University of Alberta

DESIGN AND EVALUATION OF OPTIMAL PID CONTROLLERS

by

Olugbenga Adeleye

A thesis submitted to the Faculty of Graduate Studies and Research in partial fulfillment of the requirements for the degree of **Master of Science**

in

Process Control

Department of Chemical and Materials Engineering

Edmonton, Alberta
Spring 2006

Your file Votre référence
ISBN: 0-494-13780-0
Our file Notre référence
ISBN: 0-494-13780-0

DEDICATION

I give all glory to my Heavenly Father - God Almighty, Creator of the universe; Giver of the breath of life, without which nothing is possible

ABSTRACT

Kristiansson's[1] controller design and evaluation method characterizes a control system by dividing its frequency response into four regions. Within each frequency region a criterion is defined as a measure of one of the system's properties – performance, robustness, and control activity. Constraining three of the four criteria at desired levels, controller parameters that optimize the fourth criterion are calculated so that an optimal balance of the control system's properties is attained.

This thesis presents the application of Kristiansson's[1] technique to the design, evaluation, simulation and experimental implementation of optimal PI/PID-based control systems for real and hypothetical processes. The experimental evaluation is carried out on two pilot-scale processes and an industrial control loop.

The salient points made from the application of the evaluation technique are:

- With the use of either first or second order low-pass filtering, derivative (D) control can be safely incorporated into a PI control system, hence a PID controller. Compared with the traditional PI controller, the PID controller can significantly improve output performance without excessive control activity;
- For processes having significant time-delay dominance, there's substantial improvement in closed-loop performance when a PID controller is utilized, instead of the PI controller; and
- For processes with larger time delays, the PID controller can perform better or equal to the Smith-augmented PI controller.

[1] Kristiansson, B. (2000). Evaluation and Tuning of PID Controllers. Licentiate Thesis, Dept of Signals and Systems, Chalmers University of Technology, Göteborg, Sweden

ACKNOWLEDGEMENTS

I am heavily indebted to my mentor and supervisor, Prof. Sirish L. Shah, for his excellent guidance. The warm discussions and regular meetings I had with him during the research provided the focus and direction needed to get to the finish line. I thank him for his tremendous efforts to ensure the realisation of the trial application of the PID controller design technique on an industrial control loop. My sincere gratitude to both Prof. Shah and his wife, Mrs. Anjna Shah for their pleasant hospitality and reception during the get-togethers they organized.

I would like to thank Dr. Birgitta Kristiansson of the Chalmers University of Technology, Sweden, for our numerous discussions on her control system evaluation procedure and her controller optimization MATLAB codes. The two months she spent visiting the research group encouraged my appreciation of PID controllers, whose days I hitherto thought were numbered.

The industrial application of the controller design algorithm was performed at the Petro-Canada Edmonton Refinery. I would like to show my appreciation to George Pfaff for making it possible. Thank you, George, for your prompt response to each of my numerous questions, emails, and phone-calls, despite your busy schedule.

The experimental aspect of this research would not have been possible without the Department of Chemical and Materials Engineering's permission to use the pilot-scale processes in the Computer Process Control Laboratory. Specifically, I would like to thank Prof. Shah, Prof. Fraser Forbes, and Artin Afacan, for my access into the lab. Additionally, I would like to thank the gentlemen at the Instruments Shop – Walter Boddez, Richard Cooper, and Les Dean – for their regular technical support in the use of the laboratory equipment.

The NSERC-Matrikon-ASRA Industrial Research Chair programme, the Department of Chemical and Materials Engineering, and the Faculty of Graduate Studies and Research provided the various forms of financial support for the completion of the graduate study program. Thank you all.

The high quality of system identification, control and statistics courses provided the solid academic launch pad from which I commenced this research. I thank Profs. Sirish Shah, Doug Wiens, as well as Drs. Scott Meadows, Tony Yeung, and Ivan Mizera for their high academic standards and dedication to teaching.

I am fortunate to be part of a world-class research group. I thank members of the Computer Process Control Group for the seminars and discussions presented

during group meetings, as well as for ideas, encouragement and support provided during this research.

Special thanks to Ian Alleyne, my "DCS mentor", from whom I learnt so much about the Delta V DCS and MATLAB OPC DA Toolbox.

A warm thank-you to the departmental secretaries – AnnMarie, Shona, Theresa and Leanne – for their administrative and logistics support during this graduate program.

I would like to thank my Nigerian friends here in Canada, you're too numerous to name.

I have reserved special gratitude and tribute for my family back in Nigeria. I am highly grateful for their prayers, encouragement and phone calls. Thank you, Daddy, Mummy, Yemi and Sesan. God bless you.

TABLE OF CONTENTS

LIST OF FIGURES

LIST OF TABLES

CHAPTER 1

INTRODUCTION

1.1 THE PID CONTROLLER: HISTORICAL OVERVIEW

Commercial application of the Proportional-Integral-Derivative (PID) controller for industrial activities has been on-going for nearly seventy years. According to [6], the first commercial PID controller – the *Fulscope* pneumatic controller – was introduced by Taylor Instrument Companies in 1939. Also in 1939, the Foxboro Instrument Company introduced the *Stabilog 30* pneumatic controller, which operated on the basis of the PID control algorithm as well. In 1950, the *Transet Tri-act* controller [26] was introduced. It was a serial PID controller, and became a standard form. In 1959, Foxboro presented the *Controsol*, which was the first widely-accepted electronic PID controller.

Prior to the 1930s, academic and professional institutions paid little attention to the theoretical research and development of process controllers, as development had been driven only by industrial needs and lacked a mathematically-supported foundation. The first synthesis of important ideas from several sources on PID controller design came in 1934 with Harold Hazen's paper [27] on servomechanisms, in which an examination of the control actions used in industrial instruments was included. By that time, many engineers working in instrument companies and process industries were also trying to build a body of theoretical knowledge that would assist them with future controller design problems. Grebe et al [28] at Dow Chemical Company, USA, and Ivanoff [29] in the UK, initiated this effort by publishing papers in 1933 and 1934 respectively. Later, papers on automatic control were published in the Transactions of American Society of Mechanical Engineers (ASME).

In 1940, one of the three central issues for the development of control engineering was establishing appropriate settings for PID controller design parameters. The issue was addressed in 1942 by Ziegler and Nichols [30], who presented two methods for finding suitable parameter settings. Attention paid to the development of PID control has grown tremendously since the early 1940s. There are currently numerous publications on PID tuning techniques. In [7], a survey of published papers on control theory, spanning a century, can be found. In that survey, PID tuning methods are divided into six groups:

a) Ziegler-Nichols Tuning Technique: This technique originated in the work of Ziegler and Nichols in 1942 [30]. It is still being used widely for control loops in industry.

b) Frequency Domain Tuning Techniques: These consist of a variety of frequency domain-based techniques that use information about the

desired phase and gain margins of the closed loop, as well as other system frequency response parameters.

c) Relay-Based Tuning Techniques: This technique was introduced in 1984 by Astrom and Hagglund in [39]. Since then, it has undergone several modifications.

d) Optimization-Based Tuning Techniques: The techniques in this group are based on the optimization of pre-defined performance criteria, the most common being integral criteria.

e) Internal Model Control Tuning: These techniques are based on the Internal Model Control algorithm developed by Morari and his co-workers [40, 41].

f) Other Tuning Methods: These include tuning techniques based on the identification of the transient response parameters of the second-order plus time delay process, PID tuning based on gain scheduling, PID tuning based on the dominant pole placement method, etc.

Other rich sources of PID tuning techniques are [31, 32]. Also, PID control theory is discussed at an introductory level in [4, 14].

1.2 CURRENT TRENDS AND ISSUES IN PID CONTROL

According to [5], most PID controllers in industry operate as regulators (i.e., they reject external disturbances to process variables), making regulatory performance of the controllers of primary importance. Load disturbances are often the most common disturbances in process control [33]. Consequently, several design methods focus on load disturbances. Other major functions of the PID controller in industrial processes are:

- Set point tracking
- Attenuation of sensor noise
- Robustness to model uncertainty
- Stabilization

There are approximately three million regulatory controllers in continuous process industrial facilities (based on data from Industrial Information Resources [11]), with typically between five hundred and five thousand regulatory controllers in each industry. Based on a survey of over eleven thousand controllers in the refining, chemical and pulp and paper industries, 97% of regulatory controllers utilize a PID feedback control algorithm. A minimum of three reasons are given for the predominance of the PID algorithm:

1) The PID algorithm works well in the majority of applications.
2) The PID algorithm is easy to understand. Numerous publications exist on PID implementation and tuning, and a number of software packages are available to facilitate PID tuning.

3) The PID algorithm is pre-programmed in every control system. Implementing a non-PID feedback control algorithm involves programming custom logic and could take as much as one hundred times the effort of implementing a PID algorithm, not counting the intangible lifecycle costs such as documentation, support, and troubleshooting.

Another control algorithm now in widespread use is the Model Predictive Control (MPC) [42]. According to [34], there are between two thousand and three thousand multivariable model predictive control (MPC) applications in use worldwide. When MPC is implemented, its manipulated variables are typically the set points of existing PID controllers.

Several current trends [11] suggest the gap between desired and actual controller performance in industries is widening:

1) When manufacturing sites are large enough to warrant dedicated control engineers, their time is increasingly being diluted across implementing and maintaining advanced control technologies, display building, process historian support, and traditional PID controller maintenance. Consequently, there is inadequate time for controller performance analyses.
2) Process control application engineers often lack process control troubleshooting experience.
3) Studies have shown that only about one third of industrial controllers provide an acceptable level of performance [36, 37]. Furthermore, this performance has not improved significantly in the last few years, even though many academic performance measures have been developed in that time [38].

A performance survey of twenty six thousand PID controllers [11] conducted in 2000 in a wide variety of continuous process industries classified the performance of each controller into the categories listed below. The classification was based on an algorithm combining a minimum variance benchmark [38] and an oscillation metric tuned for each measurement type (flow, pressure, level, etc). The classifications were also refined through extensive validation and industry feedback to reflect controller performance relative to practical expectations for each measurement type:

- Excellent or Acceptable (16% in each class): These refer to controllers with minor performance deviations.
- Fair or Poor (22% and 10% respectively): These refer to controllers with unacceptably sluggish or oscillatory responses.
- Open Loop (36%): This refers to controllers operating in the manual mode (i.e., process variables are held close to set points by the interventions of the operators manipulating the processes) or the output is saturated for more than 30% of the time span of the dataset.

In addition to the performance discrepancies noted above, [18, 19] list factors that could limit the achievable performance of a control system as:

- Process Dynamics
- Nonlinearities
- Uncertainties
- Disturbances

Another cause of the performance discrepancies is poor controller tuning, which arises from changes in process dynamics or the nature of the disturbances. Other causes include wear, malfunction, or failure of hardware in the control systems.

As a method of closing the desired vs. actual controller performance gap, [11] describes the Process Control Monitoring System (PCMS). The purpose of the PCMS is to provide plant control engineers with enhanced capabilities to identify problems for many controllers while minimizing additional effort and expense. The PCMS collects control loop data, computes performance assessment metrics, performs analyses, and presents the metrics in a form suitable for the control engineer to make decisions and take appropriate action on the control loop. There are three broad domains for the performance assessment metrics, one of which is the Engineering Metric (examples include dynamic model accuracy and minimum variance benchmarks). This metric helps to diagnose engineering deficiencies within the controller.

Hence, the feedback methodology for improving controller performance using PCMS would be: Minimize the deviation between current controller performance and the overall industrial/business objectives by implementing a PCMS, which empowers the control engineer with current process and control loop information obtained from metrics computation and analyses, and enables him to take the necessary corrective action.

Another issue in the industrial application of PID control is the non-usage of the derivative (D) part of the system, thus causing widespread usage of Proportional-Integral (PI) control. Derivative control is not commonly used in industrial control loops because it amplifies and transfers noise (i.e., high frequency random fluctuations in sensor measurement of process variables) to the control signal sent from the controller to the actuator. The derivative control signal is mathematically a multiple of the derivative of the process output. If the process output has an erratic trend, its derivative would also be erratic on a more severe scale. Thus, poor tuning of the D controller leads to excessive control activity and high variability in the response of the controlled process. According to [37], about 97% of the control loops in a typical Canadian paper mill use PI control.

A great amount of investigative effort has gone into PI and PID controllers, and many useful design ideas have been presented over the years (as summarized in [7, 31, 32]). However, none of the presented design methods has been widely accepted. A likely reason given in [13] is that the ultimate tuning method has not

yet been found, or perhaps one does not exist because the variety of situations where PID controllers are used is diverse. Therefore, an assortment of tuning methods is probably required.

1.3 EVALUATION OF CONTROL SYSTEMS

Evaluation of a linear control system involves the quantitative assessment of its properties, the most important of which are *performance* and *robustness* (i.e., stability, control activity, robustness to model uncertainties). In most cases, improvement of the properties of a control system in one aspect will bring deterioration in another. According to [25], for a correct comparison of various control systems, their properties must be equally restricted except for the property being compared.

A control system evaluation method proposed by Kristiansson [13] defines four evaluation criteria related to the vital performance and robustness characteristics of a control system in the frequency domain. The evaluation method has been applied in simulation to closed loops of benchmark process model examples in [8], with PI and PID controller structures used extensively. Some of the noteworthy features shown by these controllers from the application of the evaluation technique are:

1) With the augmentation of a first or second order low-pass filter, the derivative (D) controller can be implemented along with the PI controller, i.e., a PID controller with a filter, to give good control performance with moderate control activity;
2) There is an upper limit to the obtainable performance of a PI control system. That limit can be surpassed by the PID control system; and
3) In controlling a process with significant time delay, greater improvement in closed loop performance is obtainable if a PI controller is augmented with a D controller than if it is augmented with a Smith predictor [21, 22, 23, 24].

1.4 MOTIVATION

The points discussed thus far lead to the following conclusions:

1) Despite the number of alternate control algorithms with superior performance capabilities generated by research activities, PID control still has roles to play in industrial control loops. Hence, every effort and result relevant to improving the PID design method would always be applicable;
2) According to [11], if PCMS were implemented in industry, the process control engineer would find his decisions and actions progressively influenced by the business objective set points, rather than the individual performance level of his control loops alone. Hence, he would rely on

PCMS balance of detailed individual controller diagnostic metrics and overall business and operational metrics to chart the appropriate course of action. This approach suggests that measures for evaluating the various properties of a control loop (i.e., performance, robustness, and control activity) would eventually be required in computing the diagnostic metrics. Therefore, a systematic closed-loop evaluation method would be useful.

3) Research innovations in process control still have a long way to go before they can have a significant impact on industry-wide controller performance due to their generally inadequate implementation in industry. Hence, one area of focus for the academic community could be to work more closely with the industrial community and be more demonstrative of the benefits of new developments in control algorithms.

4) The overwhelming implementation of PI controllers compared with PID controllers in industry suggests there is significant potential for performance improvement of the control systems by just crossing the derivative control gap alone.

An example of the benefits of improving industrial control system performance can be found in the Industrial Information Resources report [11]. The report reveals that major US process industries spend about thirty billion dollars annually on energy and over one hundred billion dollars on facility maintenance. According to the report, even a 1% improvement in either energy efficiency or improved controller maintenance direction represents hundreds of millions of dollars in savings to process industries. Control loops not operating at optimal performance levels invariably increase energy consumption at the actuators, cause equipment wear, deviate from process operating conditions – which in turn give off-quality products and reduce production yield. These factors incur excess production costs in the form of product recycling, raw material loss, excess energy usage, loop hardware maintenance and repairs, and production downtime.

1.5 THESIS OVERVIEW

The scope of this thesis is based on Kristiansson's controller evaluation technique [13]. The features of PI and PID control systems highlighted by the technique were investigated only in simulation and for hypothetical process models. It would be desirable to verify the evaluation results experimentally using industrial processes or at least their pilot-scale versions.

It is reasonable to expect that experimental work on a real controlled process would be in the open loop (e.g., system identification) and the closed loop (e.g., controller implementation) modes. Hence, one of the objectives of this research is to obtain linear, time invariant, dynamic models for the processes employed. The models will be used for designing a range of PI and PID controllers using an optimization-based technique of the evaluation method. Closed loops consisting of the models and designed controllers will be implemented both in the simulation and real-time experimentation.

The criteria for evaluating the control systems' characteristics will be applied to the closed loops as tools for comparing the PI and PID controllers. Because the properties of major interest to plant operators and control engineers are the closed loops' performance and control activity, substantial emphasis will be placed on them in the controller comparisons.

The role of time delay in the achievable performance of control loops is a salient matter in industry. The implementation of an inappropriate control structure on a process with a significant time delay could give poor closed-loop performance. Hence, when comparing various control structures, it would be quite informative to examine the way they perform for processes in which time delay has varying degrees of dominance. In this thesis, the comparisons of control structures implemented on the real processes with varying time delays are restricted to PI and PID controllers.

In view of the fact that one of the motivating points for this research is the apparent gap between academia and industry concerning the application of innovations in controller design, it would be desirable to reproduce the results of the intended comparisons mentioned above using measures that are either already well-known to control engineers or can be easily understood. Measures used industrially are typically based on the response data for the process variables, manipulated variables, set point signals, etc, as they are readily available. Hence, the research will also consider control system comparisons that use evaluation criteria based on the sampled process data of the closed loops and not necessarily the process and controller models.

The point made in [25] on the greater benefit of adding derivative action to a PI controller, in contrast to augmenting it with a Smith predictor, will also be investigated using the models for the real processes plus the processes themselves.

Pilot-scale processes, which utilize the same physical principles (e.g., heat transfer, fluid flow, etc) as in industrial processes, are available in the Computer Process Control Laboratory for the experimental aspect of this research. A computer interface to the processes gives the flexibility of performing a wide variety of system identification experiments and implementing any control algorithm on the processes.

CHAPTER 2

CHARACTERISATION OF A CONTROL SYSTEM'S PROPERTIES

2.1 INTRODUCTION

The main exogenous and response variables of a Single-Input-Single-Output (SISO) closed loop will be discussed in this chapter, as will the common transfer functions, or the sensitivity transfer functions, of the system. The typical frequency response profile of each transfer function will be illustrated with examples, using simple process transfer functions and controllers.

The closed loop evaluation criteria proposed in [25], which are H_∞ norm-based functions of the sensitivity transfer functions, will be discussed in detail. Each criterion will be illustrated in the frequency domain, using the afore-mentioned process transfer functions and controllers.

Finally, the applicability of the evaluation criteria to controller design will be discussed.

2.2 THE SENSITIVITY TRANSFER FUNCTIONS

Figure 2.1 depicts the block diagram of a typical SISO closed-loop.

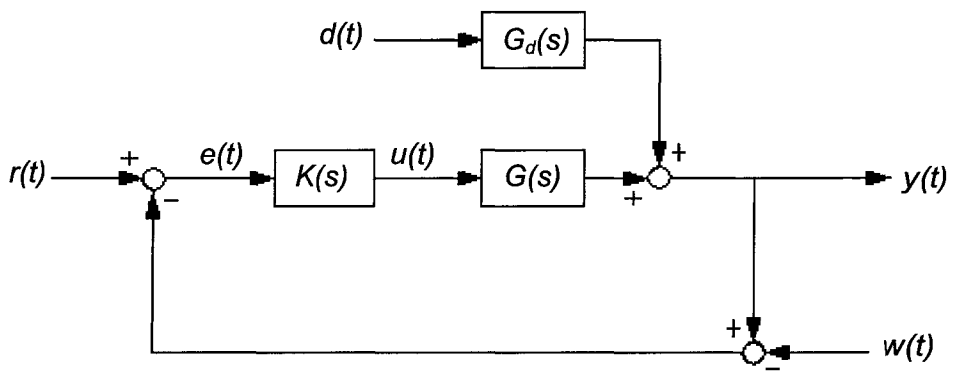

Figure 2.1: Schematic diagram of a Single-Input-Single-Output (SISO) closed loop.

The external (or exogenous) variables are:

- Set point signal, *r(t)*
- Process disturbance, *d(t)*
- Measurement noise, *w(t)*

The output variables are:

- Process output, *y(t)*
- Control signal, *u(t)*
- Error signal, *e(t)*

The relevant transfer functions are:

- The process, *G(s)*
- The disturbance, $G_d(s)$
- The controller, *K(s)*

The sensitivity transfer functions relate the external signals to the output signals. The transfer functions of interest are:

- The Sensitivity Function
- The Complementary Sensitivity Function
- The Disturbance Sensitivity Function
- The Control Sensitivity Function

Sensitivity Function

This function is defined as:

$$S(s) = \frac{1}{1 + G(s)K(s)} = G_{er} \tag{2.1}$$

Where G_{er} is the transfer function between the error signal and the set point signal.

Complementary Sensitivity Function

This function is defined as:

$$T(s) = \frac{G(s)K(s)}{1 + G(s)K(s)} = G_{yr} = G_{yw} = -G_{ew} \tag{2.2}$$

where:

G_{yr} = transfer function between the set point signal and the process output.

G_{yw} = transfer function between the measurement noise and the process output.

G_{ew} = transfer function between the measurement noise and the error signal.

S(s) and *T(s)* are the closed-loop transfer functions for disturbances and set point changes. They both provide measures of how sensitive the closed-loop system is to changes in the process. Also,

$$S(s)+T(s)=1 \tag{2.3}$$

If the controller includes integral action, offset is eliminated for set point changes and sustained disturbances, such that at low frequencies, $|T(j\omega)| \rightarrow 1$ and $|S(j\omega)| \rightarrow 0$, where $|T(j\omega)|$ and $|S(j\omega)|$ are gain magnitudes of $T(s)$ and $S(s)$ respectively. The maximum values of the gain magnitudes provide useful measures of closed-loop robustness, which will be discussed in later in this chapter.

Disturbance Sensitivity Function

This function is defined as:

$$\begin{aligned} S_v(s) &= \frac{G_d(s)}{1+G(s)K(s)} \\ &= G_{yd} \end{aligned} \tag{2.4}$$

where:

G_{yd} = transfer function between the disturbance and the process output.

For effective rejection of low frequency disturbances, the closed-loop should have a low maximum value of $|G_{yd}|$ in the low frequency region.

The PID controller evaluation method in [25] is based on the assumption that the disturbance enters the process at the control signal so that both inputs have the same dynamic effect on the process output. Typical examples given are load forces and moments in mechanical systems and fluctuating concentrations in fluid systems. Hence, $G_d(s) \approx G(s)$ so that (2.4) becomes:

$$S_v(s) = \frac{G_d(s)}{1+G(s)K(s)} \approx \frac{G(s)}{1+G(s)K(s)} \tag{2.5}$$

(2.5) will subsequently be used as the disturbance sensitivity function.

Control Sensitivity Function

This function is defined as:

$$\begin{aligned} S_u(s) &= \frac{K(s)}{1+G(s)K(s)} \\ &= G_{ur} = G_{uw} \end{aligned} \tag{2.6}$$

where:

G_{ur} = transfer function between the set point signal and the control signal.

G_{uw} = transfer function between the measurement noise and the control signal.

For effective attenuation of measurement noise transfer to the control signal, $|G_{uw}|$ should be low in the high frequency region.

Example 2.1 calculates the four sensitivity transfer functions, and illustrates their frequency response using arbitrary process and controller transfer functions:

Example 2.1: Table 2.1 shows five process transfer functions and the respective PID controllers (with first order filtering of the derivative part) used to control them in closed loops:

Table 2.1: Process and Controller Parameters for Sensitivity Transfer Functions

	PROCESS	CONTROLLER
1	$\frac{e^{-s}}{10s+1}$	$3.5536\left(1+\frac{1}{3.2602s}+\frac{0.4231s}{1+0.0701s}\right)$
2	$\frac{e^{-2s}}{10s+1}$	$2.3931\left(1+\frac{1}{4.4316s}+\frac{0.6933s}{1+0.1316s}\right)$
3	$\frac{e^{-3s}}{10s+1}$	$1.9160\left(1+\frac{1}{5.3719s}+\frac{0.9974s}{1+0.1960s}\right)$
4	$\frac{e^{-4s}}{10s+1}$	$1.6299\left(1+\frac{1}{6.1505s}+\frac{1.3315s}{1+0.2593s}\right)$
5	$\frac{e^{-5s}}{10s+1}$	$1.4308\left(1+\frac{1}{6.8131s}+\frac{1.6899s}{1+0.3194s}\right)$

Each process transfer function contains a time-delay term, which must be converted to polynomial form using the Padé approximation [14] in order to compute the sensitivity transfer functions. For simplicity, the 1/1 approximation is used. Table 2.2 shows the four transfer functions for all the processes.

Table 2.2: Computation of Sensitivity Transfer Functions

$G(s)$	$\frac{e^{-s}}{10s+1}$
$K(s)$	$3.5536\left(1+\frac{1}{3.2602s}+\frac{0.4231s}{1+0.0701s}\right)$
$S(s)$	$\frac{0.7s^4+11.5s^3+21.1s^2+2s}{0.7s^4+9.7s^3+21s^2+8.2s+2.2}$
$T(s)$	$\frac{-1.8s^3-0.1s^2+6.2s+2.2}{0.7s^4+9.7s^3+21s^2+8.2s+2.2}$

$S_v(s)$	$\frac{-0.7s^5 - 10.1s^4 - 1.8s^3 + 40.3s^2 + 4s}{7s^6 + 111.9s^5 + 415.7s^4 + 542.5s^3 + 235.4s^2 + 62.1s + 4.4}$
$S_u(s)$	$\frac{1.2s^6 + 22.7s^5 + 79.5s^4 + 92.8s^3 + 30.3s^2 + 2.2s}{0.05s^6 + 1.4s^5 + 11.2s^4 + 21.6s^3 + 8.3s^2 + 2.2s}$

$G(s)$	$\frac{e^{-2s}}{10s+1}$
$K(s)$	$2.3931\left(1 + \frac{1}{4.4316s} + \frac{0.6933s}{1+0.1316s}\right)$
$S(s)$	$\frac{1.3s^4 + 11.5s^3 + 11.1s^2 + s}{1.3s^4 + 9.5s^3 + 10.6s^2 + 2.9s + 0.5}$
$T(s)$	$\frac{-2s^3 - 0.5s^2 + 2s + 0.5}{1.3s^4 + 9.5s^3 + 10.6s^2 + 2.9s + 0.5}$
$S_v(s)$	$\frac{-1.3s^5 - 10.1s^4 - 0.3s^3 + 10.1s^2 + s}{13.2s^6 + 109.2s^5 + 211.9s^4 + 155.8s^3 + 48.21s^2 + 8.7s + 0.5}$
$S_u(s)$	$\frac{2.6s^6 + 25.8s^5 + 50.9s^4 + 35.6s^3 + 8.5s^2 + 0.5s}{0.2s^6 + 2.6s^5 + 10.9s^4 + 11s^3 + 3s^2 + 0.5s}$

$G(s)$	$\frac{e^{-3s}}{10s+1}$
$K(s)$	$1.9160\left(1 + \frac{1}{5.3719s} + \frac{0.9974s}{1+0.1960s}\right)$
$S(s)$	$\frac{2s^4 + 11.5s^3 + 7.8s^2 + 0.7s}{2s^4 + 9.2s^3 + 7.3s^2 + 1.6s + 0.2}$
$T(s)$	$\frac{-2.3s^3 - 0.46s^2 + s + 0.2}{2s^4 + 9.2s^3 + 7.3s^2 + 1.6s + 0.2}$
$S_v(s)$	$\frac{-2s^5 - 10.2s^4 - 0.1s^3 + 4.5s^2 + 0.4s}{19.6s^6 + 107.2s^5 + 145.3s^4 + 78.7s^3 + 19.8s^2 + 2.9s + 0.2}$
$S_u(s)$	$\frac{4.5s^6 + 30.2s^5 + 41.4s^4 + 21.1s^3 + 4.1s^2 + 0.2s}{0.4s^6 + 3.8s^5 + 10.7s^4 + 7.7s^3 + 1.7s^2 + 0.2s}$

$G(s)$	$\frac{e^{-4s}}{10s+1}$
$K(s)$	$1.6299\left(1+\frac{1}{6.1505s}+\frac{1.3315s}{1+0.2593s}\right)$
$S(s)$	$\frac{2.6s^4+11.6s^3+6.1s^2+0.5s}{2.6s^4+9s^3+5.7s^2+1.1s+0.1}$
$T(s)$	$\frac{-2.6s^3-0.4s^2+0.6s+0.1}{2.6s^4+9s^3+5.7s^2+1.1s+0.1}$
$S_v(s)$	$\frac{-2.6s^5-10.3s^4-0.4s^3+2.6s^2+0.3s}{25.9s^6+105.2s^5+112.3s^4+49.7s^3+10.7s^2+1.3s+0.1}$
$S_u(s)$	$\frac{6.7s^6+34.4s^5+36.2s^4+14.8s^3+2.5s^2+0.1s}{0.7s^6+4.9s^5+10.5s^4+6s^3+1.1s^2+0.1s}$

$G(s)$	$\frac{e^{-5s}}{10s+1}$
$K(s)$	$1.4308\left(1+\frac{1}{6.8131s}+\frac{1.6899s}{1+0.3194s}\right)$
$S(s)$	$\frac{3.2s^4+11.6s^3+5.1s^2+0.4s}{3.2s^4+8.7s^3+4.8s^2+0.8s+0.1}$
$T(s)$	$\frac{-2.9s^3-0.3s^2+0.4s+0.1}{3.2s^4+8.7s^3+4.8s^2+0.8s+0.1}$
$S_v(s)$	$\frac{-3.2s^5-10.3s^4-0.5s^3+1.7s^2+0.16s}{31.9s^6+103.2s^5+92.7s^4+35.3s^3+6.7s^2+0.7s+0.03}$
$S_u(s)$	$\frac{9.1s^6+38.1s^5+32.8s^4+11.3s^3+1.7s^2+0.1s}{s^6+6s^5+10.3s^4+5s^3+0.8s^2+0.7s+0.1}$

Figures 2.2(a) to 2.2(d) depict the frequency response plots of the sensitivity transfer functions for the closed loops of all the processes.

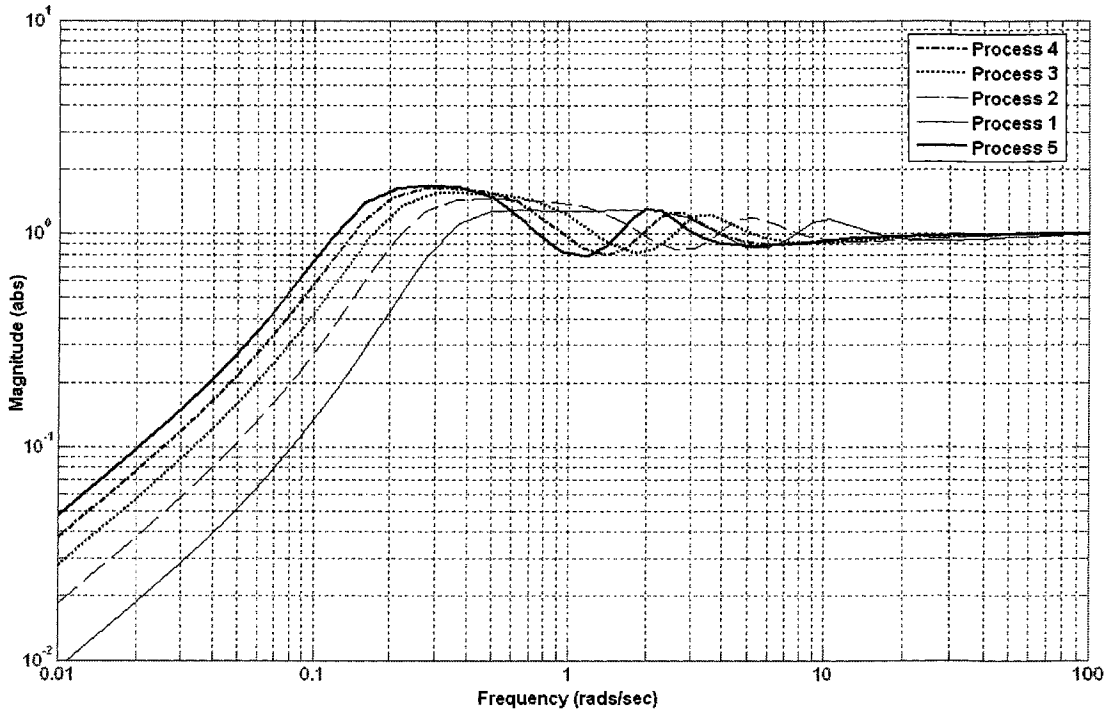

Figure 2.2(a): Frequency response of sensitivity functions.

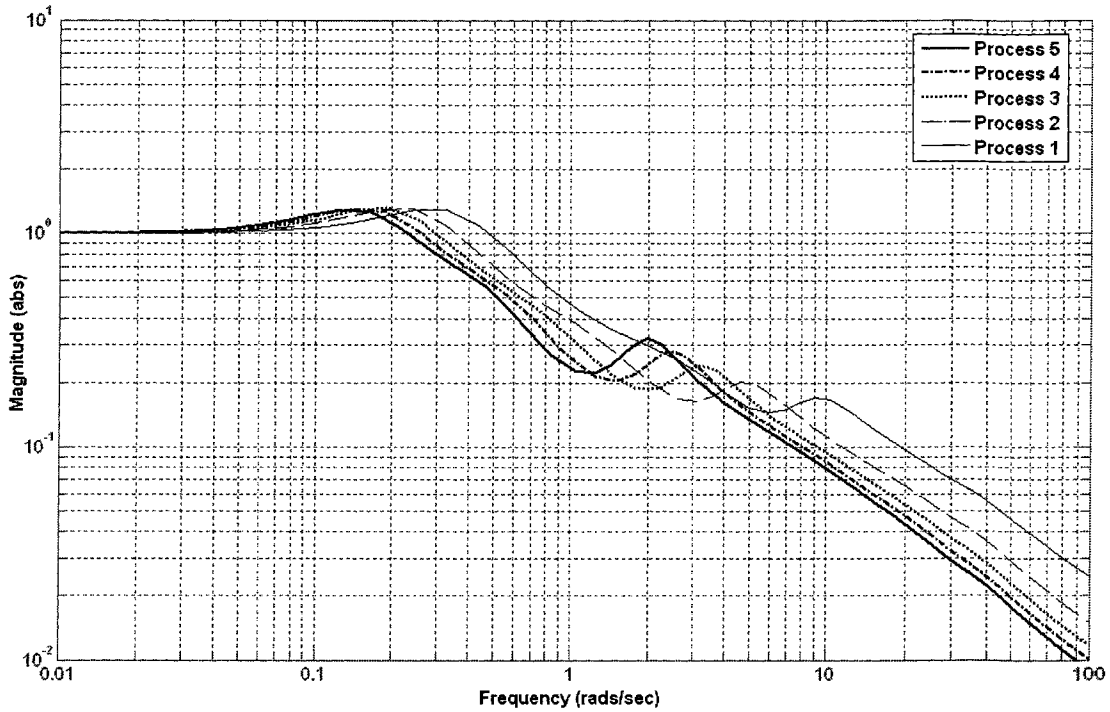

Figure 2.2(b): Frequency response of complementary sensitivity functions.

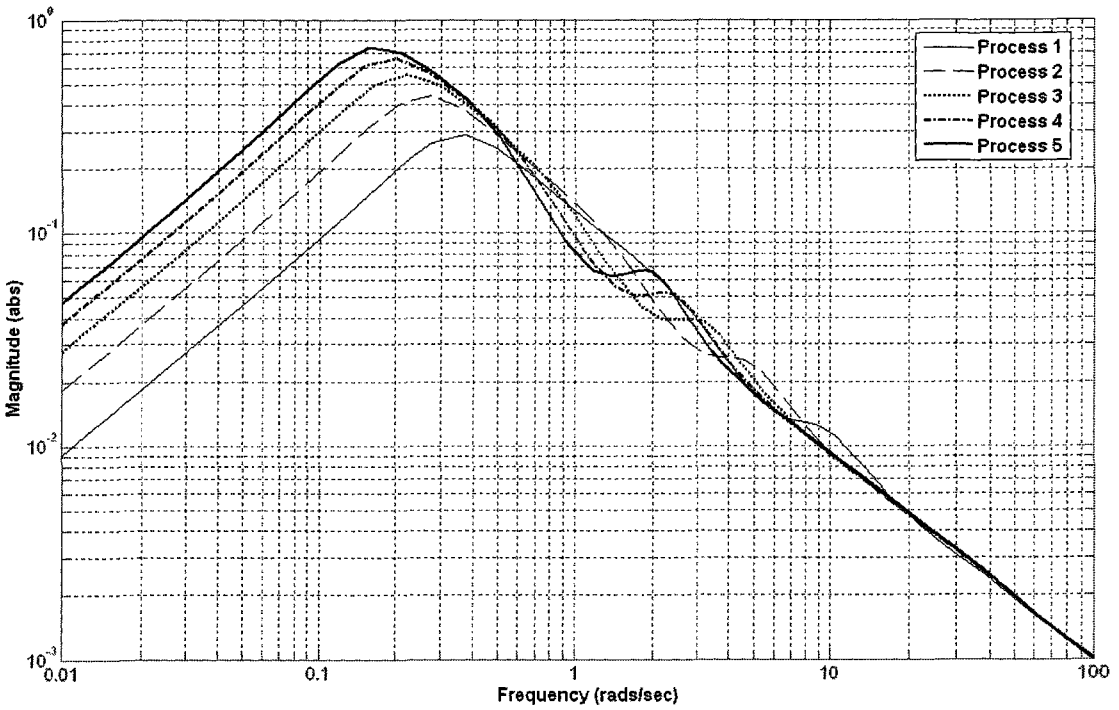

Figure 2.2(c): Frequency response of disturbance sensitivity functions.

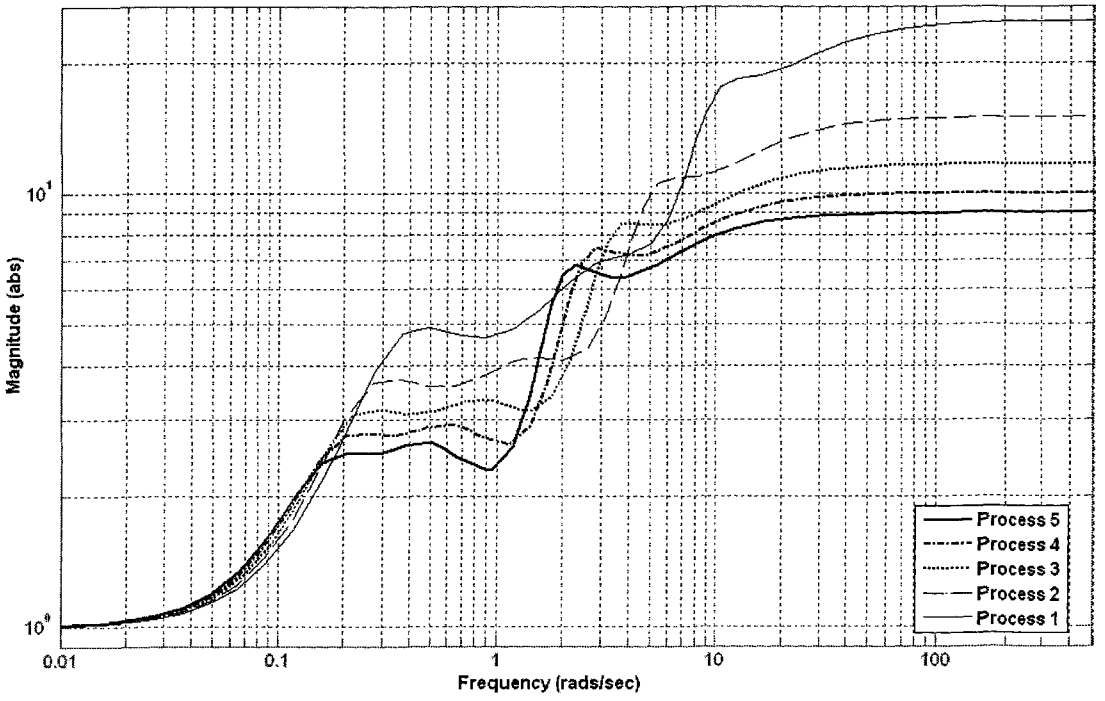

Figure 2.2(d): Frequency response of control sensitivity functions.

Figure 2.2(c) shows that the disturbance sensitivity gain initially increases with frequency in the low frequency region to a peak and subsequently drops. For good disturbance rejection, this peak should be kept as low as possible; the performance criterion in Kristiansson's evaluation method is based on it.

Figure 2.2(d) shows the control sensitivity gain increasing with frequency and converging at an upper asymptote. The asymptote shows that the most significant transfer of measurement noise to the control signal occurs at high frequencies. Hence, for effective attenuation of noise in the control signal, the high frequency asymptote should be kept as low as possible. The mid-to-high and high frequency robustness criteria in the evaluation method are based on this asymptote.

The controller, *K(s)*, can be strictly proper or just proper. When integral action is included, it has the asymptotic properties:

$$K(s) \rightarrow \begin{cases} \dfrac{k_i}{s} & s \rightarrow 0 \\ \dfrac{k_\infty}{s^m} & s \rightarrow \infty \end{cases} \tag{2.7}$$

When *K(s)* is just proper, the roll-off m is zero, $K(s) \rightarrow k_\infty$ as $s \rightarrow \infty$. The *high frequency gain*, k_∞, and the *integral gain*, k_i, are both non-zero constants.

2.3 EVALUATION CRITERIA FOR CONTROL SYSTEM'S PROPERTIES

As typified by the Bode Sensitivity Integral Theorem, which shows that the suppression of the sensitivity function's gain in one frequency region would lead to gain enhancements in other regions, improvements of the properties of a control system in one respect would cause deteriorations in the other. For each property of a control system, the demands on it vary along the frequency scale. An example can be seen in the frequency response of *T(jω)* in Figure 2.2(b). Because it is the closed-loop transfer function, it is desirable to keep its gain high in the low frequency region for enhanced closed-loop response performance. In the high frequency region, however, it must be kept low for closed-loop robustness purposes. For other sensitivity transfer functions, the demands in the low, mid-, and high frequency regions differ. Therefore, in describing the properties of a control system in the frequency domain, at least one descriptive quantity is required in each frequency region.

A control system can be characterized by its *performance* and its *robustness*. To evaluate these properties in the frequency domain, [25] divides the frequency response of the open loop transfer function *L(jω)* into four regions as shown in Figure 2.3.

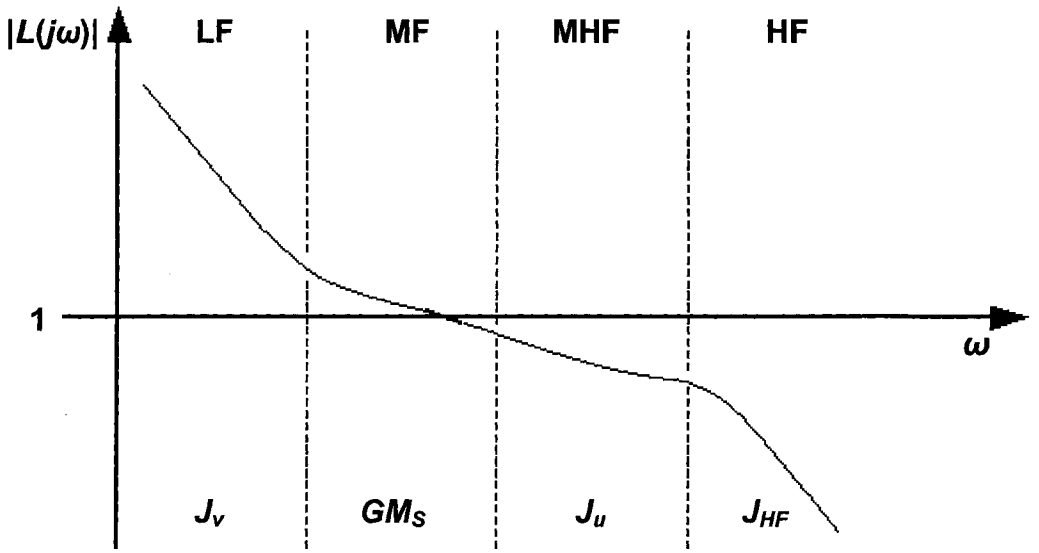

Figure 2.3: Division of frequency response of open loop transfer function into four regions.

In the low frequency (LF) band, the aim is to obtain a high loop gain in order to obtain efficient compensation of load disturbances and accurate tracking of varying set point signals, as well as robustness against process dynamics uncertainties. J_v is the proposed LF criterion, which evaluates the control system's ability to compensate low frequency load disturbances; thus, J_v is the performance criterion. Another performance criterion suitable for closed-loop servo objectives is J_r.

In the mid frequency (MF) band, which is in the vicinity of the gain and phase cross-over frequencies, the stability margins of the control system are evaluated. In this case, the general stability criterion is the *Generalized Maximum Sensitivity*, GM_S.

In the mid-to-high frequency (MHF) band, just above the bandwidth, the property of evaluation interest is the control activity. The control activity criterion defined in this frequency band is J_u. For a just proper (not strictly proper) controller, J_u can also be seen as a measure of the high-frequency robustness and of the ability of the control system to reduce high-frequency sensor noise.

The high frequency (HF) criterion is J_{HF}, and it is applicable only to control systems having strictly proper controllers. It measures their high frequency robustness and high frequency noise attenuation ability in the same way as J_u measures these properties in the mid-to-high frequency band. J_{HF} measures the extent to which high frequency measurement noise can be damped without having any significant effect on the low frequency properties of the control system.

2.3.1 PERFORMANCE CRITERIA – J_v, J_r

The main objectives of a controller [4] are listed below:

- Damping load disturbances
- Following a reference signal
- Stabilization
- Reducing the influence of uncertainties and nonlinearities
- Attenuation of sensor noise

The most common objective is damping load disturbances [33], in which case the most relevant sensitivity transfer function is the disturbance sensitivity function $S_v(s)$ from (2.5). For controllers with integral action and according to (2.7), as $\omega \to 0$ (low frequency), $G(j\omega)K(j\omega) >> 1$:

$$S_v(j\omega) = G_{yd}(j\omega) = \frac{G(j\omega)}{1+G(j\omega)K(j\omega)} \approx \frac{1}{K(j\omega)} \approx \frac{j\omega}{k_i} \tag{2.8}$$

Hence, the influence of the low frequency load disturbance on the process output is attenuated by a factor of $1/k_i$, such that the smaller its value, the smaller the influence of the disturbance on the output. [25] shows, as corroborated by [4], how for a closed loop with robust design and small undershoot in a load disturbance step response:

$$IAE = \int_0^\infty |e(t)|dt \approx |IE| = 1/k_i \tag{2.9}$$

where *IAE* is the integral of the absolute magnitude of the error signal and *IE* is the integral of the error signal. *IAE* is a common disturbance rejection performance index [4, 14, 43].

According to (2.8), $1/k_i$ is approximately equal to $(j\omega)^{-1}S_v$ and is an applicable measure of the ability of a closed loop to attenuate load disturbances. Kristiansson therefore defines the performance criterion J_v as:

$$J_v = \left\| W_v G_{yd} \right\|_\infty = \left\| W_v S_v \right\|_\infty = \max_\omega |W_v(j\omega)S_v(j\omega)| \tag{2.10}$$

where $W_v(s) = s^{-1}$

The graphic interpretation of (2.10) is that J_v is the gain peak of the disturbance sensitivity function S_v weighted by $(j\omega)^{-1}$ in the frequency domain. In addition, being an H_∞-norm-based criterion, it can be used for multiple-input-multiple-output (MIMO) systems.

Using the processes and controllers from Example 2.1 in Section 2.2, the performance criterion J_v is illustrated.

Example 2.2: Figure 2.4 shows the $(j\omega)^{-1}$-weighted disturbance sensitivity frequency response of the closed-loops for the processes and controllers in Example 2.1, J_v is indicated for each closed-loop:

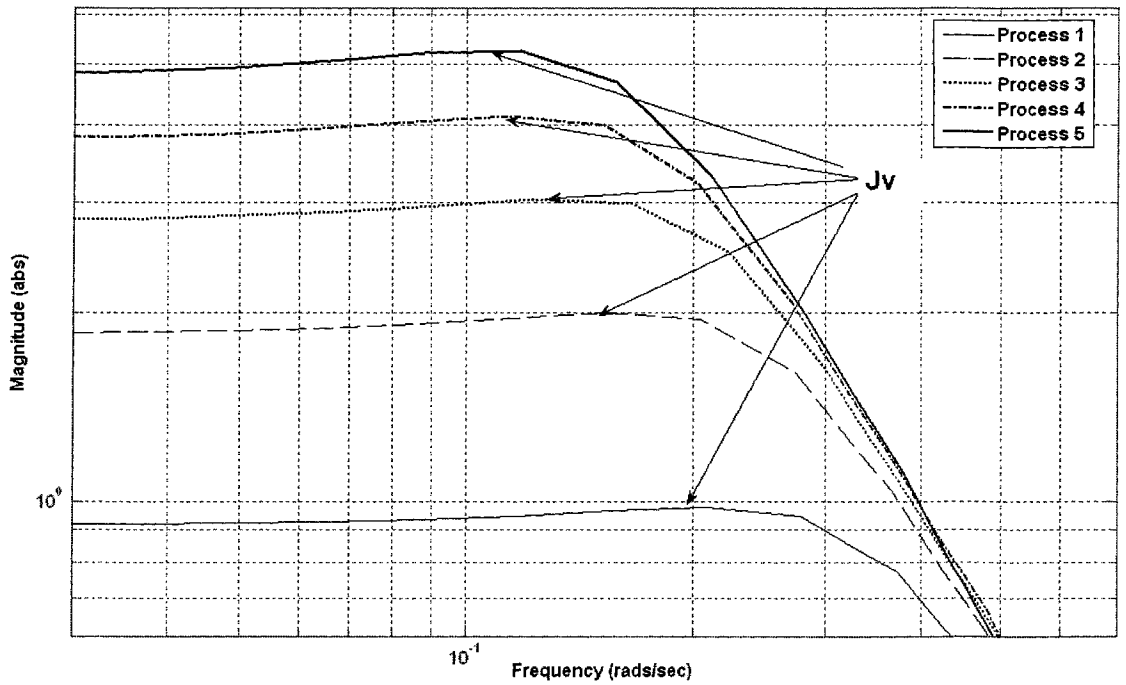

Figure 2.4: Frequency response of $(j\omega)^{-1}$-weighted disturbance sensitivity functions showing the J_v point of each closed loop.

When the main task of a control system is to follow a varying set point input, the relevant transfer function is $G_{er}(s)$ which, from (2.1), is the sensitivity function $S(s)$. As $\omega \to 0$, $L(j\omega) >> 1$. [25] defines the servo performance criterion as:

$$J_r = \|W_r G_{er}\|_\infty = \|W_r S\|_\infty = \max_\omega |W_r(j\omega)S(j\omega)| \qquad (2.11)$$

where $W_r(s) = s^{-1}$.

Now, as $\omega \to 0$, $W_r(j\omega)S(j\omega) \to G(j\omega)/k_i$. Thus J_r, unlike J_v, is plant-dependent, which makes it unsuitable as a performance criterion. In addition, [25] shows how a controller designed using (2.11) could have zeros that cancel plant poles and therefore concludes that J_v should be used as a general performance criterion, especially since a low value of J_v normally implies a low value of J_r.

2.3.2 MID-FREQUENCY ROBUSTNESS CRITERION – GM_S

The stability margin of the closed-loop is the most important factor in the mid-frequency band. A control system is stable if the Nyquist plot of its open loop transfer function $L(j\omega)$ does not encircle the point (-1,0); it must have a loop gain magnitude less than 1 at its crossover frequency, which is in the mid-frequency

region. The farther the Nyquist plot is from the point (-1,0), the higher the mid-frequency robustness of the closed loop, so that the minimum distance of the Nyquist plot from the critical point could serve as a measure of this closed-loop property. This minimum distance is the inverse of the maximum sensitivity function, $\|S(s)\|_\infty$ of the closed loop. Thus the minimum distance is maximized when the maximum value of the sensitivity function is minimized.

Based on the above description, a popular mid-frequency robustness criterion in [14] is:

$$\|S(s)\|_\infty = \frac{1}{\min_\omega |1 + G(j\omega)K(j\omega)|} \le M_S \tag{2.12}$$

Where M_S is the maximum acceptable value of $\|S(s)\|_\infty$. Typical values of M_S [4] fall between 1.4 and 2.0. When the value of M_S is specified, lower limits of the gain margin, G_m, and the phase margin, φ_m, are defined.

$$\begin{aligned} G_m &\ge \frac{M_S}{M_S - 1} \\ \varphi_m &\ge 2\sin^{-1}\left(\frac{1}{2M_S}\right) \end{aligned} \tag{2.13}$$

A typical demand on the phase margin of 45° must be met by $M_S \le 1.3$. Such a low value of M_S leads to a sluggish system. Alternatively, retaining the value of M_S and placing a constraint on the maximum of the complementary sensitivity function $\|T\|_\infty$ can meet this demand:

$$\|T\|_\infty \le M_T \tag{2.14}$$

Noting that [14]:

$$\varphi_m \ge 2\sin^{-1}\left(\frac{1}{2M_T}\right) \tag{2.15}$$

According to (2.15), setting $M_T = 1.3$ would give $\varphi_m \ge 45°$. Recommended values of M_T [3] fall between 1.2 and 2.0. However, it has been noted [41, 44] that M_T is insufficient as a mid-frequency evaluation criterion. Hence, [25] combines the criteria based on S and T in (2.12) and (2.14) to obtain a general criterion, GM_S, which serves as an applicable measure of both the control system's mid-frequency properties and phase margin requirement.

$$GM_S = \max\left(\|S\|_\infty, \alpha\|T\|_\infty\right) \tag{2.16}$$

where $\alpha = M_S / M_T$. A similar criterion is formulated by [44].

Equality between at least one of the norms and its respective restriction implies $GM_S = M_S$. Therefore, combining the constraints on the two norms ensures an acceptable phase margin, due to M_T, and a minimum distance from the Nyquist plot to the critical point in (-1, 0), due to M_S.

2.3.3 CONTROL ACTIVITY CRITERION – J_u

The general preference in the design of control loops in industry is to keep control activity as small as possible. However, since the control signal is the energy with which the controller achieves its objectives, increasing its aggressiveness enhances the achievement of those objectives. The converse also holds true. Hence, the control engineer tries to find the most advantageous trade-off between the demands on performance, i.e., J_v, and the demands on control activity. According to (2.6), the control sensitivity function S_u is the transfer function from the measurement noise to the control signal.

[25] defines the control activity criterion J_u as:

$$J_u = \|G_{uw}\|_\infty = \|S_u\|_\infty = \max_\omega |K(j\omega)S(j\omega)| \tag{2.17}$$

The graphical interpretation of (2.17) is that J_u is the peak of the frequency response of the control sensitivity function and is therefore the maximum of S_u. At frequencies above the closed-loop bandwidth, the frequency response of S_u differs depending on the controller structure used. Using Process 3 from Example 2.1, $K(j\omega)S(j\omega)$ is plotted for its closed-loop using a PI controller and two PID controllers: one with a first order low-pass filter, the other with a second order low-pass filter.

Example 2.3: Table 2.3 shows the transfer function for Process 3 with the PI and PID controllers used in the closed-loop:

Table 2.3: Transfer Functions for Process 3 with PI and PID Controllers

PROCESS	$\frac{e^{-3s}}{10s+1}$
PI CONTROLLER	$1.51\left(1+\frac{1}{6.5s}\right)$
PID CONTROLLER (with 1st order low-pass filter)	$1.9160\left(1+\frac{1}{5.3719s}+\frac{0.9974s}{1+0.1960s}\right)$
PID CONTROLLER (with 2nd order low-pass filter)	$0.36\left(\frac{1+5.57s+6.41s^2}{s(1+0.16s+0.04s^2)}\right)$

Figure 2.5 shows the frequency response plots for the three closed-loops, with the J_u point shown in each case.

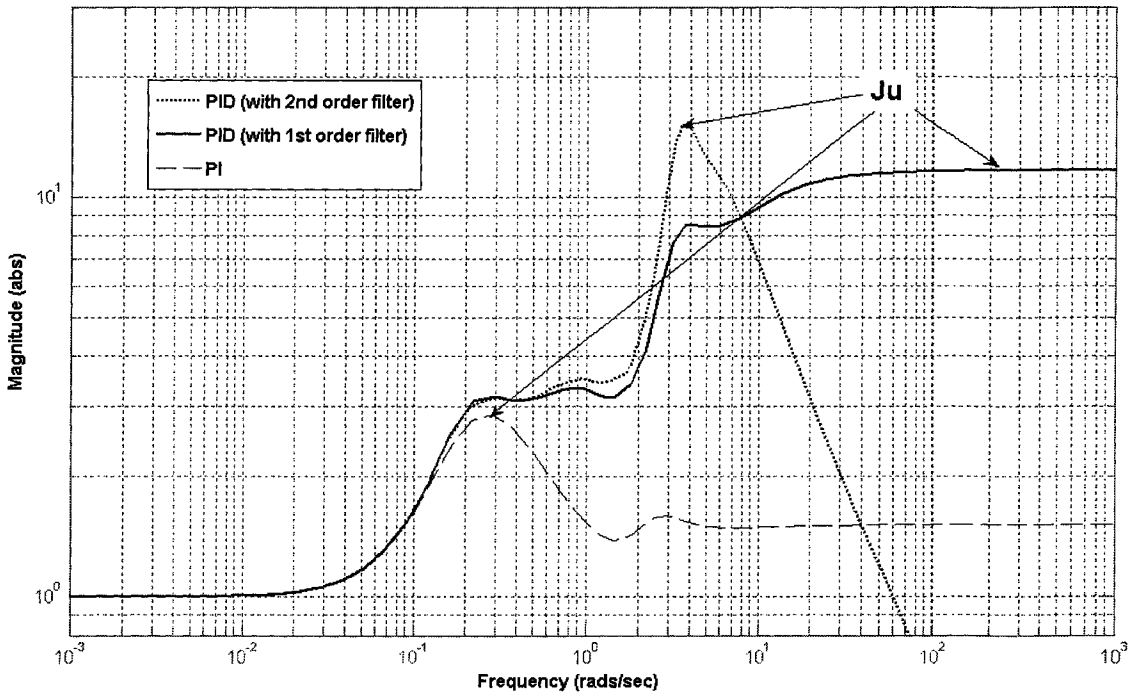

Figure 2.5: Frequency response of control sensitivity functions for closed loops using Process 3 with PI and PID (with 1st and 2nd order low-pass filters) controllers, showing the J_u points for each closed loop.

In Figure 2.5, the control signal gain of the loop with the 1st order filtered PID controller increases, within the mid-to-high frequency band, up to an asymptotic limit, where J_u is located. There is a peak in the gain of the loop with the 2nd order filtered PID controller just above the closed-loop bandwidth, beyond which the gain drops progressively. The differing high-frequency profiles of the two closed loops explains the higher noise attenuation in the control signal achieved in a closed loop using a strictly proper PID controller vis-à-vis the just proper PID controller; hence the benefit of adding the extra low-pass filter. The closed loop with the PI controller, however, has a significantly lower peak than the two PID controllers and lower high frequency asymptote, the difference being due to the missing lead action in the PI controller. This shows why the PI controller generates lower control action than the PID controller and why it is preferable for many control loops in industry. However, as will be discussed in subsequent chapters, the limited control activity of the PI controller in turn has a limiting effect on the performance of its closed loop.

2.3.4 HIGH FREQUENCY ROBUSTNESS CRITERION – J_{HF}

In the high frequency band, the just proper and strictly proper PID controllers behave differently. One way has been shown in Example 2.3, where the control signal gain profiles differ as $\omega \to \infty$. [25] mentions two relevant requirements of a closed loop in this frequency range:

- Adequate robustness of the closed loop against model uncertainties, such as un-modeled resonance and varying time delays
- Good attenuation of high frequency measurement noise transfer to the process output

To attain these two closed-loop features in the high frequency region, [25] shows the complementary sensitivity function *T(s)* as the relevant closed-loop transfer function, so that the lower the magnitude of *T(s)*, the higher the attenuation of the measurement noise transfer and the more robust the closed loop is to model uncertainties.

Now, as $\omega \to \infty$, $|L(j\omega)| << 1$, so that at high frequency,

$$T(j\omega) = \frac{L(j\omega)}{1+L(j\omega)} \approx L(j\omega) = G(j\omega)K(j\omega) \approx \frac{k_\infty}{(j\omega)^m} G(j\omega), \tag{2.18}$$

where for a just proper controller, $m = 0$ and $m > 0$ for a strictly proper controller.

The high frequency approximation of $T(j\omega)$ in (2.18) shows that performance and robustness in this frequency range are dependent on k_∞ (from (2.7)) and the process $G(j\omega)$. To make (2.18) approximately independent of the process, $T(j\omega)$ is divided by $G(j\omega)$ so that as $\omega \to \infty$,

$$\frac{T(j\omega)}{G(j\omega)} = K(j\omega)S(j\omega) = S_u \approx \frac{k_\infty}{(j\omega)^m}, \tag{2.19}$$

which is dependent on k_∞ alone. Hence, k_∞ should be given a value as low as possible to improve closed-loop performance and robustness properties at high frequencies.

Based on (2.19), Kristiansson defines the high frequency robustness and performance criterion, J_{HF}, as:

$$J_{HF} = \left\| s^m \frac{T}{G} \right\|_\infty = \max_\omega \left| \omega^m K(j\omega)S(j\omega) \right| = \max_\omega \left| \omega^m S_u(j\omega) \right| \tag{2.20}$$

The motivation for weighting S_u with s^m is that $s^m S_u(j\omega) \to k_\infty$, as $\omega \to \infty$, so that the comparison between k_∞ and J_{HF}, i.e., between high frequency peak and high frequency asymptote, would help in determining whether the roll-off of $|S_u(j\omega)|$ is

inadequate or excessive. If the roll-off is inadequate, the controller can be augmented with an extra low-pass filter and made strictly proper ($m > 0$). However, [25] points out that if the roll-off is excessive, it could lead to the build-up of a resonance peak in $T(j\omega)$ just after the crossover frequency, which could lead to the degradation of the low frequency properties of the closed loop. With a second order filter, the roll-off of $|S_u(j\omega)|$ can be adjusted by varying the filter's damping ratio, ζ_f, which will be discussed in Chapter 3: the lower its value, the higher the roll-off and vice versa. Hence, J_{HF} can be used as a measure of how much additional roll-off can be included in a system without deterioration of its low frequency properties.

For a just proper controller, i.e., $m = 0$, (2.20) reduces to (2.17), so that $J_{HF} = J_u$. Therefore, in the case of the closed loop using a just proper first order filtered PID controller, J_u serves the same evaluative purpose as J_{HF}, making the first three criteria groups discussed above adequate for evaluating the various properties of this closed loop.

Using Process 3 in five closed loops, all with second order filtered PID controllers whose filter damping ratios vary from 0.21 to 0.93, the frequency response of $s^m S_u(j\omega)$ and $T(j\omega)$ are plotted for each closed loop, as shown in Figure 2.6. J_{HF} is indicated in each case. All the closed loops have $J_u = 5$ and $GM_S \leq 1.7$.

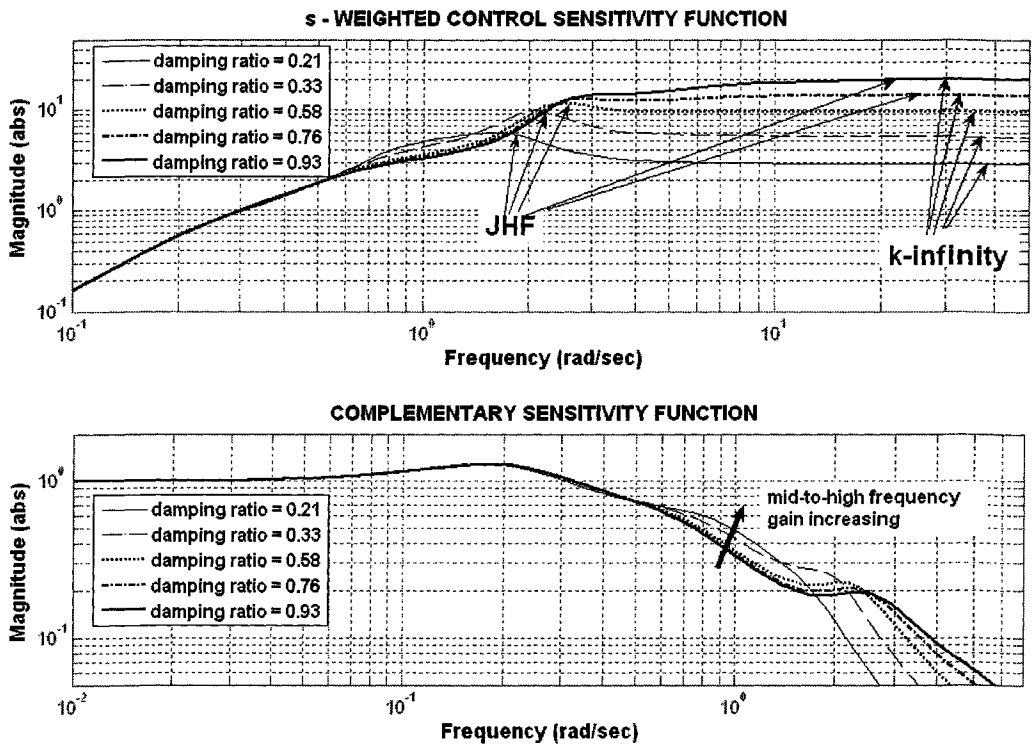

Figure 2.6: Frequency response of $s^m S_u(j\omega)$ and $T(j\omega)$ for closed loops using Process 3 with PID controllers (2nd order low-pass filters and varying damping ratios), showing the J_{HF} points for each closed loop and the k_∞ asymptote.

The above figure shows that for a high damping ratio, $s^m S_u(j\omega)$ has a high frequency peak that is approximately equal to k_∞. Therefore, $J_{HF} \approx k_\infty$. The roll-off of $S_u(j\omega)$ in this case may or may not be considered inadequate. Hence, the controller filter's damping ratio could be reduced for extra roll-off. However, the figure shows the effect of reducing the filter's damping ratio, J_{HF} becomes more significant compared to k_∞ to the extent that it is twice the value of the asymptote for a damping ratio of 0.21. In the plot of $T(j\omega)$, the gain is increasing, between mid-frequency and mid-to-high frequency regions, as the damping ratio is decreasing. The gain increase with decrease in damping ratio leads to the build-up of a resonance peak, which is considered inimical to the closed loop's high frequency robustness and low frequency performance.

It has thus been shown that the closer the J_{HF} value of a strictly proper control system to its k_∞ value, the wider the flexibility for increasing the roll-off of its high frequency controller gain and the less significant the effect of the filter augmentation on the system's low frequency characteristics. To strike a good balance between sufficient roll-off and good performance (both in the low and high frequencies), [25] recommends controller filter damping ratios of 0.4 to 0.5.

2.3.5 APPLICABILITY OF CRITERIA TO EVALUATION OF CONTROL SYSTEMS

When designing a controller, the design parameters must be specified. All the design parameters for a controller can collectively form a tuning vector ρ. In the PID controller, for example, ρ contains the controller gain, integral time constant, derivative time constant, and derivative filter constant. Using the four groups of evaluation criteria discussed in the preceding sections, an objective method of evaluating a control system in terms of its performance, robustness, or control activity can be formulated. This involves keeping three of the four criteria constant, or upper bound, and varying the elements of ρ until the fourth criterion has been favourably optimized. The method can be formulated as a constrained optimization procedure with ρ as the optimization variable vector.

For example, to design a controller whose closed-loop low frequency performance is optimized while keeping the stability and control activity constrained, the optimization problem can be formulated as:

$$\min_{\rho} \{J_V(\rho) : GM_S \le M_S, J_u \le C_u, J_{HF} \le C_{HF}\}, \tag{2.21}$$

where M_S, C_u, and C_{HF} are arbitrarily chosen constraints.

Throughout this thesis, any controller designed by solving (2.21) is referred to as an *optimal controller*. Other features of the evaluation method in [25] are its applicability to comparing different controller structures, comparing different

tuning methods used on the same controller structure, as well as studying the trade-off between any two properties in an individual controller.

The main purpose of this research is to design, simulate and experimentally implement optimal PI and PID controllers by solving (2.21) and secondly to study the performance-control activity trade-off for these control systems.

CHAPTER 3

DESIGN OF OPTIMAL PI AND PID CONTROLLERS

3.1 INTRODUCTION

Optimal PID and PI controllers can be designed using the evaluation criteria presented in Chapter 2. The design is based on the solution of a constrained optimization formulation, in which the low frequency performance criterion is optimized while specified constraints are imposed on the mid, mid-to-high, and high frequency robustness criteria of the control system.

In this chapter, the reformulation of the PI and PID controllers will first be discussed and the new design parameters are presented. Next, the design formulation for the optimal controllers will be discussed, with numerical examples presented for illustration.

The closed-loop response of the designed optimal controllers will be simulated and plotted to provide insight into the optimization design's controller tuning quality.

3.2 REFORMULATION OF THE PID CONTROLLER

The classical PID and PI controllers with the one-degree-of-freedom structure have the respective transfer functions:

$$K(s) = k_c\left(1 + \frac{1}{\tau_i s} + \tau_d s\right)$$
$$K(s) = k_c\left(1 + \frac{1}{\tau_i s}\right) \qquad (3.1)$$

where:

k_c is the proportional gain

τ_i is the integral time constant

τ_d is the derivative time constant

The PID controller's transfer function has the flaw of not being proper, and therefore unrealizable. To make the structure proper, the derivative part is augmented with a low-pass filter, which is a transfer function with a steady gain of one and is usually of first order with time constant τ_f. It could also be of higher order. Hence, the filtered PID controller is formulated as:

$$K(s) = k_c\left(1 + \frac{1}{\tau_i s} + \frac{\tau_d s}{\tau_f s + 1}\right) \tag{3.2}$$

The filter imposes a bound on the high frequency gain of the controller, which makes it applicable for the attenuation of high frequency measurement noise. According to [10], the derivative filter time constant τ_f is typically chosen as $\tau_f = \tau_d / N$, where N is in the range of 2 – 10. For Proportional-Derivative (PD) controllers, typical values of N fall between 5 and 20 [14], with 10 being the common choice. Kristiansson has shown in [13] that optimal PID controllers designed by solving (2.21) always have complex zeros and therefore reformulates the PID controller in (3.2) as:

$$K(s) = k_i\left(\frac{1 + 2\zeta\tau s + \tau^2 s^2}{s(1 + s\tau/\beta)}\right) \tag{3.3}$$

Hence, the new controller parameters are k_i(already defined in (2.7)), τ, ζ, β. (3.3) ensures that any PID controller having $\zeta < 1$ would have complex zeros. For an optimal PI controller, $\zeta = 1$, $\beta = 1$. Therefore:

$$K(s) = k_i\left(\frac{1 + \tau s}{s}\right) \tag{3.4}$$

From (3.3), the controller high frequency gain, k_∞, defined in (2.7), is given as:

$$k_\infty = k_i \tau \beta \tag{3.5}$$

For PID controllers used in some processes, measurement noise can be a considerable problem, e.g., level control in flow processes. With these systems, the roll-off of the controller's high-frequency gain offered by a first order low-pass filter might not be adequate for satisfactory noise attenuation. [13] proposes exchanging the PID controller's first order filter for a second order filter and formulates the controller structure as:

$$K(s) = k_i\left(\frac{1 + 2\zeta\tau s + \tau^2 s^2}{1 + 2\zeta_f \frac{\tau}{\beta} s + \frac{\tau^2}{\beta^2} s^2}\right) \tag{3.6}$$

(3.6) gives a PID controller with complex zeros and possibly complex poles. ζ_f is the damping ratio of the filter poles, which was briefly discussed in Chapter 2. Varying ζ_f has an effect on the roll-off of the control sensitivity function $S_u(j\omega)$ and hence on the control activity. The lower the ratio, the more effective the roll-off will be and, correspondingly, the lower the control activity. Using the process

and second order filtered PID controller in Example 2.3, the control sensitivity function is plotted for values of ζ_f ranging from 0.21 to 0.93 as shown in Figure 3.1.

However, an adverse effect occurs as the damping ratio is progressively reduced. For low values of ζ_f, a resonance peak is building up in the complementary sensitivity function $T(j\omega)$, also shown in Figure 3.1, which is not good for high frequency robustness or low frequency performance. The resonance peak occurs at frequencies above the phase crossover frequency. For an optimal balance of high frequency robustness and sufficient roll-off in the control sensitivity transfer function, [13] recommends ζ_f be set at 0.4 or 0.5 in the optimization procedure.

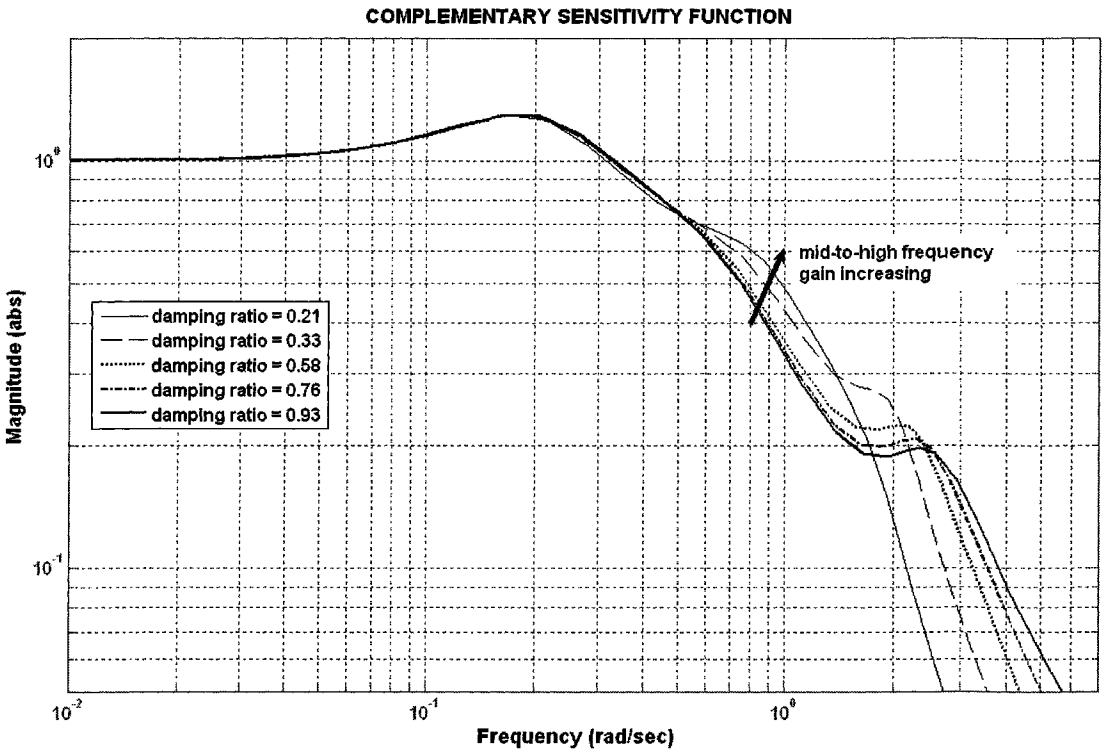

Figure 3.1: Frequency response of $T(j\omega)$ for closed loops using Process 3 with PID controllers (2^{nd} order low-pass filters and varying damping ratios), showing the build-up of a gain peak in the mid-to-high frequency region.

It must be noted that the controller high frequency gain k_∞ for the PID controller with a second order filter has an expression different from (3.5).

$$k_\infty = k_i \beta^2 \tag{3.7}$$

3.3 CONSTRAINED OPTIMIZATION FORMULATION FOR OPTIMAL PID CONTROLLERS WITH FIRST ORDER LOW-PASS FILTERS

Designing an optimal controller, whether PID (with first or second order filter) or PI, involves the solution of (2.21). In this section, an optimal PID controller with a first order filter will be designed, thus $J_{HF} = J_u$. In addition, [13] shows how for a PID controller with a first order filter, such as (3.3), the high frequency controller gain, k_∞, is approximately equal to J_u. Also, (3.5) relates the control activity criterion to the controller parameters, so that specifying a value for J_u (via k_∞) constrains one of the controller parameters, which reduces the number of optimization variables and reduces the time taken for (2.21) to converge at optimal values. [13] recommends a GM_S bound of 1.7; this value ensures that the control system's gain margin is at least 2.4 and the phase margin is at least 45°. Consequently, a GM_S constraint of 1.7 is used throughout this thesis. (2.21) can then be re-stated as:

$$\min_{\rho}\{J_V(\rho) : GM_S \le 1.7, k_\infty \le C_u\} \tag{3.8}$$

Once a constraint on k_∞ has been specified, (3.8) can be solved for $\rho = [k_i, \tau, \zeta, \beta]$.

Example 3.1 illustrates the design of an optimal PID controller with the pre-specification of GM_S and J_u.

Example 3.1: Consider the process:

$$\frac{e^{-3s}}{10s+1}$$

An optimal PID controller, with first order filtering, that meets the criteria: $GM_S \le 1.7$ and $J_u = 10$ will be designed for the process.

(3.8) thus becomes:

$$\min_{\rho}\{J_V(\rho) : GM_S \le 1.7, k_\infty = 10\} \tag{3.9}$$

The MATLAB Optimization Toolbox is used to solve (3.9) and will be used for all the constrained optimization functions formulated in this thesis. In order to compute the relevant sensitivity transfer functions in the objective functions, it is necessary to compute the Padé approximation of the time delay terms coming from the plant models. For the solution of all constrained optimizations in this thesis, the 4/4 Padé approximation of the time delay terms will be computed. Alternatively, the frequency response of the sensitivity transfer functions could be computed with the non-approximated delays in the transfer functions.

The optimal PID controller, with minimum J_v and which satisfies (3.9), is obtained with the following parameters:

Table 3.1: Parameters for Optimal PID Controller

$G(s)$	$\frac{e^{-3s}}{10s+1}$
k_∞	10
J_v	2.6302
J_u	9.9998
k_i	0.39503
τ	2.787
ζ	1.0769
β	9.0832
GM_S	1.7

Figure 3.2 shows the frequency response plots of the s^{-1}-weighted disturbance and control sensitivity functions for the optimized PID controller.

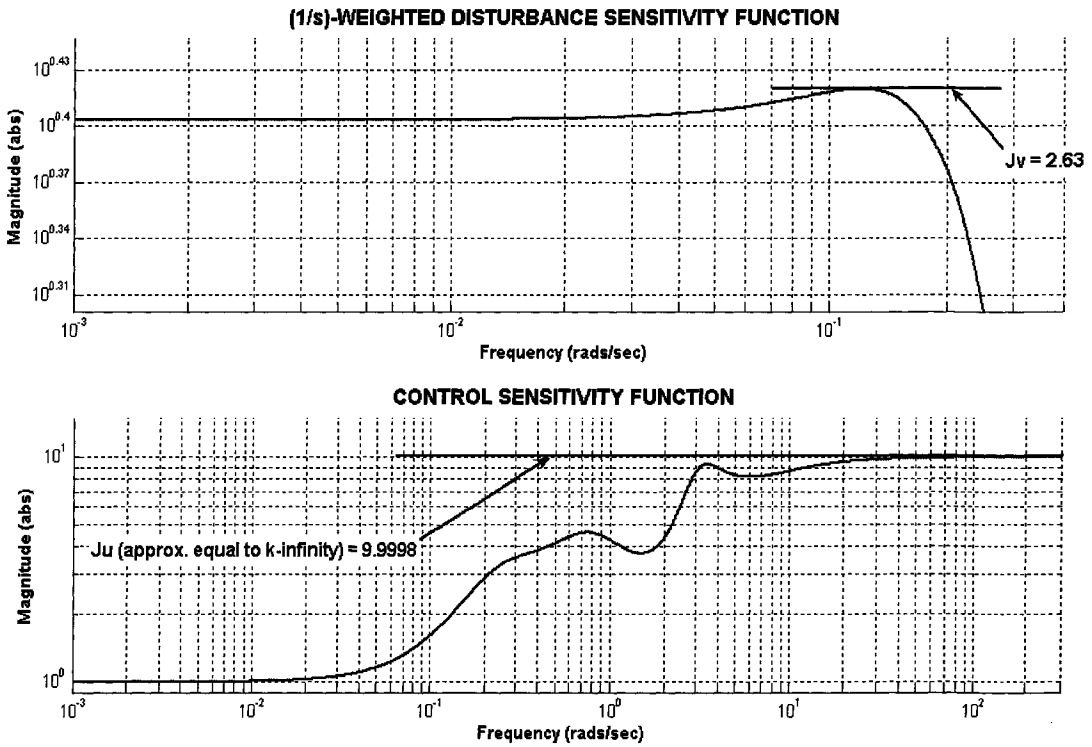

Figure 3.2: Frequency response of (1/s)-weighted disturbance sensitivity function and complementary sensitivity function using optimal PID controller; showing the J_v and J_u peaks respectively.

The closed loop is implemented in simulation using SIMULINK. Figure 3.3 shows the block diagram of the closed loop used for the simulation.

Figure 3.4 shows the closed loop's response to a step in the set point signal and the process input disturbance.

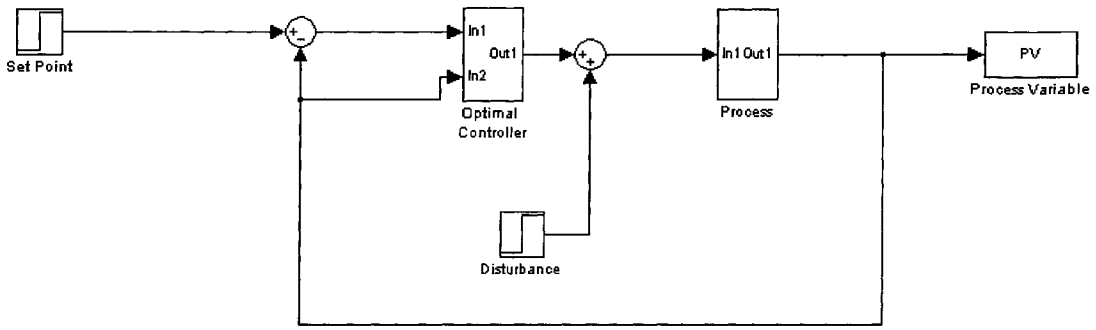

Figure 3.3: SIMULINK block diagram for simulation of closed loop response using optimal controller.

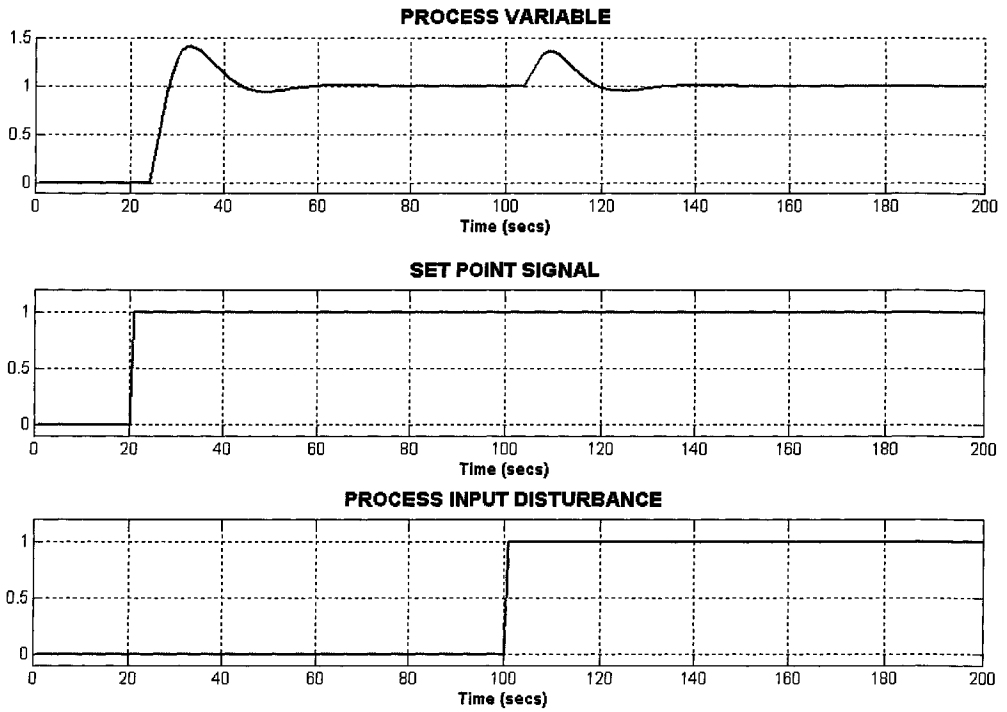

Figure 3.4: Closed-loop response of optimal PID controller to steps in set point signal and disturbance.

The process' disturbance response is satisfactory, but there is a significant overshoot in the set point tracking. This is to be expected because the PID controller designed is a J_V-optimal controller, which favours disturbance rejection. To improve the set point tracking performance of the closed loop, a J_r-optimal controller could be designed. However, as discussed in the previous chapter, J_r is plant dependent, making it less suitable than J_V as a performance criterion.

Alternatively, [25] recommends use of the J_V-optimal controller along with a pre-filter for the set point signal. Figure 3.5 shows the closed-loop block diagram with the addition of a pre-filter. Figure 3.6 shows the closed-loop response using the same process and controller as in Figure 3.4, as well as a first order set point pre-filter with the transfer function $\frac{1}{6s+1}$.

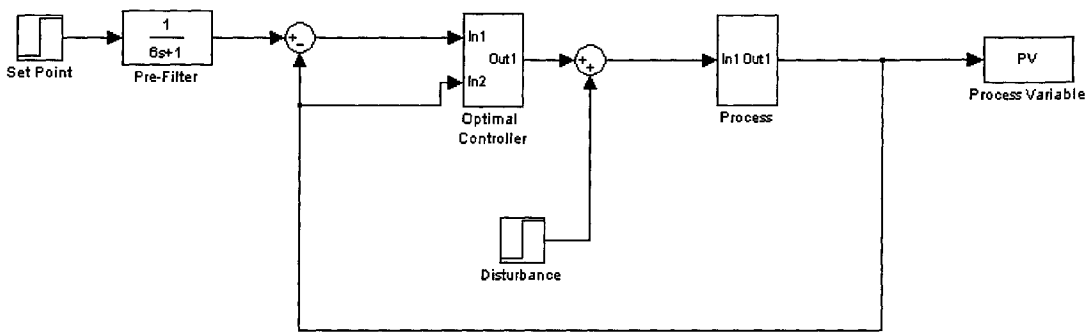

Figure 3.5: SIMULINK block diagram for simulation of closed-loop response using optimal PID controller and set point pre-filter.

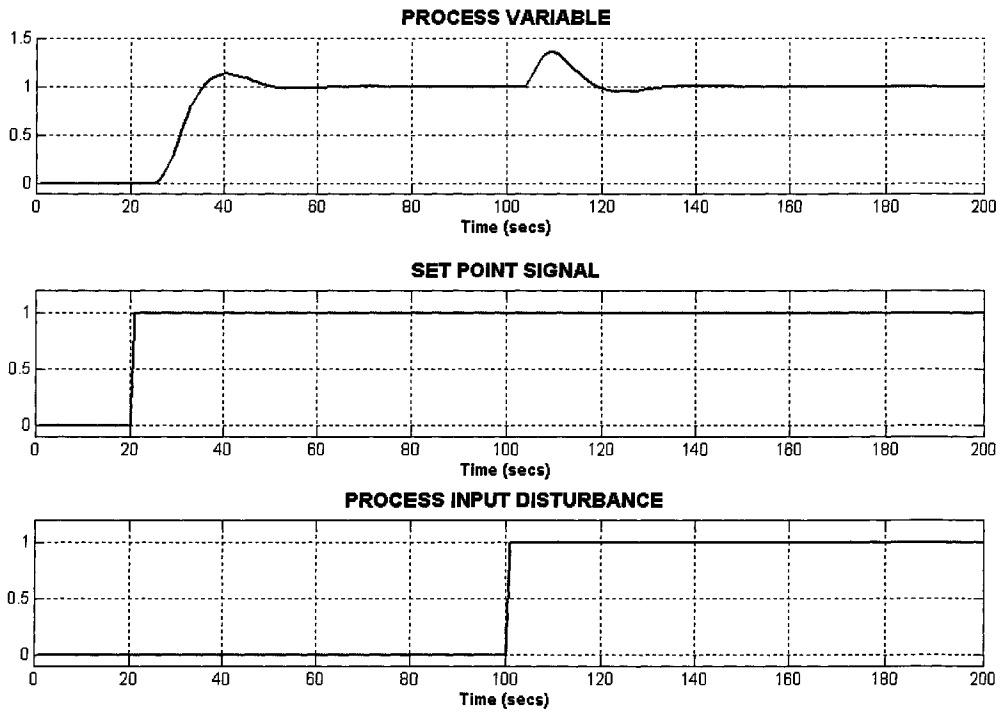

Figure 3.6: Closed-loop response of first order filtered optimal PID controller to steps in set point signal and disturbance with the use of set point pre-filter.

There is less overshoot with the use of the pre-filter for the set point signal, as can be seen in Figure 3.6. At the same time, the closed-loop response to the set point is slightly more sluggish than the unfiltered signal. The sluggish response becomes significant as the time constant of the pre-filter is increased, which

concomitantly suppresses the overshoot. Hence, in designing a set point pre-filter, a reasonable trade-off must be struck between the damping of the overshoot and the reduction in the tracking response speed of the closed loop.

3.4 CONSTRAINED OPTIMIZATION FORMULATION FOR OPTIMAL PI CONTROLLERS

The optimal PI controller is of the structure depicted in (3.4). Again, (2.21) is solved and, just as in the design of the optimal PID controller with a first order filter, $J_{HF} = J_u$. However, unlike the PID controller, the high frequency controller gain, k_∞, is not approximately equal to J_u. This can be seen in Figure 2.5, in which the control sensitivity gain increases to a peak (corresponding to J_u) slightly below the crossover frequency and then drops to the high frequency asymptote (k_∞). Thus, J_u would be constrained in (2.21), not k_∞ as was done for the PID controller. Also, GM_S would be bounded by a value of 1.7. In addition, ζ and β are both set to 1 for this controller, so that k_i and τ are the optimization variables in the tuning vector ρ. Hence, $\rho = [k_i, \tau]$.

Example 3.2 illustrates the design of an optimal PI controller with the pre-specification of GM_S and J_u.

Example 3.2: Consider the process:

$$\frac{e^{-3s}}{10s+1}$$

An optimal PI controller that meets the criteria: $GM_S \leq 1.7$ and $J_u = 1.5$ will be designed for the process.

(2.21) becomes:

$$\min_{\rho} \{J_V(\rho) : GM_S \leq 1.7, J_u = 1.5\} \tag{3.10}$$

The J_V-optimal controller designed has the following parameters:

Table 3.2: Parameters for Optimal PI Controller

$G(s)$	$\frac{e^{-3s}}{10s+1}$
k_∞	1.5
J_v	7.8794
J_u	1.5
k_i	0.12691
τ	6.8942
ζ	1
β	1
GM_S	1.3576

Figure 3.7 shows the frequency response plots of the s^{-1}-weighted disturbance and control sensitivity functions for the optimized PI controller.

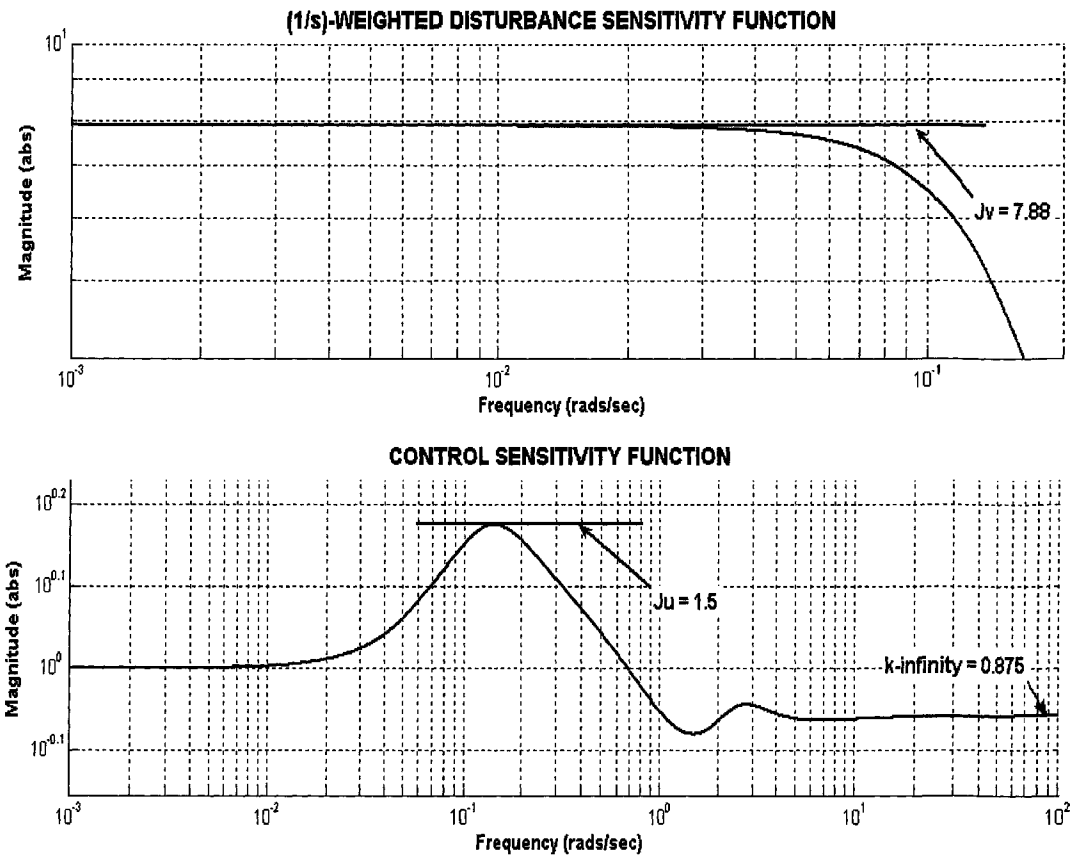

Figure 3.7: Frequency response of (1/s)-weighted disturbance sensitivity function and complementary sensitivity function using optimal PI controller, showing the J_v and J_u peaks respectively.

The closed-loop simulation response is shown in Figure 3.8. A set point pre-filter is not included in the closed loop.

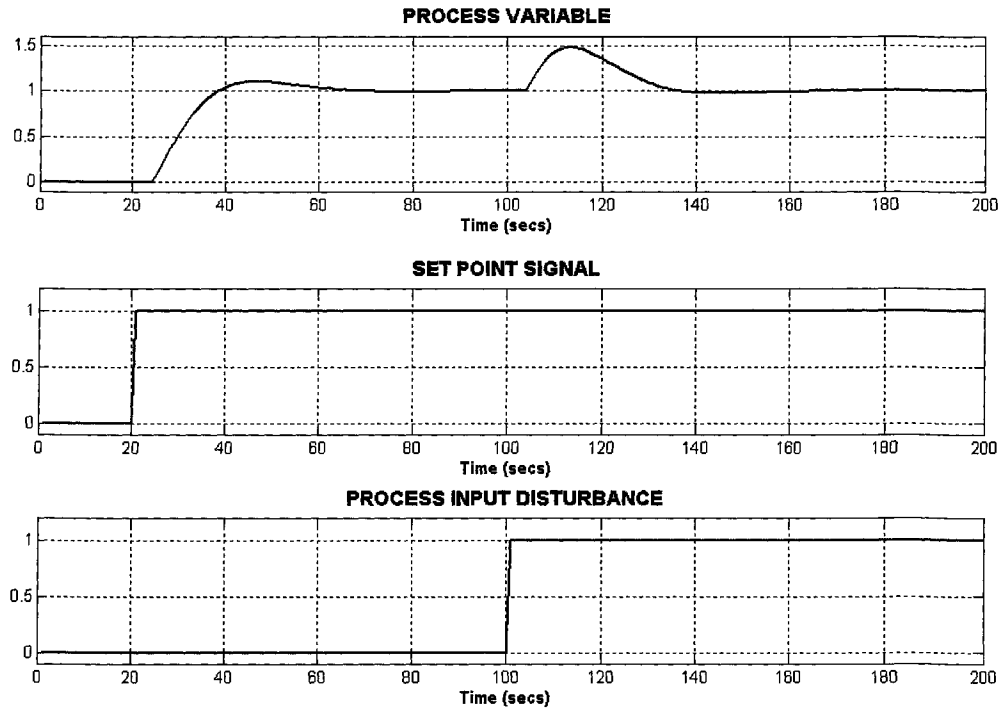

Figure 3.8: Closed-loop response of optimal PI controller to steps in set point signal and disturbance.

In Figure 3.7, the dissimilarity between k_∞ and J_u is shown, which is characteristic of the optimal PI controller. The GM_S value obtained is less than the constraint, indicating that the optimal PI controller is quite robust. In Figure 3.8, the closed-loop's set point response has a small overshoot, compared with the optimal PID's response in Figure 3.4, despite not using a pre-filter. However, the rejection of the step disturbance is slow. The optimal PI controller has a smaller integral gain k_i than the optimal PID, due to the difference in the J_u constraints imposed on the two controllers, and therefore has lower control action. Thus, the disturbance rejection performance of the optimal PI controller could be improved by increasing the value of its J_u constraint.

3.5 CONSTRAINED OPTIMIZATION FORMULATION FOR OPTIMAL PID CONTROLLERS WITH SECOND ORDER LOW-PASS FILTERS

The optimal PID controller with a second order filter is of the structure depicted in (3.6). Again, (2.21) is solved, but here $J_{HF} \neq J_u$, so that a separate constraint for J_{HF} would have to be specified. The high frequency gain of this controller is generally not asymptotic. With a second order filter it takes the form k_∞ / s, where

k_∞ is given by (3.7). In addition, (3.6) suggests an extra parameter, namely the filter's damping ratio ζ_f, should be included in the tuning vector ρ. Hence, $\rho = [k_i, \tau, \zeta, \beta, \zeta_f]$. Again, GM_S will be bounded by a value of 1.7. Therefore, the optimization of J_v, for the design of the strictly proper PID, requires more parameters than the PI and just proper PID controllers; thus, the computational duration before the optimization converges is longer. To enhance the design procedure's convergence, and perhaps shorten the computational duration, the optimized values of the parameters of a just proper PID, having the same J_u and GM_S values as the strictly proper PID, will be chosen as the initial values for ρ. ζ_f will be given an initial value of 0.4 based on the recommendation in [25].

Example 3.3 illustrates the design of an optimal PID controller with a second order low-pass filter. GM_S, J_u, and J_{HF} are pre-specified.

Example 3.3: Consider the process:

$$\frac{e^{-3s}}{10s+1}$$

An optimal PID controller, with second order filtering, that meets the criteria: $GM_S \leq 1.7$, $J_u = 5$, $J_{HF} \leq 11$.

(2.21) becomes:

$$\min_{\rho} \{J_v(\rho) : GM_S \leq 1.7, J_u = 5, J_{HF} \leq 11\} \tag{3.11}$$

The J_V-optimal controller obtained has the parameters presented in Table 3.3

Table 3.3: Parameters for Optimal PID Controller with Second Order Low-pass Filter

$G(s)$	$\frac{e^{-3s}}{10s+1}$
k_∞	7.0958
J_v	3.1563
J_u	5
J_{HF}	11
k_i	0.3303
τ	2.7835
ζ	1.1099
ζ_f	0.444
β	4.6347
GM_S	1.7

Figure 3.9 shows the frequency response plots of the s^{-1}-weighted disturbance and control sensitivity functions for the second order filtered optimized PID controller. Figure 3.10 shows the closed-loop response of the controller to steps in the set point and the disturbance.

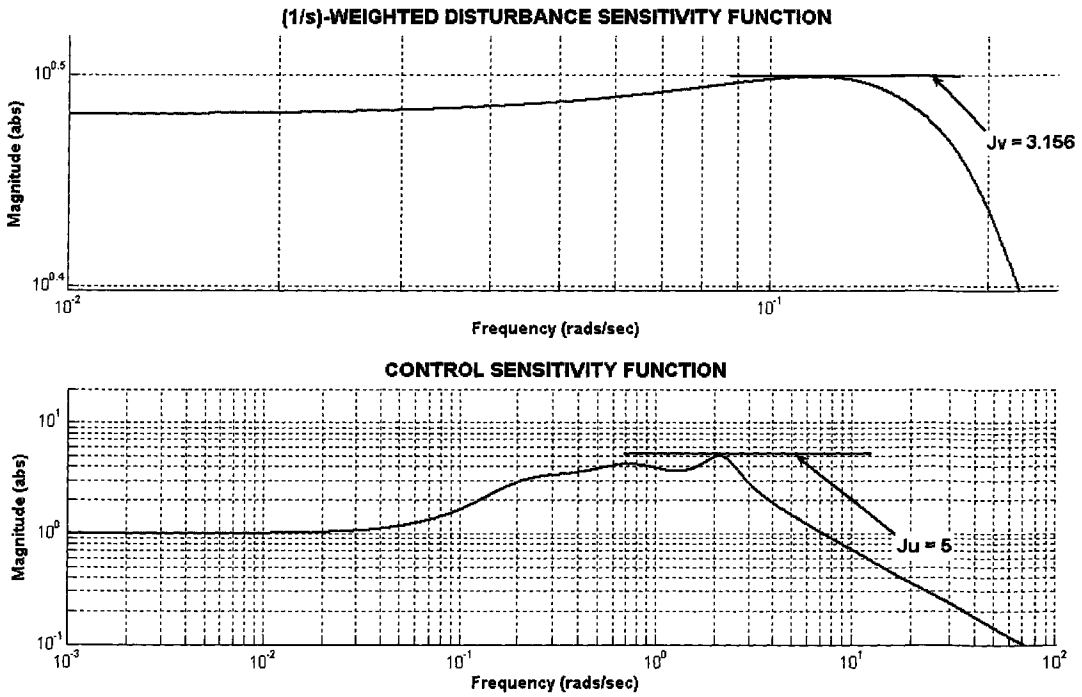

Figure 3.9: Frequency response of (1/s)-weighted disturbance sensitivity function and complementary sensitivity function using optimal PID controller with a second order filter, showing the J_v and J_u peaks respectively.

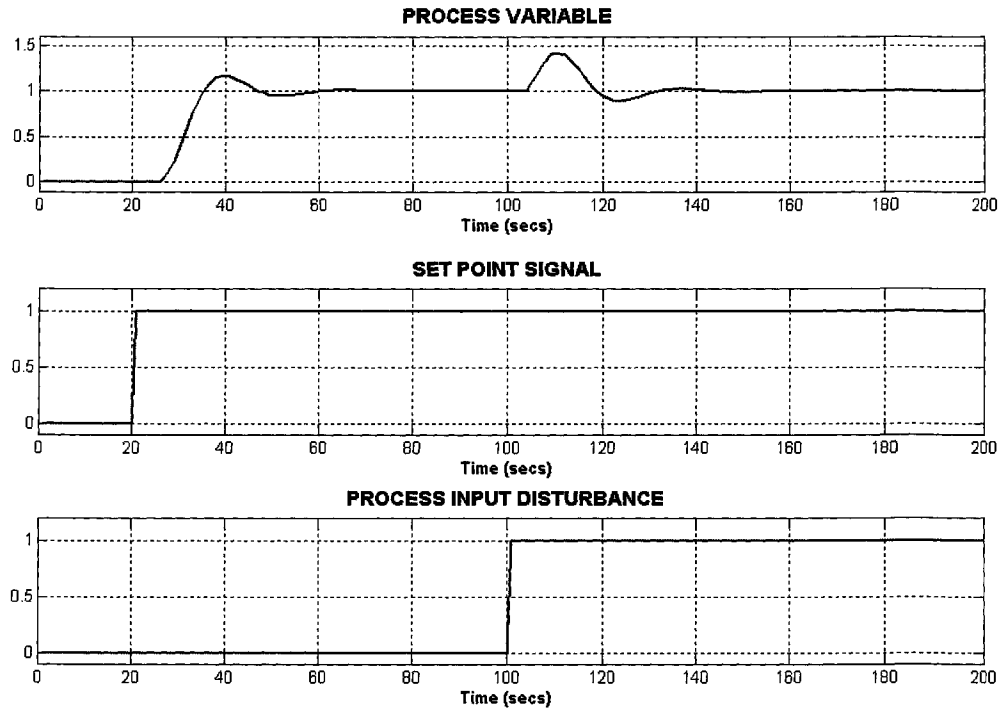

Figure 3.10: Closed-loop response of second order filtered optimal PID controller to steps in set point signal and disturbance.

CHAPTER 4

THE QUADRUPLE-TANK PROCESS

4.1 INTRODUCTION

The Quadruple-Tank Process serves as a laboratory-scale example of an interacting, multivariable process that can be controlled in a multiloop configuration. PI or PID controllers are usually used in multiloops; the controller tuning techniques in such configurations differ from the SISO control loop tuning methods due to loop interactions, which aren't taken into consideration in the latter methods. A popular multiloop controller design approach is to tune the controller for each loop as though all the loops were non-interacting, i.e., to assume the multiloop consists of decoupled SISO closed loops Each loop's PI/PID controller is tuned using typical SISO PID design methods. The loops in the multiloop are then closed and their controllers are de-tuned by trial and error to accommodate loop interactions, until the multiloop's performance becomes acceptable.

The main objective of this chapter is to present the design, simulation and implementation of PID controllers for the multiloop of the Quadruple-Tank Process using the control system evaluation method in [25], which has already been discussed and applied to SISO loop controller design in previous chapters. Because the evaluation method requires process models for the controller design procedure, the chapter will initially focus on the open-loop identification of linear, time-invariant models from sampled data of the process' response to pre-designed excitation signals. The computed models will form multivariable process matrices, the phase dynamics of which will also be discussed.

The Relative Gain Array method will be applied to the Quadruple-Tank's multiloop to determine which controller input/process output pairing is appropriate for the process' open-loop dynamics.

Finally, the multiloop's PID controllers, designed by applying a combination of a multiloop controller tuning method and solving the optimization procedure in (2.21), will be implemented experimentally and through simulation.

4.1.1 PROCESS DESCRIPTION

The Quadruple-Tank system consists of four equally-sized transparent tanks that have orifices. The system also has two water pumps and split-valves, which determine the distribution of flow into the tanks. The schematic diagram in Figure 4.1 illustrates the set-up of the four-tank system, showing the pumps, split valves and the inter-connection of the four tanks. A computer interface, consisting of the Emerson's Delta V hybrid DCS and MATLAB OPC DA Toolbox, facilitates the

performance of various experiments on the four-tank system, ranging from process identification to controller implementation.

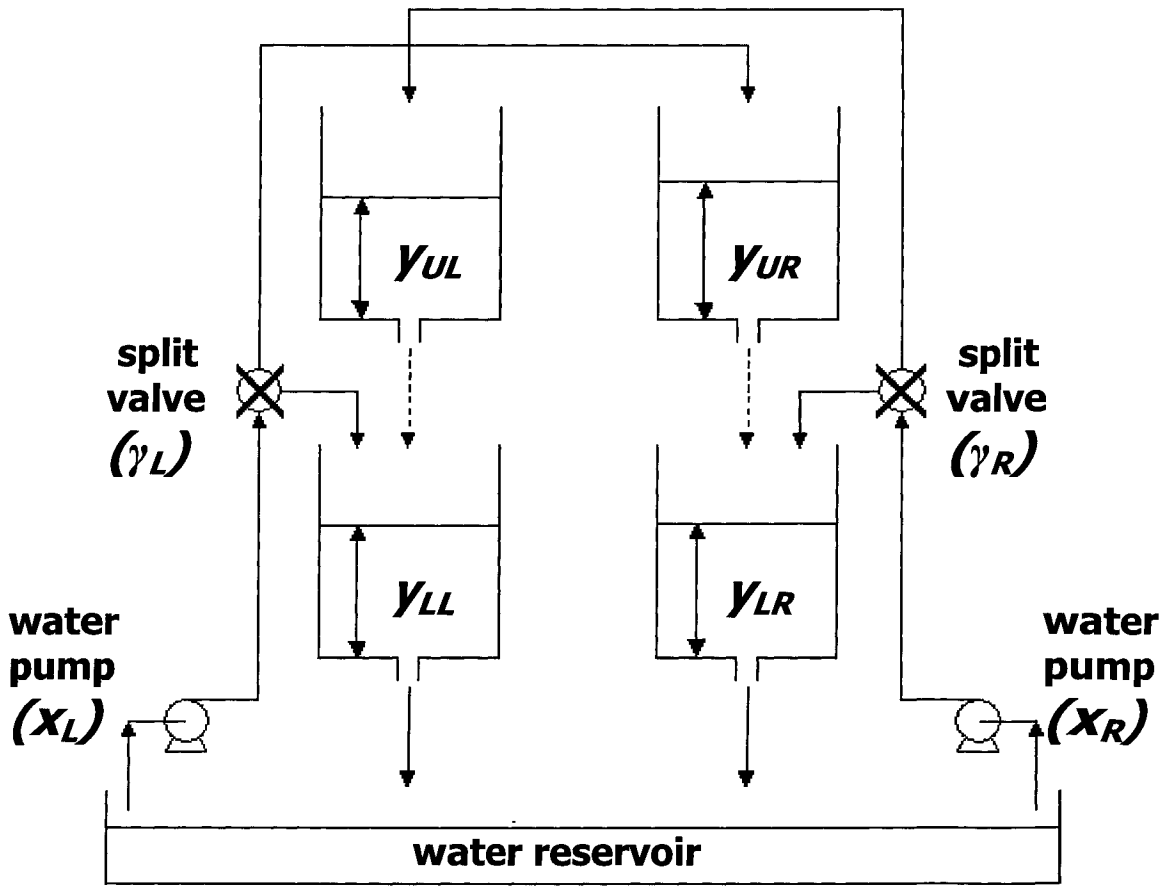

Figure 4.1: Process schematic of Quadruple-Tank Process.

y_{UL} = upper left tank water level
y_{UR} = upper right tank water level
y_{LL} = lower left tank water level (process output 1)
y_{LR} = lower right tank water level (process output 2)
x_L = left pump discharge rate (process input 1)
x_R = right pump discharge rate (process input 2)
γ_L = left split valve ratio
γ_R = right split valve ratio

The two pumps draw water from the reservoir. Depending on the fractional settings of the split valves, γ_L and γ_R (which are usually adjusted at the beginning of an experiment and held fixed throughout), the flow from each pump is split between the closer lower tank and an upper tank diagonally above the lower tank as shown by the solid arrows. In addition to the apportioned flow from the pump, each lower tank also receives water flowing out from the tank vertically above it

as shown by the dashed arrows. The outflows from the lower tanks are discharged to the water reservoir. Thus, the process is cyclic. The input variables are the pump discharge rates, u_L and u_R, and the output variables are the water levels in the lower left and right tanks, h_{LL} and h_{LR} respectively. Based on the physical dynamics of the process, the water level in each lower tank is a function of the flow input from both pumps and the split valve settings.

MATLAB OPC DA Client makes it possible to construct the input sequences for left and right pump discharge rates, feed them to the system, and record the input and output data. The Delta V DCS provides the interface between the OPC DA Client and the physical system.

Assuming the influence of the pump dynamics on the discharge rates is negligible, mass balances and the Torricellian Law can be used to formulate the linear, time-invariant, multivariable transfer function of the system's input to output variables as:

$$\begin{bmatrix} h_{LL} \\ \\ h_{LR} \end{bmatrix} = G(s) \cdot \begin{bmatrix} u_L \\ \\ u_R \end{bmatrix}$$

$$G(s) = \begin{bmatrix} \dfrac{K_{LL}^{L} e^{-T_{dLL,L}s}}{\tau_{LL}s+1} & \dfrac{K_{LL}^{R} e^{-T_{dLL,R}s}}{(\tau_{LL}s+1)(\tau_{UL}s+1)} \\ \dfrac{K_{LR}^{L} e^{-T_{dLR,L}s}}{(\tau_{LR}s+1)(\tau_{UR}s+1)} & \dfrac{K_{LR}^{R} e^{-T_{dLR,R}s}}{\tau_{LR}s+1} \end{bmatrix} \qquad (4.1)$$

where:

h_i = deviational height of water level in tank i, i.e. $y_j - y_{jo}$; subscript $i = \{LL, LR, UL, UR\}$

u_j = deviational discharge flow-rate of pump j

v_o = nominal value of variable v; $v = \{u_L, u_R, h_{LL}, h_{LR}, h_{UL}, h_{UR}\}$

u_j = $x_j - x_{jo}$; subscript $j = \{L, R\}$

K_i^j = level gain for tank i from pump j; subscript $i = \{LL, LR, UL, UR\}$; superscript $j = \{L, R\}$

τ_i = time constant for tank i

T_{dij} = response time delay of tank i to pump j

γ_j = split fraction of flow from pump j

C_i = coefficient of discharge for the orifice of tank i

According to [1],

$$K_i^j = f(\gamma_j, h_{io})$$

τ_i = $f(h_{io}, C_i,$ tank i dimensions)

4.1.2 MULTIVARIABLE ZERO

According to [1], the zeros of the transfer matrix in (4.1) are the zeros of the numerator polynomial of the rational function:

$$det[G(s)] = \frac{K_{LR}^R K_{LL}^L e^{-(T_{dLL,L}+T_{dLR,R})s}}{(\tau_{LL}s+1)(\tau_{LR}s+1)} - \frac{K_{LL}^R K_{LR}^L e^{-(T_{dLR,L}+T_{dLL,R})s}}{(\tau_{LL}s+1)(\tau_{LR}s+1)(\tau_{UR}s+1)(\tau_{UL}s+1)} \quad (4.2)$$

Typically, for quadruple-tank processes,

$\tau_i >> T_{dij}$; subscript i = {LL, LR, UL, UR}, superscript j = {L, R};

Thus, the process is time-constant dominated so that the time delay terms can be dropped from the function, and it becomes:

$$det[G(s)] \approx \frac{K_{LR}^R K_{LL}^L}{(\tau_{LL}s+1)(\tau_{LR}s+1)} - \frac{K_{LL}^R K_{LR}^L}{(\tau_{LL}s+1)(\tau_{LR}s+1)(\tau_{UR}s+1)(\tau_{UL}s+1)} \quad (4.3)$$

$$= K_{LR}^R K_{LL}^L \prod_{i=UL,UR,LL,LR} \left(\frac{1}{\tau_i s+1}\right)\left[(\tau_{UL}s+1)(\tau_{UR}s+1) - \left(\frac{K_{LL}^R K_{LR}^L}{K_{LR}^R K_{LL}^L}\right)\right]$$

The zeros of the numerator polynomial of (4.3) are the two zeros of the quadratic equation:

$$(\tau_{UL}s+1)(\tau_{UR}s+1) - \left(\frac{K_{LL}^R K_{LR}^L}{K_{LR}^R K_{LL}^L}\right) = 0 \quad (4.4)$$

4.1.3 MINIMUM PHASE DYNAMICS

According to [1], $G(s)$ follows minimum phase dynamics if the two zeros from (4.4) both lie on the left half plane. This condition is met if:

$$(\tau_{UL}+\tau_{UR})^2 > (\tau_{UL}+\tau_{UR})^2 - 4(\tau_{UL}\tau_{UR})\left(1 - \frac{K_{LL}^R K_{LR}^L}{K_{LR}^R K_{LL}^L}\right)$$

$$\Rightarrow 1 - \frac{K_{LL}^R K_{LR}^L}{K_{LR}^R K_{LL}^L} > 0$$

$$\Rightarrow K_{LR}^R K_{LL}^L > K_{LL}^R K_{LR}^L$$

$$\Rightarrow K_{LR}^{R}(\gamma_R)K_{LL}^{L}(\gamma_L) > K_{LL}^{R}(\gamma_R)K_{LR}^{L}(\gamma_L) \tag{4.5}$$

4.1.4 NON-MINIMUM PHASE DYNAMICS

G(s) follows non-minimum phase dynamics if one of the zeros from (4.4) lies on the right half plane. The process follows such dynamics if:

$$(\tau_{UL}+\tau_{UR})^2 < (\tau_{UL}+\tau_{UR})^2 - 4(\tau_{UL}\tau_{UR})\left(1-\frac{K_{LL}^{R}K_{LR}^{L}}{K_{LR}^{R}K_{LL}^{L}}\right)$$

$$\Rightarrow K_{LR}^{R}(\gamma_R)K_{LL}^{L}(\gamma_L) < K_{LL}^{R}(\gamma_R)K_{LR}^{L}(\gamma_L) \tag{4.6}$$

Assuming the coefficients of discharge are 1 so that the Torricellian law becomes the Bernoulli law, the minimum phase condition in (4.5) can be restated as:

$$1 < \gamma_L + \gamma_R < 2 \tag{4.7a}$$

Also, the non-minimum phase condition in (4.6) can be restated as:

$$0 < \gamma_L + \gamma_R < 1 \tag{4.7b}$$

Thus, the split valve settings determine whether the process is minimum phase or non-minimum phase. Because the transfer function matrix in the minimum phase is diagonally dominant, it is intuitively preferable to control the lower left tank level, h_{LL}, using the left pump flow rate, u_L, and similarly preferable for the lower right tank level and right pump flow rate. With the transfer function matrix in the non-minimum phase being anti-diagonally dominant, input-output pairing rules converse to the minimum phase's are preferable. The Relative Gain Array Method [45] will be later applied to the transfer function matrices of the two phases to confirm the input-output pairing rules.

For this identification experiment, two pairs of split valve settings are chosen such that a model for each phase can be computed.

4.2 PROCESS IDENTIFICATION

4.2.1 EXCITATION EXPERIMENT

An excitation experiment is performed on the Quadruple-Tank Process to obtain the relationship between the inputs (pump flow rates) and the outputs (tank water levels). The following steps are performed:

i. The split fractions of the left and right pump flows are set in accordance with the desired level of interaction between the two flows on the lower tanks. The choice of interaction levels for the excitation experiments will be discussed in the next section.

ii. Positive and negative step tests of various magnitudes are performed to determine a linear range around the nominal point of each lower tank level.

iii. From the step test results, the excitation frequency ranges of interest are determined and Random Binary Sequence (RBS) input sequences are designed accordingly.

iv. The RBS input signals are applied to one pump at a time, while the other pump is kept at a constant nominal discharge rate, so the level response of both tanks to each pump input can be sampled separately.

v. Using the sampled data of the level responses, discrete-time models are computed using the *pem* function in MATLAB.

Applying the *idproc* function – also in MATLAB – converts the discrete-time models into continuous-time models while imposing the model structures in (4.1).

4.2.2 STEP TEST RESULTS AND EXCITATION SIGNAL DESIGNS

Several step test magnitudes were performed. However, good signal-to-noise ratios and approximately linear level dynamics were obtained with perturbations of ± **1 L/min,** and using nominal input flowrates of **18 L/min** and **18 L/min** respectively for the left (split valve set at 73%:27% split) and right (split valve set at 72%:28% split) pumps for the minimum phase experiments; and **13 L/min** and **12 L/min** respectively for the left (split valve set at 28%:72% split) and right (split valve set at 30%:70% split) pumps for the non-minimum phase experiments. Step test results for the lower left tank level are shown in Figure 4.2. Sampling period, $\mathbf{t_s}$, was **1 second** for the excitation experiments. The level response data were thereafter down-sampled to **10 seconds** for the model computations.

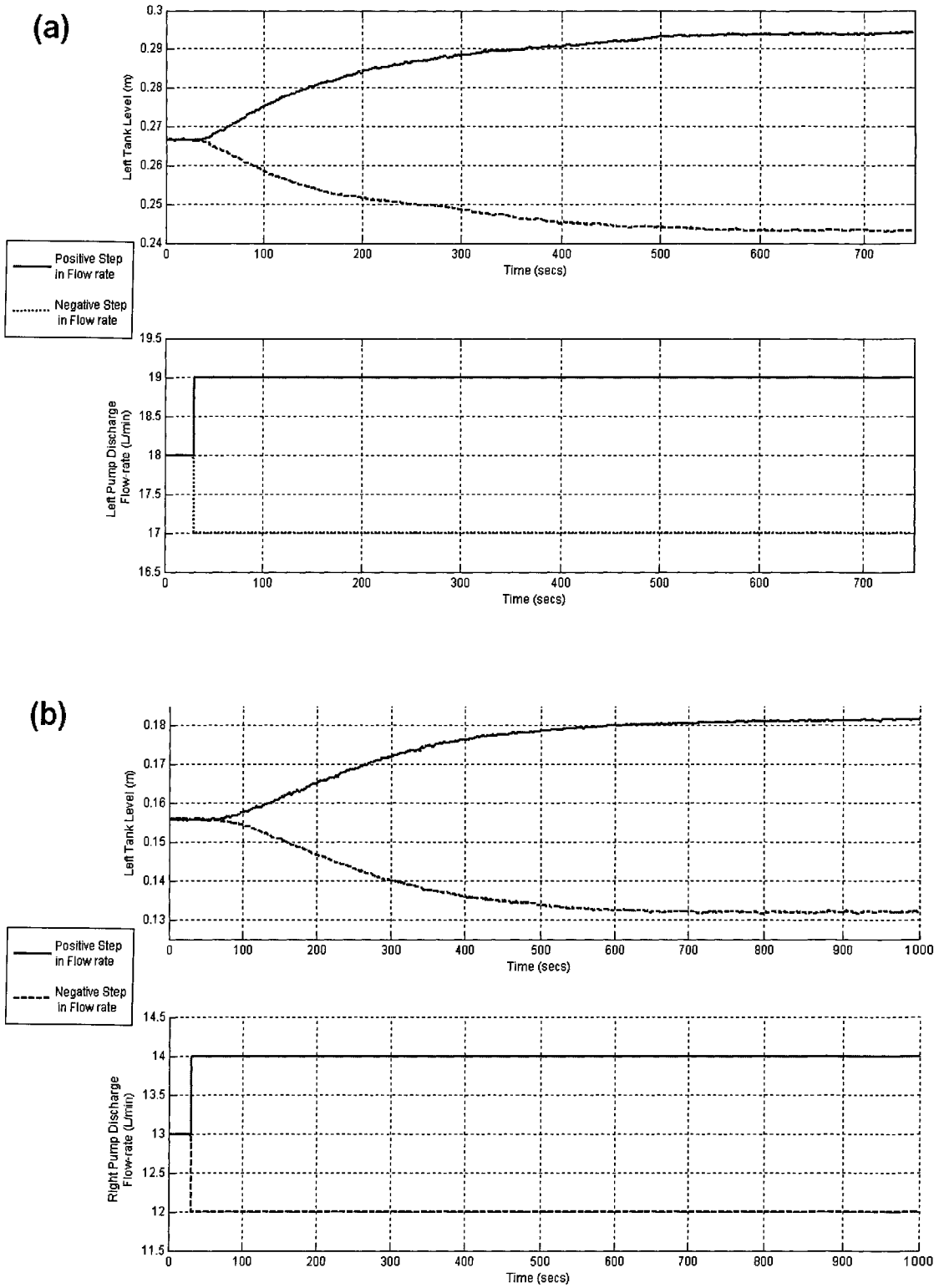

Figure 4.2: Level responses of the lower left tanks to positive (solid) and negative (dashed) step inputs in the minimum (a) and non-minimum (b) phases.

The step response data were used to compute parameter estimates for first order model approximations to determine the appropriate Nyquist frequency ranges to specify for the Random Binary Sequences (RBS), to be used for exciting the system. Dynamic data obtained from these tests are presented in Table 4.1.

Table 4.1: 1st Order Approximation Constants from the Step Tests

Process Dynamics	Gain (m-min/L)	Time constant (sec)	Time delay (sec)
Minimum Phase	0.0274	157.2	6.6
Non-Minimum Phase	0.0255	231	39

Using the approximate time constants from Table 4.1, the following Nyquist frequency bands of interest were determined: 0 - 0.05 (minimum phase) and 0 - 0.01 (non-minimum phase). A smaller Nyquist frequency band was used for the non-minimum phase excitation because of its higher time constant, which meant more time was required for the level response to attain steady state. Consequently, an input signal of lower frequency was designed with sampling time of 1 sec.

Table 4.2: RBS Inputs used for Process Dynamics Identification (sampling rate = 1 sec)

Process Dynamics	Nyquist Frequency band	Levels (L/min)	# of input points
Minimum Phase	0 to 0.05	±1.0	18071
Non-Minimum Phase	0 to 0.01	±1.0	24861

4.2.3 LEVEL RESPONSES AND MODEL COMPUTATION

The left and right pumps were sequentially excited with the designed RBS signals for both phases. Figures 4.3(a), 4.3(b), 4.4(a), and 4.4(b) show the level responses of the lower left and right tank levels to the excitations, as well as the input signals, for the minimum phase and non-minimum phase dynamics.

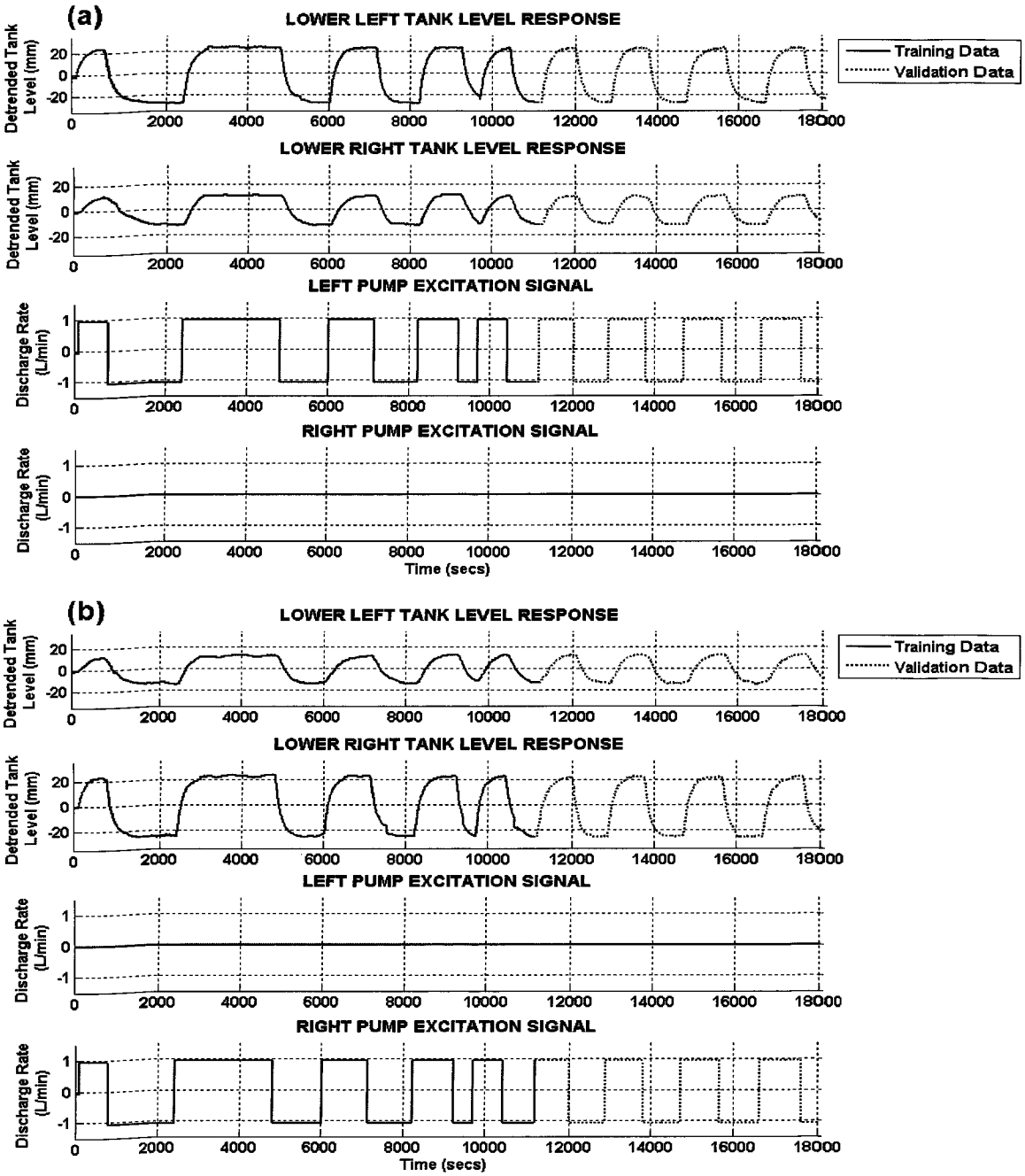

Figure 4.3: Minimum phase responses of the lower tank levels to RBS excitation inputs applied to (a) left Pump, and (b) right pumps.

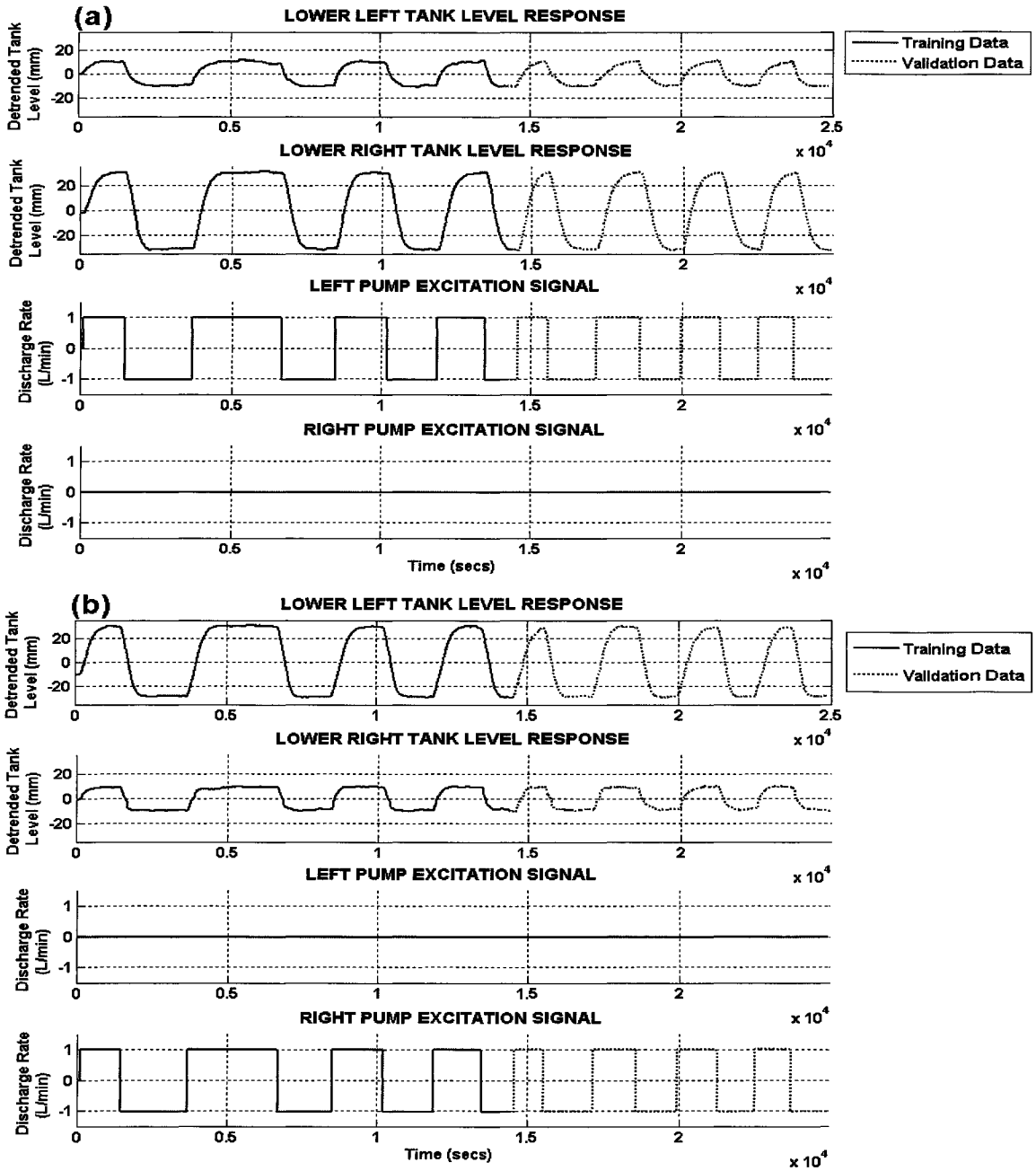

Figure 4.4: Non-minimum phase responses of the lower tank levels to RBS excitation inputs applied to (a) left pump, and (b) right pumps.

4.2.3.1 MINIMUM PHASE COMPONENT MODELS

a) *Left Pump to Lower Left Tank Model - $G_{min}(1,1)$*

Model Structure: $\dfrac{Ke^{-T_d s}}{\tau s + 1}$

K = 25.944 mm-min/L

τ = 155 secs
T_d = 5.0004 secs

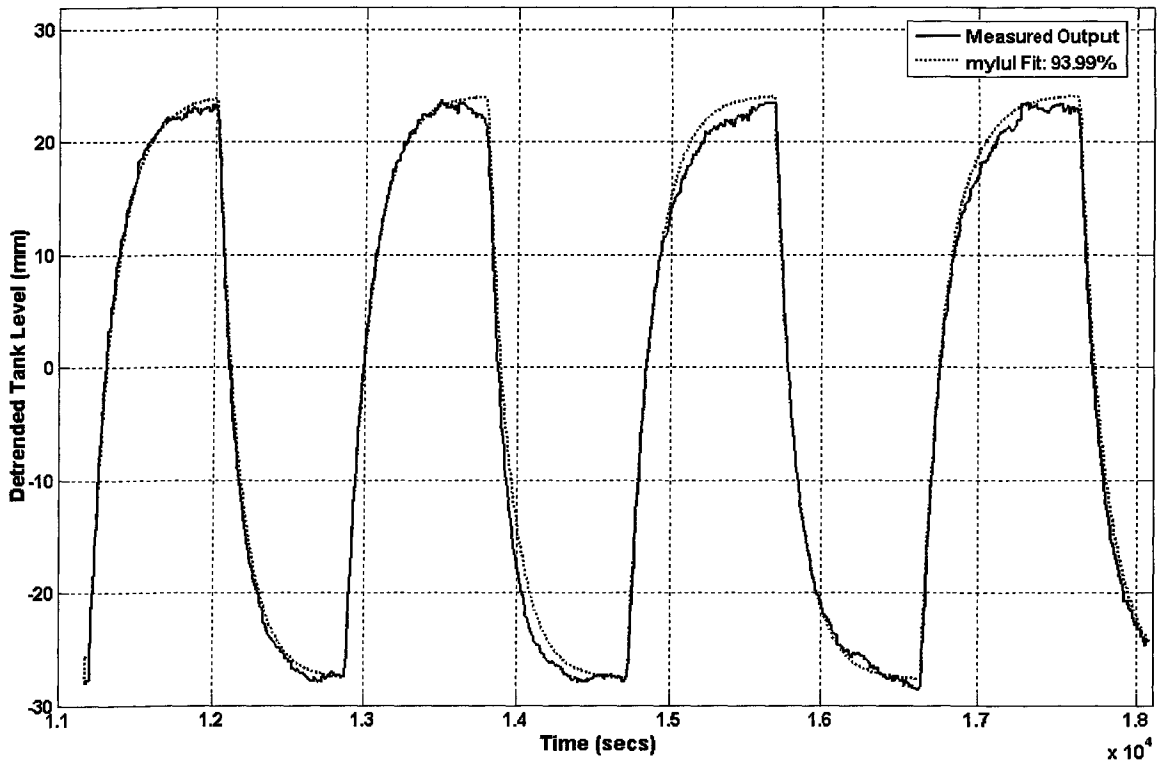

Figure 4.5(a): Validation of continuous-time model for component transfer function $G_{min}(1,1)$.

b) *Left Pump to Lower Right Tank Model - $G_{min}(2,1)$*

Model Structure: $\dfrac{Ke^{-T_d s}}{\tau_1 \tau_2^2 s^2 + (\tau_1 + \tau_2)s + 1}$

K = 11.478 mm-min/L
τ_1 = 117.55 secs
τ_2 = 117.55 secs
T_d = 10.274 secs

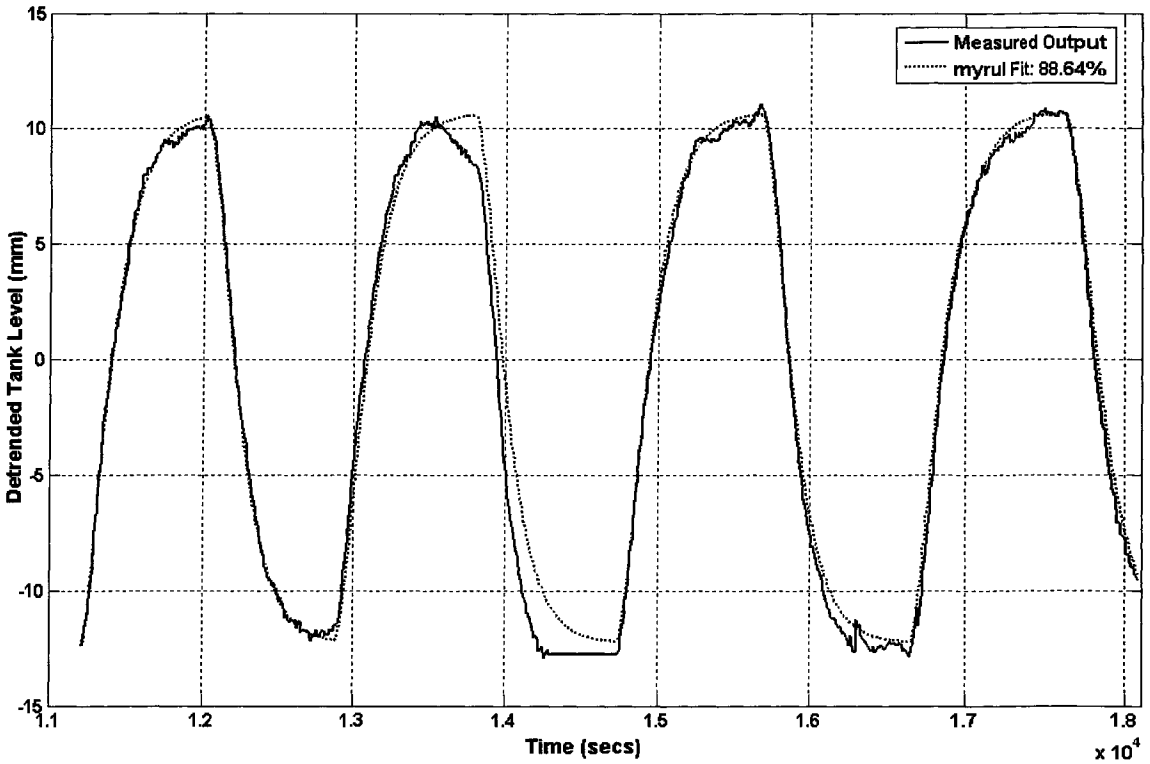

Figure 4.5(b): Validation of continuous-time model for component transfer function $G_{min}(2,1)$.

c) *Right Pump to Lower Left Tank Model - $G_{min}(1,2)$*

Model Structure: $\dfrac{Ke^{-T_d s}}{\tau^2 s^2 + 2\tau\zeta s + 1}$

K = 12.932 mm-min/L
τ = 127.33 secs
ζ = 1.0204 secs
T_d = 15.921 secs

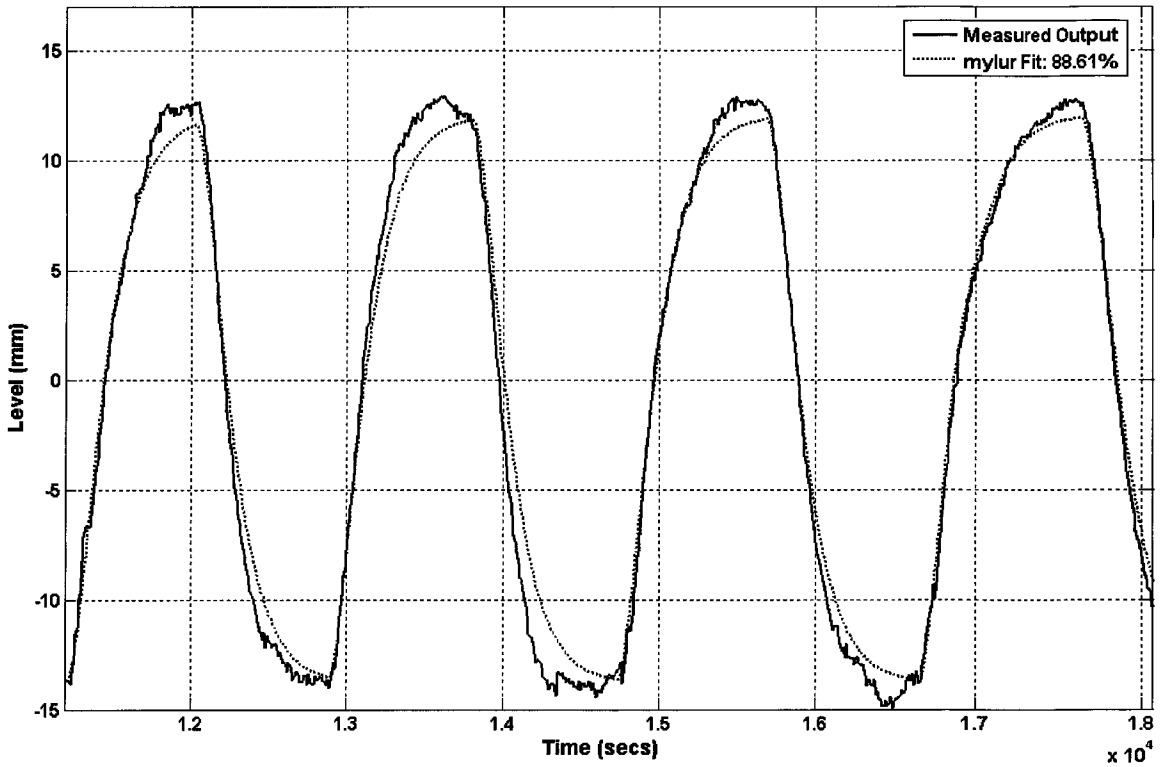

Figure 4.5(c): Validation of continuous-time model for component transfer function $G_{min}(1,2)$.

d) *Right Pump to Lower Right Tank Model - $G_{min}(2,2)$*

Model Structure: $\frac{Ke^{-T_d s}}{\tau s + 1}$

K = 23.933 mm-min/L
τ = 145.05 secs
T_d = 5.8182 secs

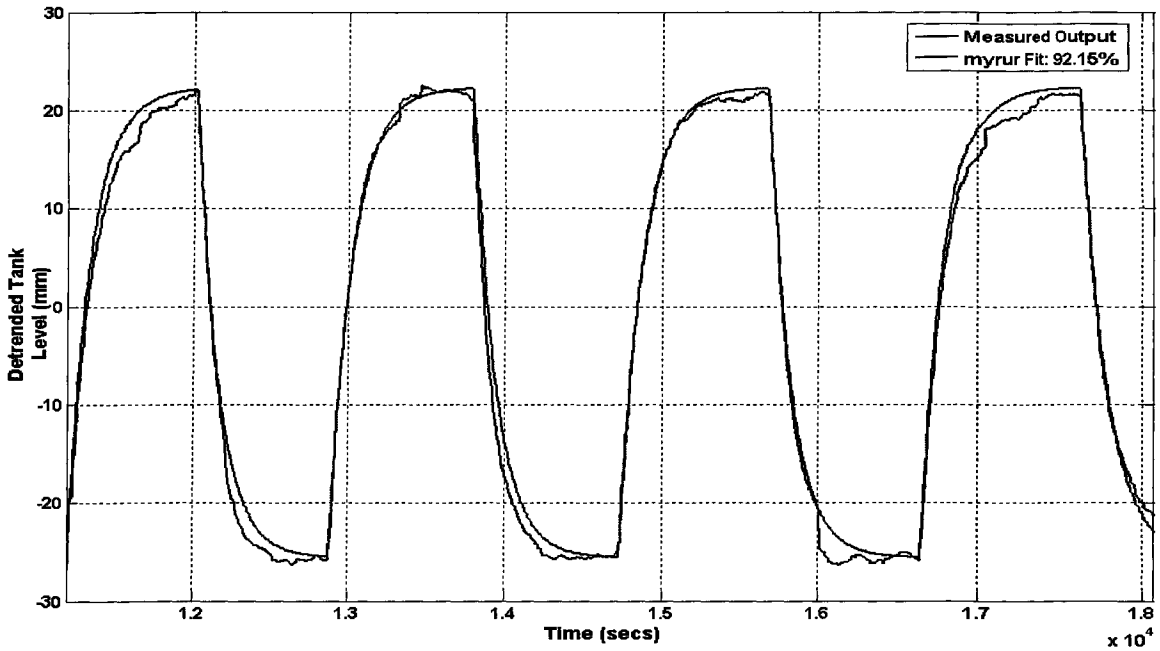

Figure 4.5(d): Validation of continuous-time model for component transfer function $G_{min}(2,2)$.

4.2.3.2 NON-MINIMUM PHASE COMPONENT MODELS

a) *Left Pump to Lower Left Tank Model - $G_{nonmin}(1,1)$*

Model Structure: $\dfrac{Ke^{-T_d s}}{\tau s + 1}$

K = 10.061 mm-min/L
τ = 200.56 secs
T_d = 4.1318 secs

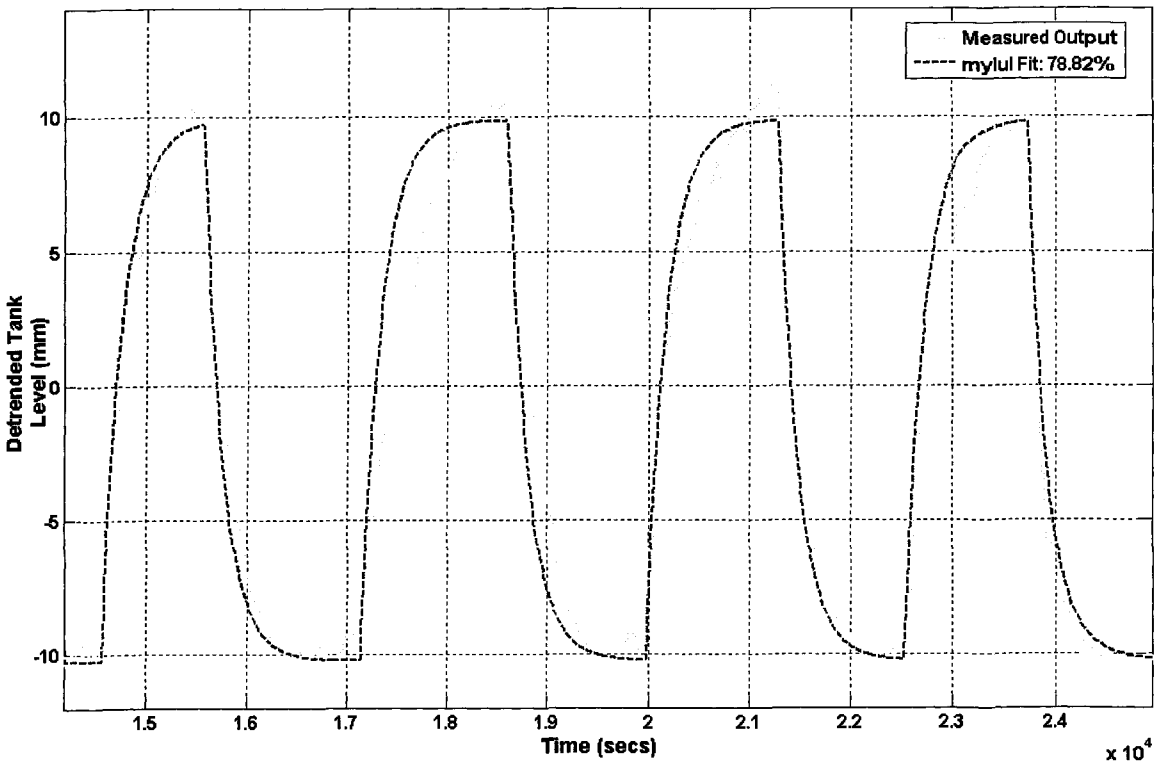

Figure 4.6(a): Validation of continuous-time model for component transfer function $G_{nonmin}(1,1)$.

b) *Left Pump to Lower Right Tank Model - $G_{nonmin}(2,1)$*

Model Structure: $$\frac{Ke^{-T_d s}}{\tau_1\tau_2 s^2 + (\tau_1 + \tau_2)s + 1}$$

K = 31.044 mm-min/L
τ_1 = 153.3 secs
τ_2 = 144.19 secs
T_d = 33.517 secs

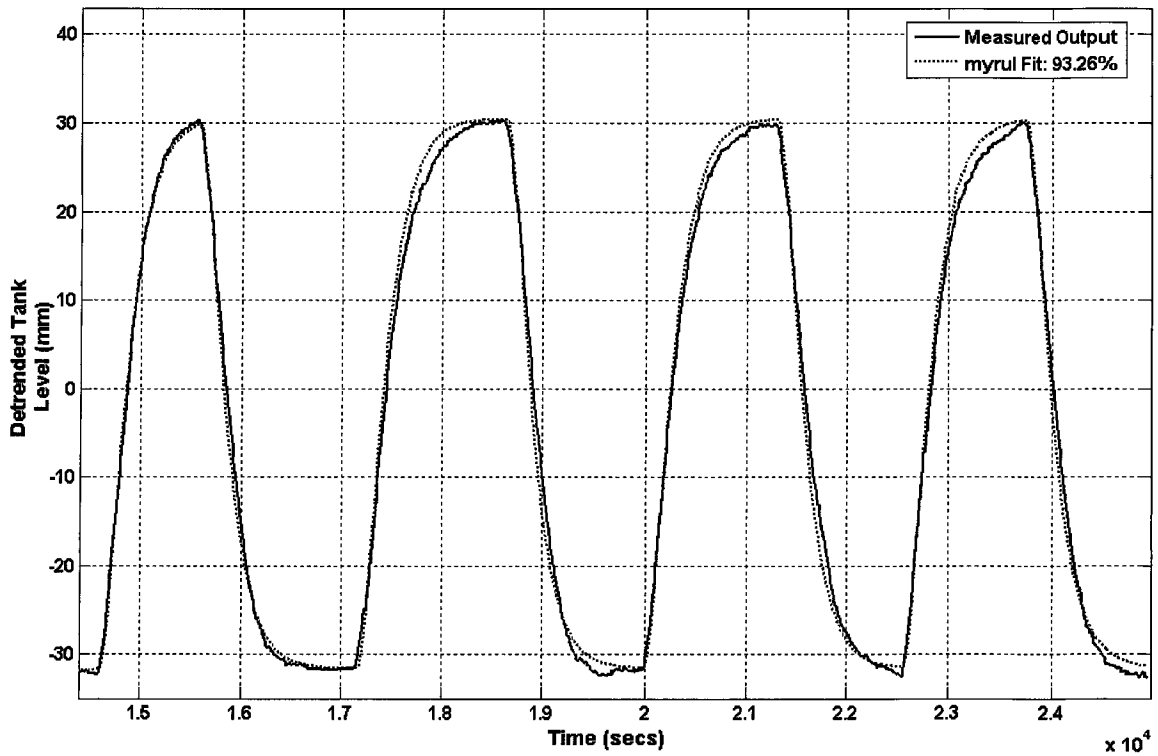

Figure 4.6(b): Validation of continuous-time model for component transfer function $G_{nonmin}(2,1)$.

c) *Right Pump to Lower Left Tank Model - $G_{nonmin}(1,2)$*

Model Structure: $$\frac{Ke^{-T_d s}}{\tau_1\tau_2 s^2 + (\tau_1 + \tau_2)s + 1}$$

K = 28.596 mm-min/L
τ_1 = 150.86 secs
τ_2 = 150.86 secs
T_d = 24.116 secs

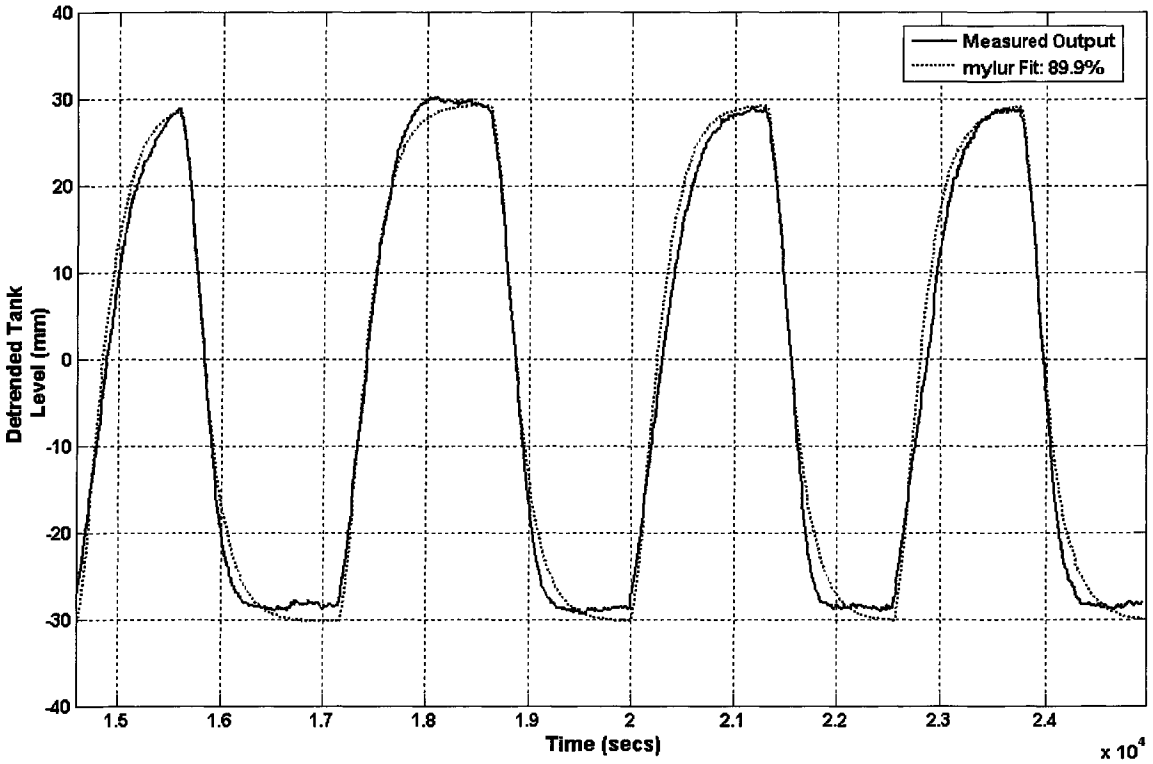

Figure 4.6(c): Validation of continuous-time model for component transfer function $G_{nonmin}(1,2)$.

d) *Right Pump to Lower Right Tank Model - $G_{nonmin}(2,2)$*

Model Structure: $\frac{Ke^{-T_d s}}{\tau s + 1}$

K = 9.2785 mm-min/L
τ = 124.24 secs
T_d = 9.2746 secs

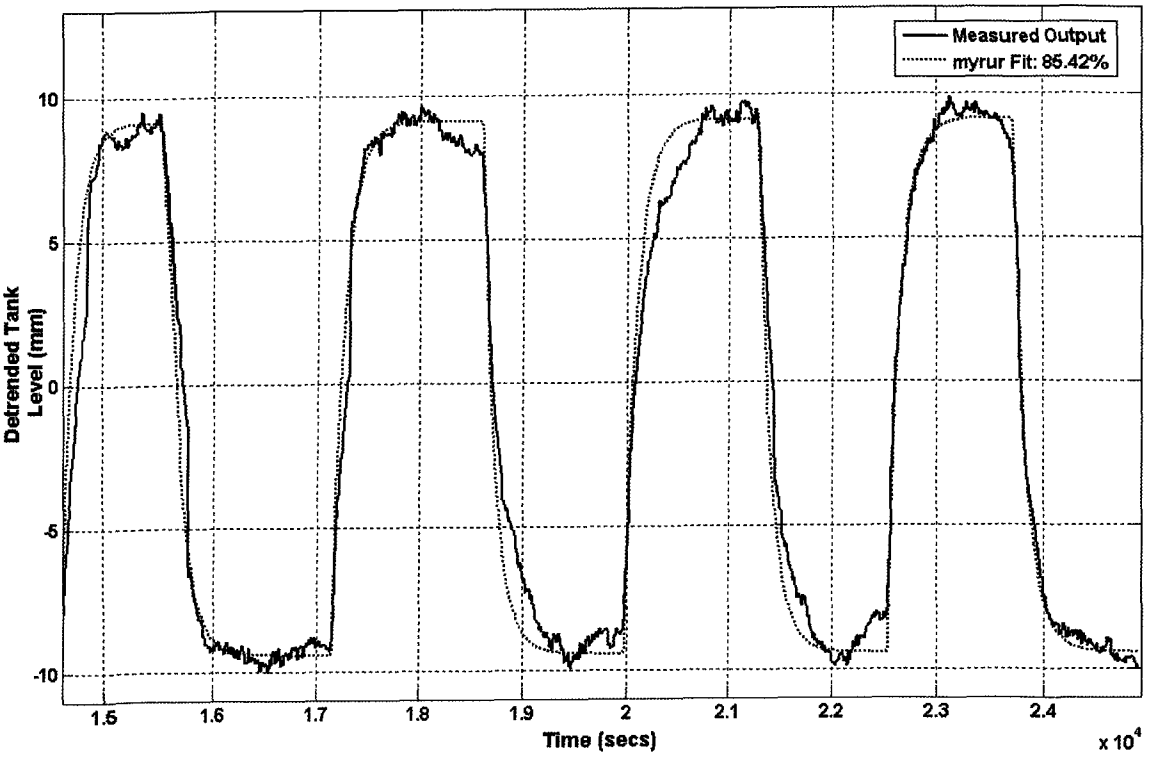

Figure 4.6(d): Validation of continuous-time model for component transfer function $G_{nonmin}(2,2)$.

Thus, (4.1) for the minimum phase can be written as:

$$G_{min}(s) = \begin{bmatrix} \dfrac{25.944e^{-5.0004s}}{155s+1} & \dfrac{12.932e^{-15.921s}}{(16212.93s^2+259.86s+1)} \\ \dfrac{11.478e^{-10.274s}}{(13818.0025s^2+235.1s+1)} & \dfrac{23.933e^{-5.82s}}{145.05s+1} \end{bmatrix} \quad (4.8a)$$

The non-minimum phase's model is:

$$G_{nonmin}(s) = \begin{bmatrix} \dfrac{10.061e^{-4.1318s}}{200.56s+1} & \dfrac{28.596e^{-24.12s}}{(22758.74s^2+301.72s+1)} \\ \dfrac{31.044e^{-33.517s}}{(22104.33s^2+297.49s+1)} & \dfrac{9.2785e^{-9.275s}}{124.24s+1} \end{bmatrix} \quad (4.8b)$$

4.3 INPUT-OUTPUT PAIRING USING THE RELATIVE GAIN ARRAY METHOD

Because the objective of computing the minimum and non-minimum phase models of the Quadruple-Tank Process is to design decentralized optimal PI and PID controllers for the process, it is important to determine how to pair the

manipulated (input) and controlled (output) variables for minimal process interactions and acceptable closed-loop performance. Intuitively, the elements of the process matrix for the minimum phase suggest that the lower left tank water level should be controlled using the left pump, since the transfer function between the two variables has a larger gain than the transfer function between the tank level and the other pump. The same explanation applies to the lower right tank water level and the right pump. For the non-minimum phase process, on the other hand, it is apparently preferable to control the lower left tank water level using the right pump and vice versa for the lower right tank water level.

The Relative Gain Array (RGA) Method, presented by Bristol in [45], provides a systematic approach for the analysis of multivariable process control problems, based on the concept of a *relative gain*, and provides insight into the process interaction measure and the most effective pairing of the controlled and manipulated variables. For a process with n controlled variables and n manipulated variables, the relative gain λ_{ij} between a controlled variable y_i and a manipulated variable u_j is defined to be the dimensionless ratio of the two steady-state gains:

$$\lambda_{ij} = \frac{(\partial y_i / \partial u_j)_u}{(\partial y_i / \partial u_j)_y} = \frac{open\text{-}loop\ gain}{closed\text{-}loop\ gain} \tag{4.9}$$

for $i = 1, 2, \ldots, n$ and $j = 1, 2, \ldots, n$.

For a 2 × 2 transfer function matrix such as (4.8a) and (4.8b), with two manipulated variables and two controller variables, the relative gains can be calculated by using the steady-state form of the process model [14]:

$$\begin{bmatrix} y_1 \\ \\ y_2 \end{bmatrix} = \begin{bmatrix} K_{11} & K_{12} \\ \\ K_{21} & K_{22} \end{bmatrix} \cdot \begin{bmatrix} u_1 \\ \\ u_2 \end{bmatrix} \tag{4.10}$$

where K_{ij} denotes the steady-state gain between y_i and u_j, for a stable process:

$$K_{ij} = \lim_{s \to 0} \left(\frac{y_i(s)}{u_j(s)} \right) \tag{4.11}$$

[14] derives the expressions for λ_{ij} ($i, j = 1, 2$) in terms of the steady-state gains:

$$\lambda_{11} = \frac{1}{1 - \frac{K_{12}K_{21}}{K_{11}K_{22}}}$$
$$\lambda_{12} = \lambda_{21} = 1 - \lambda_{11} \qquad (4.12)$$
$$\lambda_{22} = \lambda_{11}$$

Thus, the RGA for the 2 × 2 process can be expressed as

$$\Lambda = \begin{bmatrix} \lambda & 1-\lambda \\ 1-\lambda & \lambda \end{bmatrix} \qquad (4.13)$$

where $\lambda = \lambda_{11}$.

From (4.12), λ depends on the relative magnitudes of the diagonal and anti-diagonal elements of the steady-state matrix in (4.10), which in turn depends on how the input and output variables have been paired.

[45] recommends that the input-output pairing for the 2 × 2 process should have an RGA, like (4.13), in which λ is as close to one as possible. The implication of this recommendation to (4.12) is that the product $K_{11}K_{22}$ should be made as large as possible compared to $K_{12}K_{21}$. Therefore, (4.10) should be made as diagonally dominant as possible.

From (4.8a) and (4.8b), the steady-state matrices of the models can be expressed as

$$G_{min}(0) = \begin{bmatrix} 25.944 & 12.932 \\ 11.478 & 23.933 \end{bmatrix}$$
$$G_{nonmin}(0) = \begin{bmatrix} 10.061 & 28.596 \\ 31.044 & 9.2785 \end{bmatrix} \qquad (4.14)$$

From (4.12) and (4.14), the RGA matrices – in the form of (4.13), for the minimum and non-minimum phase models, using the h_{LL}-u_L / h_{LR}-u_R and the h_{LL}-u_R / h_{LR}-u_L pairings – are computed as shown in Table 4.3.

Table 4.3: RGAs for all Input-Output Pairings of the Minimum and Non-Minimum Phase Models

PROCESS MODEL	RGA (h_{LL}-u_L/ h_{LR}-u_R PAIRING)	RGA (h_{LL}-u_R/ h_{LR}-u_L PAIRING)
MINIMUM PHASE	$\begin{bmatrix} 1.314 & -0.314 \\ -0.314 & 1.314 \end{bmatrix}$	$\begin{bmatrix} -0.314 & 1.314 \\ 1.314 & -0.314 \end{bmatrix}$
NON-MINIMUM PHASE	$\begin{bmatrix} -0.118 & 1.118 \\ 1.118 & -0.118 \end{bmatrix}$	$\begin{bmatrix} 1.118 & -0.118 \\ -0.118 & 1.118 \end{bmatrix}$

From Table 4.a, λ is closer to one for the minimum phase model, if the left pump is paired with the lower left tank water level and the right pump with the lower right tank level, than the converse pairing. For the non-minimum phase model, the right pump can control the lower left tank level more effectively than the left pump. Thus, the recommended pairings by RGA analysis agree with the intuitive selections.

In the next section, the decentralised optimal PI and PID controllers will be designed and implemented.

4.4 MULTILOOP CONTROL DESIGN

The multiple-input/multiple-output (MIMO) transfer function matrices in (4.8a) and (4.8b) have process interactions, but the RGA matrices in Table 4.3 show that the process matrices are significantly diagonal or anti-diagonal. Thus, either multiloop or multivariable control schemes [14] can be applied to controlling the processes.

Multiloop (also known as decentralized) PID control systems are often used to control interacting MIMO processes. They consist of single-input/single-output (SISO) PID controllers acting in a multiloop fashion. Figure 4.7 shows a typical multiloop system for a 2 × 2 process like (4.8a) and (4.8b).

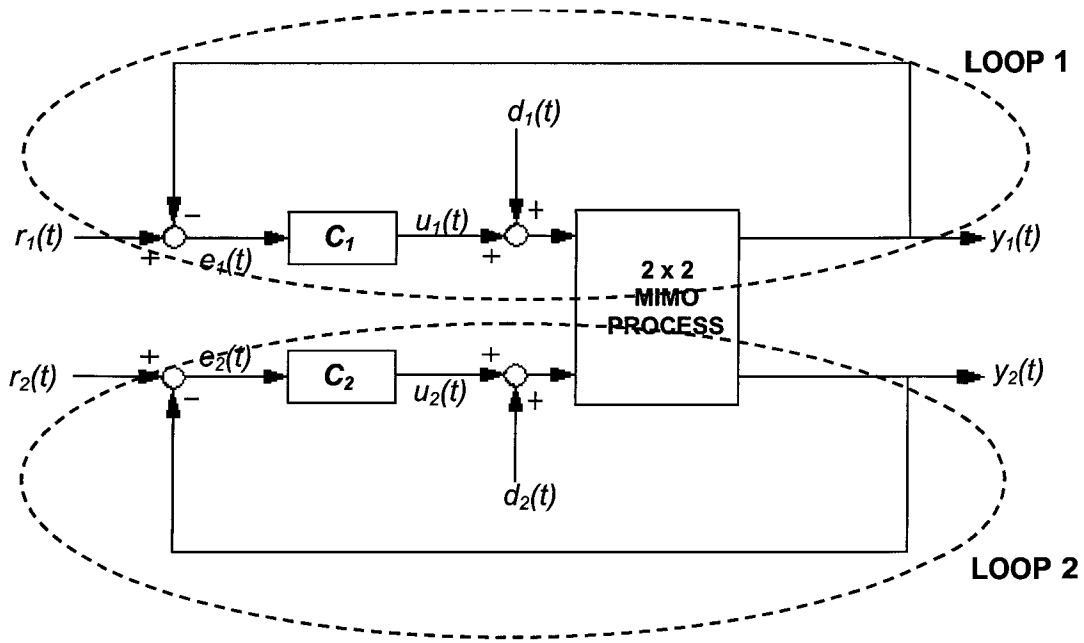

Figure 4.7: Multiloop control block diagram for a typical 2 x 2 MIMO process.

where:

$r_i(t)$ = set point signal to Loop i; i = 1, 2
$e_i(t)$ = error signal in Loop i
$u_i(t)$ = control signal in Loop i
$d_i(t)$ = process input disturbance to Loop i
$y_i(t)$ = process output at Loop i
C_i = SISO controller (PI or PID) utilized in Loop i

Decentralized control is commonly implemented in MIMO systems because of its relative simplicity, and because it is potentially robust to sensor and control actuator failure. In a multiloop system, after a control structure is fixed, control performance is determined mainly by tuning each single-loop PID controller. Another advantage of multiloop controllers is that loop failure tolerance of the resulting control system can be easily checked. [46] lists and briefly discusses the main types of tuning methods for multiloop PID control systems:

- Detuning methods
- Sequential loop closing methods
- Iterative or trial-and-error methods
- Simultaneous equation solving or optimization methods
- Independent methods

The sequential loop closing method will now be discussed. In this method, each controller in the multiloop is designed in sequence, i.e., a MIMO process is treated as a sequence of SISO systems. This approach is applicable to [25]'s control system design procedure because the procedure is formulated essentially for SISO processes. The sequential loop closing method involves closing the

loops in the multiloop one after the other. A controller is designed for a selected loop using a single loop tuning method and the loop is closed. Another controller is tuned for the next loop while the first loop remains closed, and it too is then closed and so on. This method differs from detuning methods in that it takes into consideration the loop interactions in the sequence of SISO processes. According to [46, 47, 48, 49, 50, 51], the sequential loop closing method has been used in designing controllers for quite a number of multiloop control systems in recent years.

A method proposed by Shen and Yu [17] is a multivariable autotuning procedure, which is based on the sequential identification and the modified Ziegler-Nichols controller design method. The method is an iterative form of the sequential loop closing method; it is illustrated using a 2 × 2 process in a multiloop structure similar to Figure 4.7. Assuming the manipulated and controlled variables have been paired by the RGA method, Loop 1 is closed using a relay as shown in Figure 4.8(a), while Loop 2 is left open.

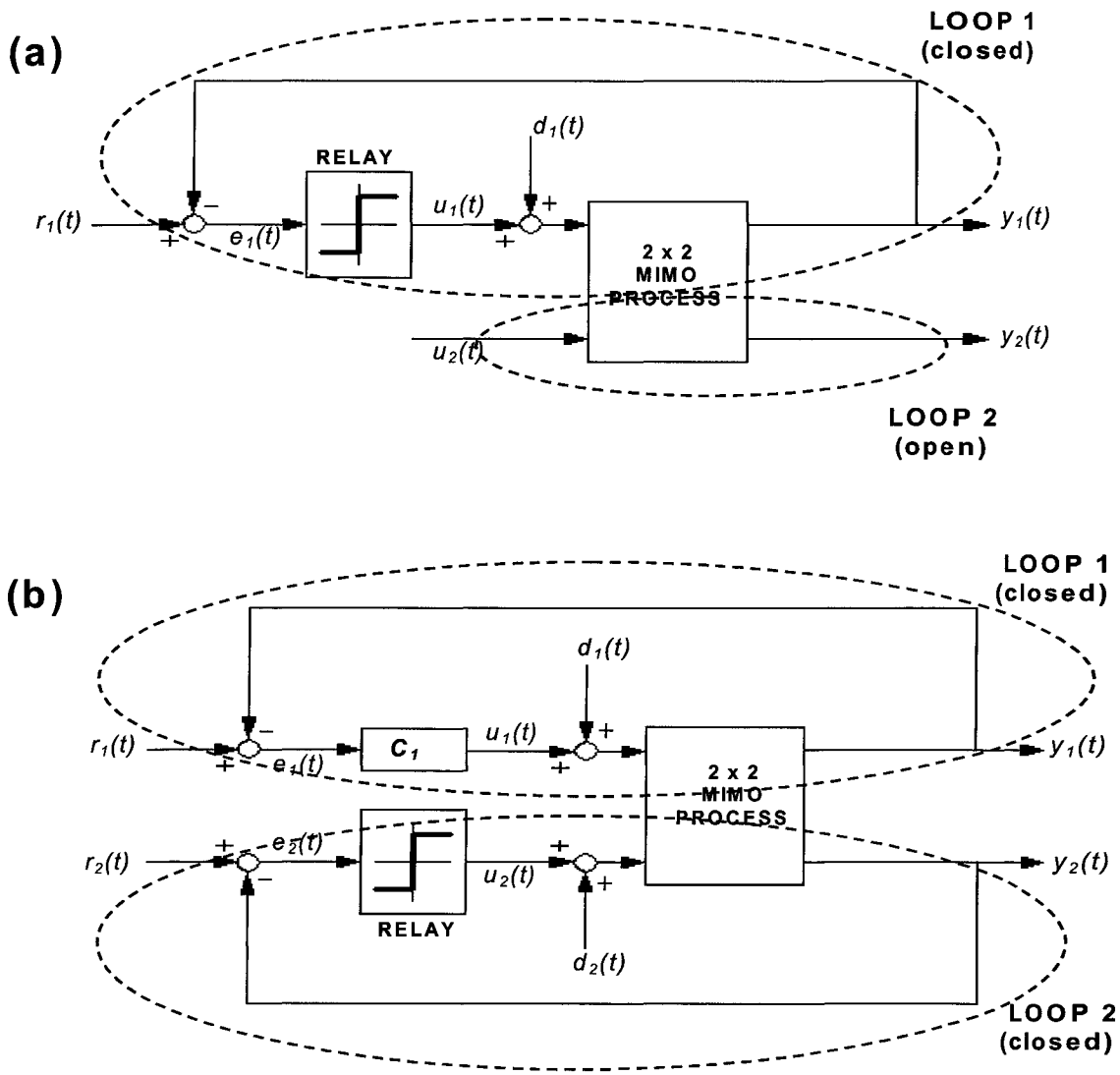

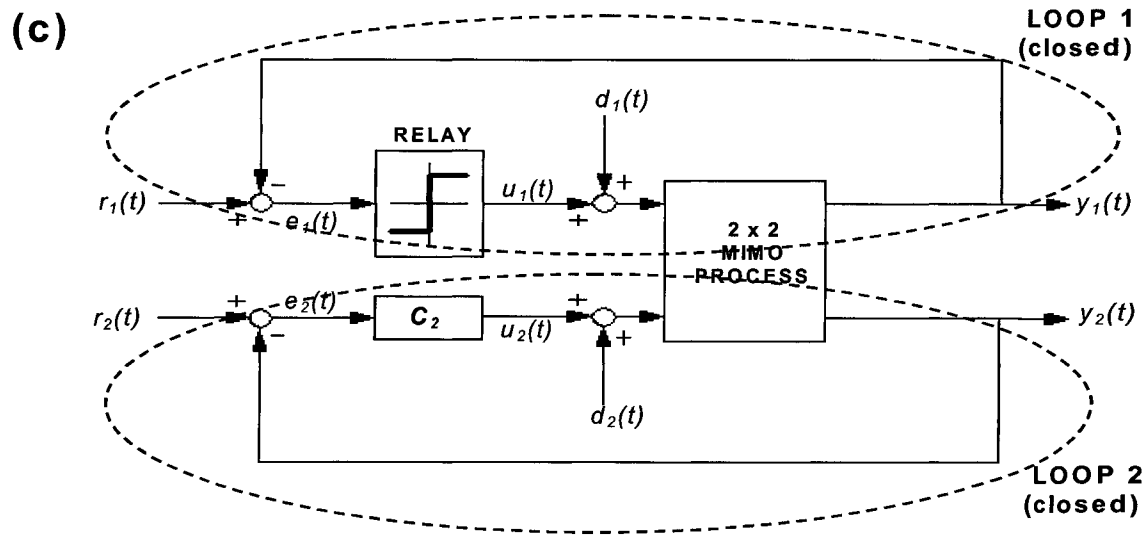

Figure 4.8: Sequential tuning procedure for a 2 x 2 multiloop.

The relay-feedback test [39] is performed, and controller C_1 is designed from the ultimate gain K_u and the ultimate frequency ω_u. Next, a relay-feedback test is performed on Loop 2, while Loop 1 remains closed with C_1 as shown in Figure 4.8(b), and the controller C_2 is designed for Loop 2. Then Loop 2 is closed with C_2 and another experiment is performed on Loop 1, as shown in Figure 4.8(c), to obtain new controller constants for C_1. The procedures in Figure 4.8(b) and Figure 4.8(c) are iteratively followed until the parameters for C_1 and C_2 converge. Because the MIMO process is treated as a sequence of SISO processes, the method has the advantage of simplicity. Figures 4.8(b) and Figure 4.8(c) can be simplified into the SISO closed-loops in 4.9(a) and Figure 4.9(b) respectively:

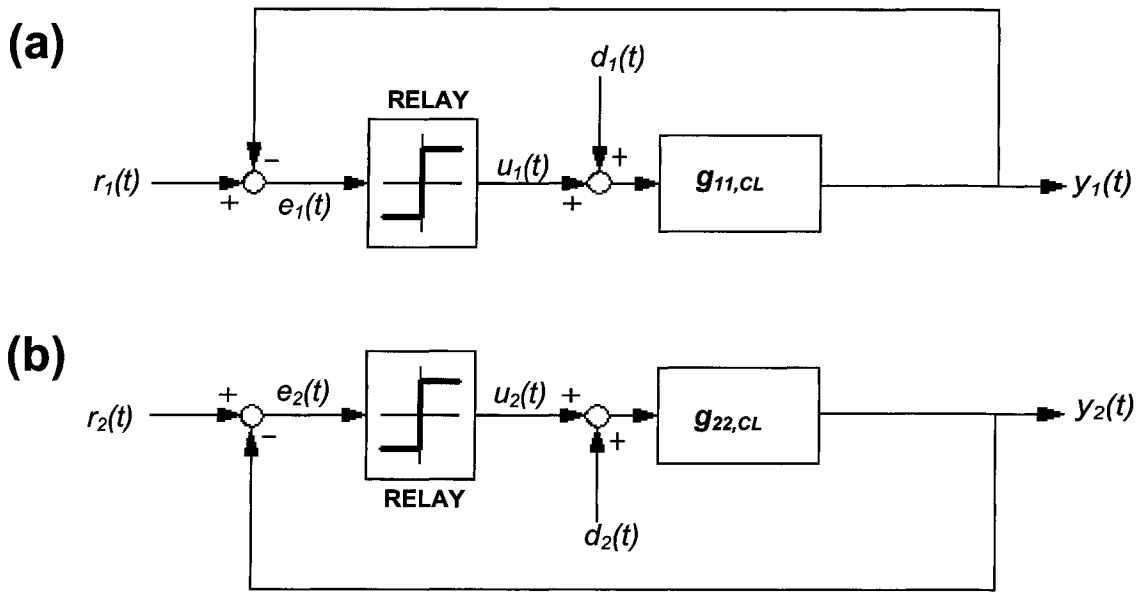

Figure 4.9: Simplification of 2 x 2 multiloop into a sequence of 2 SISO closed loops.

where:

$$g_{11,CL} = g_{11}\left(1 - \frac{g_{12}g_{21}}{g_{11}g_{22}}h_2\right) \tag{4.15}$$

$$g_{22,CL} = g_{22}\left(1 - \frac{g_{12}g_{21}}{g_{11}g_{22}}h_1\right) \tag{4.16}$$

$$h_1 = \frac{g_{11}C_1}{1 + g_{11}C_1} \tag{4.17}$$

$$h_2 = \frac{g_{22}C_2}{1 + g_{22}C_2} \tag{4.18}$$

Hence, C_1 and C_2 can be designed iteratively from $g_{11,CL}$ and $g_{22,CL}$, using suitable controller tuning methods for single loops. In investigating the convergence property of the iterative sequential tuning procedure, Monte Carlo experiments were performed on 2 × 2 multiloops in [17], using randomly generated first-order plus dead time transfer functions. All cases considered met the specified convergence criterion.

4.5 DESIGN OF MULTILOOP OPTIMAL PID CONTROLLERS FOR QUADRUPLE TANK PROCESS

In the design of optimal PID controllers for the multiloop in Figure 4.7, a tuning procedure similar to the iterative sequential loop closing procedure in [17] is considered. However, instead of applying Astrom and Hagglund's autotuning method in [39] to design C_1 and C_2, Kristiansson's optimal PID design procedure [25] is used. Thus, (2.21) is solved for the controllers iteratively until their parameters converge.

4.5.1 MINIMUM PHASE MULTILOOP

The RGA matrices in Table 4.3 suggest an h_L-u_L / h_R-u_R pairing for the quadruple-tank's minimum phase multiloop. Thus, Figures 4.9(a) and 4.9(b) are modified to Figures 4.10(a) and 4.10(b) respectively.

$G_{min}(s)$ in (4.8a) can be expressed as

$$G_{min}(s) = \begin{bmatrix} \dfrac{25.944e^{-5.0004s}}{155s+1} & \dfrac{12.932e^{-15.921s}}{(16212.93s^2+259.86s+1)} \\ \dfrac{11.478e^{-10.274s}}{(13818.0025s^2+235.1s+1)} & \dfrac{23.933e^{-5.82s}}{145.05s+1} \end{bmatrix} \quad (4.19)$$

$$= \begin{bmatrix} G_{11}^{min} & G_{12}^{min} \\ G_{21}^{min} & G_{22}^{min} \end{bmatrix}$$

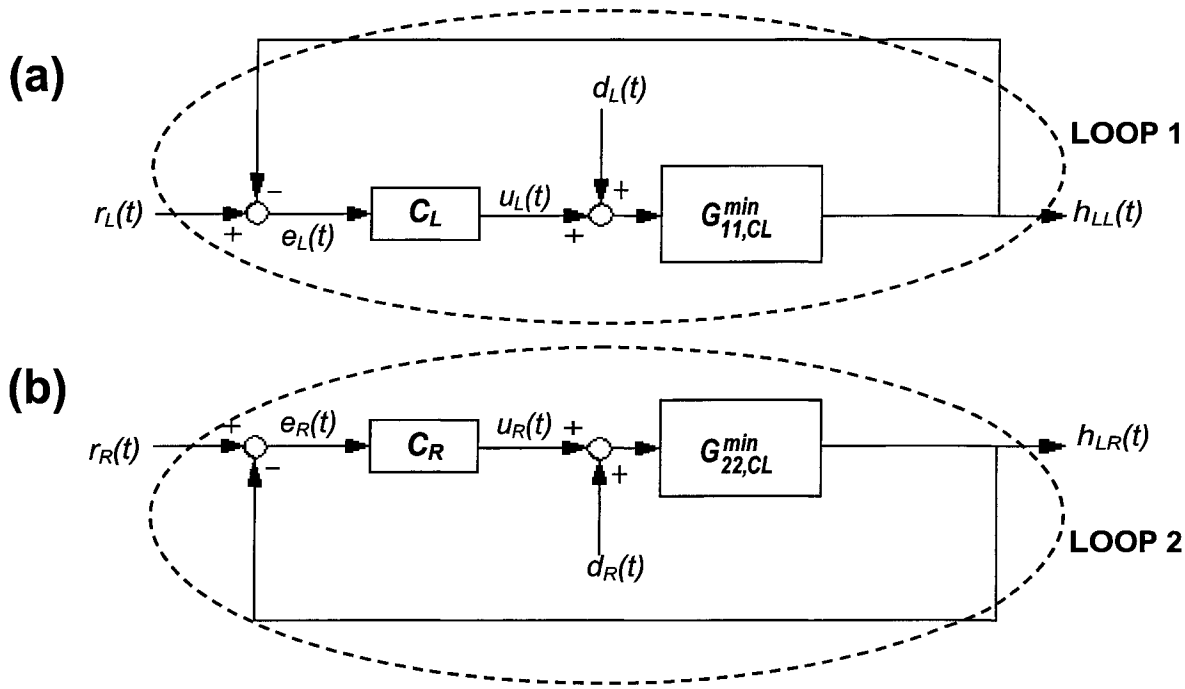

Figure 4.10: Simplification of minimum phase multiloop into 2 SISO closed loops.

where:

$r_L(t)$, $r_R(t)$ = set point signals to lower left and right tank level closed loops (Loops 1 and 2) respectively

C_L, C_R = PID controllers manipulating left and right pumps respectively

e_L, e_R = error signals in Loops 1 and 2 respectively

d_L, d_R = process input disturbance to Loops 1 and 2 respectively

(4.15) to (4.18) are expressed in terms of (4.19) as

$$G_{11,CL}^{min} = G_{11}^{min}\left(1 - \frac{G_{12}^{min}G_{21}^{min}}{G_{11}^{min}G_{22}^{min}}h_R\right) \quad (4.20)$$

$$G_{22,CL}^{min} = G_{22}^{min}\left(1 - \frac{G_{12}^{min}G_{21}^{min}}{G_{11}^{min}G_{22}^{min}}h_L\right) \tag{4.21}$$

$$h_L = \frac{G_{11}^{min}C_L}{1 + G_{11}^{min}C_L} \tag{4.22}$$

$$h_R = \frac{G_{22}^{min}C_R}{1 + G_{22}^{min}C_R} \tag{4.23}$$

The iterative sequential loop closing method of designing PID controllers for the Quadruple-Tank Process' multiloop, using Kristiansson's single loop optimal controller design method [25], is itemized in the following steps:

Step 1.1: Specify constraints on GM_S, J_u (or k_∞) and J_{HF} (for the optimal PID controller with a second order filter) for Loops 1 and 2.

Step 1.2: Solve (2.21), with the constraints specified in **Step 1.1**, for Loop 1 in Figure 4.10(a), with the modification of using G_{11}^{min} as the process model instead of $G_{11,CL}^{min}$. Set the optimal parameters in ρ as the initial parameters for controller C_L.

Step 1.3: Solve (2.21), with the constraints specified in **Step 1.1**, for Loop 2 in Figure 4.10(b) and using $G_{22,CL}^{min}$ as the process model. Set the optimal parameters in ρ as the parameters for controller C_R.

Step 1.4: Solve (2.21) for Loop 1 in Figure 4.10(a) and using $G_{11,CL}^{min}$ as the process model. Set the optimal parameters in ρ as the parameters for controller C_L.

Step 1.5: Follow **Steps 1.3** and **1.4** iteratively until the parameters for C_L and C_R converge.

C_L and C_R are both designed as optimal PID controllers with first and second order filters. For the just proper optimal PID controllers, (2.21) is formulated as

$$\min_{\rho}\{J_V(\rho) : GM_S \le 1.7, k_\infty = 6\}; \qquad \rho = [k_i, \tau, \zeta, \beta] \tag{4.24}$$

Table 4.4 presents the results of the iterative procedure, while Table 4.5 presents the final parameters of multiloop controllers after the iteration converges.

Table 4.4: Tuning of Just Proper Optimal PID Controllers for the Minimum Phase Model of the Quadruple-Tank Process using the Iterative Sequential Loop Closing Method

ITERATION NO.	C_L				C_R			
	k_i	τ	ζ	β	k_i	τ	ζ	β
0	0.024819	8.7595	1.5418	27.599				
1	0.025148	8.807	1.5251	27.091	0.020548	9.8264	1.4997	29.716
2	0.025148	8.807	1.5251	27.091	0.02055	9.8262	1.4996	29.714
3	0.025148	8.807	1.5251	27.091	0.02055	9.8262	1.4996	29.714

Table 4.5: Final Parameters for Just Proper Optimal PID Controllers for the Minimum Phase Model of the Quadruple-Tank Process

PARAMETERS	C_L	C_R
k_∞	6	6
J_v	39.765	48.663
J_u	5.9999	5.9999
k_i	0.025148	0.02055
τ	8.807	9.8262
ζ	1.5251	1.4996
β	27.091	29.714
GM_S	1.7	1.7

For the strictly proper optimal PID controllers, (2.21) is formulated as:

$$\min_{\rho}\{J_v(\rho): GM_S \le 1.7, J_u = 6, J_{HF} \le 25\}; \qquad \rho = [k_i, \tau, \zeta, \zeta_f, \beta] \tag{4.25}$$

Table 4.6 shows the results of the iterative procedure, while Table 4.7 shows the final parameters of multiloop controllers when the iteration converges.

Table 4.6: Tuning of Strictly Proper Optimal PID Controllers for the Minimum Phase Model of the Quadruple-Tank Process using the Iterative Sequential Loop-Closing Method

ITERATION NO.	C_L					C_R				
	k_i	τ	ζ	ζ_f	β	k_i	τ	ζ	ζ_f	β
0	0.024899	8.5477	1.5878	0.41318	28.881					
1	0.025061	8.7347	1.5389	0.45561	27.848	0.020496	9.765	1.5095	0.47007	31.017
2	0.025061	8.7347	1.5389	0.45561	27.848	0.020495	9.7651	1.5095	0.47007	31.018
3	0.025061	8.7347	1.5389	0.45561	27.848	0.020495	9.7651	1.5095	0.47007	31.018

Table 4.7: Final Parameters for Strictly Proper Optimal PID Controllers for the Minimum Phase Model of the Quadruple-Tank Process

PARAMETERS	C_L	C_R
k_∞	19.434	19.719
J_v	39.903	48.792
J_u	6	6
J_{HF}	25	25
k_i	0.025061	0.020495
τ	8.7347	9.7651
ζ	1.5389	1.5095
ζ_f	0.45561	0.47007
β	27.848	31.018
GM_S	1.7	1.7

The tuned optimal controllers are implemented on the multiloop of the minimum phase of the Quadruple-Tank Process, in simulation and experimentally. Steps in the set point of the lower left and right tank levels, r_L and r_R, are introduced, one after the other, to the multiloop, as well as steps in the load disturbance to the left and right pump discharge rates, d_L and d_R. The simulations are performed using SIMULINK (Figure 4.11). Set point pre-filters are used in the multiloop to reduce the excessive overshoots typical of J_V-optimal PID controllers.

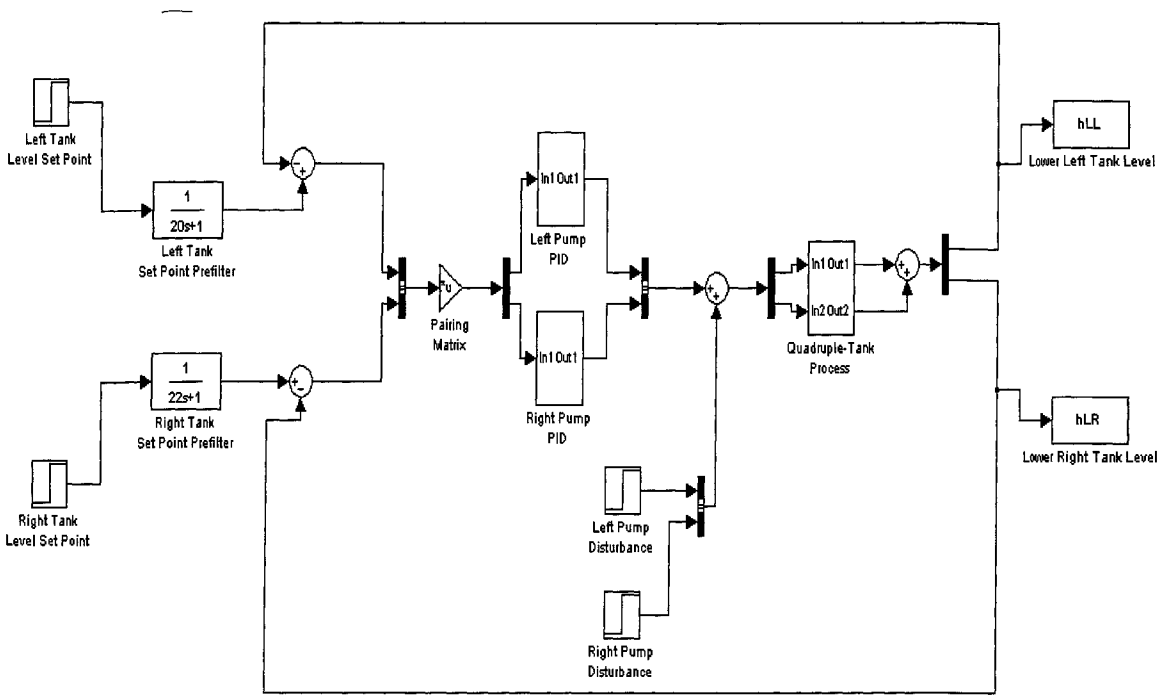

Figure 4.11: SIMULINK block diagram for simulation of quadruple-tank multiloop.

Figures 4.12(a) and (b) show the level responses of the simulated minimum phase multiloop, using the just proper optimal PID controllers along with the set point and disturbance steps. The control signal sent to each pump is also shown. The level responses for the multiloop using strictly proper optimal PID controllers are shown in Figures 4.13(a) and (b). Figures 4.14(a) and (b) and 4.15(a) and (b) show the level responses of the experimental implementation of the just proper and strictly proper optimal PID controllers, respectively, on the quadruple-tank process in the laboratory. The split valves of the process have been adjusted so that it follows the minimum phase dynamics similar to (4.8a). The set point pre-filters used for the simulations were also used in the experimental implementation of the controllers.

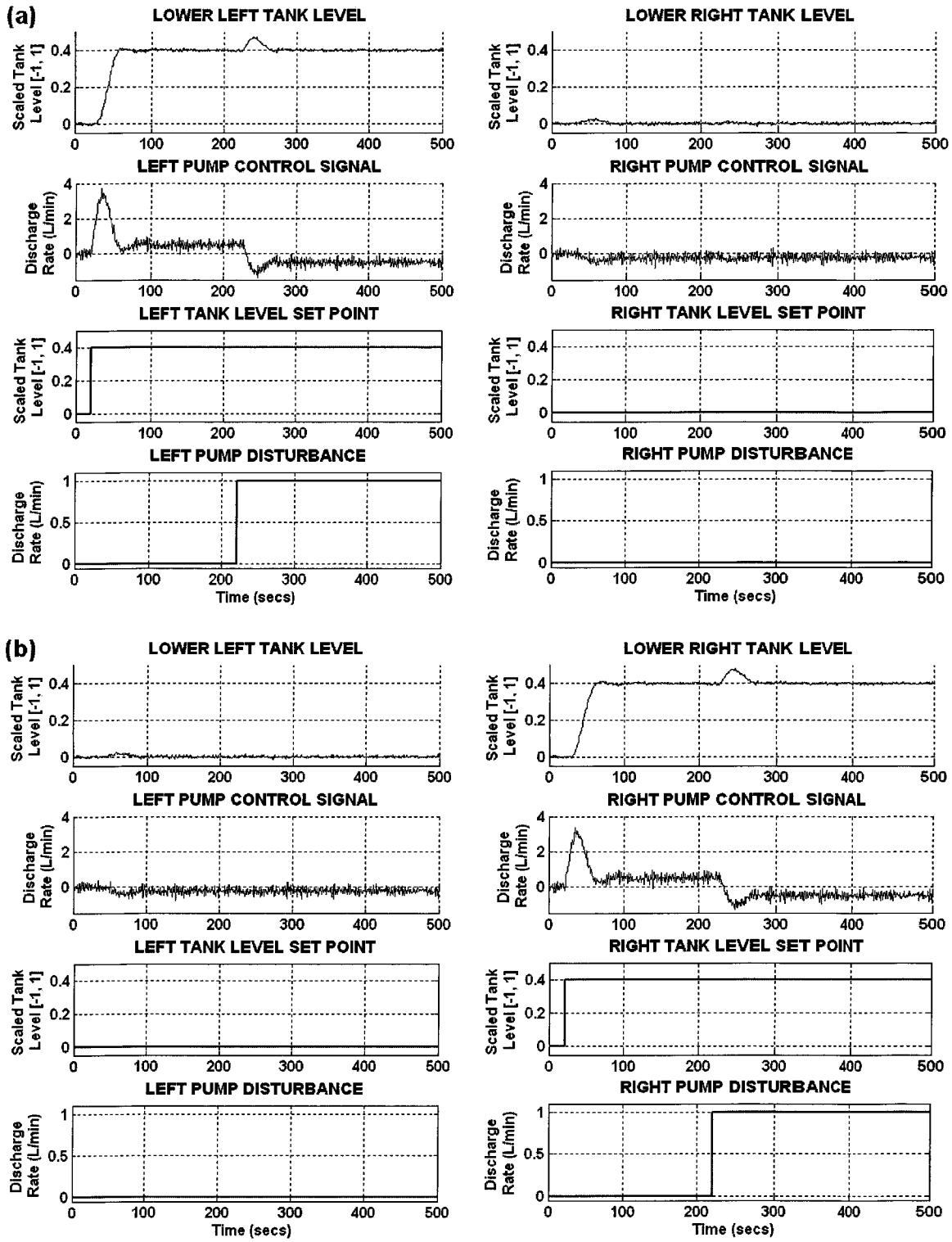

Figure 4.12: Level responses of left and right tanks to steps in (a) left tank level set point and left pump input disturbance, and (b) right tank level set point and right pump input disturbance for simulated multiloop of minimum phase of Quadruple-Tank Process, using just proper PID controllers.

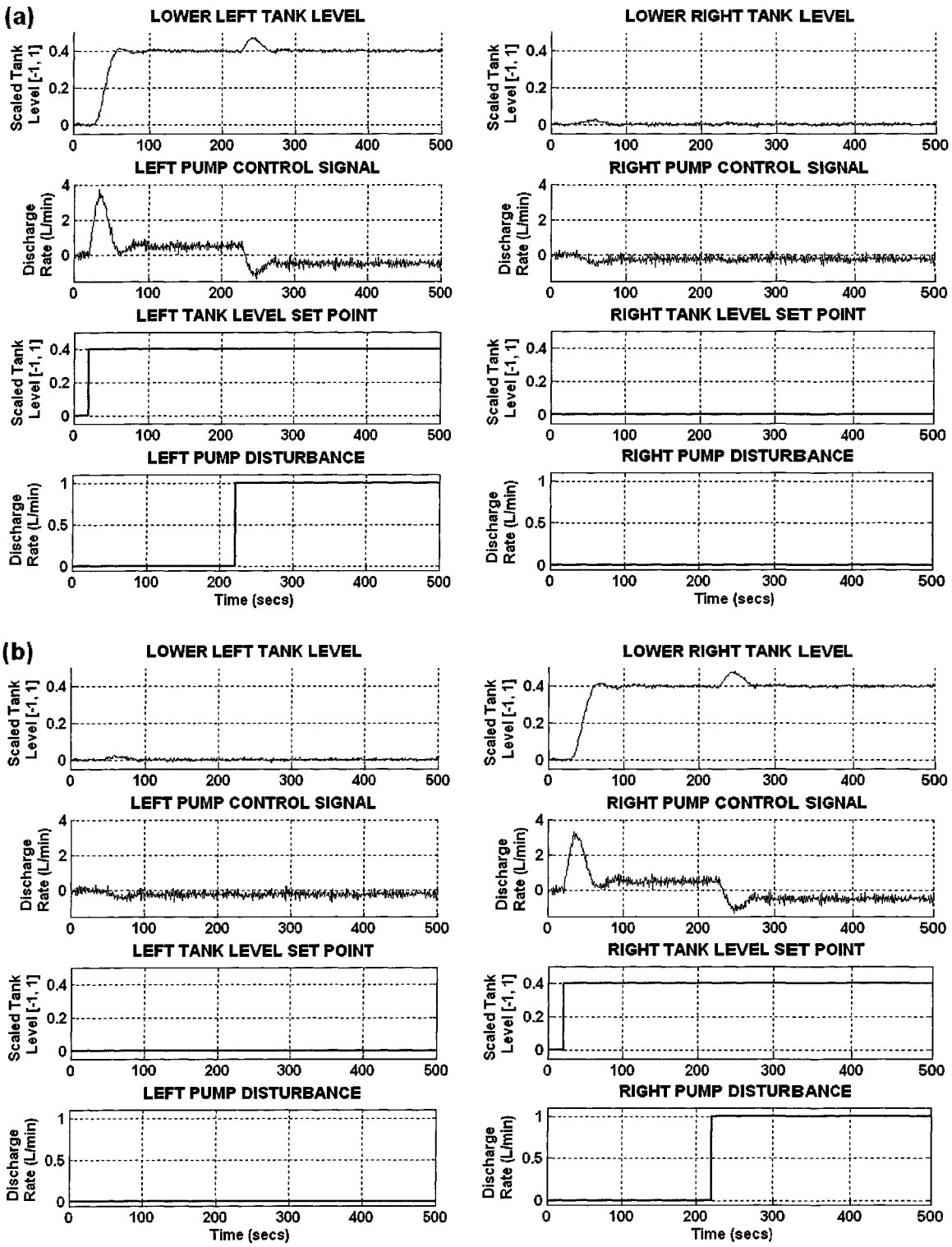

Figure 4.13: Level responses of left and right tanks to steps in (a) left tank level set point and left pump input disturbance, and (b) right tank level set point and right pump input disturbance for simulated multiloop of minimum phase of Quadruple-Tank Process, using strictly proper PID controllers.

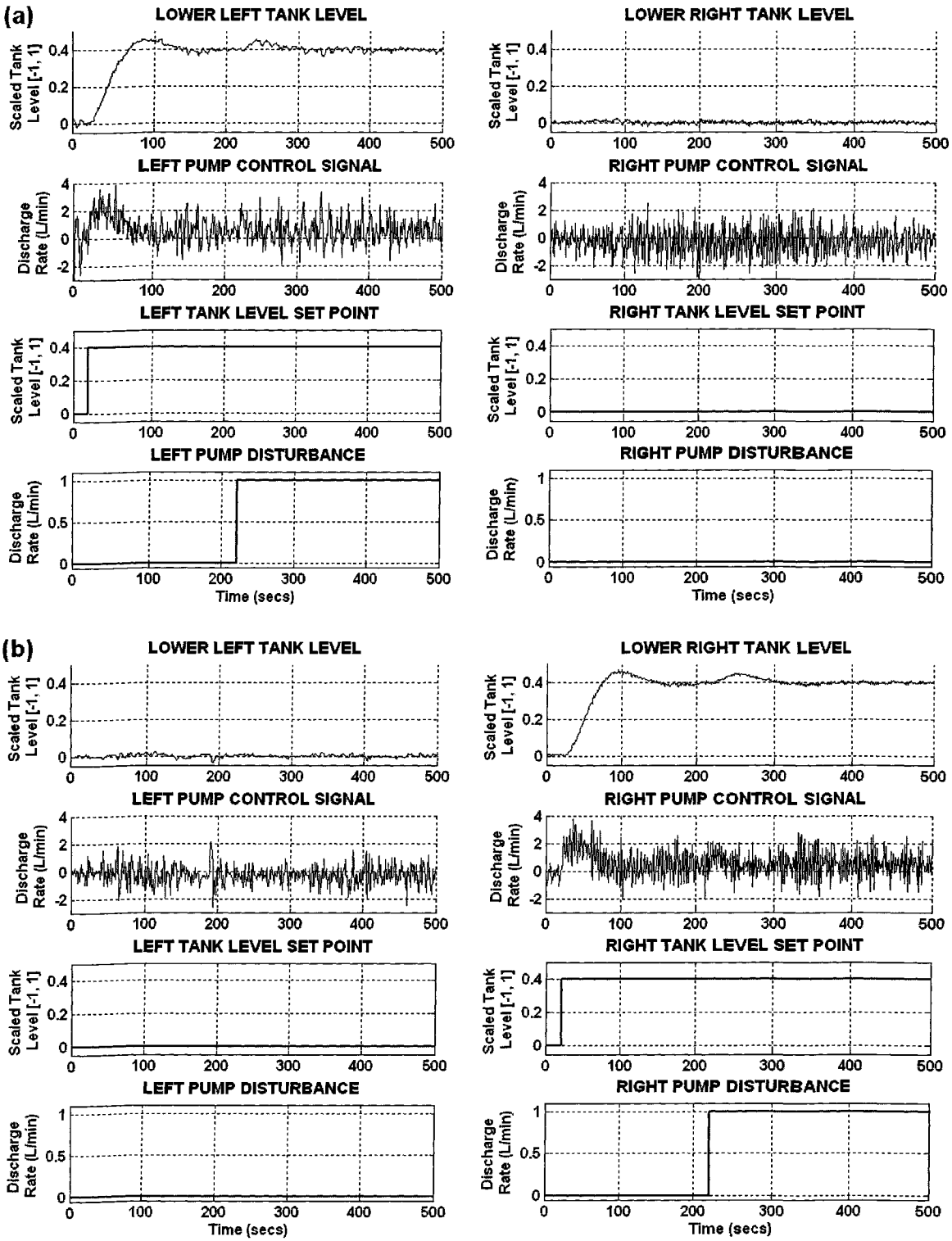

Figure 4.14: Level responses of left and right tanks to steps in (a) left tank level set point and left pump input disturbance, and (b) right tank level set point and right pump input disturbance for experimentally implemented multiloop of minimum phase of Quadruple-Tank Process, using just proper PID controllers.

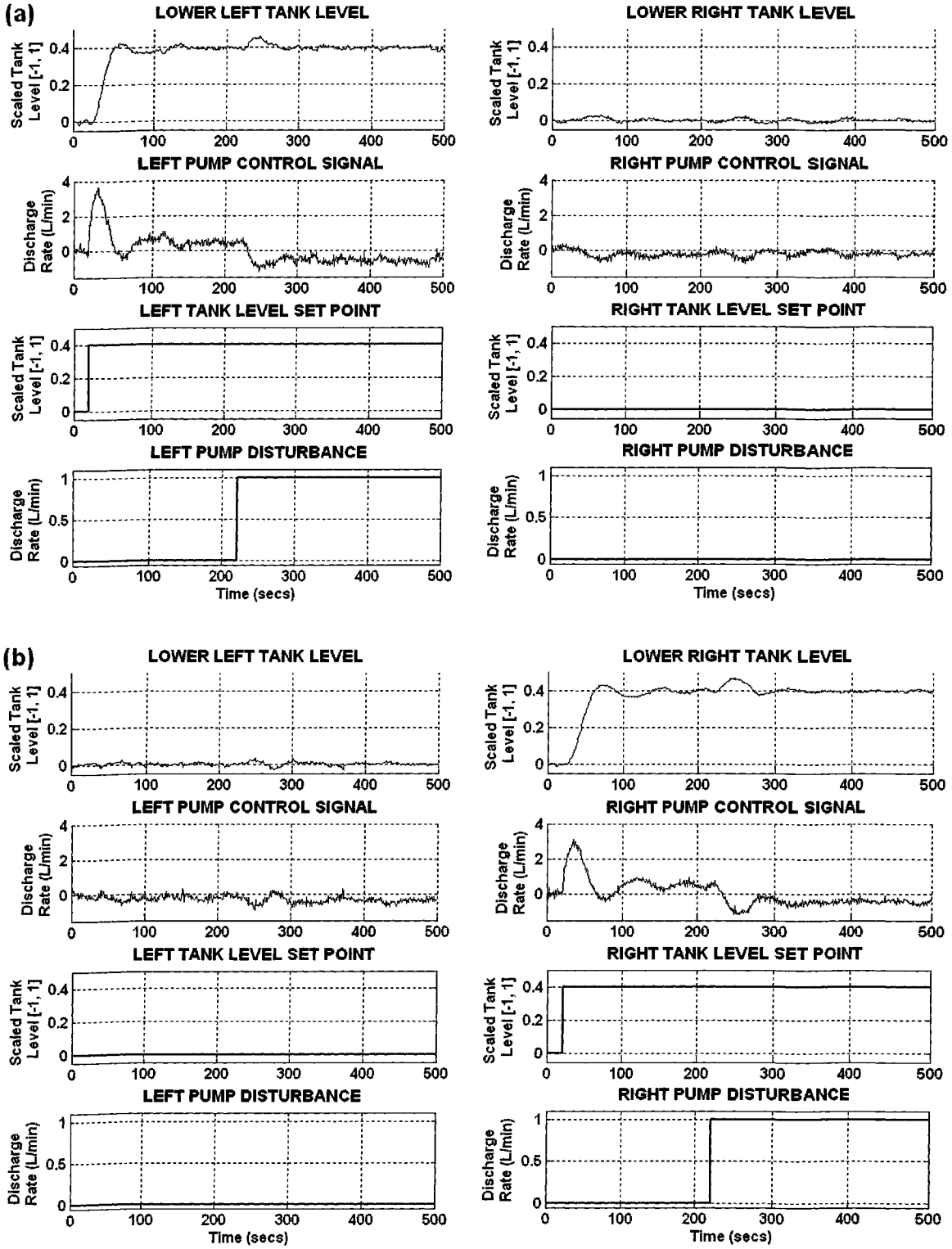

Figure 4.15: Level responses of left and right tanks to steps in (a) left tank level set point and left pump input disturbance, and (b) right tank level set point and right pump input disturbance for experimentally implemented multiloop of minimum phase of Quadruple-Tank Process, using strictly proper PID controllers.

4.5.2 NON-MINIMUM PHASE MULTILOOP

For the non-minimum phase multiloop of the quadruple-tank process, the h_{LL}-u_R / h_{LR}-u_L pairing will be used. Figures 4.9(a) and 4.9(b) are modified to Figures 4.16(a) and 4.16(b) respectively.

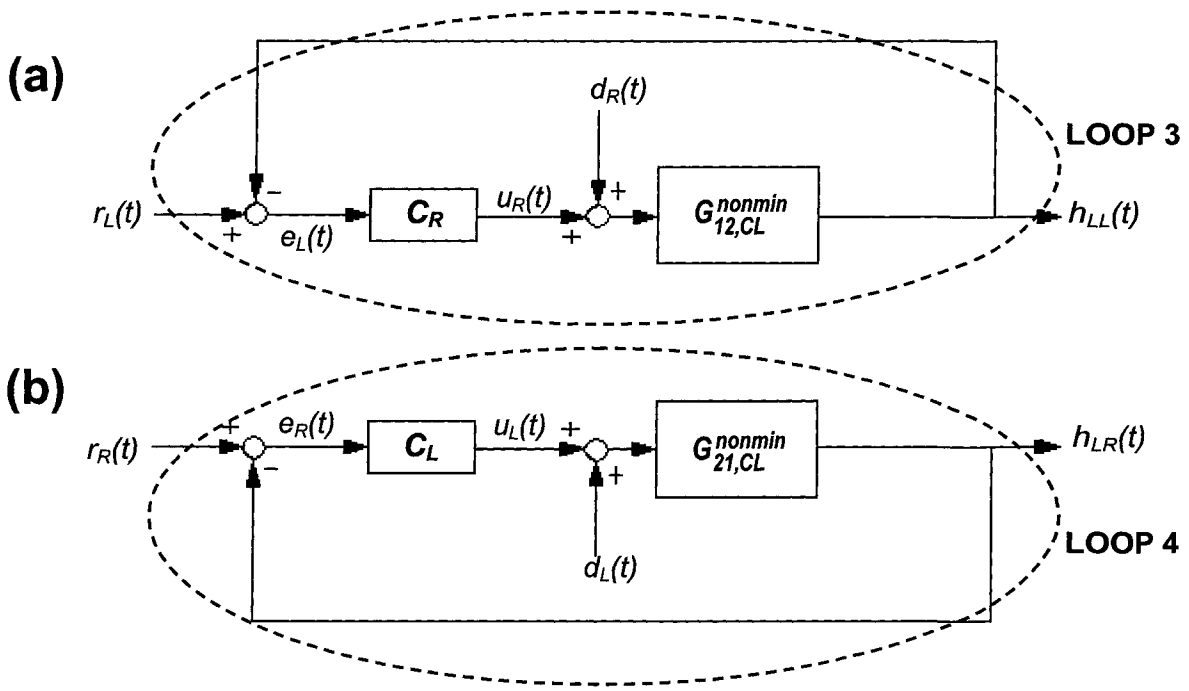

Figure 4.16: Simplification of non-minimum phase multiloop into 2 SISO closed loops.

$G_{nonmin}(s)$ in (4.8b) can be expressed as

$$G_{nonmin}(s) = \begin{bmatrix} \dfrac{10.061e^{-4.1318s}}{200.56s+1} & \dfrac{28.596e^{-24.12s}}{(22758.74s^2+301.72s+1)} \\ \dfrac{31.044e^{-33.517s}}{(22104.33s^2+297.49s+1)} & \dfrac{9.2785e^{-9.275s}}{124.24s+1} \end{bmatrix} \quad (4.26)$$

$$= \begin{bmatrix} G_{11}^{nonmin} & G_{12}^{nonmin} \\ G_{21}^{nonmin} & G_{22}^{nonmin} \end{bmatrix}$$

(4.15) to (4.18) are expressed in terms of (4.26) as

$$G_{12,CL}^{nonmin} = G_{12}^{nonmin}\left(1 - \frac{G_{11}^{nonmin} G_{22}^{nonmin}}{G_{12}^{nonmin} G_{21}^{nonmin}} h_R\right) \quad (4.27)$$

$$G_{21,CL}^{non\,min} = G_{21}^{non\,min}\left(1 - \frac{G_{11}^{non\,min} G_{22}^{non\,min}}{G_{12}^{non\,min} G_{21}^{non\,min}} h_L\right) \tag{4.28}$$

$$h_L = \frac{G_{12}^{non\,min} C_R}{1 + G_{12}^{non\,min} C_R} \tag{4.29}$$

$$h_R = \frac{G_{21}^{non\,min} C_L}{1 + G_{21}^{non\,min} C_L} \tag{4.30}$$

The iterative sequential loop-closing method, using Kristiansson's single loop optimal controller design method, is itemized in the following steps:

Step 2.1: Specify constraints on GM_S, J_u (or k_∞) and J_{HF} (for the optimal PID controller with a second order filter) for Loops 3 and 4.

Step 2.2: Solve (2.21), with the constraints specified in **Step 2.1**, for Loop 3 in Figure 4.16(a), with the modification of using $G_{12}^{non\,min}$ as the process model instead of $G_{12,CL}^{non\,min}$. Set the optimal parameters in ρ as the initial parameters for controller C_R.

Step 2.3: Solve (2.21), with the constraints specified in **Step 2.1**, for Loop 4 in Figure 4.16(b) and using $G_{21,CL}^{non\,min}$ as the process model. Set the optimal parameters in ρ as the parameters for controller C_L.

Step 2.4: Solve (2.21) for Loop 3 in Figure 4.16(a) and using $G_{12,CL}^{non\,min}$ as the process model. Set the optimal parameters in ρ as the parameters for controller C_R.

Step 2.5: Follow **Steps 2.3** and **2.4** iteratively until the parameters for C_L and C_R converge.

C_L and C_R are designed both as optimal PID controllers with first and second order filters. For the just proper optimal PID controllers, (2.21) is formulated as

$$\min_{\rho}\{J_V(\rho) : GM_S \le 1.7, k_\infty = 6\}; \qquad \rho = [k_i, \tau, \zeta, \beta] \tag{4.31}$$

Table 4.8 presents the results of the iterative procedure, while Table 4.9 presents the final parameters of multiloop controllers when the iteration converges.

Table 4.8: Tuning of Just Proper Optimal PID Controllers for the Non-Minimum Phase Model of the Quadruple-Tank Process using the Iterative Sequential Loop-Closing Method

ITERATION NO.	C_L				C_R			
	k_i	τ	ζ	β	k_i	τ	ζ	β
0					0.009238	143.47	0.78769	4.5268
1	0.01389	128.11	0.94801	3.3717	0.008839	151.74	0.73799	4.4736
2	0.016318	123.47	0.81585	2.9781	0.009027	154.51	0.73691	4.3016
3	0.016114	123.72	0.82846	3.0094	0.008999	154.37	0.73592	4.3192
4	0.016177	123.62	0.82502	3.0002	0.009006	154.44	0.73601	4.3138
5	0.016164	123.62	0.82583	3.0026	0.009005	154.44	0.73592	4.3141
6	0.016168	123.62	0.82563	3.002	0.009006	154.44	0.73594	4.314
7	0.016167	123.62	0.82567	3.0021	0.009005	154.44	0.73594	4.314
8	0.016167	123.62	0.82566	3.0021	0.009005	154.44	0.73594	4.3141
9	0.016167	123.62	0.82566	3.0021	0.009005	154.44	0.73594	4.3141

Table 4.9: Final Parameters for Just Proper Optimal PID Controllers for the Non-Minimum Phase Model of the Quadruple-Tank Process

PARAMETERS	C_L	C_R
k_∞	6	6
J_v	71.47	122.66
J_u	6.0786	6
k_i	0.016167	0.009005
τ	123.62	154.44
ζ	0.82566	0.73594
β	3.0021	4.3141
GM_S	1.7	1.7

For the strictly proper optimal PID controllers, (2.21) is formulated as:

$$\min_{\rho}\{J_V(\rho): GM_S \le 1.7, J_u = 6, J_{HF} \le 0.25\}; \qquad \rho = [k_i, \tau, \zeta, \zeta_f, \beta] \tag{4.32}$$

Table 4.10 shows the results of the iterative procedure, while Table 4.11 shows the final parameters of multiloop controllers after the iteration converges.

Table 4.10: Tuning of Strictly Proper Optimal PID Controllers for the Non-Minimum Phase Model of the Quadruple-Tank Process using the Iterative Sequential Loop-Closing Method

ITERATION NO.	C_L					C_R				
	k_i	τ	ζ	ζ_f	β	k_i	τ	ζ	ζ_f	β
0						0.0003299	122.37	0.872	0.478	4.735
1	0.0003673	138.35	0.84317	0.650	4.836	0.0003157	131.98	0.860	0.484	4.874
2	0.0003704	134.86	0.85703	0.631	4.803	0.0003018	135.82	0.814	0.497	5.027
3	0.0003692	134.95	0.85504	0.630	4.810	0.0003039	136.4	0.814	0.502	5.023
4	0.0003693	135.05	0.85482	0.631	4.810	0.0003043	136.22	0.815	0.502	5.018
5	0.0003693	135.04	0.85486	0.631	4.810	0.0003040	136.24	0.815	0.502	5.019
6	0.0003693	135.03	0.85488	0.631	4.810	0.0003041	136.24	0.815	0.502	5.019
7	0.0003693	135.03	0.8549	0.631	4.810	0.0003042	136.23	0.815	0.502	5.019
8	0.0003693	135.03	0.8549	0.631	4.810	0.0003042	136.23	0.815	0.502	5.019

Table 4.11: Final Parameters for Strictly Proper Optimal PID Controllers for the Non-Minimum Phase Model of the Quadruple-Tank Process

PARAMETERS	C_L	C_R
k_∞	0.24606	0.22524
J_v	96.939	119.44
J_u	6	6
J_{HF}	0.25	0.25
k_i	0.0003693	0.0003042
τ	135.03	136.23
ζ	0.8549	0.815
ζ_f	0.631	0.502
β	4.810	5.019
GM_S	1.7	1.7

The tuned optimal controllers are implemented on the non-minimum phase of the quadruple-tank process multiloop, both in simulation and experimentally. Steps in the set point of the lower left and right tank levels, r_L and r_R, are introduced, one after the other, to the multiloop. This is also done for the load disturbance to the left and right pump discharge rates, d_L and d_R. The simulations are performed using SIMULINK. Set point pre-filters are used in the multiloop to reduce the excessive overshoots typical of J_V-optimal PID controllers.

Figures 4.17(a) and (b) show the level responses of the simulated non-minimum phase multiloop, using the just proper optimal PID controllers along with the set point and disturbance steps. The control signal sent to each pump is also shown. The level responses for the multiloop using strictly proper optimal PID controllers are shown in Figures 4.18(a) and 4.18(b). Figures 4.19(a), 4.19(b), 4.20(a) and 4.20(b) show the level responses of the experimental implementation of the just

proper and strictly proper optimal PID controllers, respectively, on the quadruple-tank process in the laboratory. The split valves of the process have been adjusted so that it follows the non-minimum phase dynamics similar to (4.8b). The same set point pre-filters used for the simulations were used in the experimental implementation of the controllers.

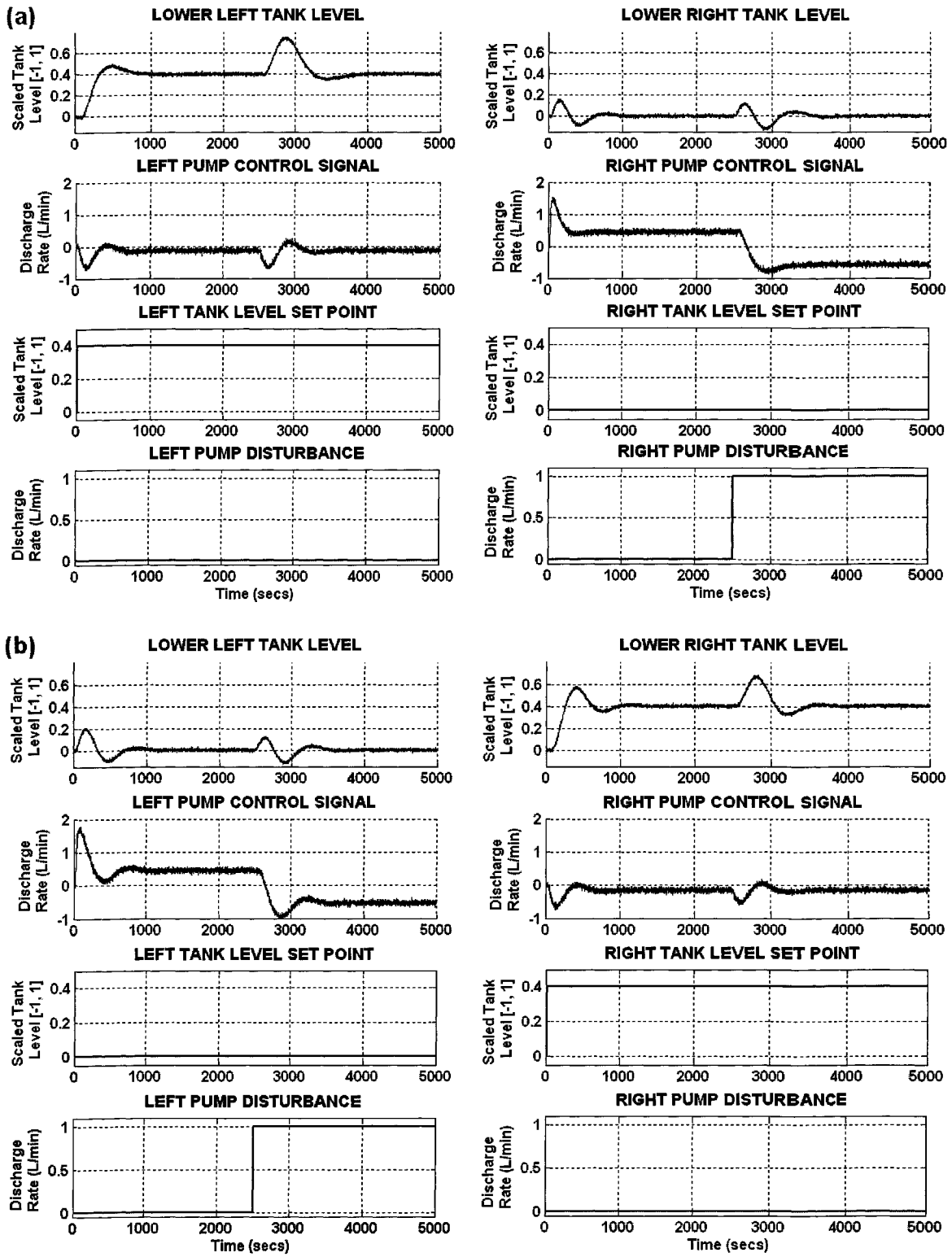

Figure 4.17: Level responses of left and right tanks to steps in (a) left tank level set point and right pump input disturbance, and (b) right tank level set point and left pump input disturbance for simulated multiloop of non-minimum phase of Quadruple-Tank Process, using just proper PID controllers.

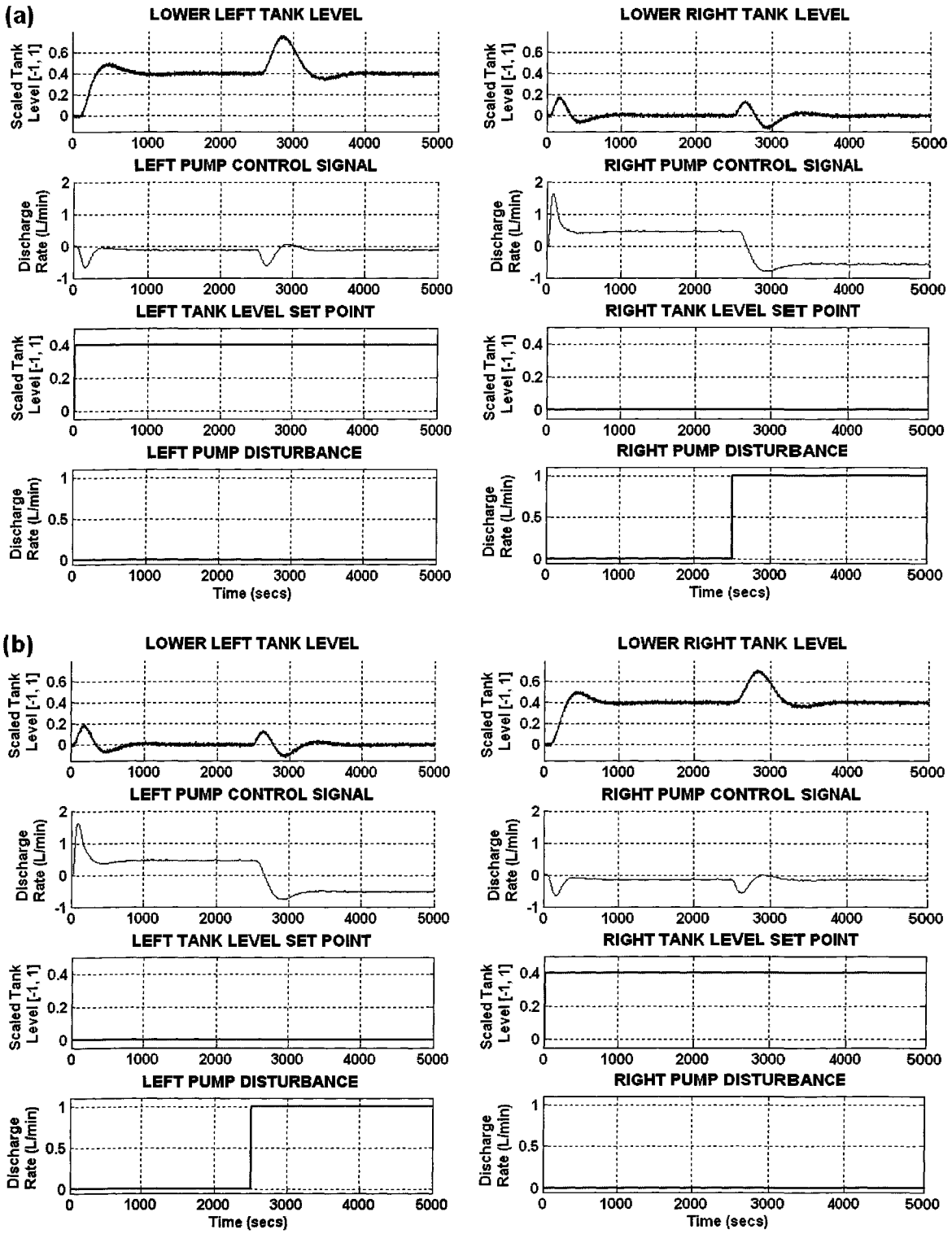

Figure 4.18: Level responses of left and right tanks to steps in (a) left tank level set point and right pump input disturbance, and (b) right tank level set point and left pump input disturbance for simulated multiloop of non-minimum phase of Quadruple-Tank Process, using strictly proper PID controllers.

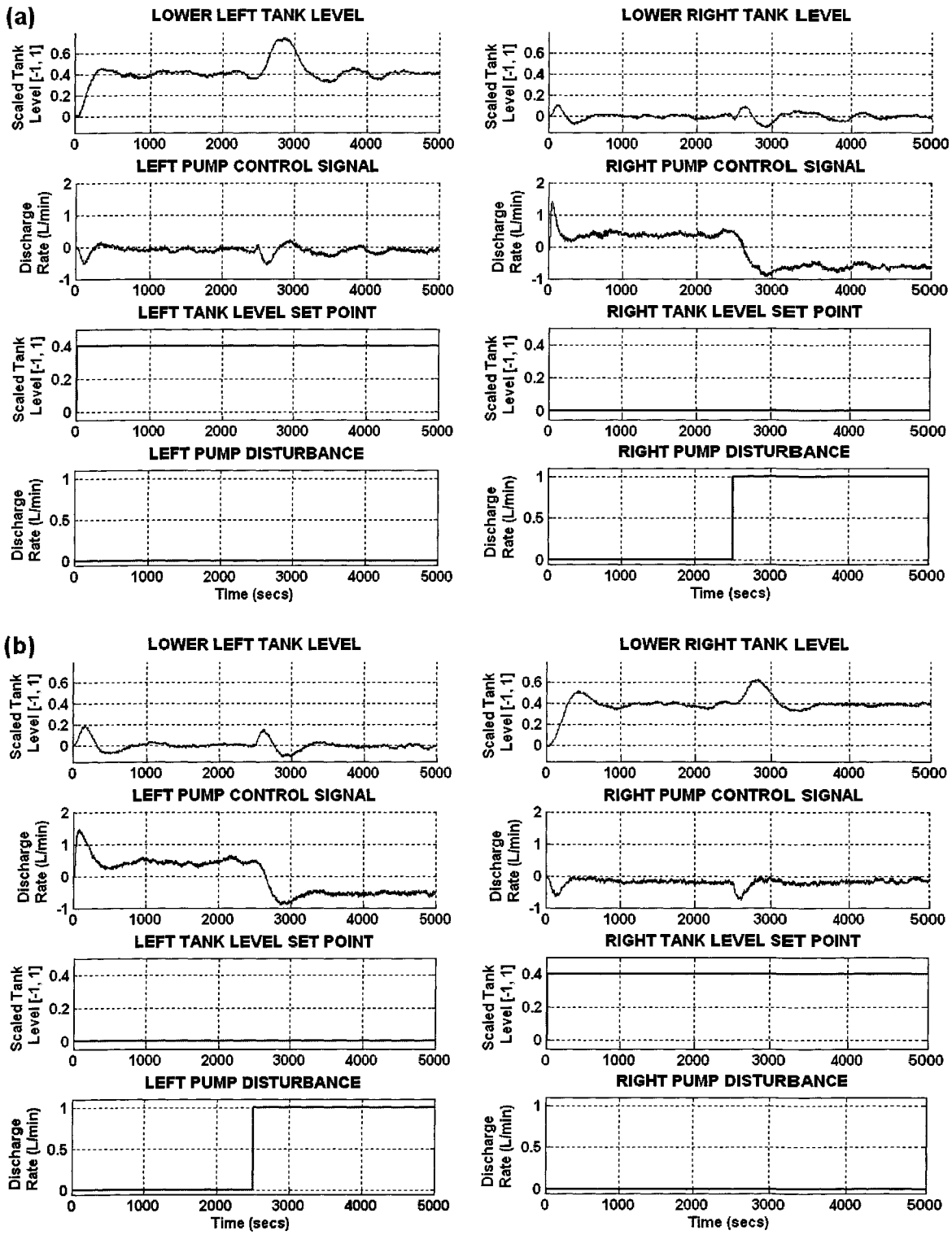

Figure 4.19: Level responses of left and right tanks to steps in (a) left tank level set point and right pump input disturbance, and (b) right tank level set point and left pump input disturbance for experimentally implemented multiloop of minimum phase of Quadruple-Tank Process, using just proper PID controllers.

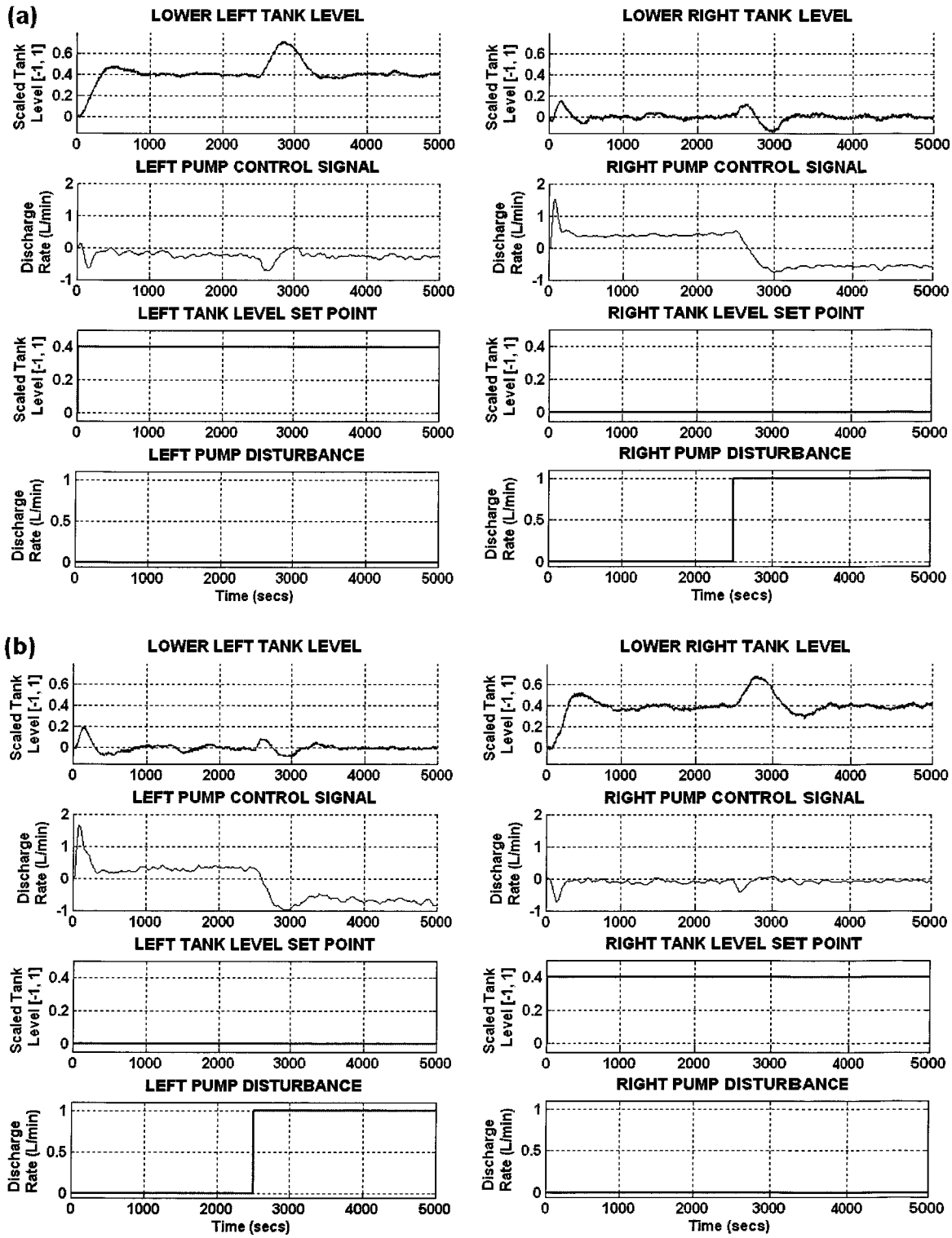

Figure 4.20: Level responses of left and right tanks to steps in (a) left tank level set point and right pump input disturbance, and (b) right tank level set point and left pump input disturbance for experimentally implemented multiloop of minimum phase of Quadruple-Tank Process, using strictly proper PID controllers.

The level responses of the multiloops appear satisfactory, both in simulation and experimentally. All responses attain their set points, without oscillations and sluggish offset damping. In some cases, however, one of the two tank levels appears to significantly overshoot its final value before settling, compared to the other tank's level response. This problem could be solved by either adjusting the J_u or k_∞ constraints on the controller designs in (4.24), (4.25), (4.31) and (4.32). Identical constraint values were chosen by default for the two loops, which is not compulsory for the design, the values could differ. Also, the set point pre-filter constants could be adjusted.

Overall, the optimal controllers designed for the multiloops give satisfactory disturbance rejection performance. Assessment of the closed-loop performance of the optimal controllers, in both set point tracking and disturbance rejection, is an area that will be extensively examined in subsequent chapters.

CHAPTER 5

TRADE-OFFS BETWEEN PROPERTIES IN OPTIMAL CONTROL SYSTEMS

5.1 INTRODUCTION

The control system evaluation criteria have been applied to the design of optimal PI and PID controllers for the multiloops of the minimum and non-minimum phases of the Quadruple-Tank Process. The controllers were designed by solving (2.21), i.e., finding controller parameters, which optimized the closed-loop performance criterion and at the same time conformed to the constraints imposed on the control activity and stability criteria. Because the control system evaluation criteria [25] allow the control engineer to study inter-relationships amongst the closed-loop characteristics, the relationship between two important properties – performance and control activity – will be considered.

Assessing closed-loop performance is of interest to the engineer in the process industry because it is analogous to profitability, while control activity is analogous to the operating cost incurred to achieve profitability. Therefore, the performance-control activity relationship of several control systems with optimal PI and PID controllers will be computed and examined in this chapter. The profiles will be computed by solving (2.21), but in this case the constraint on the control activity criterion, J_u, will have a range of values, with the performance criterion, J_v, optimized for each value. The first control system to be considered will be the closed loop of a simple, hypothetical process with a first order plus dead time (FOPDT) transfer function. Next, J_v-J_u profiles of the multiloops for the Quadruple-Tank Process will be computed.

Other evaluation criteria, based on the time domain characteristics of the control systems, will be considered for suitability as comprehensible substitutes of J_v and J_u respectively. Thus, the profiles for the multiloops will be computed using the time domain-based criteria and compared with the J_v-J_u profiles for similarity.

Finally, the performance-control activity profiles for closed loops of processes with varying degrees of dead time dominance will be examined. The objective of this procedure is to determine the influence of time delay on the closed-loop characteristics of optimal PI controllers vis-à-vis optimal PID controllers.

5.2 J_v-J_u PROFILES FOR SISO OPTIMAL PI/PID CONTROL SYSTEMS

The J_v-J_u profile for simple SISO closed-loops, with optimal PI and PID controllers, is studied using Process 1 from Example 2.1, i.e.,

$$G(s) = \frac{e^{-s}}{10s+1}$$

For the optimal PI controller, (2.21) is expressed as

$$\min_{\rho}\{J_V(\rho) : GM_S \le 1.7, J_u \in C\} \tag{5.1}$$

$\boldsymbol{C}$ is a vector of values for J_u; for the above SISO process, $\boldsymbol{C}$ consists of elements ranging from 4 to 9.5. For each value of J_u in $\boldsymbol{C}$, the parameters for a J_V-optimal PI controller are computed.

For the optimal PID controller with a first order low-pass filter, (2.21) is expressed as

$$\min_{\rho}\{J_V(\rho) : GM_S \le 1.7, k_\infty \in Q\} \tag{5.2}$$

$\boldsymbol{Q}$ is a vector of values for k_∞; for Process 1, the elements of $\boldsymbol{Q}$ vary from 8.4 to 30. Figure 5.1 shows the J_V-J_u profiles for the closed loops for Process 1 using optimal PI and just proper optimal PID controllers, designed by solving (5.1) and (5.2) respectively. The controller and evaluation parameters for all the controllers are listed in Tables A.1 and A.2 in Appendix A.

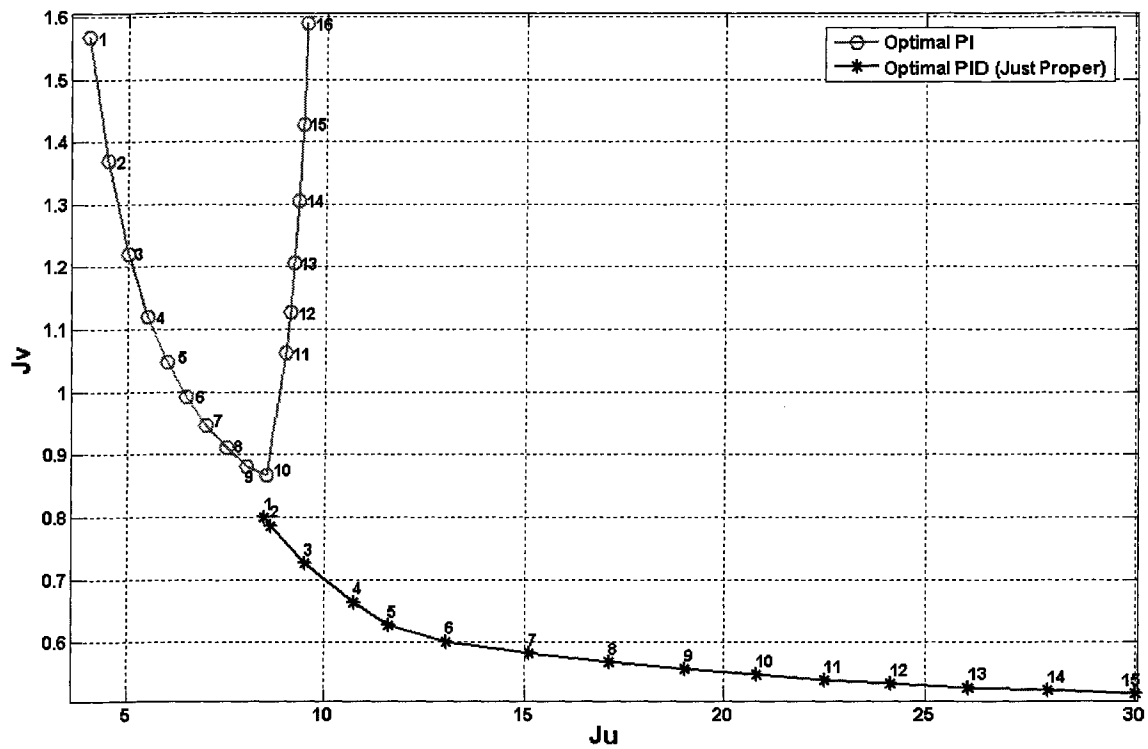

Figure 5.1: J_V-J_u profiles for closed loops for Process 1 using optimal PI and optimal (just proper) PID controllers. $GM_S \le 1.7$.

For closed loops with optimal PI controllers, J_V decreases exponentially as the value of J_u is increased. J_V attains a minimum point with Optimal PI Controller 10

at J_u = 8.5, beyond which it increases progressively. Figure 5.1 suggests that the low frequency disturbance rejection performance of the closed loop with an optimal PI controller improves up to a limit as the permissible control activity is increased, and rapidly deteriorates as the control activity is increased beyond this limit. On the other hand, the J_v for the optimal PID controller decreases exponentially to an asymptotic limit as J_u is increased. Thus increasing control activity improves its disturbance rejection performance, but does not degrade it. However, the optimal PID control loop's marginal performance improvement decreases, making the increase in control activity eventually ineffective and uneconomical. The profiles for the optimal PI and PID controllers depicted in Figure 5.1 are consistent with those reported in [13, 25].

To obtain insight into the implications of the above J_v-J_u profiles to the time domain behaviour of the closed loop, its rejection response to a step disturbance in the process input, using some selected controllers from Figure 5.1, are simulated.

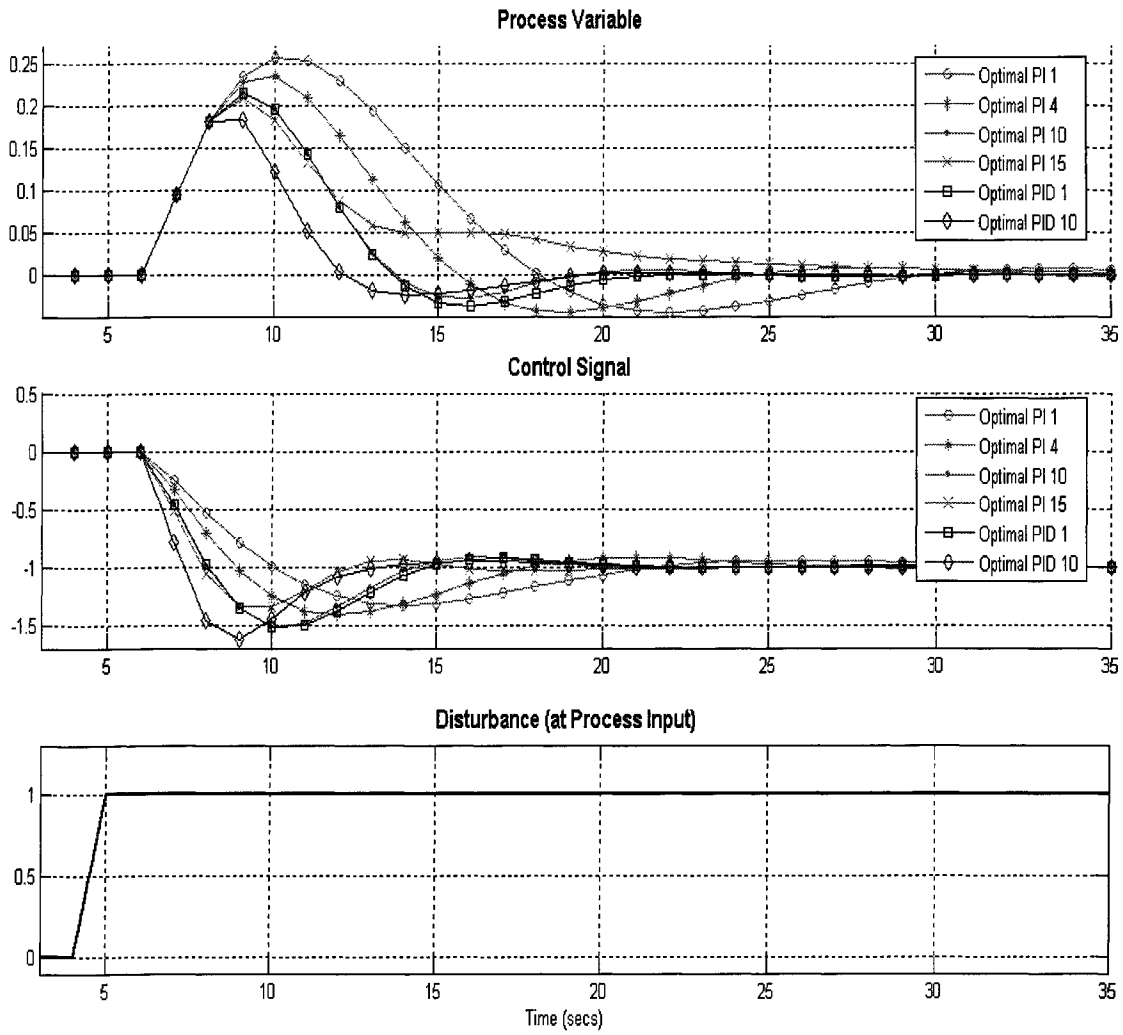

Figure 5.2: Load disturbance step response of Process 1 with selected optimal controllers from Figure 5.1.

Amongst the selected optimal controllers, Optimal PI Controller 1's step response has the highest overshoot, lowest undershoot, and the longest settling time, thus giving the lowest step response performance, which is consistent with its J_v location in Figure 5.1. Its control signal has the slowest response and longest settling time, thus leading to the observed trend in the closed-loop's step response. The control signal's trend suggests low controller gain, which explains the low value of the control activity criterion J_u.

Closed-loops with Optimal PI Controllers 4 and 10 have progressively smaller J_v values than Controller 1, as well as lower overshoots, higher undershoots and shorter settling times. Overall, their step response performances are better than Controller 1's. Their control signals have steeper responses and shorter settling times, suggesting higher controller gains (shown by their higher J_u values). Optimal PI Controller 15's closed-loop has a slightly smaller overshoot than Controllers 10's. Hence the smallest overshoot amongst the selected optimal PI controllers, but the longest settling time due to a sluggish damping of the process output's offset. The small overshoot suggests higher controller gain than the other PI controllers', which is shown by its J_u value. However, the sluggish offset damping suggests low integral action, i.e., high integral time. Thus, amongst the selected PI controllers, Optimal PI Controller 10's closed loop gives the best step disturbance response performance, which corroborates its position as a minimum point in the J_v-J_u profile for optimal PI controllers in Figure 5.1.

The closed-loop responses for Optical PID Controllers 1 and 10 have smaller overshoots than the optimal PI controllers discussed above, as well as shorter settling times. Their control signals have steeper responses and also shorter settling times, meaning higher controller gains as shown by their J_u values. The closed-loop step responses and control outputs of Optimal PI Controller 10 and Optimal PID Controller 1 appear to be nearly identical, which is to be expected from the closeness of their (J_u, J_v) coordinates in Figure 5.1.

To obtain clearer insight into the characteristics of the control signals in Figure 5.2, the parameters $\rho = [k_i, \tau, \zeta, \beta]$ of the optimal controllers are expressed in terms of the traditional PID controller structure, i.e., $[k_c, \tau_i, \tau_d, \tau_f]$ from (3.2), which are used to calculate the gains of the three components of the controller. Figure 5.3 shows the optimal PI and PID controllers' proportional gain (k_c), integral gain (k_c / τ_i), and derivative gain ($k_c \tau_d$).

Although the profile for the optimal PID controller appears to be disjointed from the optimal PI controller's, [25] shows that it is possible for the optimal PID controller's performance curve to connect to the optimal PI's at its minimum-J_v point.

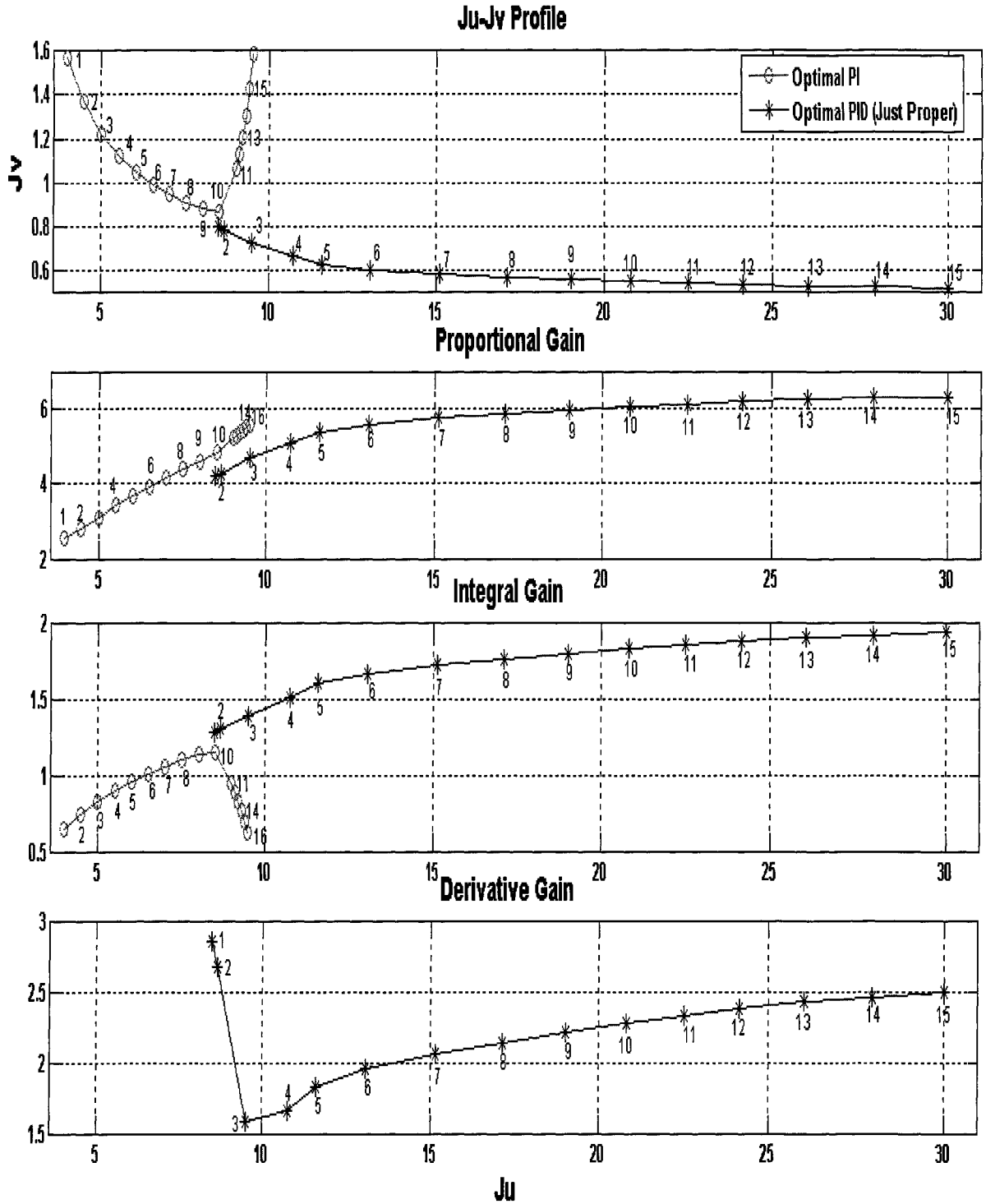

Figure 5.3: Proportional, integral and derivative gains of optimal PI and PID controllers for Process 1.

The proportional gain of the optimal PI controller increases almost linearly with J_u. Its integral gain also increases with J_u up to Controller 10, which has the

minimum J_v for the optimal PI controllers, and decreases thereafter. The optimal PI controller has no derivative gain. Hence, the improving closed-loop performance with increasing control activity between Optimal PI Controllers 1 and 10 is due to the combined effect of increasing proportional and integral gains. There is a progressive deficiency in integral action for Optimal PI Controllers 11 to 15, although the proportional gain is increasing. This explains the sluggish settling of the step response of the closed loop with Controller 15, which was observed in Figure 5.2, combined with the relatively small overshoot. Also, lack of derivative action contributes to the exponential deterioration of closed-loop performance as J_u increases beyond 8.5. The optimizer's computation of controller parameters, which increase proportional gain with J_u, at the expense of decreasing integral gain, ensures all the optimal PI controllers meet the mid-frequency robustness constraint $GM_S \leq 1.7$.

For the optimal PID controllers, both proportional and integral action increase asymptotically. There is an initial drop in the derivative action as J_u increases, after which it also increases to an asymptotic limit. The asymptotic profiles of the three gains explain the corresponding asymptote in the J_v-J_u profile of the optimal PID controllers. Consequently, although the increase in the permissible control action of the optimal PID controller buys non-deteriorating performance improvement, the diminishing returns on performance, due to the asymptote, eventually makes the increase uneconomical.

From the design and simulation of optimal controllers for the simple SISO process above, it can be concluded that if the stability (mid-frequency robustness) criterion of its closed loop is constrained, increasing the control activity limit of the closed loop leads to an improved disturbance rejection performance when either an optimal PI or PID controller is used. However, in the case of the optimal PI, the performance improvement with control activity has an upper limit, beyond which it deteriorates. With the optimal PID controller, performance also improves to an upper limit but does not deteriorate. The J_v-J_u profiles for the two groups of controllers show that optimal PID controllers can give better closed loop performance than the optimal PI controllers, and demonstrate the advantage of including the derivative (D) control portion with a PI controller in the closed loop.

The above investigation of the J_v-J_u profiles has been restricted to a stable SISO process transfer function with one pole, no zero and a small time delay. In contrast, Kristiansson presents profiles in [13] for optimal PI and PID controllers used to control SISO processes with transfer functions having a wide variety of structures, including high order and non-minimum phase structures. The results show that there is usually a corresponding minimum in the J_v/J_u graph when a PI controller is used in the closed loop, a point made in [3]. The results also show clear improvements in closed-loop performance when derivative control is utilized. For an optimal PI controller controlling a process with a first-order plus delay model, [15] shows how the minimum J_v can be calculated analytically. For non-minimum phase systems controlled by optimal PID controllers, [16]

demonstrates theoretically that a lower limit for J_v, corresponding to the asymptote, does exist.

5.3 J_v-J_u PROFILES FOR QUADRUPLE-TANK MULTILOOP

In the last section, an important feature observed in the J_v-J_u profiles was that if the GM_S criterion of a SISO optimal PI closed loop is constrained, increasing its control action criterion, J_u, improves its step response performance up to a limit, beyond which its performance deteriorates. If an optimal PID controller is used in the closed loop, its step response performance, generally better than the optimal PI's, improves with increasing control action up to an asymptotic, non-deteriorating limit. Hence, derivative control plays a significant role in enhancing closed-loop performance.

Although the profiles investigated were for SISO closed loops, the J_v-J_u graphs for the multiloops of the minimum and non-minimum phase models of the Quadruple-Tank Process would also be examined. The basis for investigating the J_v-J_u relationships for the multiloops comes from the concept of the iterative sequential loop closing method [17] discussed in Chapter 4, which allows a multiloop to be represented by a sequence of SISO closed loops. For example, the multiloop for the minimum phase dynamics of the quadruple-tank process can be expressed as decoupled SISO closed-loops Loop 1 and Loop 2 as shown in Figures 4.10(a) and 4.10(b) respectively. Hence, the J_v-J_u graphs are plotted separately for Loop 1, Loop 2, as well as Loop 3 and Loop 4 (Figures 4.16(a) and 4.16(b) respectively).

Computing the J_v-J_u profiles for the four closed-loops requires the design of a range of optimal PI and PID controllers for the minimum and non-minimum phase multiloops. **Steps 1.1** to **1.5** and **2.1** to **2.5** in Chapter 4 are followed to design the multiloops' optimal PI and PID controllers; for the just proper optimal PID, (4.31) is modified to (5.2) with $\boldsymbol{Q}$ consisting of elements ranging from 0.9 to 4.5. For the optimal PI, (4.31) is modified to

$$\min_{\rho}\{J_V(\rho): GM_S \le 1.7, J_u \in W\}; \qquad \rho = [k_i, \tau] \tag{5.3}$$

$\boldsymbol{W}$'s values range from 0.1 to 0.8. The parameters for the optimal controllers designed for the minimum and non-minimum phase multiloops can be found in Tables A.3 to A.10 of Appendix A. Figures 5.4 to 5.7 show the J_v-J_u profiles for the four loops mentioned above.

The performance-control action characteristics for the four loops are similar to Figure 5.1, thus providing the same comparative assessment on the closed-loop performance of optimal PI and PID controllers. In the multiloop for the two phases of the Quadruple-Tank Process, optimal PID controllers can give improved performance in the level responses of the two lower tanks, compared to optimal PI controllers.

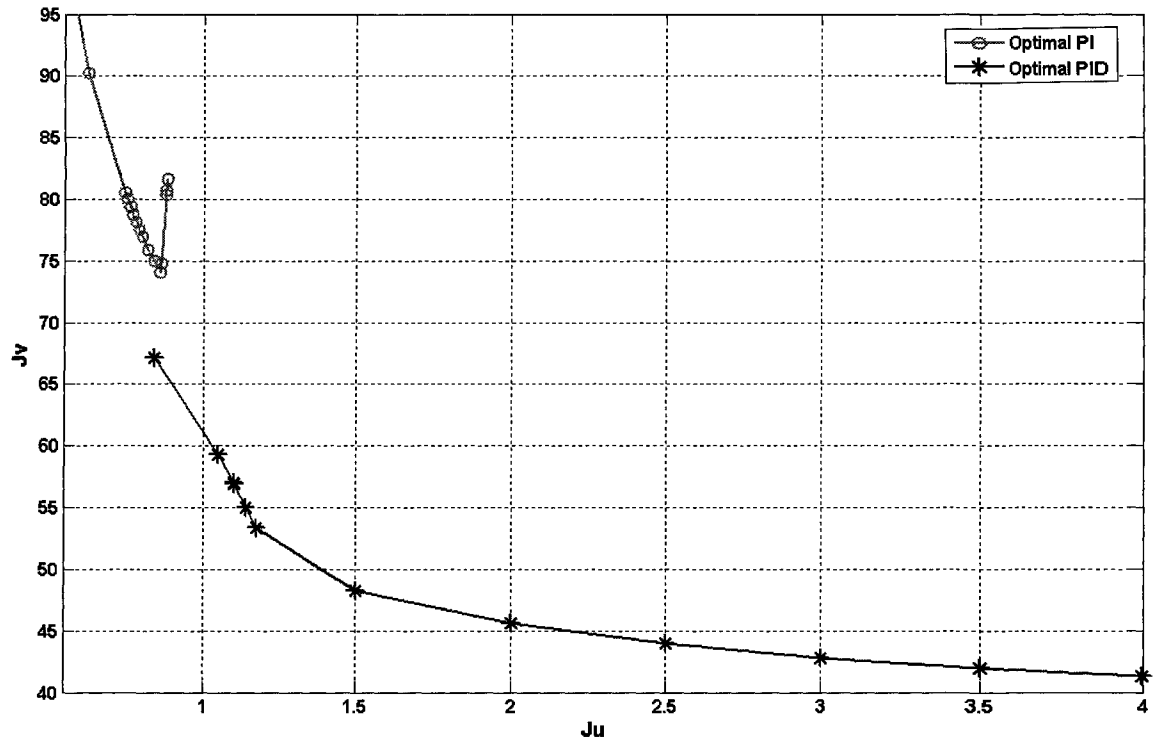

Figure 5.4: J_V-J_u profiles for Loop 1 of the minimum phase multiloop of the Quadruple-Tank Process using optimal PI and optimal (just proper) PID controllers. $GM_S \leq 1.7$.

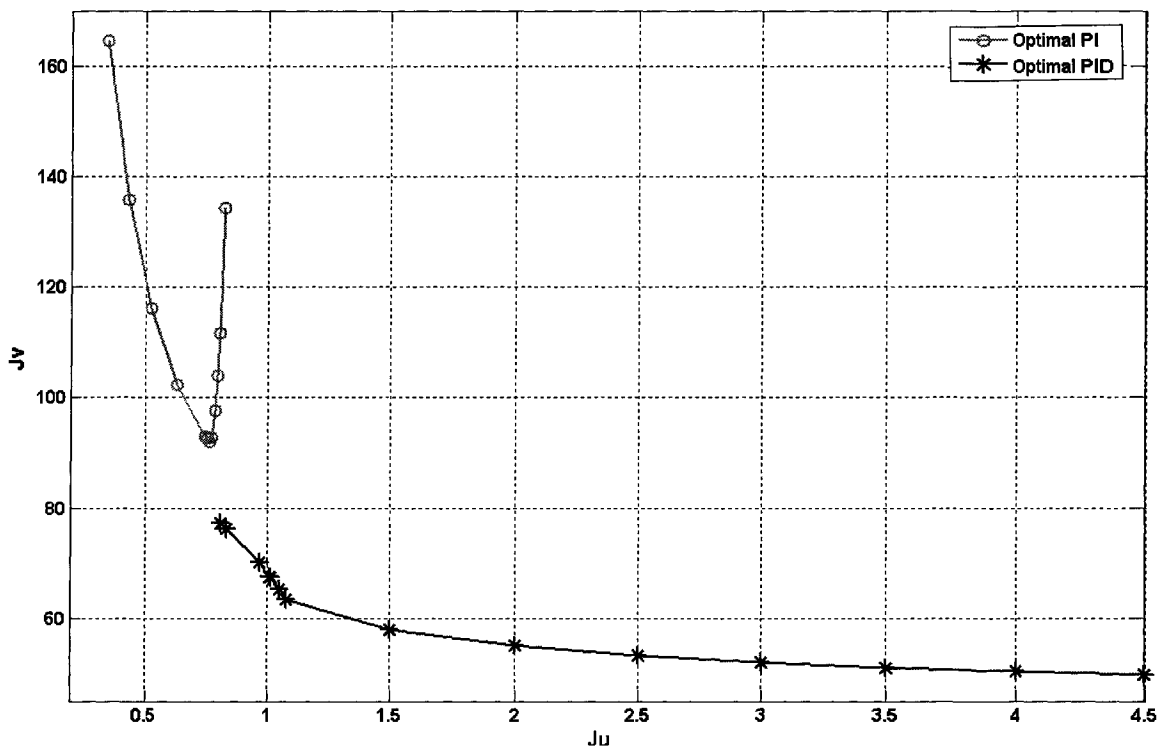

Figure 5.5: J_V-J_u profiles for Loop 2 of the minimum phase multiloop of the Quadruple-Tank Process using optimal PI and optimal (just proper) PID controllers. $GM_S \leq 1.7$.

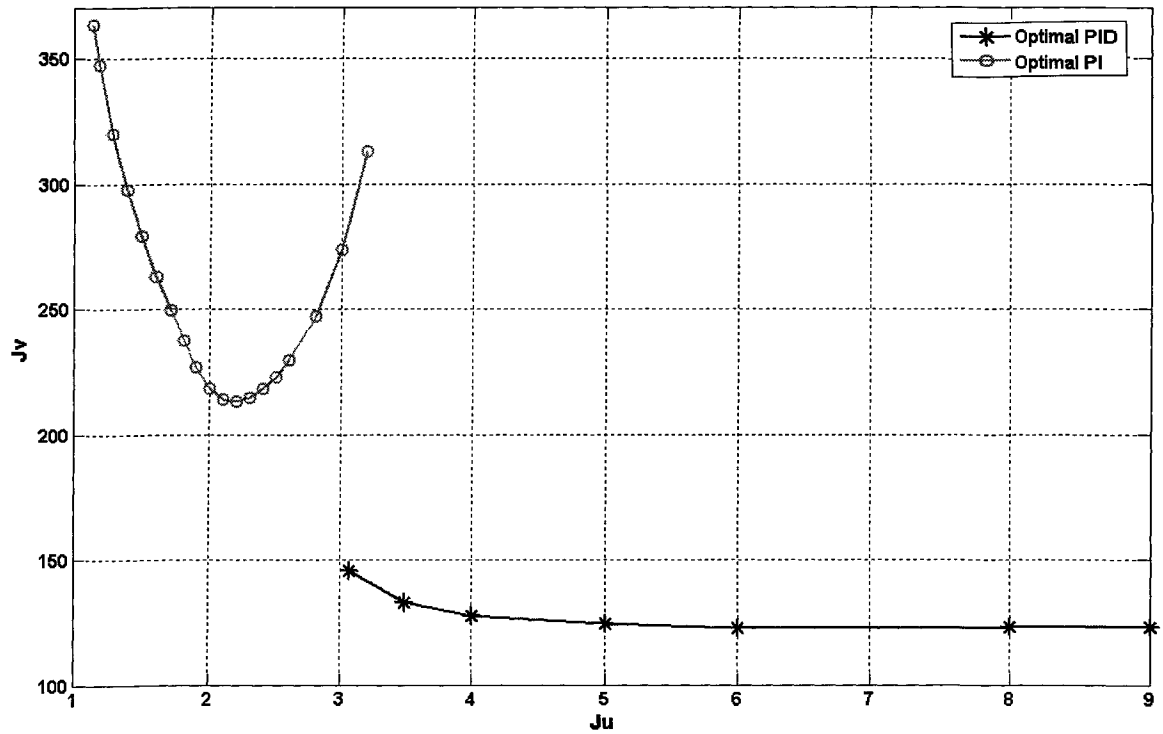

Figure 5.6: J_v-J_u profiles for Loop 3 of the non-minimum phase multiloop of the Quadruple-Tank Process using optimal PI and optimal (just proper) PID controllers. $GM_S \leq 1.7$.

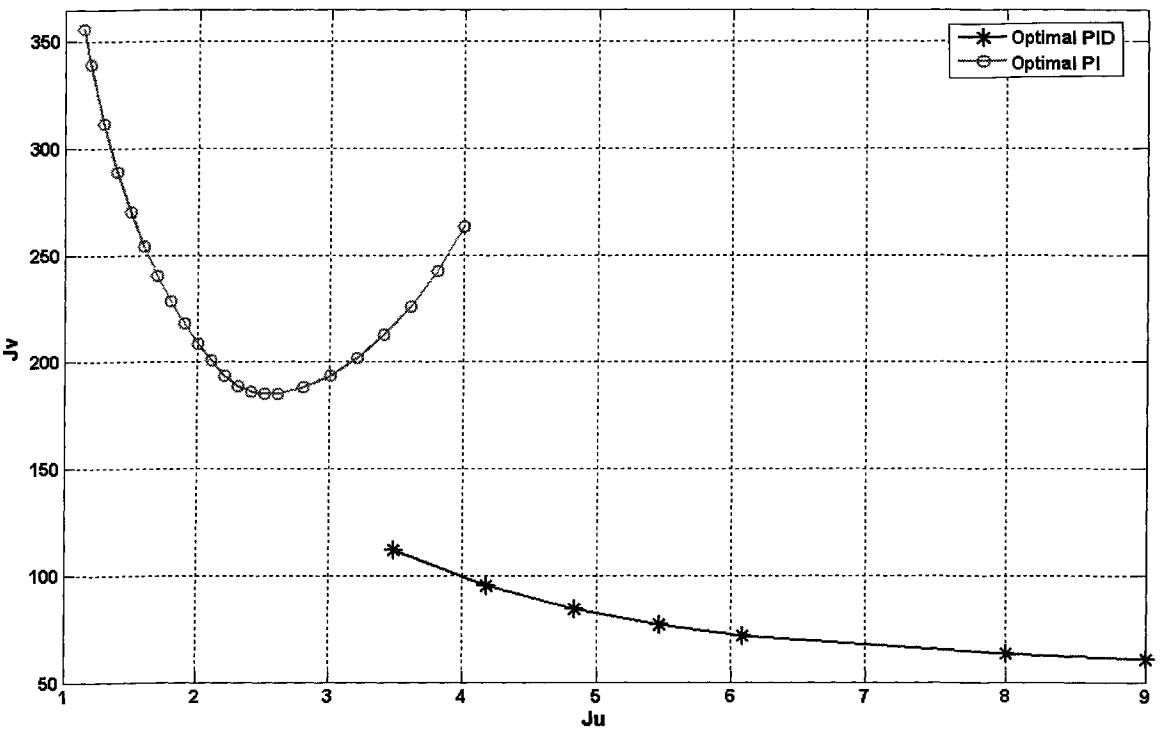

Figure 5.7: J_v-J_u profiles for Loop 4 of the non-minimum phase multiloop of the Quadruple-Tank Process using optimal PI and optimal (just proper) PID controllers. $GM_S \leq 1.7$.

5.4 TIME DOMAIN EVALUATION CRITERIA

J_u and J_v are criteria for evaluating a closed loop's control activity and low frequency disturbance rejection performance respectively. Their mathematical definitions in (2.17) and (2.10) respectively imply that transfer functions for both the process and the controller are required to compute them. In industry, process models are not always available. Where they are available, variations in process dynamics may render existing models invalid and make their regular updating necessary. Thus, computations of the two criteria for industrial control loops may not always be accurate: closed-loop evaluations and controller comparisons may be misleading. Furthermore, with (2.17) and (2.10) being frequency domain-based criteria, physically relating them to controller aggressiveness and loop performance may not be straightforward to a plant operator. On the other hand, the insights provided by the J_v-J_u graphs in Figure 5.1 and 5.4, concerning closed-loop properties would be useful in assisting process engineers and operators tune control loops.

Thus, it would be desirable to represent the observed performance-control action characteristics for closed loops of optimal PI and PID controllers, described by the J_v-J_u profiles, using criteria that can be physically related to the loop properties being evaluated and easily comprehended. It would also be convenient to be able to compute these criteria using process information readily available to the plant operator, such as sampled time domain data for the closed loop's process output and the control signal.

In Chapter 2, J_v was shown to be approximately equal to $1/k_i$, the inverse of the PID controller's integral gain, which is equal to the integral of the error signal, *IE*. For small undershoots in load step disturbance, *IE* was shown to be approximately equal to *IAE*, the integral of the absolute error. *IAE* is considered the most common SISO closed-loop performance index. Another well-known index for SISO closed loops is the integral of the squared error, *ISE*. They are defined in [4, 14] as:

$$IAE = \int |e(t)|dt \tag{5.4}$$

$$ISE = \int e(t)^2 dt \tag{5.5}$$

For closed loops with disturbance rejection control objectives, $r(t) = 0$. Therefore

$$e(t) = -y(t)$$

$$|e(t)| = |y(t)|$$

$$e(t)^2 = y(t)^2$$

If process data are sampled for duration, t_f, that is sufficiently long to capture the closed loop's settling response at the attainment of steady state, then for disturbance rejection, (5.4) and (5.5) respectively become

$$IAE \approx \int |y(t)| dt \tag{5.6}$$

$$ISE \approx \int y(t)^2 dt \tag{5.7}$$

Thus, *IAE* and *ISE* are measures that could be applied to evaluate closed-loop performance in the same way as J_v. Moreover, they can be easily calculated from the sampled data for the process output, *y(t)*.

The above time-domain performance measures are for SISO closed loops. It would be of interest to measure the performance of a multiloop using a time domain criterion. A 2 x 2 multiloop performance criterion is proposed in this thesis for the Quadruple-Tank Process is $NORM[e_L, e_R]$, defined as:

$$NORM[e_L(t_f), e_R(t_f)] = \sqrt{\sum_{t=0}^{t_f} \left(e_L(t)^2 + e_R(t)^2\right)}, \tag{5.8}$$

where e_L and e_R are the error signals for Loops 1 and 2 (or Loops 3 and 4) respectively. Again, for disturbance rejection, (5.8) can be written in terms of the process output, instead of the error signals. For the Quadruple-Tank Process, h_L and h_R are its multiloop's process outputs. (5.8) then becomes:

$$NORM[e_L(t_f), e_R(t_f)] = \sqrt{\sum_{t=0}^{t_f} \left(h_L(t)^2 + h_R(t)^2\right)} \tag{5.9}$$

As the performance of a closed loop/multiloop improves, the values of the aforementioned time domain performance measures are expected to decrease, just like J_v, but otherwise increase.

The control activity criterion, J_u, is based on the control sensitivity function, S_u, which is the transfer function between sensor noise, *w(t)*, and the control signal, *u(t)*. Its value increases as the gain of the transfer function increases. As an illustration, consider a SISO closed loop, whose controller parameters can be altered so that its J_u value varies. If the process output, *y(t)*, of the closed-loop response is corrupted by the same stochastic sensor noise signal each time the controller parameters are altered, it is expected that the degree of stochasticity, or volatility, of the loop's control signal, due to S_u, would increase as the J_u value

of the loop increases. For stochastic systems, [43] mentions the variance of the control signal, *u(t)*, as a likely measure of control activity. However, a time domain criterion proposed in this thesis for measuring control activity of a disturbance rejection closed loop is the variance of the *differenced* control signal, $VAR[\Delta u]$. The differenced signal, Δu, is obtained from the control signal through the relationship:

$$\Delta u(t) = u(t) - u(t-1); \qquad t = 1,2,...,t_f \tag{5.10}$$

Differencing the control signal calculates the trend in which the control signal's value changes from one sampling instance to another. Calculating the variance of the differenced signal measures the overall amplitude of value changes in the control signal, thus measuring the volatility of the signal. Therefore, it is expected that a control signal significantly affected by sensor noise, or by a stochastic disturbance like coloured noise, would possess an equally significant degree of volatility, and hence a high variance for its differenced signal.

For a SISO closed loop tracking a set point signal, the proposed measure for control activity is the *Median of Absolute Deviation* (MAD) of the differenced control signal, which is discussed in [55]. It is defined as:

$$MAD[\Delta u] = MEDIAN\Big|_{t=0}^{t_f} \{|\Delta u(t) - MEDIAN[\Delta u(t)]|\} \tag{5.11}$$

For the Quadruple-Tank Process' multiloop, a time domain evaluation criterion proposed for the combined control activity of its controllers is $VAR[\Delta u_L, \Delta u_R]$, given by:

$$VAR[\Delta u_L, \Delta u_R] = VAR[\Delta u_L + \Delta u_R] \tag{5.12}$$

5.5 TIME DOMAIN PERFORMANCE-CONTROL ACTIVITY EVALUATION CRITERIA FOR QUADRUPLE-TANK MULTILOOP

Having discussed several time domain evaluation criteria for measuring the performance and control action of a control system, the next step is to apply these criteria to the multiloop of the Quadruple-Tank Process and compare their performance-control activity profiles with those given by J_v and J_u in Figures 5.4 to 5.7. Because these criteria rely on process data for their computation, it becomes necessary to implement the multiloop using the controllers designed in Section 5.3, and obtain data for the system's response for each pair of controllers implemented. Controller implementation is carried in simulation, via SIMULINK, and experimentally on the Quadruple-Tank Process in the laboratory. The following loop excitation experiments are performed and response data sampled:

Excitation 5.1: Set point step in r_L introduced to Loop 1, while keeping r_R and disturbance inputs d_L and d_R at their nominal values.

Excitation 5.2: Set point step in r_L introduced to Loop 3, while keeping r_R and disturbance inputs d_L and d_R at their nominal values.

Excitation 5.3: Step in disturbance d_L introduced to Loop 1, while keeping d_R and set point inputs r_L and r_R at their nominal values.

Excitation 5.4: Step in disturbance d_R introduced to Loop 3, while keeping d_L and set point inputs r_L and r_R at their nominal values.

Excitation 5.5: Set point step in r_R introduced to Loop 2, while keeping r_L and disturbance inputs d_L and d_R at their nominal values.

Excitation 5.6: Set point step in r_R introduced to Loop 4, while keeping r_L and disturbance inputs d_L and d_R at their nominal values.

Excitation 5.7: Step in disturbance d_R introduced to Loop 2, while keeping d_L and set point inputs r_L and r_R at their nominal values.

Excitation 5.8: Step in disturbance d_L introduced to Loop 4, while keeping d_L and set point inputs r_L and r_R at their nominal values.

Excitation 5.9: Steps in disturbances d_L and d_R introduced to multiloop of minimum phase process, while keeping set point inputs r_L and r_R at their nominal values.

Excitation 5.10: Steps in disturbances d_L and d_R introduced to multiloop of non-minimum phase process, while keeping set point inputs r_L and r_R at their nominal values.

Figures 5.8 to 5.21 show the performance-control activity profiles for the above excitation experiments, computed using the time domain evaluation criteria.

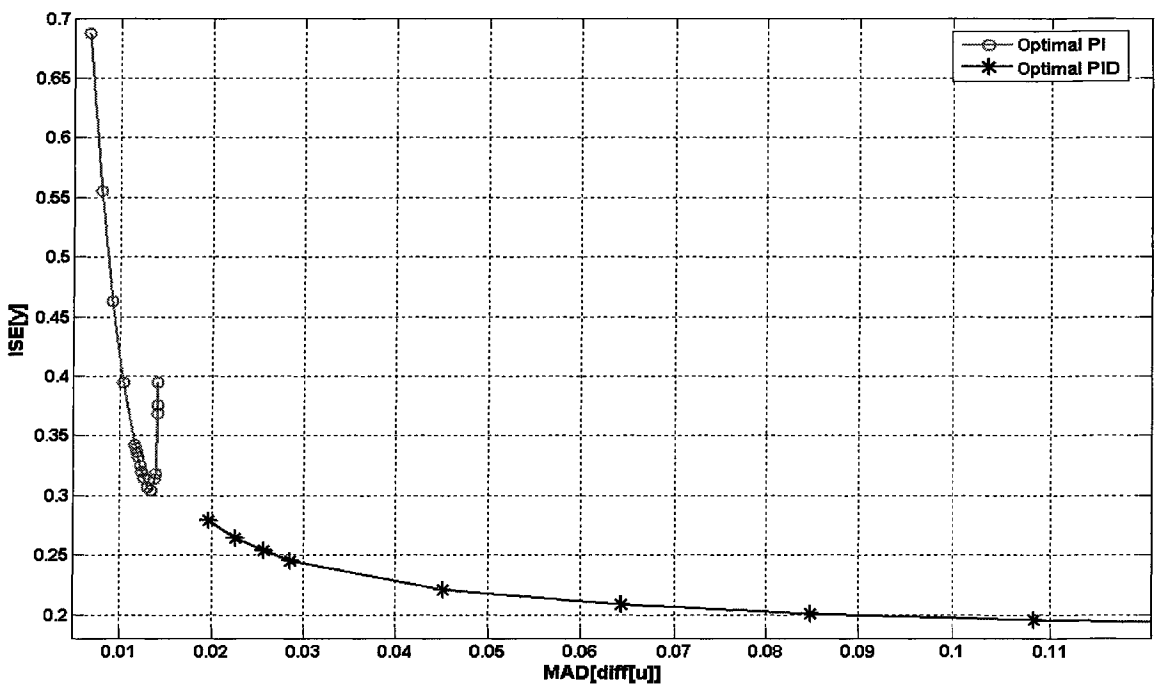

Figure 5.8: *ISE*[*y*]-*MAD*[Δu] profiles for **Excitation 5.5** implemented in simulation.

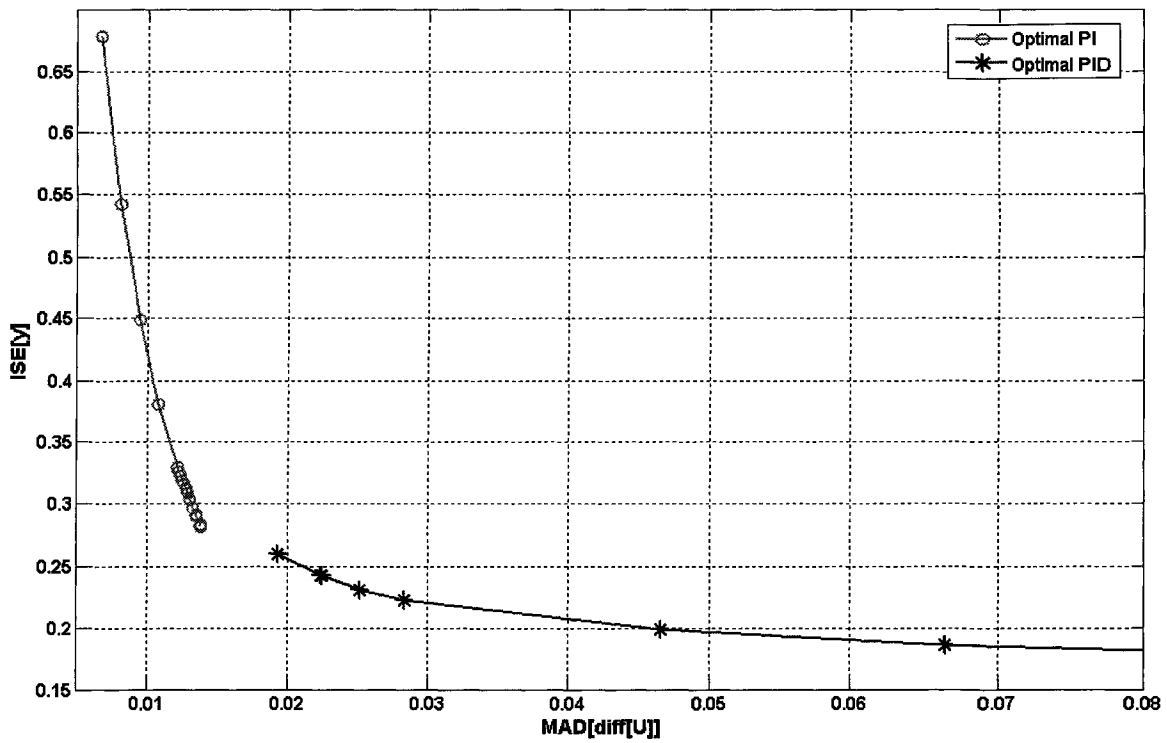

Figure 5.9: *ISE*[*y*]-*MAD*[Δu] profiles for **Excitation 5.1** implemented in simulation.

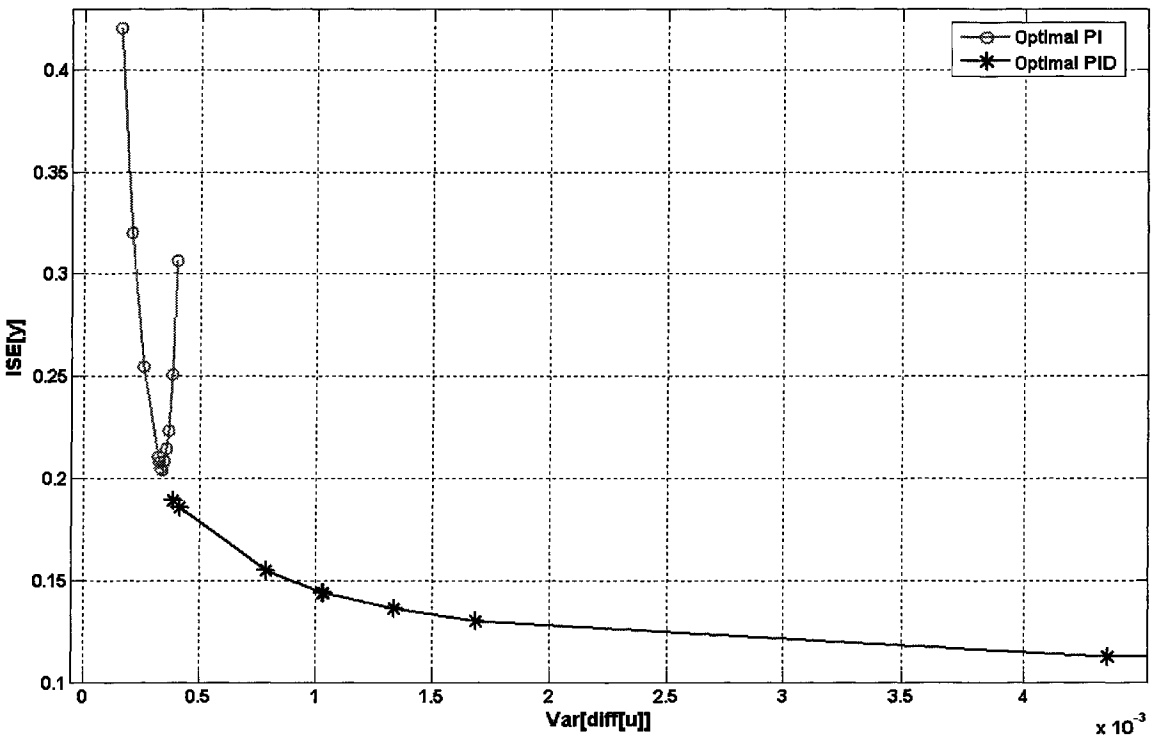

Figure 5.10: *ISE*[*y*]-*VAR*[Δu] profiles for **Excitation 5.7** implemented in simulation.

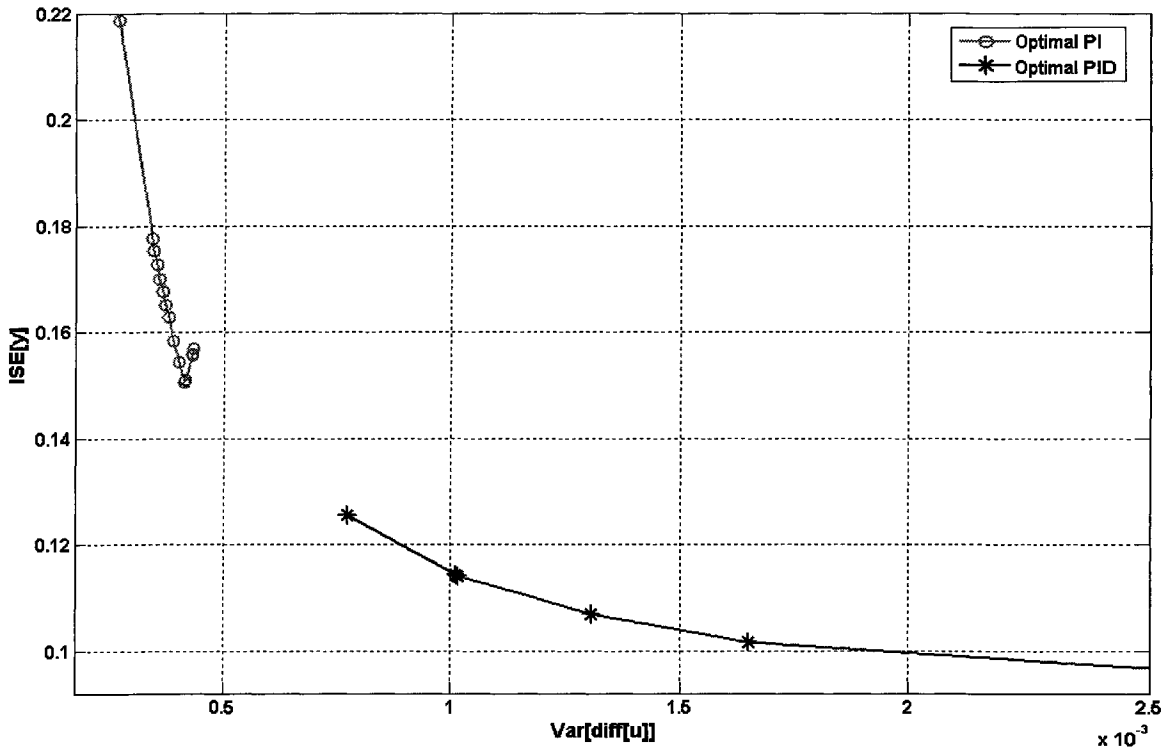

Figure 5.11: *ISE*[*y*]-*VAR*[Δ*u*] profiles for **Excitation 5.3** implemented in simulation.

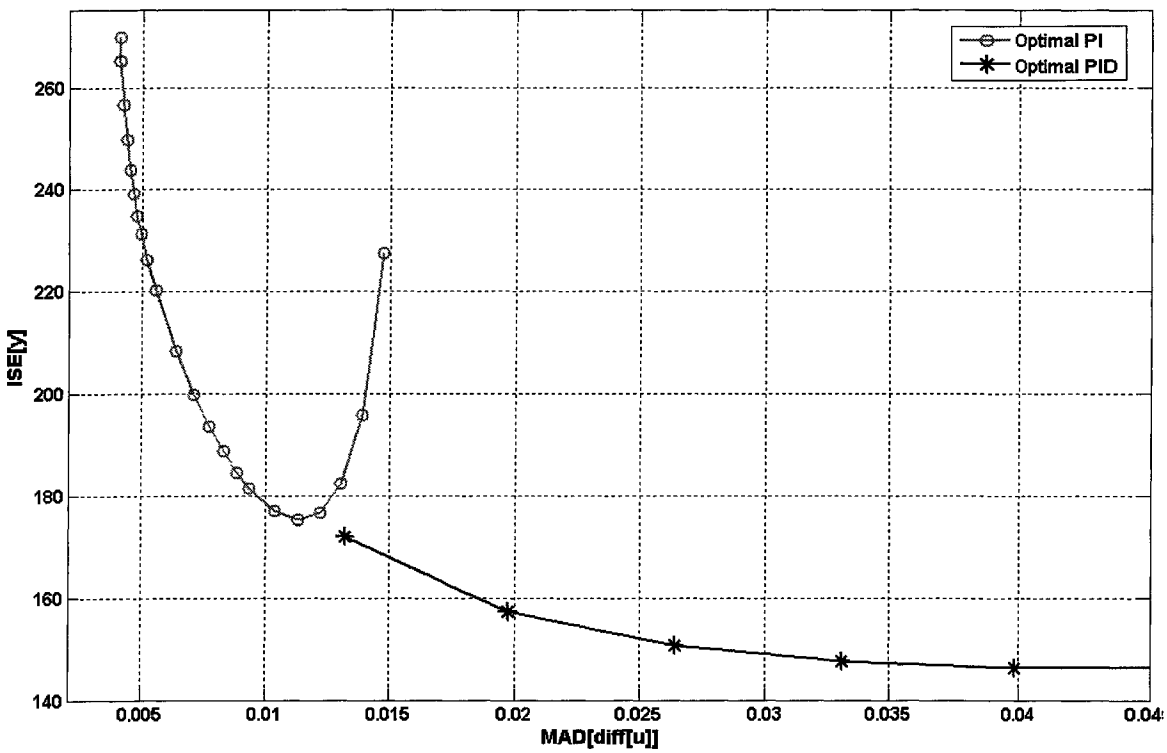

Figure 5.12: *ISE*[*y*]-*MAD*[Δ*u*] profiles for **Excitation 5.2** implemented in simulation.

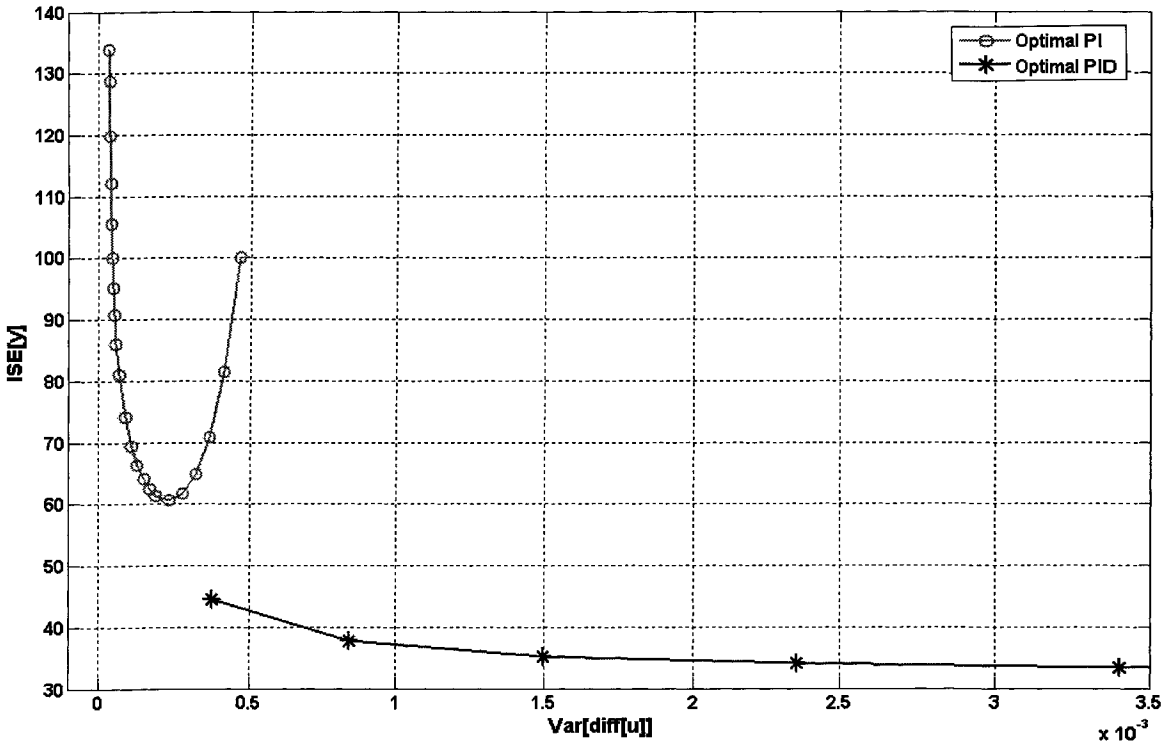

Figure 5.13: *ISE*[*y*]-*VAR*[Δu] profiles for **Excitation 5.4** implemented in simulation.

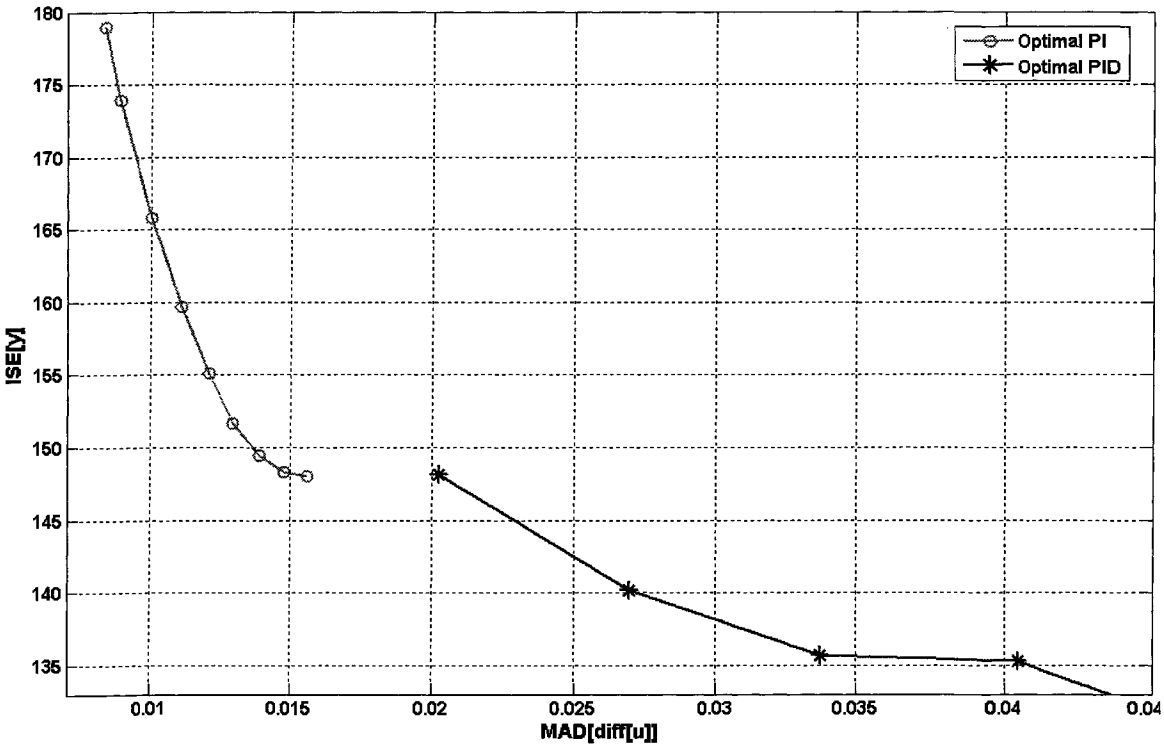

Figure 5.14: *ISE*[*y*]-*MAD*[Δu] profiles for **Excitation 5.6** implemented in simulation.

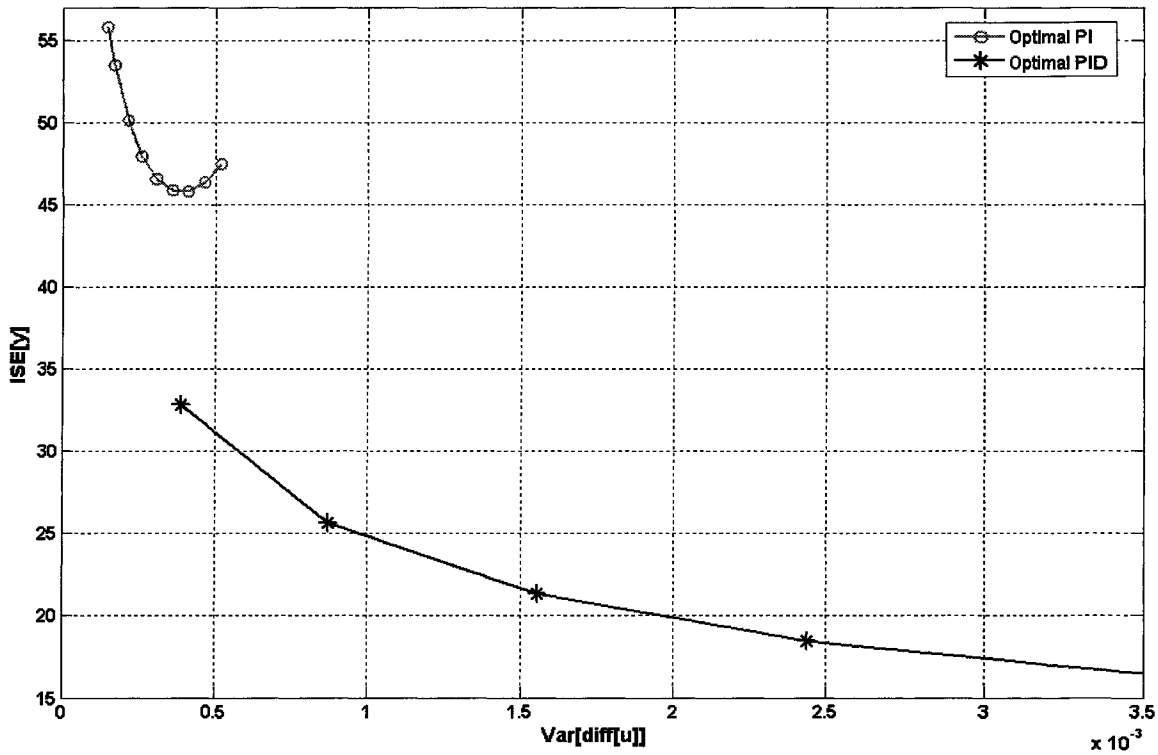

Figure 5.15: *ISE*[*y*]-*VAR*[Δu] profiles for **Excitation 5.8** implemented in simulation.

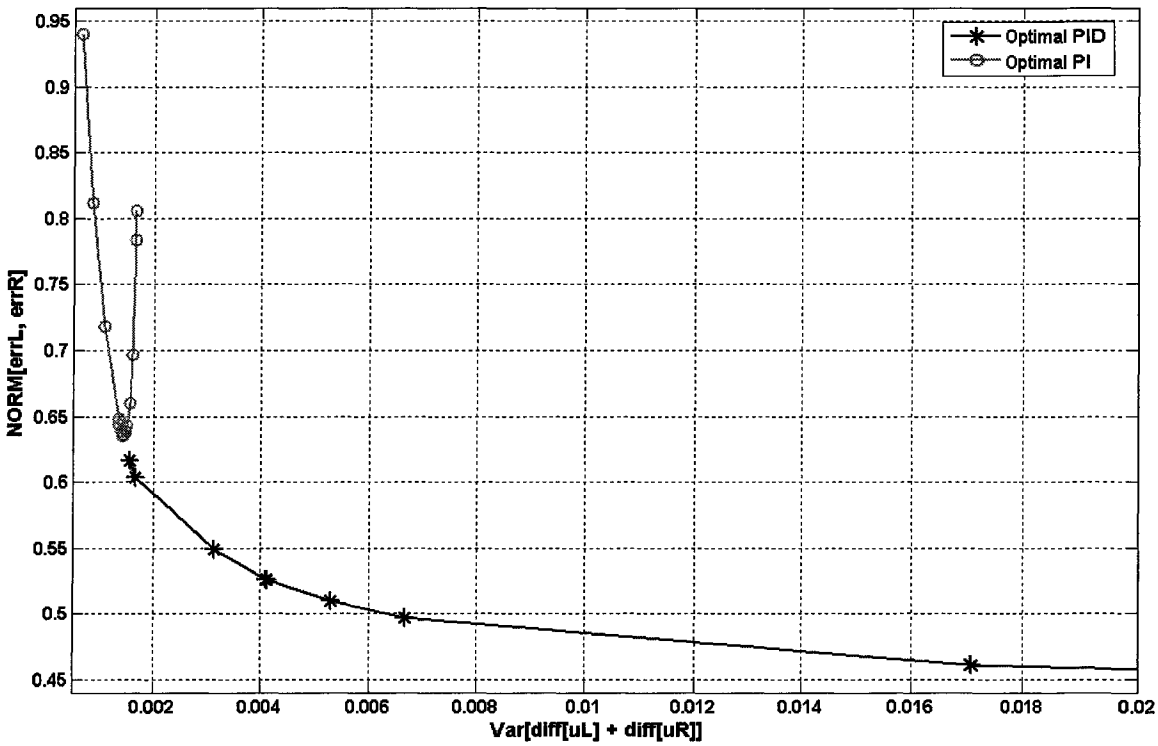

Figure 5.16: *NORM*[e_L, e_R]-*VAR*[Δu_L + Δu_R] profiles for **Excitation 5.9** implemented in simulation.

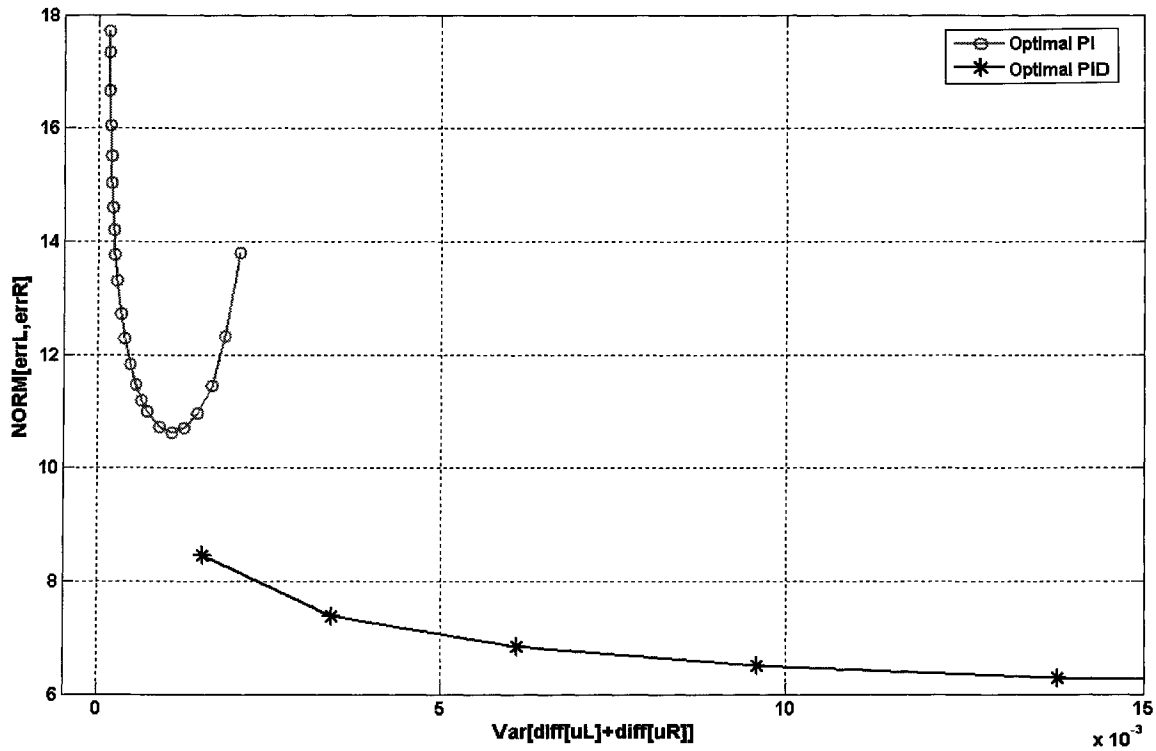

Figure 5.17: *NORM*[e_L, e_R]-*VAR*[Δu_L + Δu_R] profiles for **Excitation 5.10** implemented in simulation.

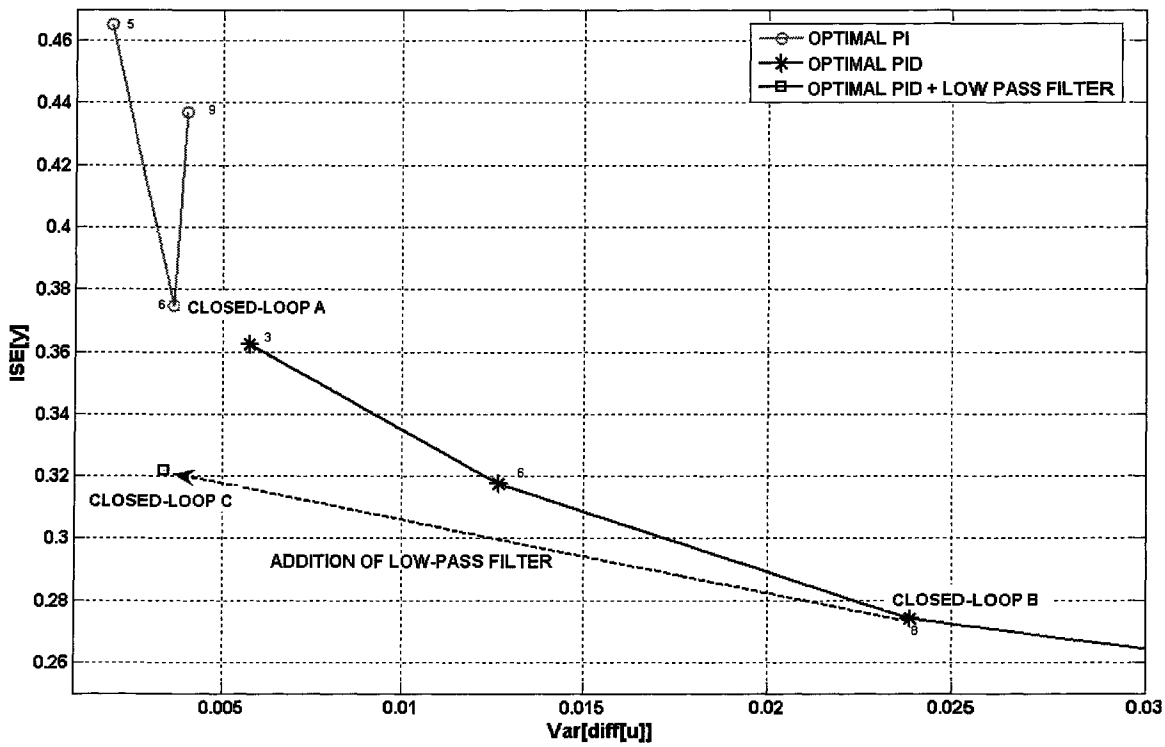

Figure 5.18: *ISE*[*y*]-*VAR*[Δu] profiles for **Excitation 5.3** implemented experimentally on Quadruple-Tank Process.

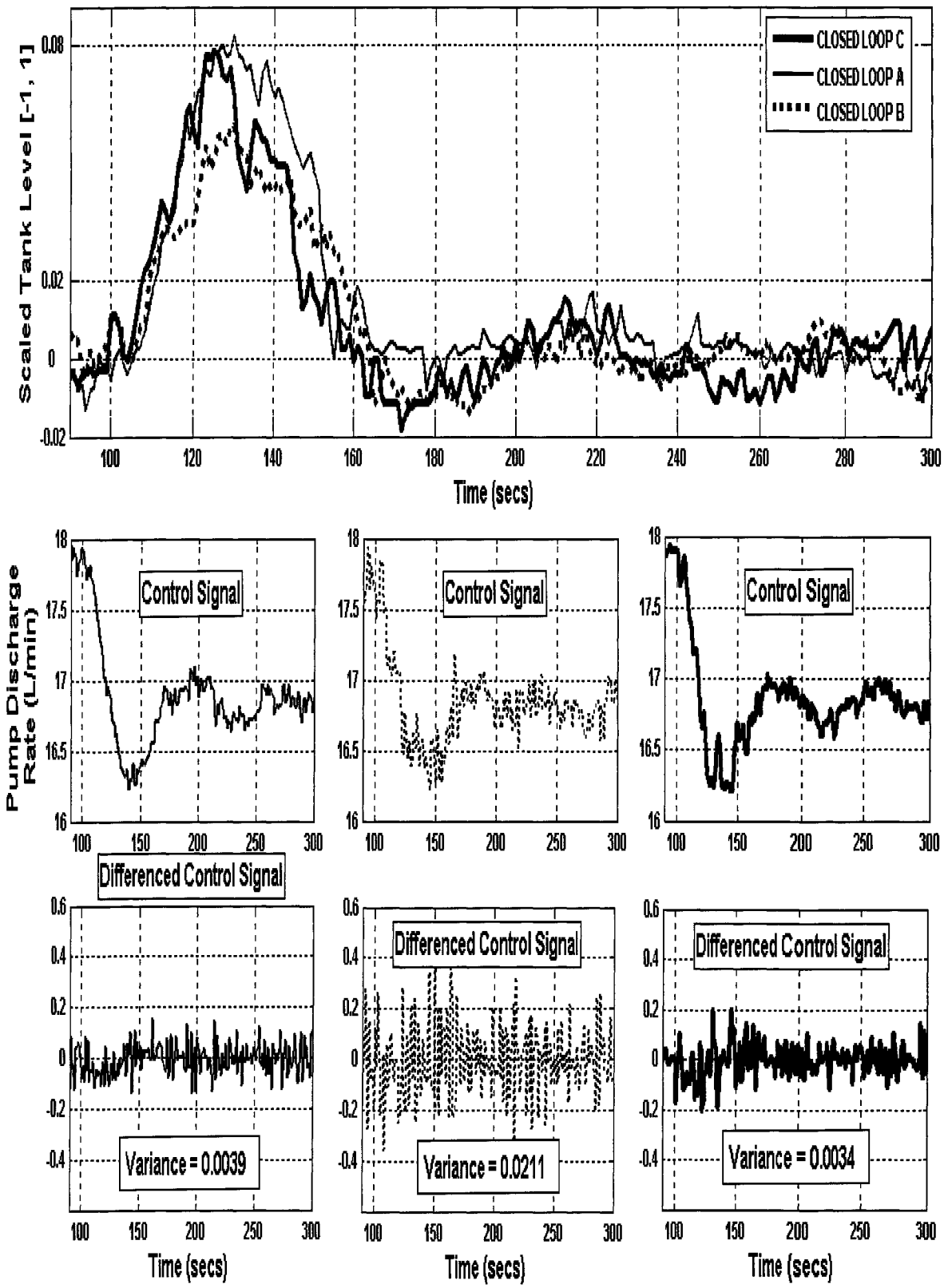

Figure 5.19: Response of selected closed loops (in Figure 5.17) from **Excitation 5.3** implemented experimentally on Quadruple-Tank Process.

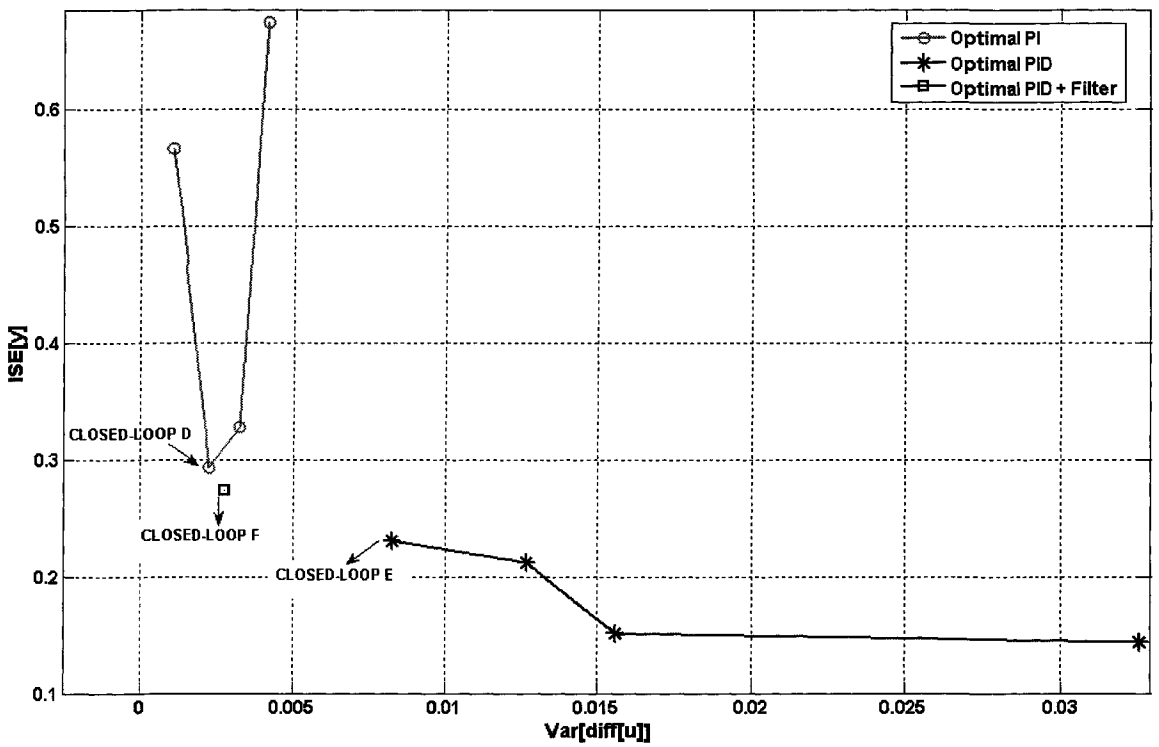

Figure 5.20: *ISE*[*y*]-*VAR*[Δu] profiles for **Excitation 5.7** implemented experimentally on Quadruple-Tank Process.

Based the experimental implementation of the optimal controllers, the process output, control signal and differenced control signal are shown in Figures 5.19 and 5.21 for the closed loops of the optimal PI controller (whose closed loop has the smallest *ISE*[*y*] value), a selected optimal PID controller with a first order filter, and an optimal PID controller with a second order filter.

The performance-control activity plots, obtained using the time domain-based evaluation criteria, show the same profiles obtained with J_v and J_u in Figures 5.4 to 5.7. The optimal PID controllers generally give better closed-loop performance than the optimal PI controllers. However, as shown by the *VAR*[Δu] values in those figures, the price to be paid by the PID controllers for improved performance is greater control activity. The optimal PID controllers with second order filters generate less control activity than the PID controllers with first order filters. There is, however, a slight deterioration in performance. Thus, the second order-filtered PID controllers improve the performance of the PI controllers and generate control activity less aggressive than the first order-filtered PID controllers.

The time domain criteria also show, in agreement with the J_v-J_u profiles, that the performance of the optimal PID controller is asymptotic, i.e., performance improvement with increasing control activity is progressively marginal until no significant improvement is achievable.

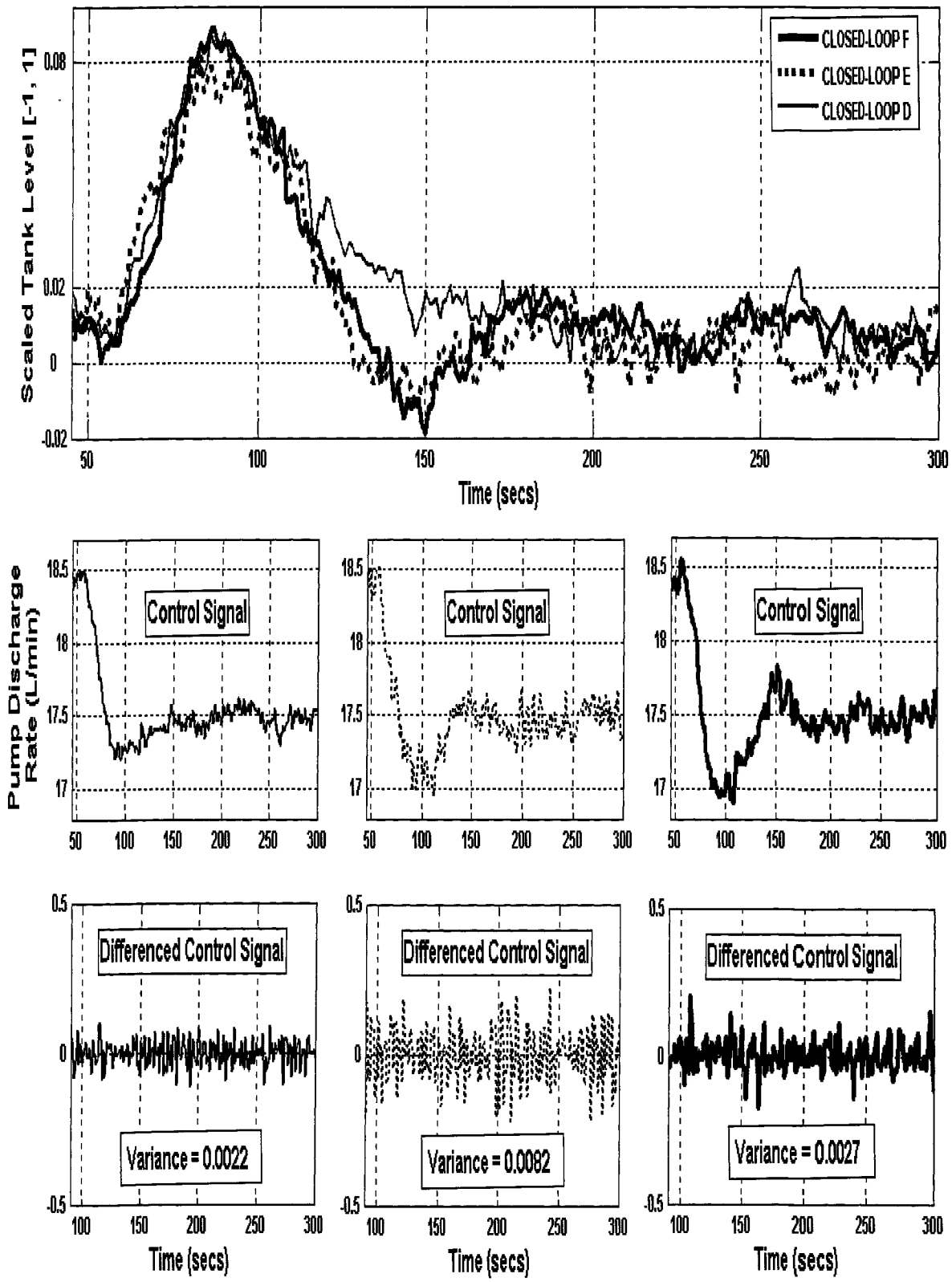

Figure 5.21: Response of selected closed loops (in Figure 5.19) from **Excitation 5.7** implemented experimentally on Quadruple-Tank Process.

The tank level responses from the simulation of Closed Loops A, B, C, D, E, and F showed similar behaviour to the experimental time trends in 5.19 and 5.21 and supported the performance comparisons shown in Figures 5.18 and 5.20 respectively, i.e. inclusion of derivative control improves the closed-loop performance of the PI controller and careful filtering of its control signal makes it as moderate as the plain PI controller's.

5.6 TRADE-OFFS FOR PROCESSES WITH VARIOUS TIME DELAY-TIME CONSTANT RATIOS

An attractive feature of the control system evaluation method [25] is that the performance criteria of various control systems can be compared while other property criteria are constrained equally for all the systems. If these systems use the same controller structure but different processes, then it is possible to gain some insight to how process dynamics influence closed-loop performance. Process dynamics is one of the factors that limit the achievable performance of a control system [5, 18, 19].

The influence of a process' time delay on the closed-loop's performance is of major interest, as quite a number of industrial processes have significant dead times due to the presence of distance velocity lags, recycle loops, and the analysis time associated with composition measurement. The presence of process time delay limits the performance of a conventional feedback control system. In terms of a feedback loop's frequency response, time delay adversely affects the system's stability by adding phase lag to the loop. Consequently, the controller gain must be reduced below the value that can be used if no time delay were present, and the response of the closed loop would be sluggish compared to that of the delay-free process. Many processes can be represented by a first-order-plus-dead-time (FOPTD) model:

$$G(s) = \frac{Ke^{-\theta s}}{\tau s + 1}$$

A typical measure of the dominance of the time delay in a process is the *fractional dead time*, also known as the *normalized dead time* [4], defined as $\theta/\theta+\tau$. In this thesis, θ/τ, i.e., the time delay-time constant ratio, is used. In this section, the J_V-J_U profiles for feedback loops of simple, hypothetical processes with small to moderate time delay-time constant ratios, and using optimal PI and PID controllers, are computed to study the benefits of derivative action as the ratio increases. Table 5.1 shows the transfer functions for the processes. Their time delay-time constant ratios vary from 0.1 to 0.4, but their gains and time constants are unaltered. Figure 5.22 shows the J_V-J_U profiles of the closed loops for the processes controlled by optimal PI and PID controllers.

Table 5.1: Transfer Functions and Time Delay-Time Constant Ratios of Simple Processes

PROCESS MODEL	TIME DELAY – TIME CONSTANT RATIO
$\frac{24.37e^{-15.47s}}{154.7s+1}$	0.1
$\frac{24.37e^{-30.94s}}{154.7s+1}$	0.2
$\frac{24.37e^{-46.41s}}{154.7s+1}$	0.3
$\frac{24.37e^{-61.88s}}{154.7s+1}$	0.4

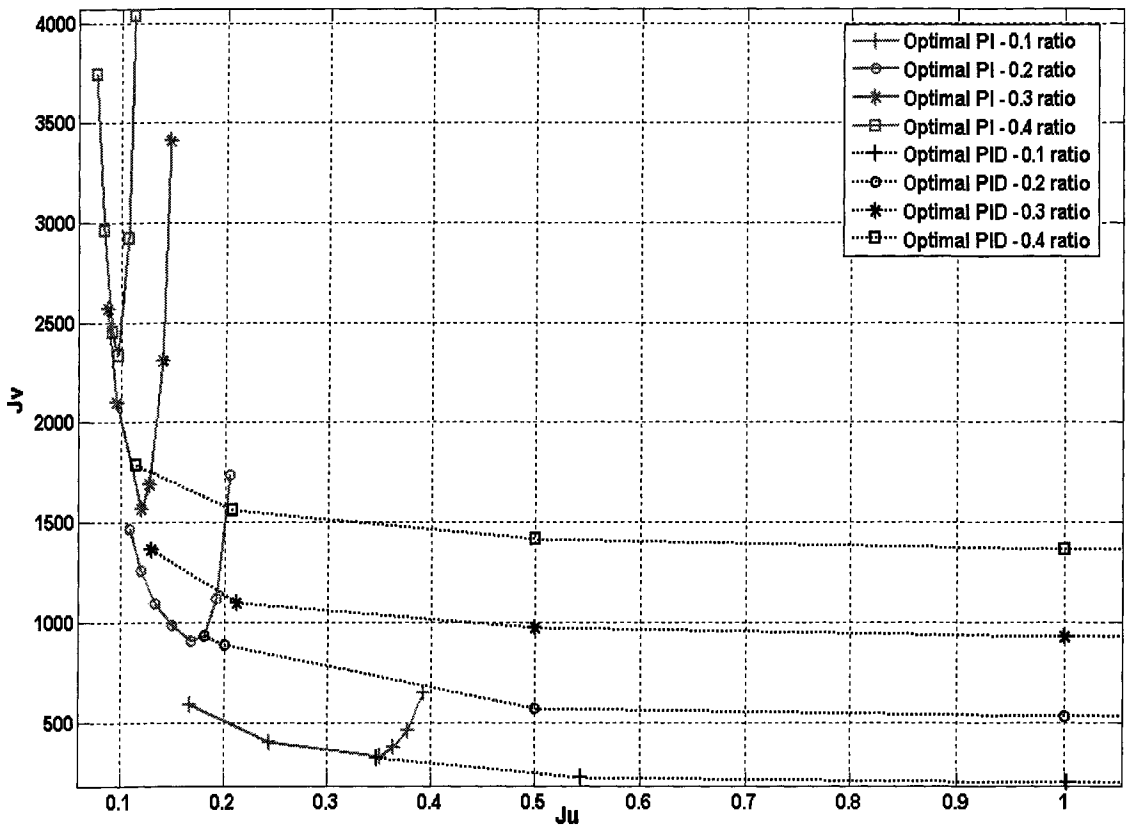

Figure 5.22: J_V-J_u profiles of closed loops for processes in Table 5.1 using optimal PI and optimal (just proper) PID controllers. $GM_S \leq 1.7$.

The J_V-J_u profiles in Figure 5.22 show the already-discussed performance improvement derivative control brings to a PI-controlled closed loop. Additionally, they show that the performance of closed loops using either PI or PID controllers generally deteriorates as the process' time delay dominance increases. Thus, for processes that are highly time delay-dominated, the PID control algorithm might

not be adequate for meeting control objectives, in which case other algorithms and control schemes should be considered.

Another interesting feature of the profiles in Figure 5.22 is that as the time delay dominance in a process increases, the performance gap between the optimal PID closed loop's J_v asymptote and the minimum-J_v point of the optimal PI closed loop increases. Thus, even though the PID structure is not the best control system for processes with large time delays, inclusion of derivative control makes a significant difference in the performance of the PI controller. This improvement is due to the predictive property of the derivative controller, which is able to estimate future, un-sampled values of the process output via linear extrapolation and generate the corrective control action based on the estimate before the actual output is sampled. However, for most processes, linear extrapolations do not provide accurate predictions of future outputs [5], thus requiring other techniques for improved predictions. At the same time, generating control action for a future process output measurement, based on a linearly-extrapolated prediction, is of greater benefit than control action based on the actual, but delayed, measurement. Moreover, the mid-frequency constraint of $GM_S \leq 1.7$, imposed on all closed loops in Figure 5.22, implies that the controllers optimized for the processes with greater time delays must have smaller controller gains to retain closed loop stability. The reduction in controller gains, as shown by the decreasing J_u values of the PI controllers, with minimum J_v values in Figure 5.22, implies reduced controller aggressiveness, which in turn implies reduced performance capability. Thus, the closed loop performance of the PI controller deteriorates significantly as the process' time delay increases, and its performance gap from the PID closed loop also increases.

The time domain evaluation criteria applied to the loops of the Quadruple-Tank Process are also applied to the closed loops of the processes in Table 5.1, the objective being to see whether the performance-control activity profiles in Figure 5.22 can also be represented by these criteria. In this case, two forms of disturbance would be introduced to the closed loops: a step in the disturbance at the process input, and an integrated white noise signal added to the process output. An integrated white noise signal is obtained by sending a Gaussian white noise signal through an integrating filter $1/s$. Figure 5.23 shows the block diagram for generating an integrated noise signal and the time plots of the unfiltered and filtered signals. Figures 5.24 and 5.25 show the SIMULINK block diagrams for the closed loops excited by step and integrated white noise disturbances respectively.

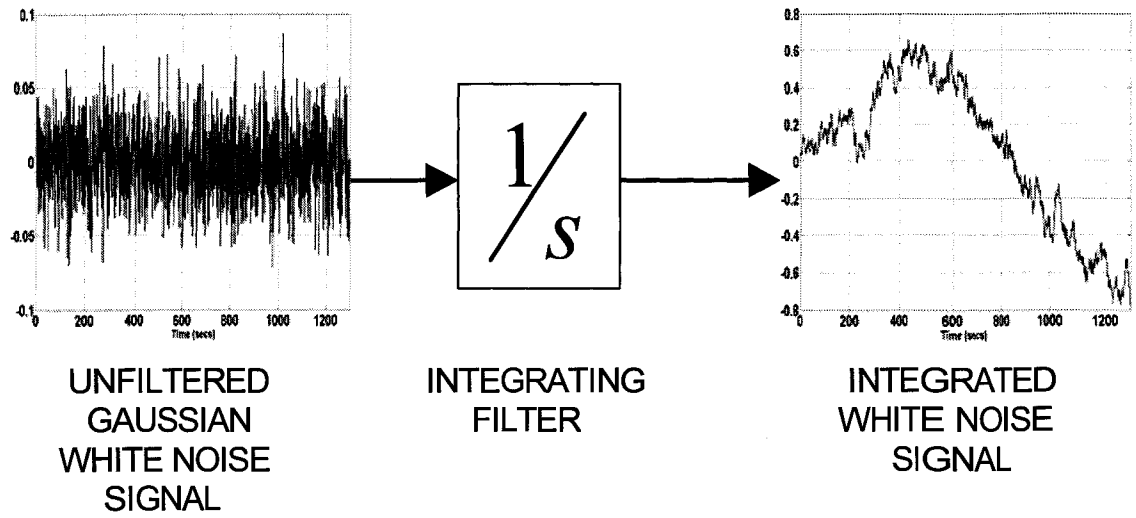

Figure 5.23: Generation of integrated noise disturbance from Gaussian white noise signal.

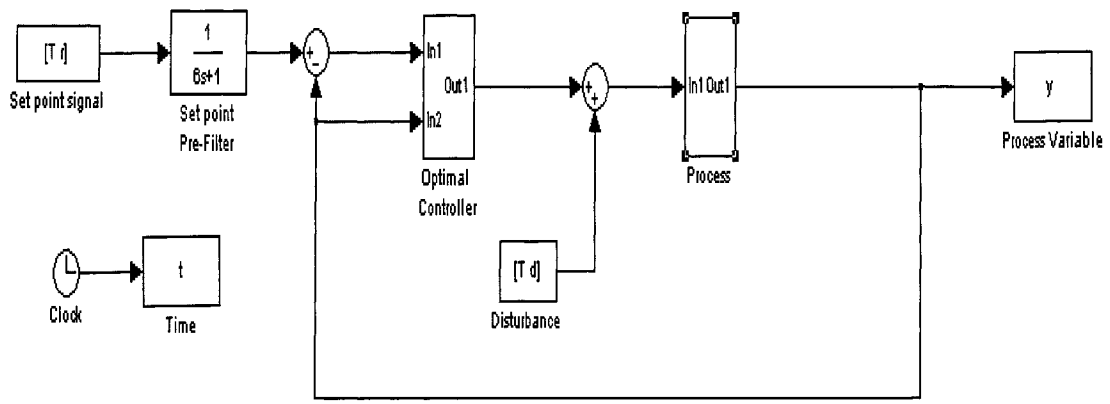

Figure 5.24: SIMULINK block diagram for closed loop with step disturbance introduced at process input.

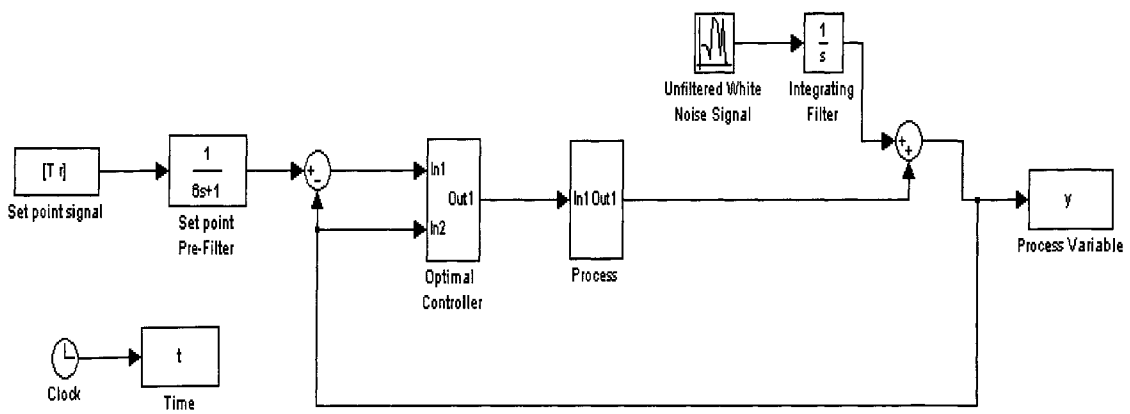

Figure 5.25: SIMULINK block diagram for closed loop with integrated white noise disturbance introduced at process output.

To plot the performance-control activity profiles for the closed loops of the processes using the time domain evaluation criteria, the following excitation experiments are performed on the SIMULINK closed loops and response data sampled:

Excitation 5.10: Step in process input disturbance, *d*, while keeping other exogenous variables at nominal values.

Excitation 5.11: Integrated white noise disturbance introduced to process output, while keeping set point, *r*, and input disturbance, *d*, at nominal values.

Excitation 5.12: Step in set point, *r*, while keeping other exogenous variables at nominal values.

Figures 5.26 to 5.28 show the performance-control activity profiles for the above excitation experiments, computed using the time domain evaluation criteria.

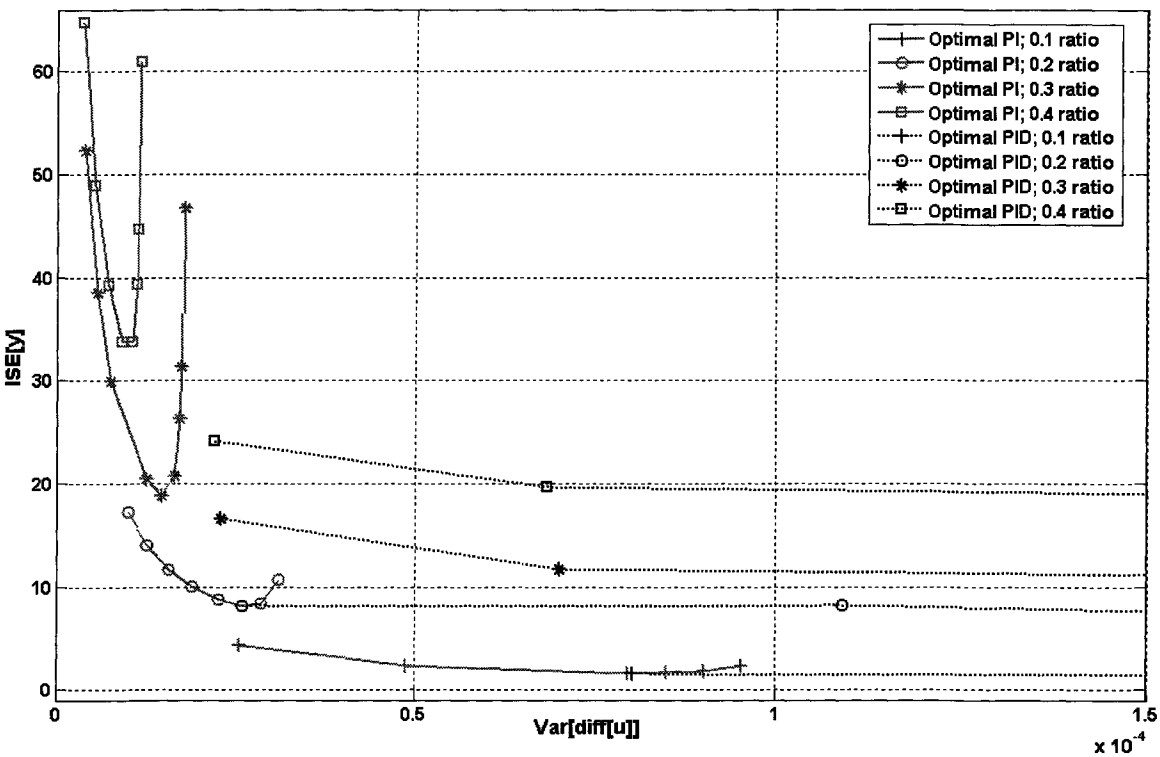

Figure 5.26: *ISE*[*y*]-*VAR*[Δu] profiles for **Excitation 5.10** implemented in simulation.

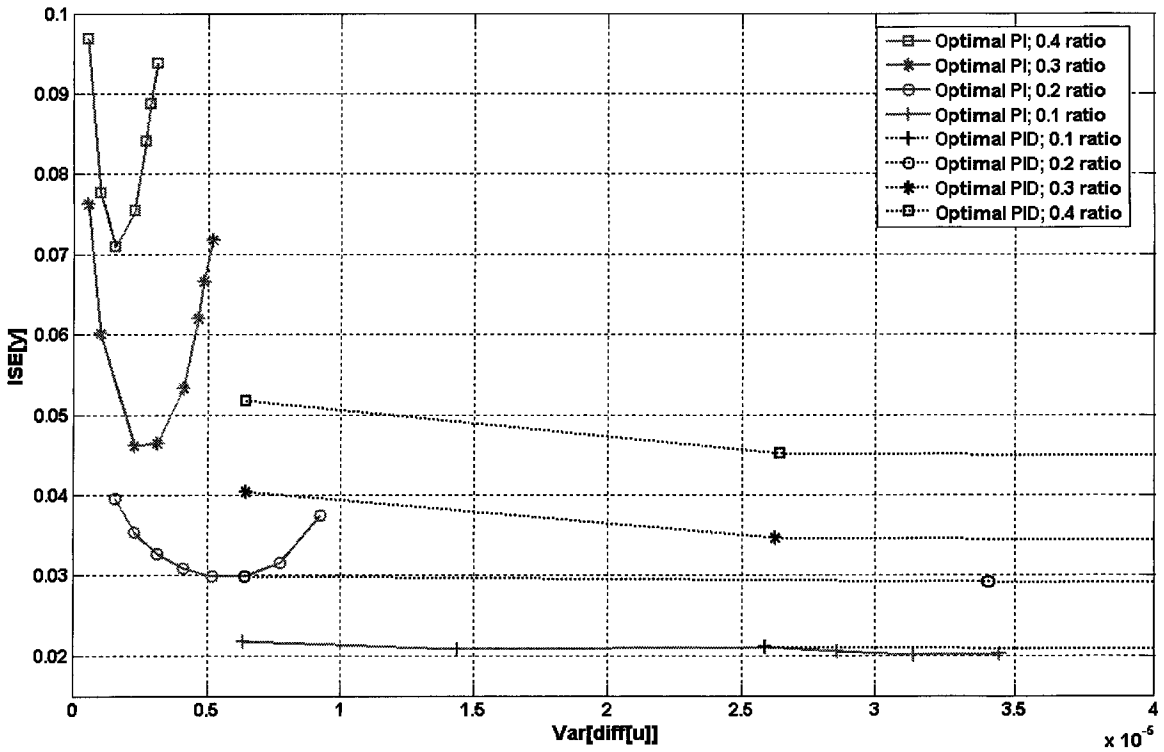

Figure 5.27: *ISE*[*y*]-*VAR*[Δu] profiles for **Excitation 5.11** implemented in simulation.

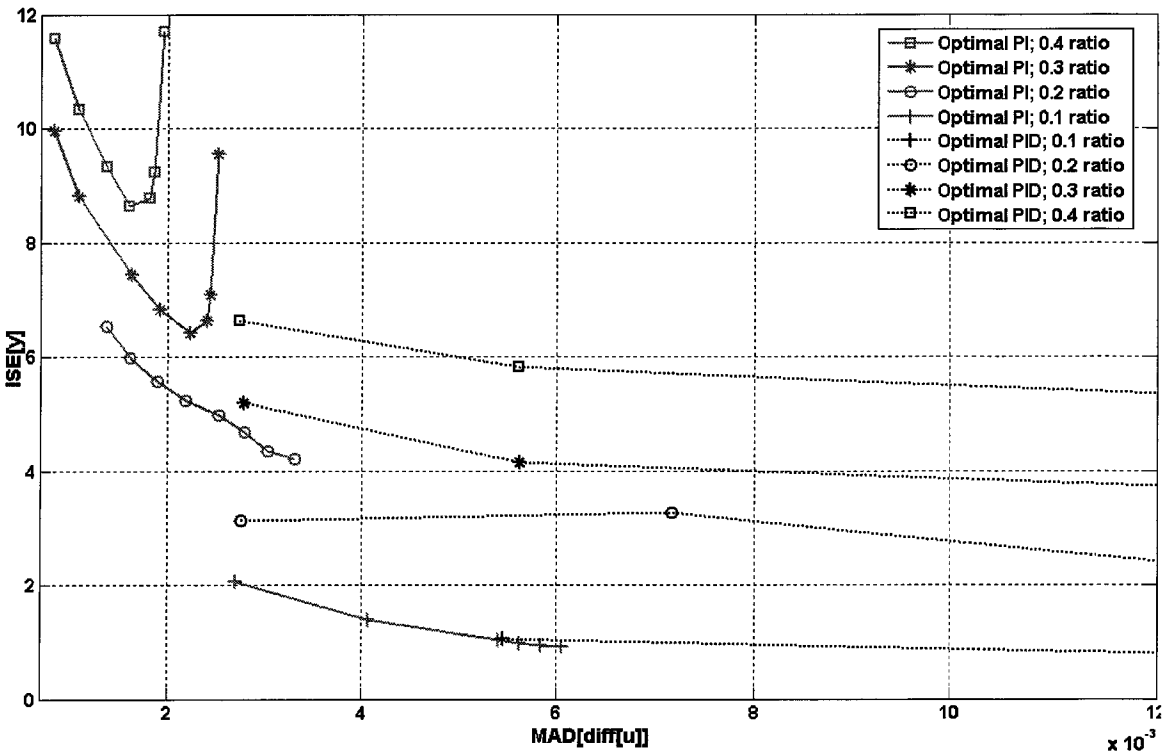

Figure 5.28: *ISE*[*y*]-*MAD*[Δu] profiles for **Excitation 5.12** implemented in simulation.

The profiles in Figures 5.26 to 5.28 are consistent with those in Figure 5.22. The PI controller's closed-loop performance is highly restricted for processes with significant time delays. On the other hand, the asymptotic profile of the PID controller shows a progressively widening performance gap from the PI controller. Hence, for closed loops of dead time-dominated processes, in which the control structure options are restricted to PI or PID controllers, performance benefits are obtainable by implementing the PID controllers instead of the PI controllers. First or second order filtering of the PID control signal can be applied to reduce its aggressiveness, if found to be excessive. Since the above conclusion has been drawn from closed-loop simulations and using hypothetical process transfer functions, it would be desirable to validate it on a real process having adjustable dead time dominance features. Such a process will be discussed in the next chapter.

CHAPTER 6

THE HEATED TANK PROCESS

6.1 INTRODUCTION

In Chapter 5, closed-loop simulations of processes with various degrees of time delay dominance showed that time delay imposes limitations on the performance of optimal PI and PID controllers, and moreover that the performance gap between optimal PI and PID controllers widens as the delay dominance becomes more significant. Thus, the simulations showed that for time delay dominated control systems, in which controller choice is restricted to either the PI or PID structure, the derivative action of the PID controller gives it an advantage over the PI controller in terms of its potential for performance improvement. The next step is to experimentally confirm the simulation results through a pilot-scale process.

The Heated Tank Process will be considered for the experimental investigation. It has a process output sensor configuration that allows the time delay dominance of its dynamics to be alterable; this feature will be discussed in the next section. Thus, one of the research objectives to be addressed in this chapter is the implementation of open-loop excitation experiments on the Heated Tank Process and identification of linear, time-invariant, continuous-time models, having various values of the time delay-time constant ratio, from the sampled response data. The other objective is the design of optimal PI and PID controllers for the models, by solving (2.21), and implementation of their closed loops in simulation and experimentation. The performance-control activity profiles for the closed loops will be computed using the J_V-J_u criteria, as well as the time domain evaluation criteria discussed in Chapter 5.

6.2 PROCESS DESCRIPTION

The Heated Tank system consists of a transparent glass tank. The system has a cold-water inlet, which introduces water into the tank from the utilities line. The system has a heating coil located inside the tank, near its base. Steam flowing through this coil from the utilities line heats the water in the tank. The tank has two outlet lines, each with a valve that controls the flow-rate of water exiting the tank. The first outlet line enables the direct discharge of water from the tank, while the second line allows the flow of the exiting water into a winding pipe; thermocouples are inserted at various points along the pipe's length to measure the water temperature. A computer interface, consisting of the Emerson's Delta V hybrid DCS and MATLAB OPC DA Toolbox, facilitates the implementation of various experiments on the heated tank system, ranging from process identification to controller implementation. Three controllers in the Delta V system control the flow of the steam and cold-water into the tank:

a) The Cold-Water Flow Controller (FIC-104), which facilitates the manual or automatic control of cold-water flow into the tank;

b) The Steam Controller (FIC-105), for the manual or automatic control of steam flow through the heating coil in the tank; and

c) The Water Level Controller (LIC-101), which regulates the water level in the tank around a set point.

The diagram in Figure 6.1 illustrates the set-up of the heated tank system, showing the tank, flow outlet lines and valves, the steam coil, plus the flow and level controllers.

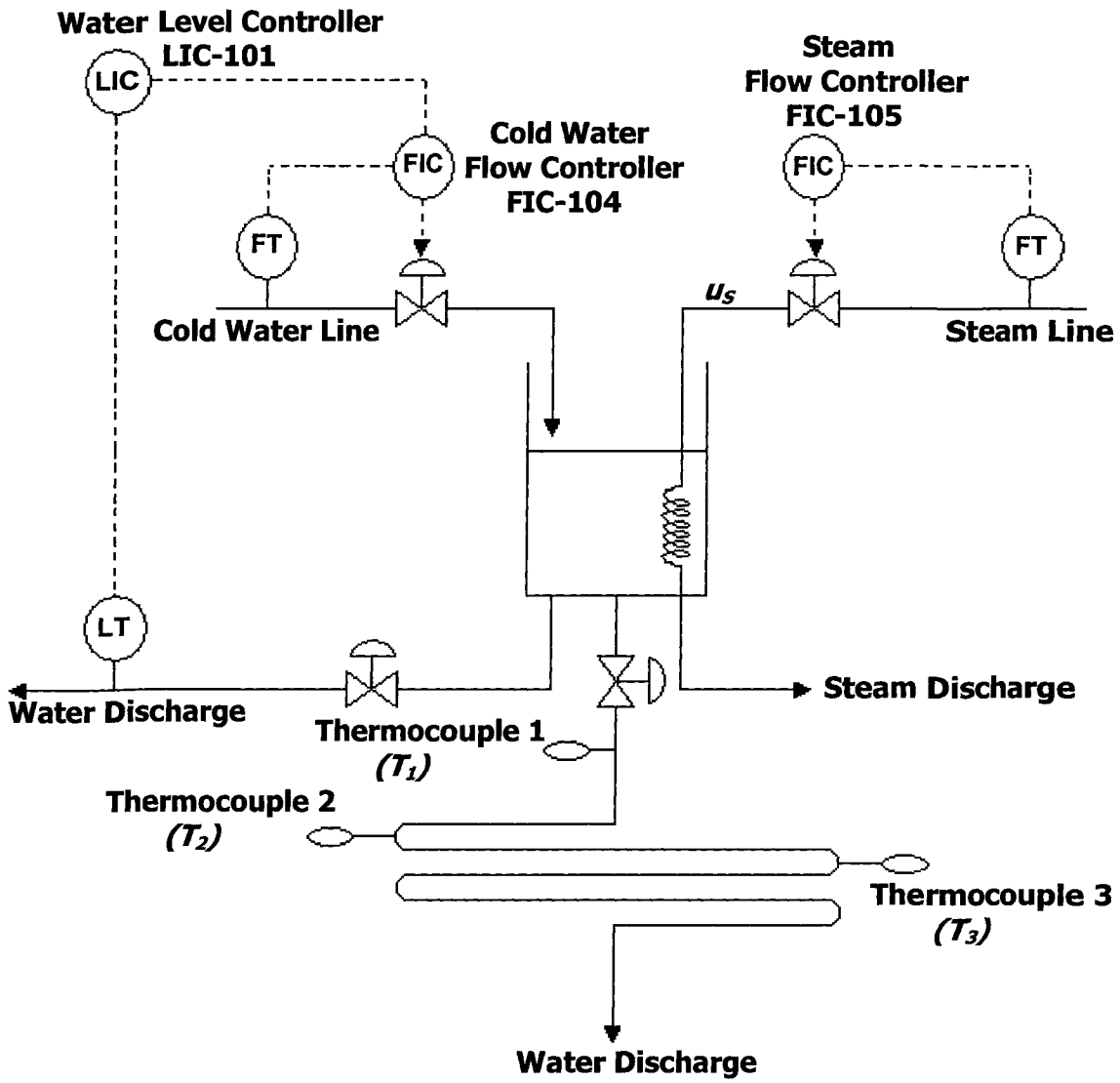

Figure 6.1: Process schematic of the Heated Tank Process.

The cold-water controller introduces water into the tank, which exits the tank via the outlet lines. Due to the flow resistance at the outlets, the water is retained in the tank, thereby causing its level to rise until a constant level is attained. Next,

the steam controller sends steam through the coil and heats the water in the tank. The thermocouples on the winding pipe measure the temperature of the exiting water at various distances from the tank. The farther the thermocouple's distance from the tank outlet, the longer the delay in its measurement of the water temperature. The cold-water controller can be cascaded with the level controller, so that the configuration keeps the water level in the tank constant at a chosen set point.

MATLAB OPC DA Client makes it possible to construct the input sequences for the steam flow rates, introduce them to the system and record the input and output data. The Delta V DCS provides the interface between the OPC DA client and the physical system.

The following assumptions are made about the process conditions:

a) There is thorough mixing of cold and heated water in the tank, so that the water temperature is homogenous;

b) Heat loss/gain along the winding pipe is negligible;

c) The water level in the tank is kept constant by the level controller;

d) The closed-loop dynamics of the steam controller is negligible;

e) Convective heat transfer within the exiting water, while flowing between the tank and the thermocouples, is negligible.

The energy balance of the process can be used to formulate the linear, time-invariant, univariate transfer function of the system's input-to-output variables as:

$$T_l(s) = G_l(s) \cdot u_S(s)$$

$$G_l(s) = \frac{k_l e^{-T_{dl}s}}{\tau_l s + 1} \qquad (6.1)$$

where:

T_l = Deviational temperature of exiting water, measured at thermocouple l; l = 1, 2, 3

u_S = Deviational steam flow-rate

T_{dl} = Transport delay of temperature measurements at thermocouple l

τ_l = Time constant of temperature response at thermocouple l

k_l = Gain of temperature response at thermocouple l

k_l is a function of the steam's latent heat of vapourization, specific heat capacity, water density, and the cold-water flow rate. τ_l is a function of the volume of water in the tank and the cold-water flow rate.

(6.1) is a first-order, linear model, whose parameters will be estimated using sampled temperature response data from excitation experiments.

6.3 PROCESS IDENTIFICATION

6.3.1 EXCITATION EXPERIMENT

An excitation experiment is implemented on the Heated Tank Process to obtain the relationship between the input (steam flow set point) and the outputs (temperature measurements at Thermocouples 1, 2, and 3). The following steps are performed:

a) The cold-water controller is cascaded with the level controller; the water level set point value is chosen as 0.17m. The system is then allowed to attain steady level.

b) The steam controller is set to the AUTOMATIC mode and the nominal steam flow rate set point is chosen as 11 kg/hr.

c) Positive and negative step tests of various magnitudes are performed to determine a linear range around the nominal point.

d) From the step test results, the frequency ranges of interest are determined and Random Binary Sequence (RBS) input sequences are designed accordingly.

e) The RBS input signals are introduced to the steam controller via the MATLAB OPC.

f) The process' temperature response at each thermocouple (Thermocouples 1, 2, and 3) is sampled using the MATLAB OPC.

6.3.2 STEP TEST RESULTS AND EXCITATION SIGNAL DESIGNS

Several step magnitudes were tested. Good signal-to-noise ratios and approximately linear level dynamics were obtained with perturbations of **± 3 kg/hr,** nominal input steam flow-rate of **11 kg/hr,** and sampling the temperature response from Thermocouple 1 with **65°** and **15°**, respectively, for the valve positions of water outlet valves 1 and 2. Step test results for water temperature are shown in Figure 6.2. Sampling period, t_s, was **1 second** for the excitation experiments. The temperature-response data were thereafter down-sampled to **5 seconds** for the model computations.

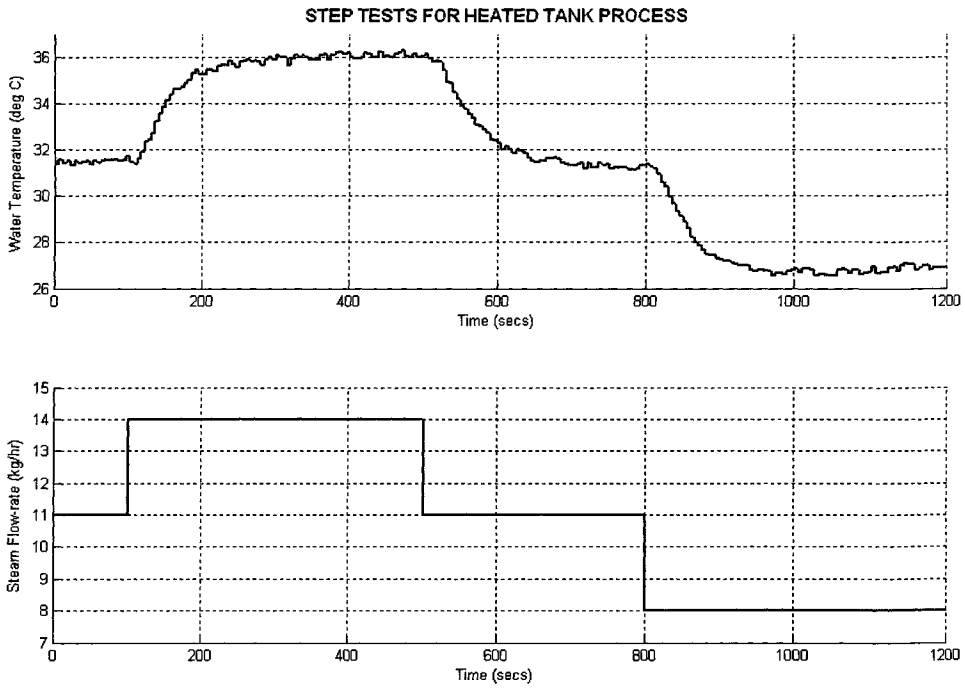

Figure 6.2: Water temperature response of Heated Tank Process to positive and negative step changes in the steam flow rate.

The step-response data were used to compute parameter estimates for first order model approximations to design the Random Binary Sequences (RBS) for exciting the system. Parameter estimates obtained from these tests are presented in Table 6.1.

Table 6.1: 1st Order Approximation Constants from the Step Tests

Gain (°C-hr/kg)	Time constant (sec)	Time delay (sec)
1.5	40	11

6.3.3 TEMPERATURE RESPONSES AND MODEL COMPUTATION

The steam controller was excited with the designed RBS set point signal for the thermocouples. Figures 6.3(a) – (d) show the temperature responses of Thermocouples 1, 2 and 3 to the excitation, as well as the input signal.

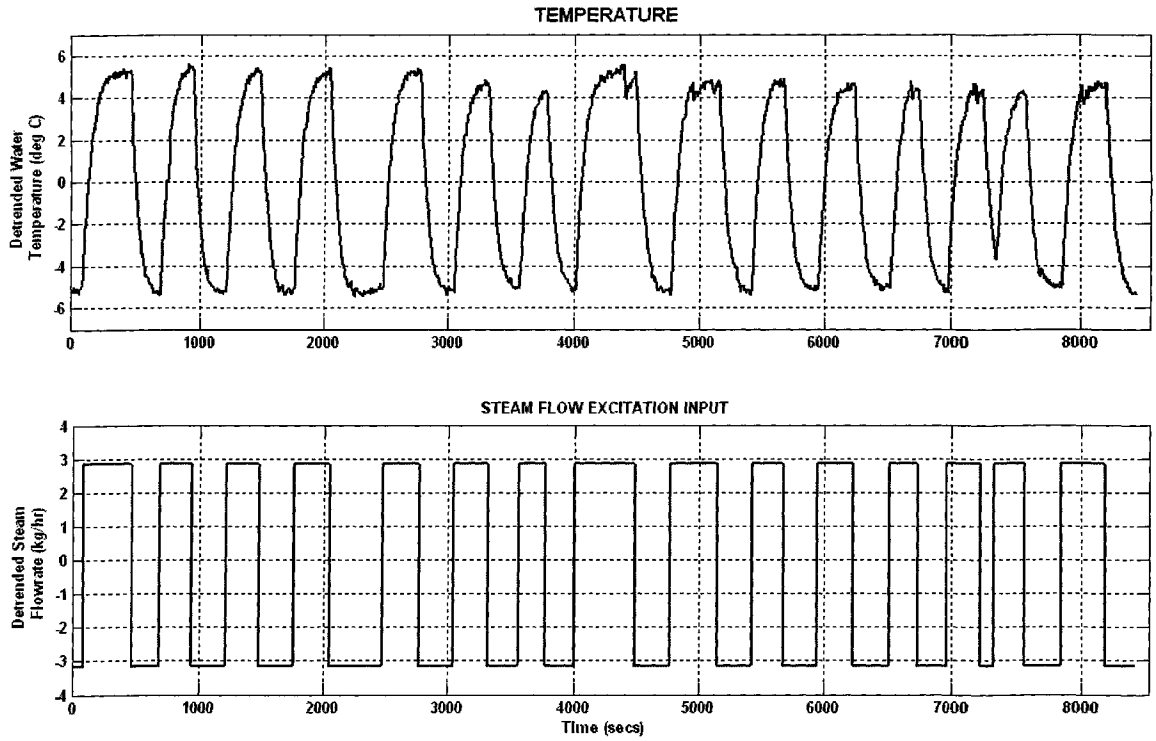

Figure 6.3(a): Water temperature response measurement at Thermocouple 1.

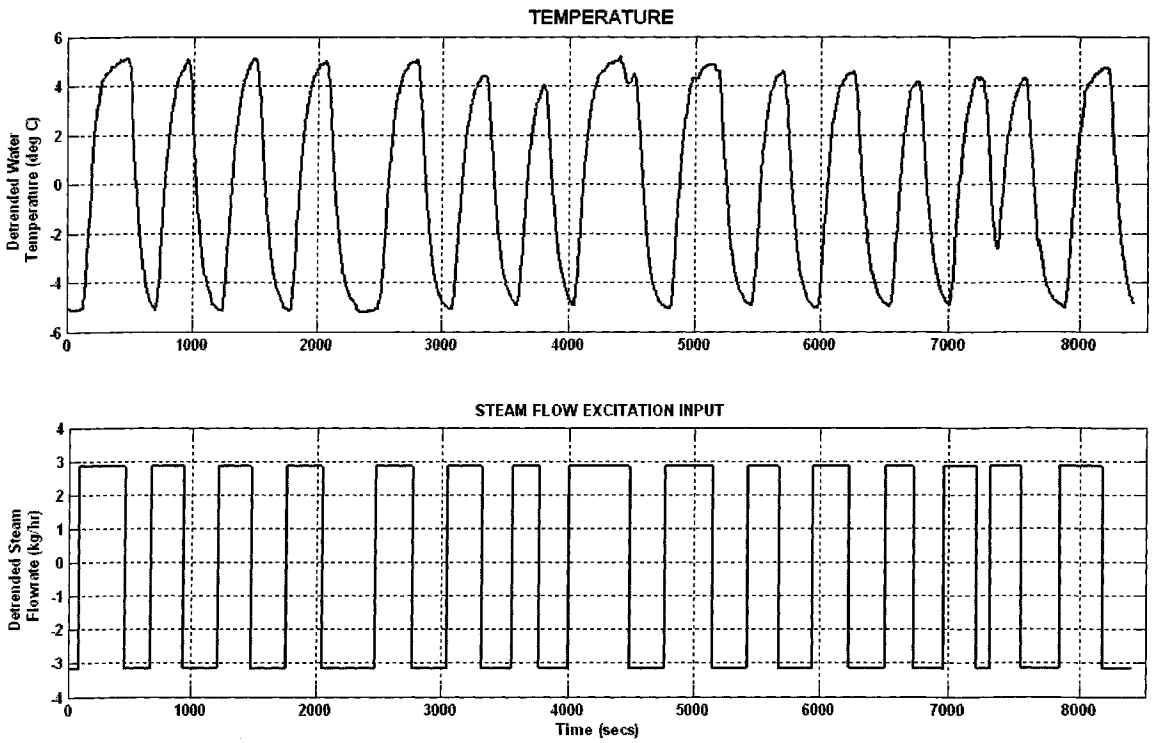

Figure 6.3(b): Water temperature response measurement at Thermocouple 2.

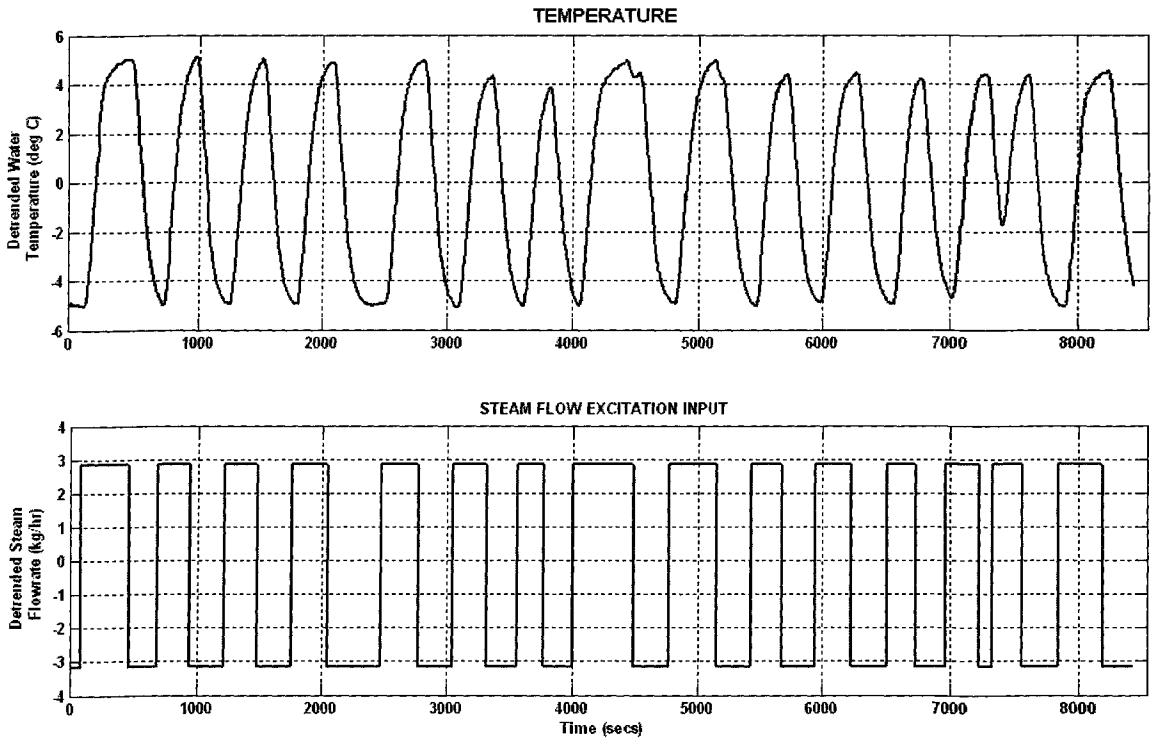

Figure 6.3(c): Water temperature response measurement at Thermocouple 3.

Using the *pem* and *idproc* functions in MATLAB, for continuous-time model identification, and imposing the model structures in (6.1) on the identification functions, the transfer functions for the temperature measurements at the thermocouples were computed.

Figure 6.4 shows the division of the excitation data into the training data sets and the validation data sets.

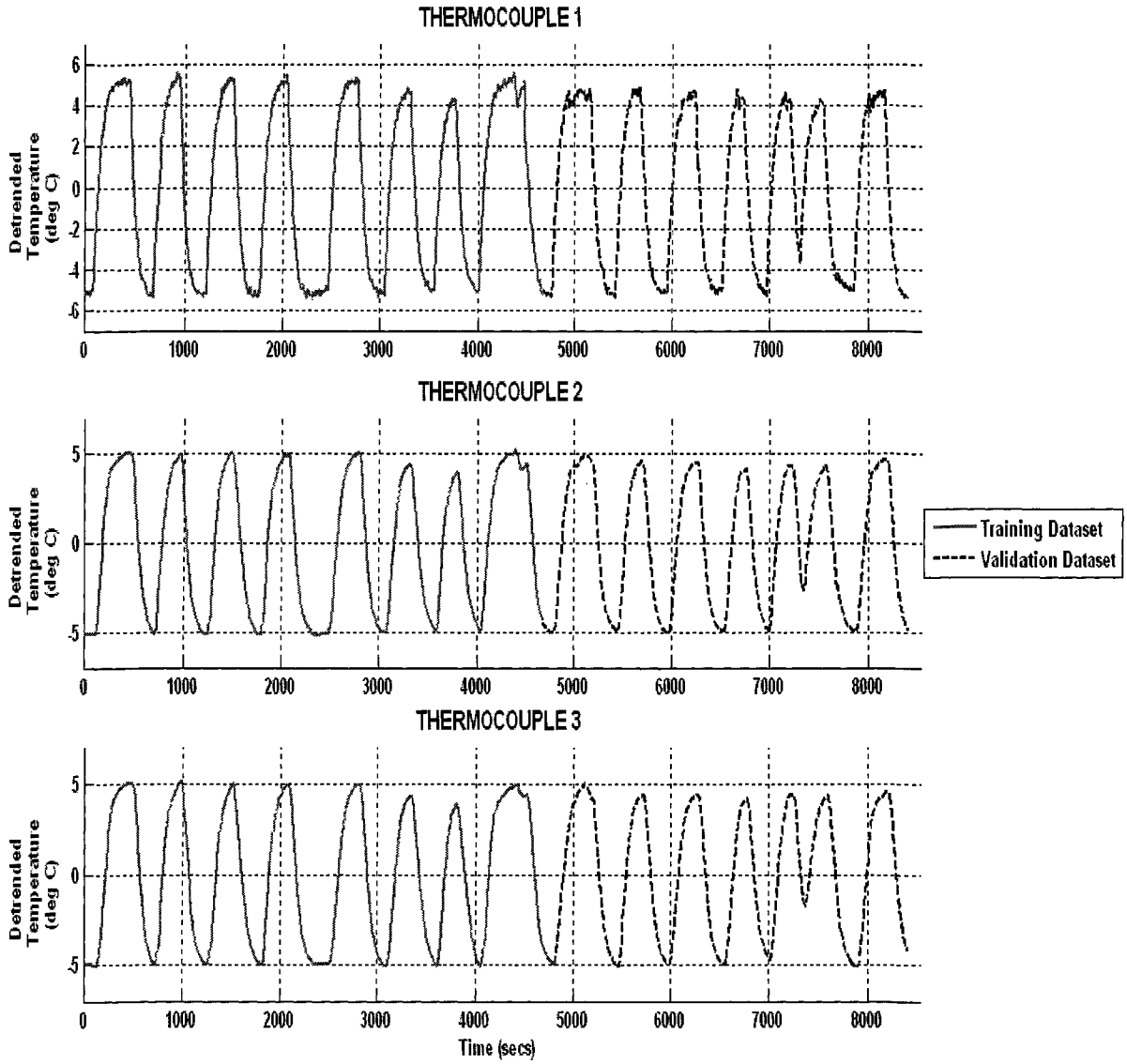

Figure 6.4: Training and validation datasets for temperature measurements at thermocouples.

6.3.3.1 THERMOCOUPLE 1 MODEL

Model Structure: $\frac{Ke^{-T_d s}}{\tau s + 1}$

K = 1.7021 °C-hr/kg
τ = 57.192 secs
T_d = 7.81 secs

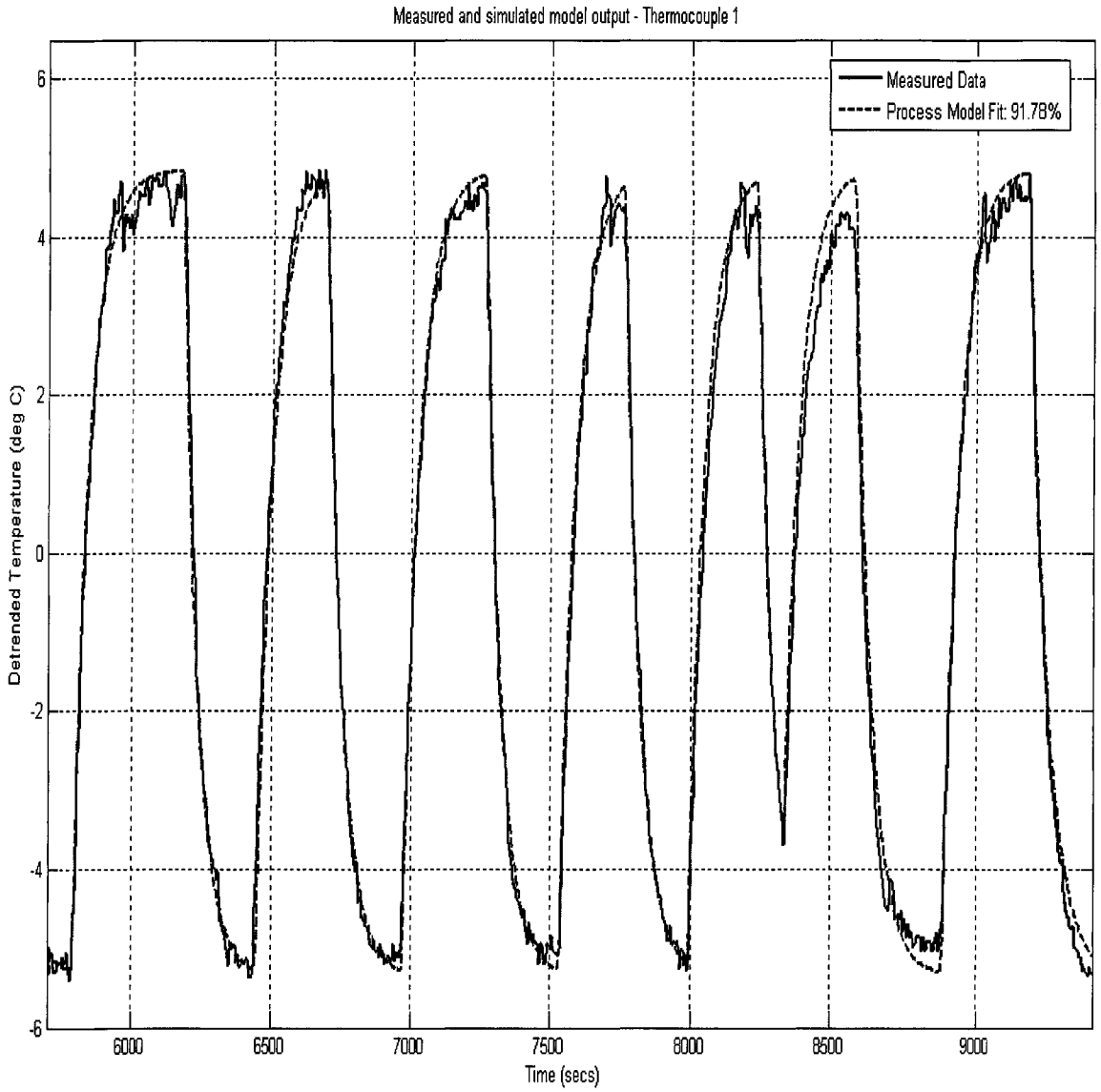

Figure 6.5(a): Validation of continuous-time model for transfer function at Thermocouple 1.

6.3.3.2 THERMOCOUPLE 2 MODEL

Model Structure: $\frac{Ke^{-T_d s}}{\tau s + 1}$

K = 1.719 °C-hr/kg
τ = 73.087 secs
T_d = 48.93 secs

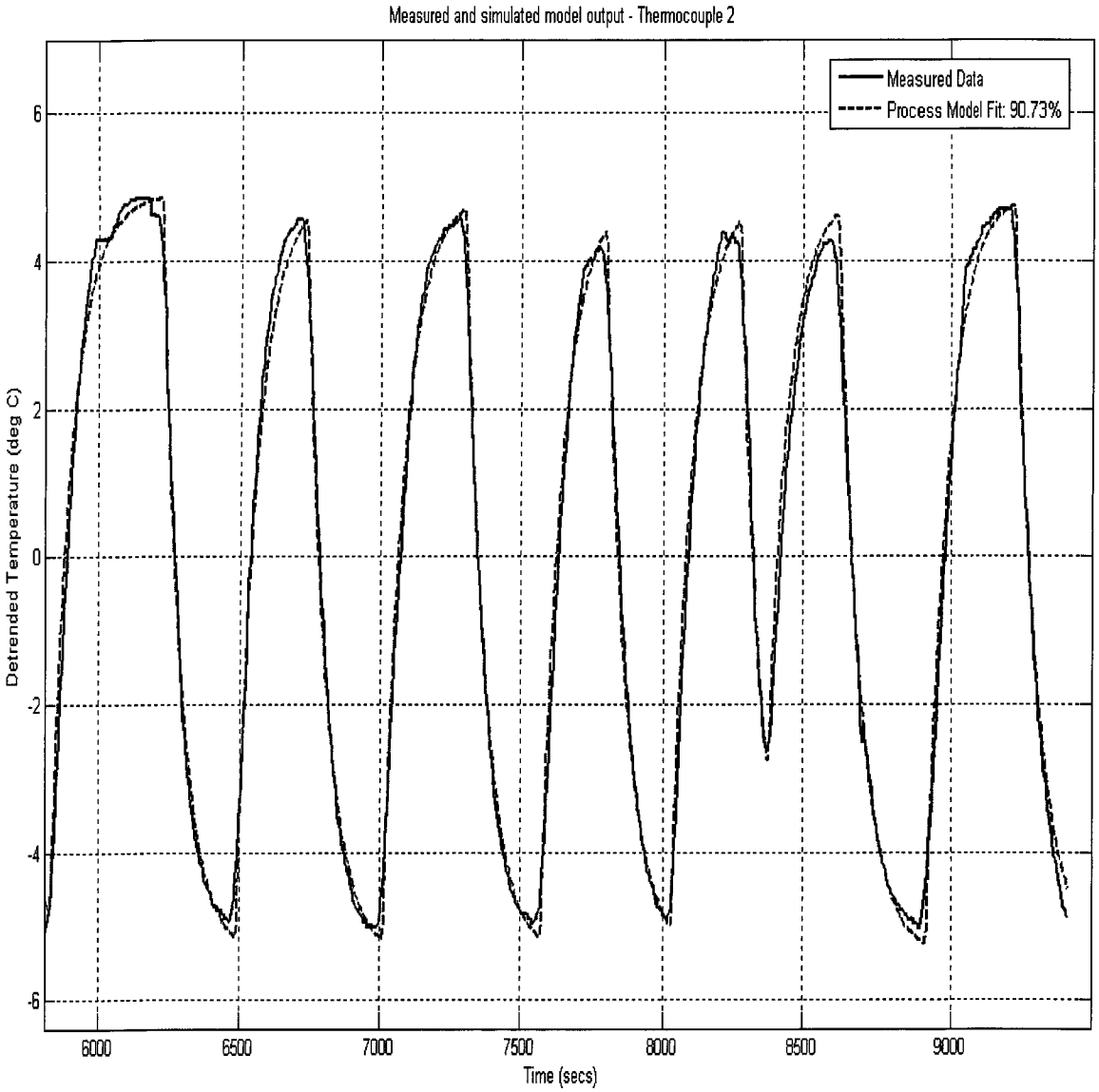

Figure 6.5(b): Validation of continuous-time model for transfer function at Thermocouple 2.

6.3.3.3 THERMOCOUPLE 3 MODEL

Model Structure: $\frac{Ke^{-T_d s}}{\tau s + 1}$

K = 1.738 °C-hr/kg
τ = 81.1 secs
T_d = 68.562 secs

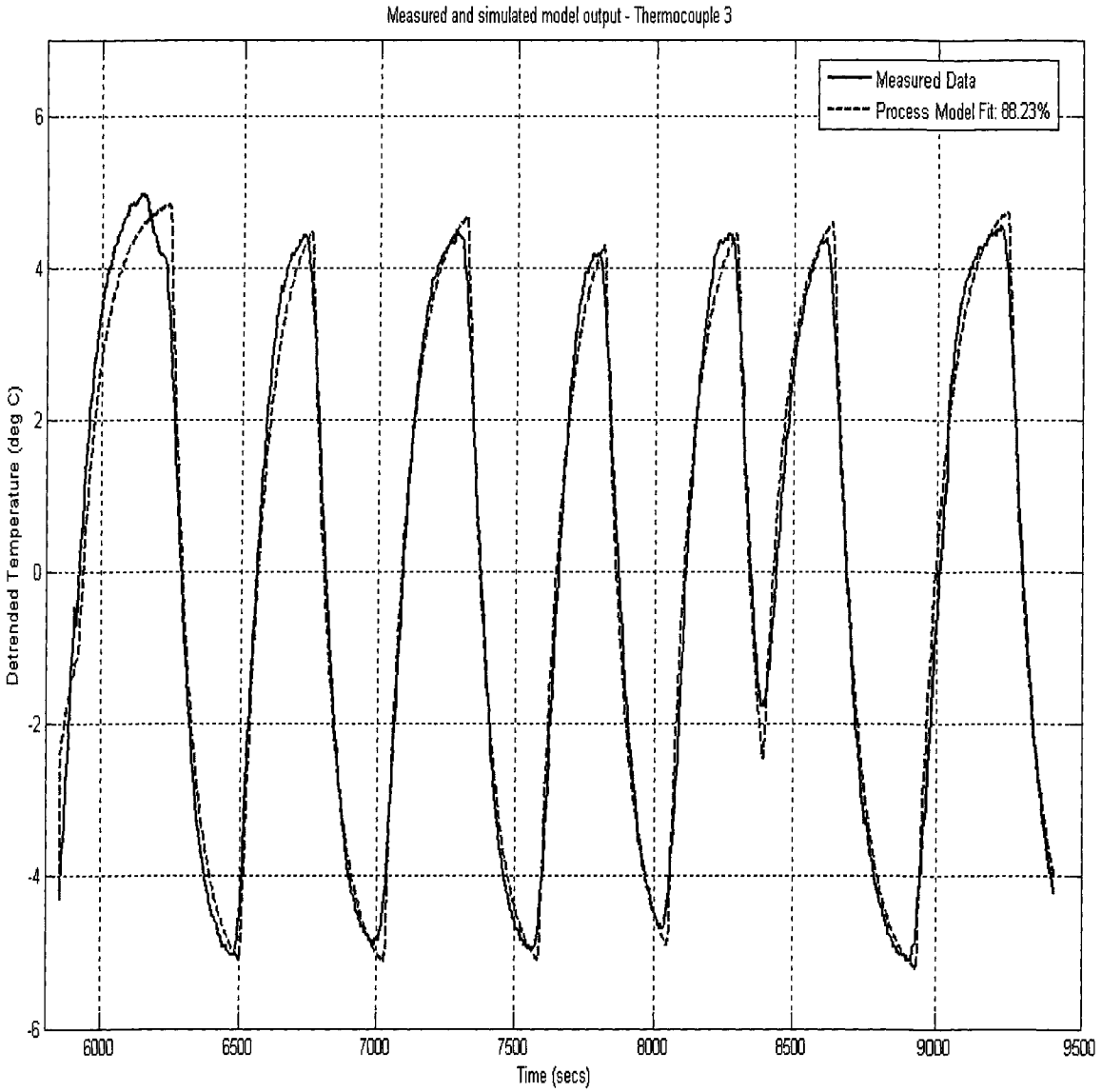

Figure 6.5(c): Validation of continuous-time model for transfer function at Thermocouple 3.

Table 6.2 summarizes the model identification results for the thermocouples.

Table 6.2: Process Models for Temperature Measurements of Heated Tank Process

SENSOR	PROCESS MODEL	TIME DELAY – TIME CONSTANT RATIO
Thermocouple 1	$G_1(s) = \frac{1.7021e^{-7.81s}}{(57.192s+1)}$	0.1366
Thermocouple 2	$G_2(s) = \frac{1.719e^{-48.93s}}{(73.087s+1)}$	0.6695
Thermocouple 3	$G_3(s) = \frac{1.738e^{-68.562s}}{(81.1s+1)}$	0.8454

The models obtained for the three thermocouples show that the transport delay of temperature measurement at a thermocouple increases with the thermocouple's distance from the tank. It can also be observed that the process gain and time constant increase with the time delay. This observation can be attributed to convective heat transfer dynamics occurring within the exiting water in the spiral pipe as it flows between successive thermocouples.

6.4 DESIGN OF OPTIMAL PI AND PID CONTROLLERS

The consecutively increasing time delay-time constant ratios of the transfer functions in Table 6.2 provide a practical example of processes approximately similar to those in Table 5.1, and therefore enable the experimental evaluation of the performance differences between closed loops with optimal PI and PID controllers as process time delay increases. To design the optimal PI and PID controllers for a range of J_u constraints, (5.1) and (5.2) are respectively solved for the transfer functions.

The parameters for the designed optimal controllers can be found in Tables A.11 to A.16 of Appendix A. Next, the J_v-J_u profiles for the closed loops are plotted, as well as the *ISE[y]-VAR[Δu]* profiles for closed loops perturbed by steps in load disturbance at the process inputs and integrated noise signals added to process outputs.

6.5 OPTIMAL PI AND PID PERFORMANCE-CONTROL ACTION PROFILES

Figure 6.6 shows the J_v-J_u plots for the closed loops of the processes $G_1(s)$, $G_2(s)$, and $G_3(s)$, using optimal PI and PID controllers. Figures 6.7(a) and 6.7(b) show the *ISE[y]-VAR[Δu]* profiles for simulated closed loops with input step and integrated white noise disturbances respectively. Figure 6.7(c) shows the *ISE[y]-MAD[Δu]* profiles for the simulated closed loops with steps in their set point signals.

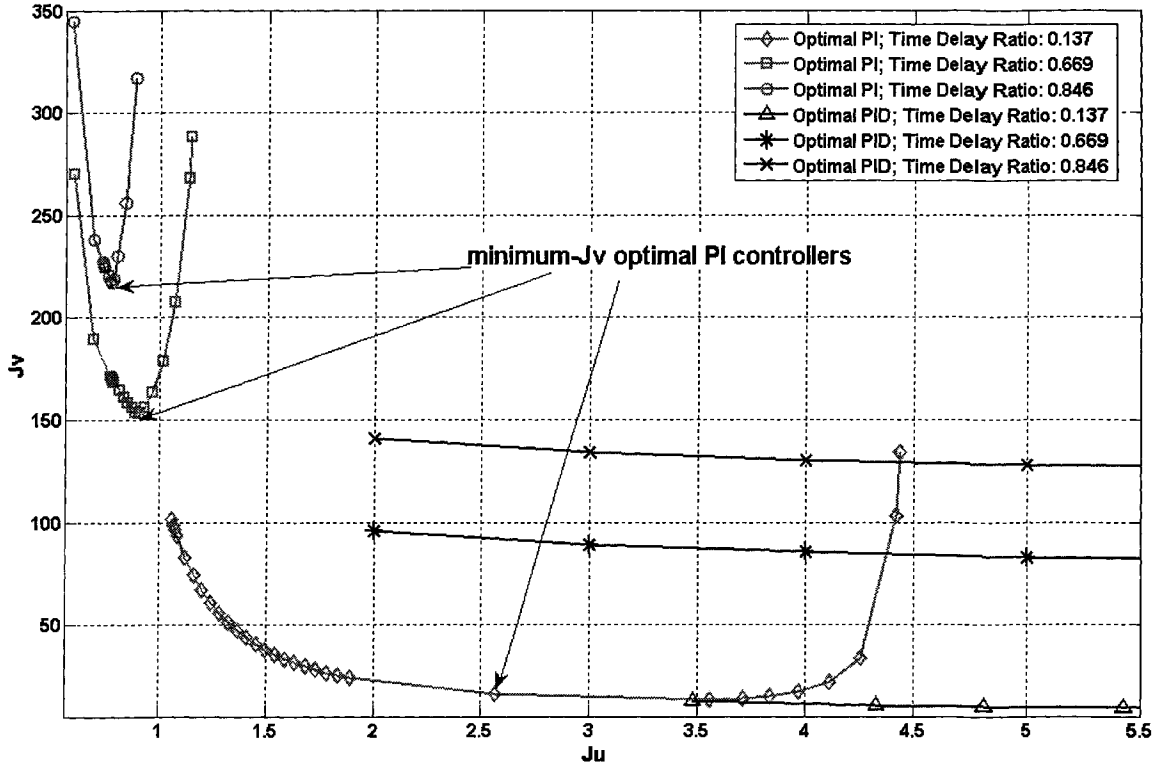

Figure 6.6: J_v-J_u profiles of closed loops for Heated Tank Process.

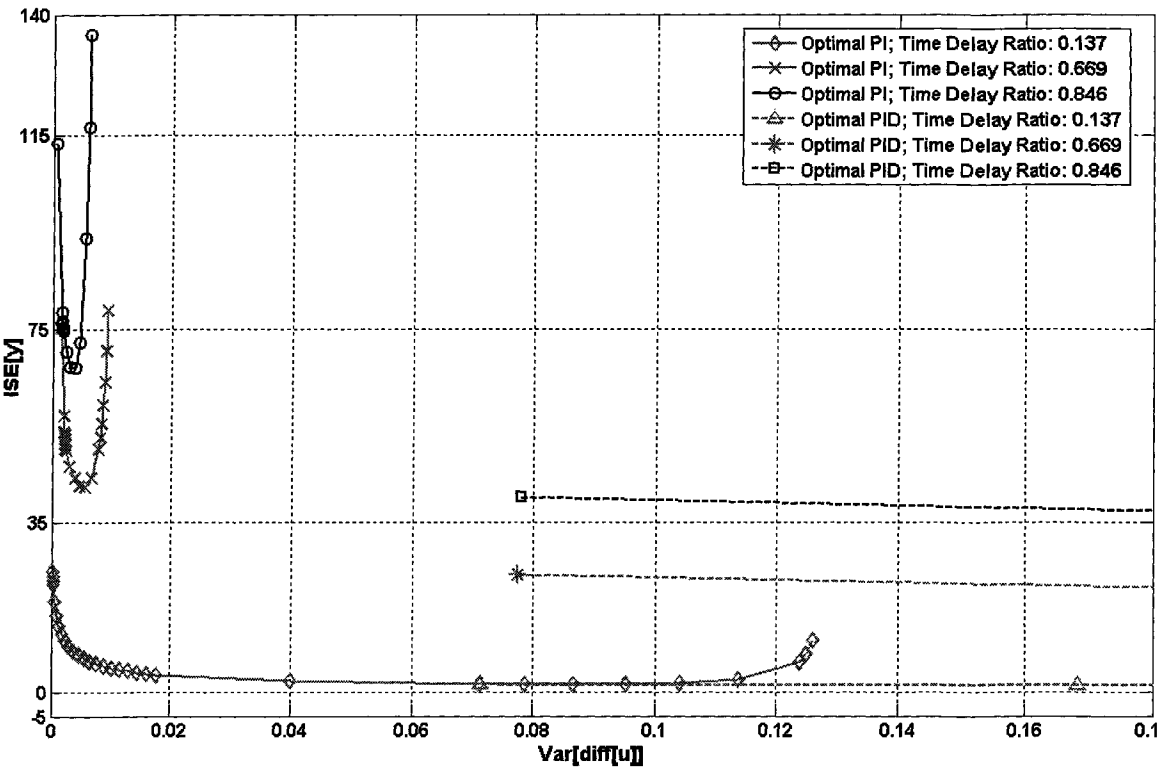

Figure 6.7(a): *ISE[y]-VAR[Δu]* profiles from simulation of Heated Tank closed loops perturbed by input step disturbances.

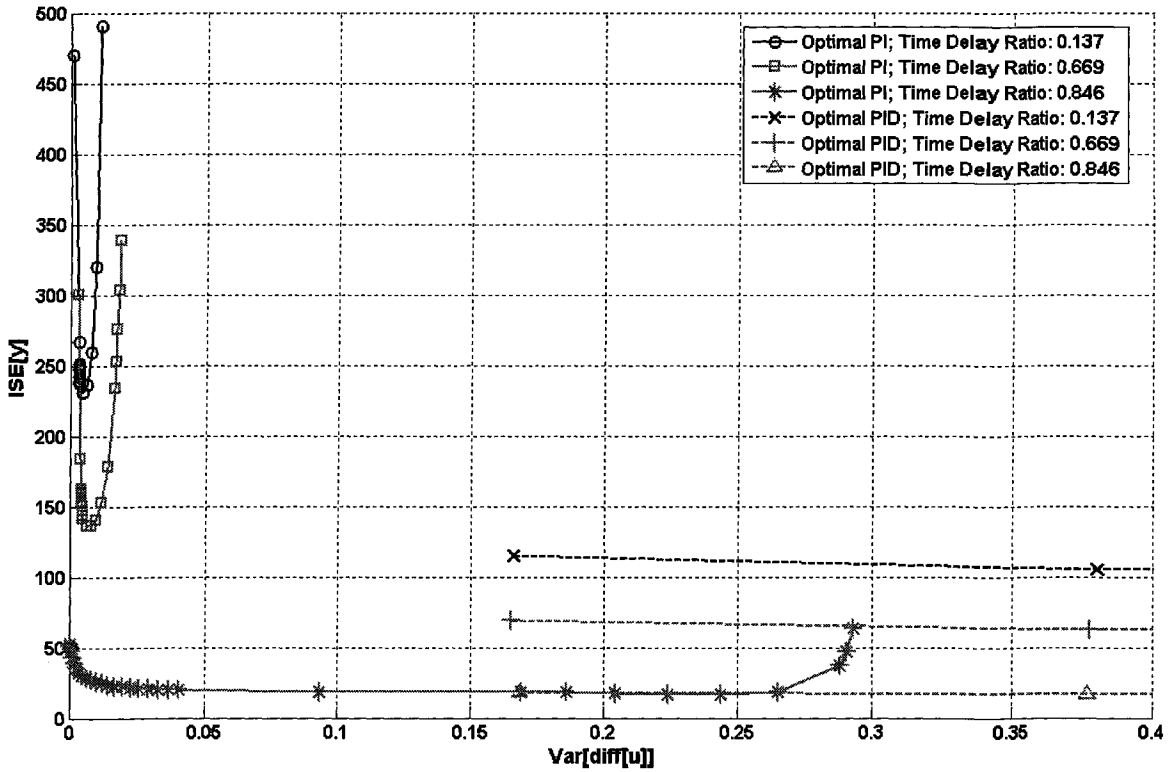

Figure 6.7(b): *ISE[y]-VAR[Δu]* profiles from simulation of Heated Tank closed loops perturbed by integrated white noise disturbances.

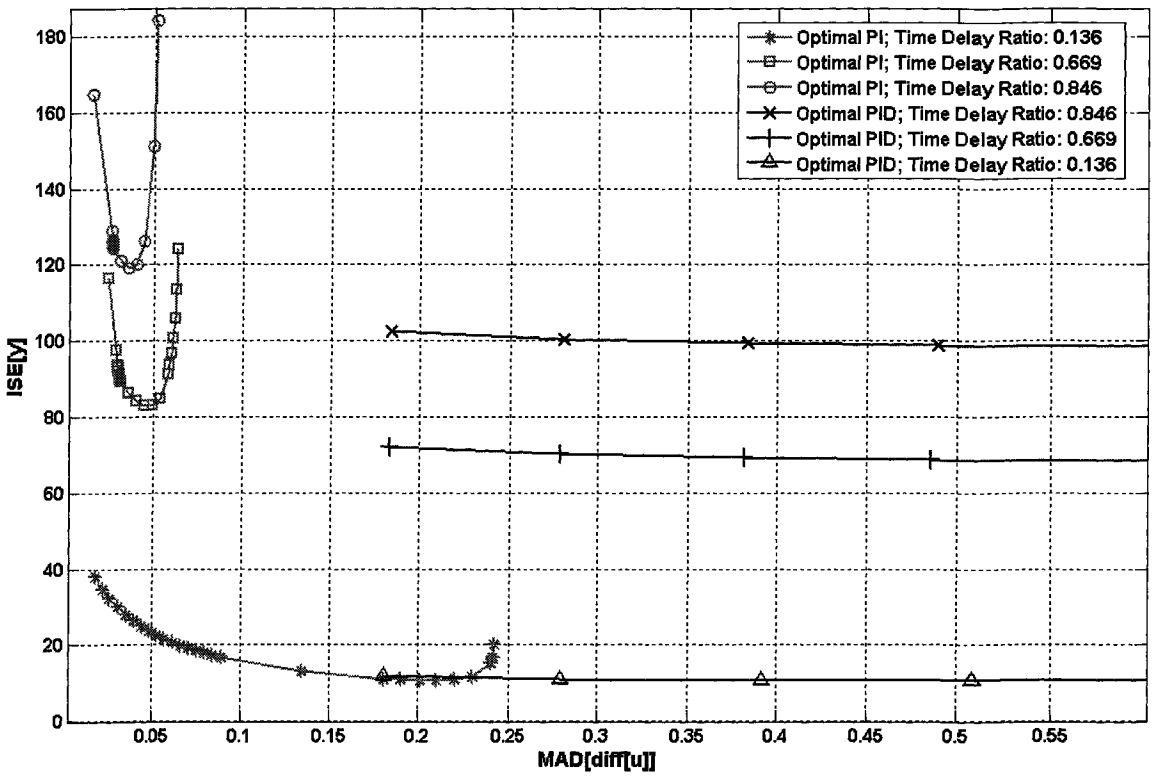

Figure 6.7(c): *ISE[y]-MAD[Δu]* profiles from simulation of Heated Tank closed loops perturbed by step in set point signal.

Figures 6.7(a), 6.7(b), and 6.7(c) show that the capability of the optimal PI controller becomes more restricted as the system's time delay increases; the profiles also show that the potential improvement derivative action offers to the PI controller increases with the system's time delay. To obtain clearer insight into the improvement offered to the closed loop by using a PID controller, the disturbance responses of the loop to the input step, integrated white noise, and set point step signals, using the minimum-J_v PI controllers and some selected PID controllers for each temperature model, are plotted in Figures 6.8(a), 6.8(b), and 6.8(c).

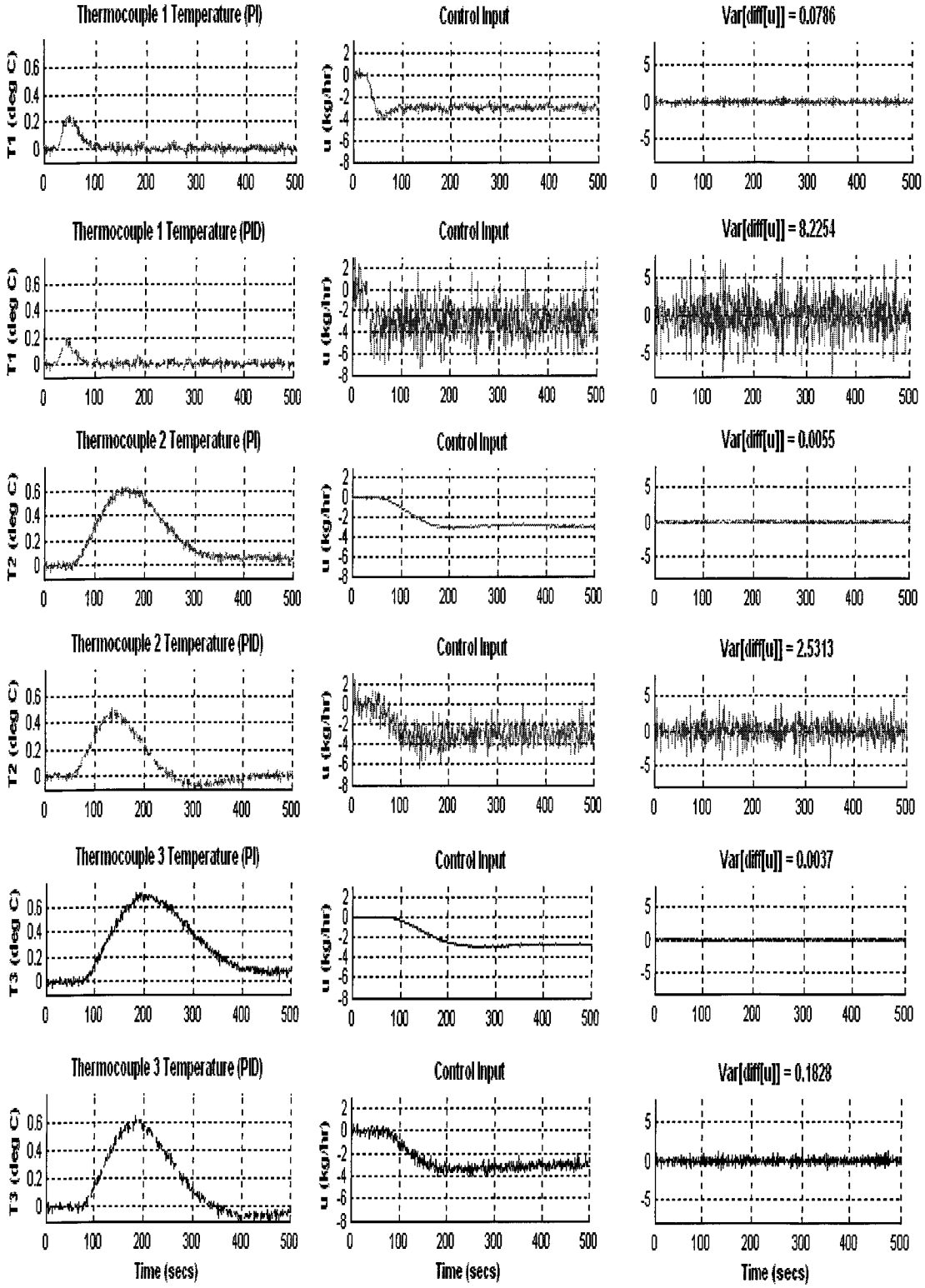

Figure 6.8(a): Temperature response of simulated closed loops to input step disturbance using minimum-J_v PI controllers and selected PID controllers.

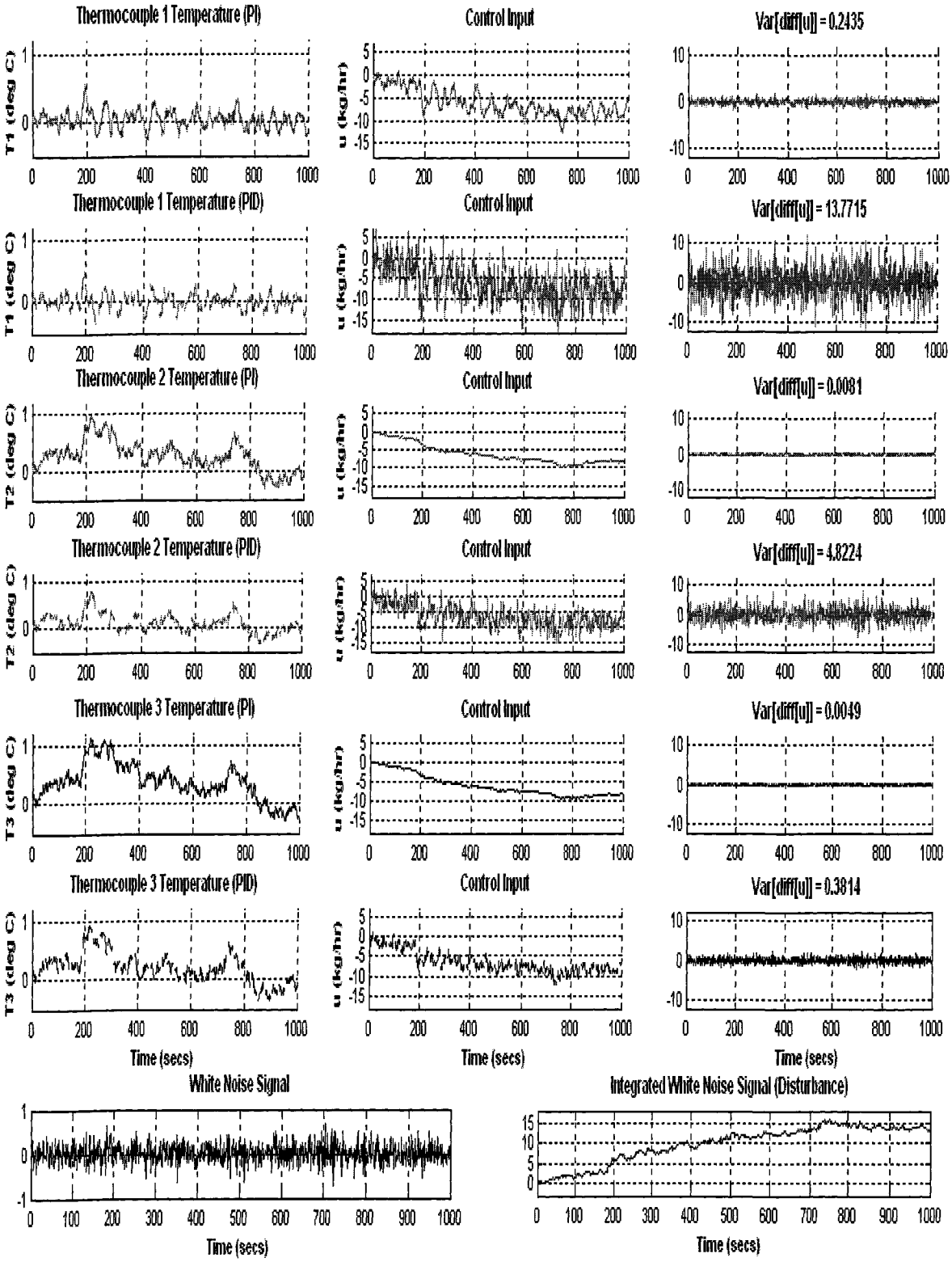

Figure 6.8(b): Temperature response of simulated closed loops to integrated white noise disturbance using minimum-J_v PI controllers and selected PID controllers.

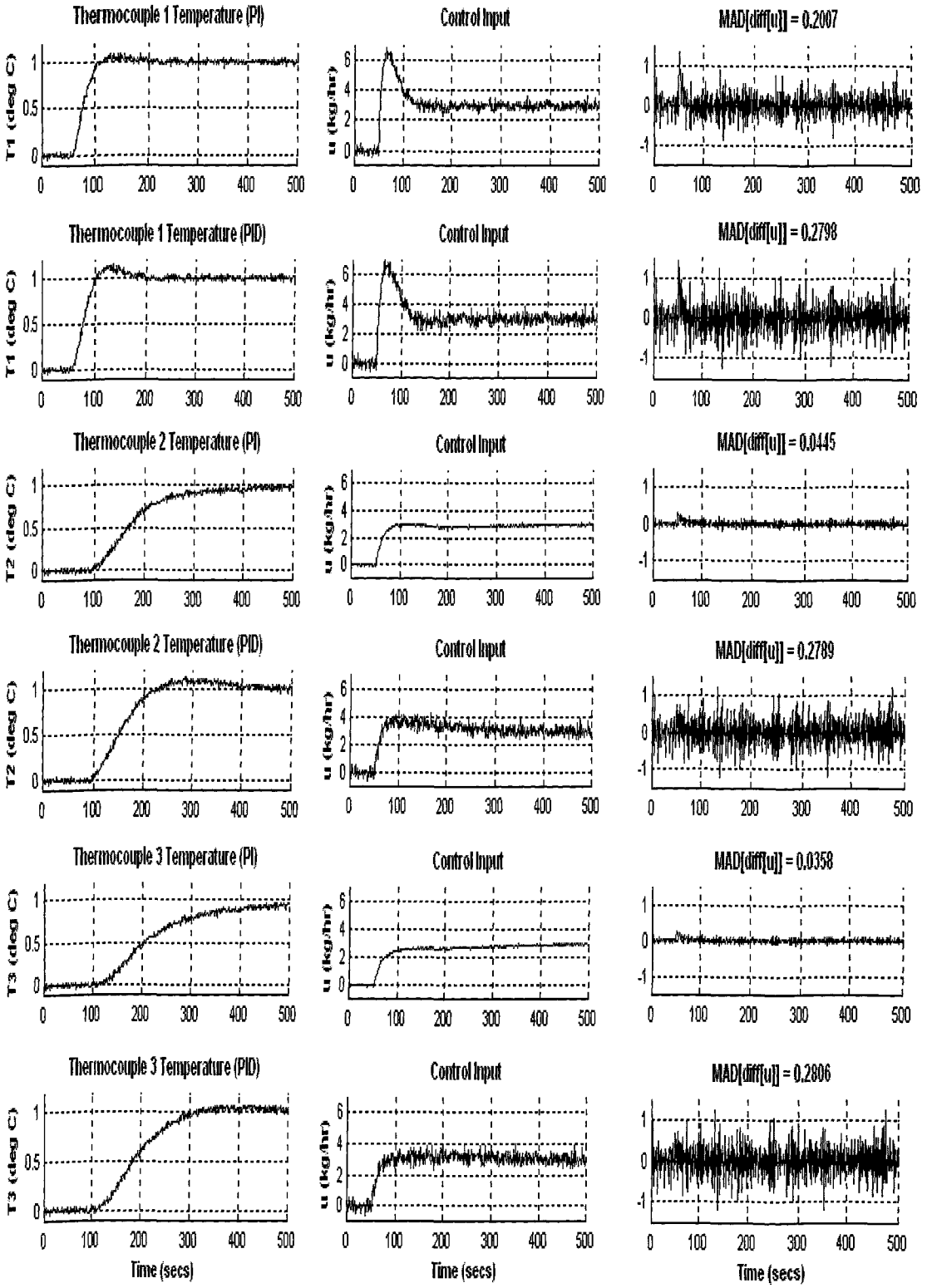

Figure 6.8(c): Temperature response of simulated closed loops to steps in set point signals using minimum-J_v PI controllers and selected PID controllers.

Figures 6.8(a), 6.8(b), and 6.8(c) show that, in simulation, the regulatory and servo performance of the closed loops with PID controllers are better than the PI controllers' as the process' time delay increases. One explanation for the increasing performance gap that derivative action creates is the restriction on the control activity of the PI controllers as time delay increases, as shown in Figures 6.6, 6.7(a), 6.7(b), and 6.7(c). This restriction is necessary so that the optimal PI controllers do not violate their mid-frequency robustness demand, specified by GM_S. However, the cost to be paid by the PID controller for improved performance is greater control action, as shown by the *VAR[Δu]* and *MAD[Δu]* values of control input plots above. The closed loop for Thermocouple 3, for example, generates control action with variance about 60 times greater if a PID controller is used, in comparison to the PI controller.

The PID controller used on Thermocouple 3's closed loop is augmented with an extra low-pass filter (strictly proper controller) by solving the optimization function similar to (3.11). The GM_S and J_u constraints are held equal to those for the selected just proper PID controller implemented above and a constraint on J_{HF} is imposed. Figure 6.9 shows the location of the strictly proper PID controller in the *ISE[y]-VAR[Δu]* profiles for Thermocouple 3's closed loop with input step disturbances, as well as the minimum-J_v PI controller and selected just proper PID controller. Figure 6.10 shows the disturbance response of the three closed loops.

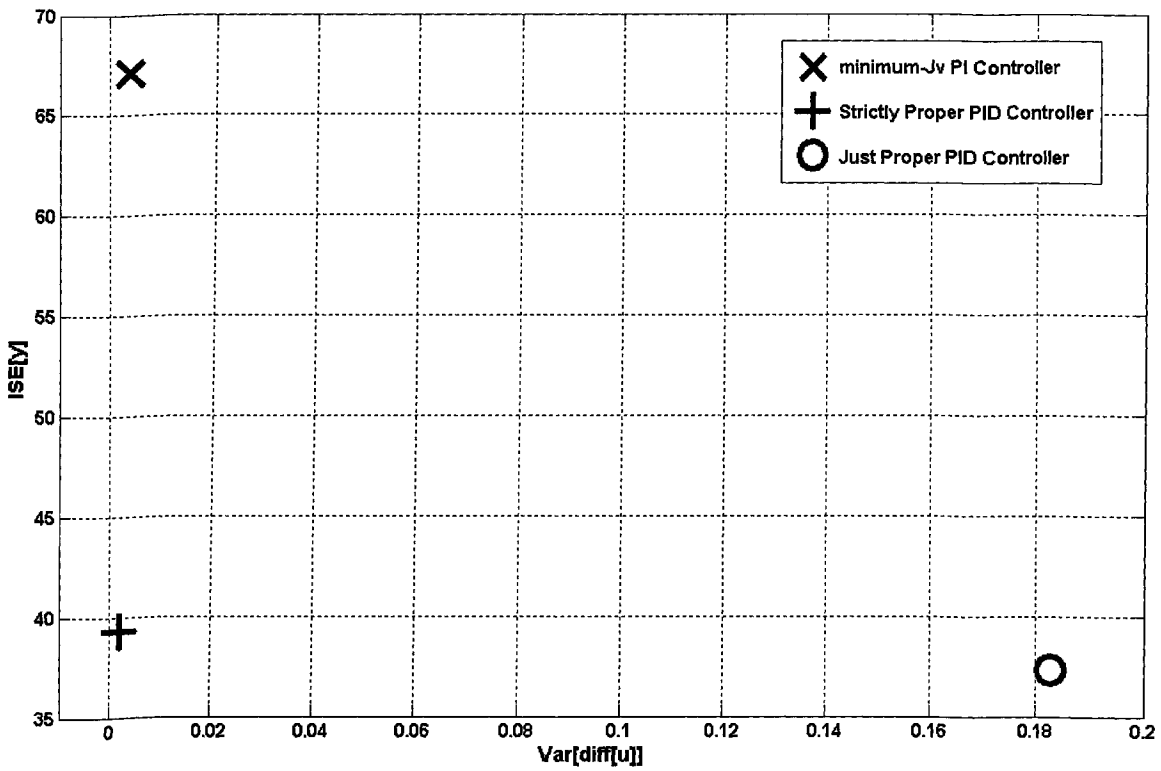

Figure 6.9: *ISE[y]-VAR[Δu]* profiles for input step disturbance rejection from simulation of Thermocouple 3 closed loops using minimum-J_v optimal PI, selected just proper and strictly proper PID controllers.

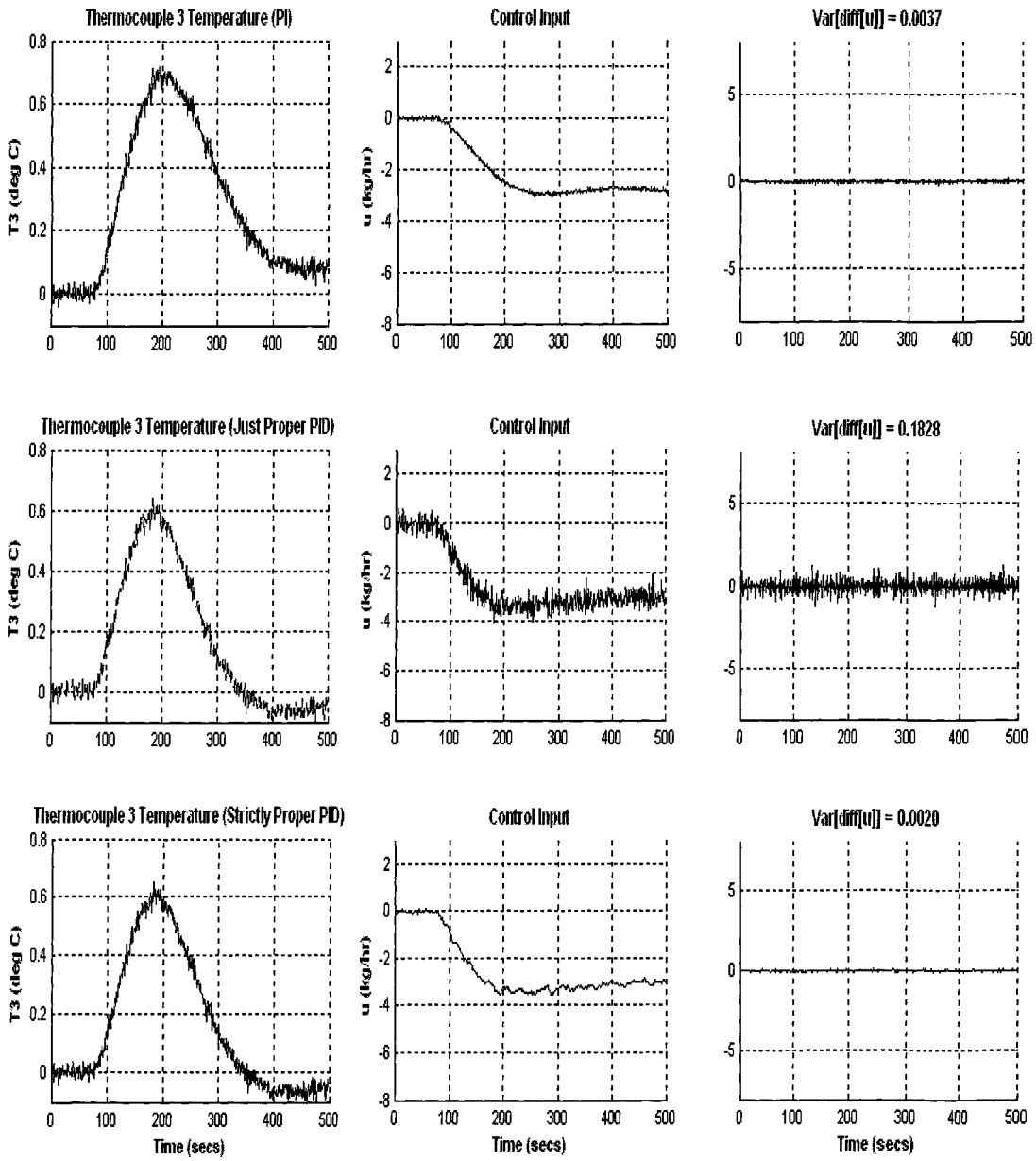

Figure 6.10: Temperature response of Thermocouple 3's simulated closed loops to input step disturbance using minimum-J_v PI controller, selected just proper and strictly proper PID controllers.

Figures 6.9 and 6.10 clearly demonstrate the advantage of the strictly proper PID controller over the shortcomings of the PI and just proper PID controllers, in the areas of performance and control action respectively. The strictly proper PID controller has a smaller control action variance than the just proper PI controller and yet its closed loop has a smaller overshoot and shorter settling time, and thus better performance. A property of the closed loops for the three controllers worth discussing is their mid-frequency robustness, i.e., their stability margins. Figure 6.11 shows the bode plot for the three closed loops, highlighting their respective gain and phase margins.

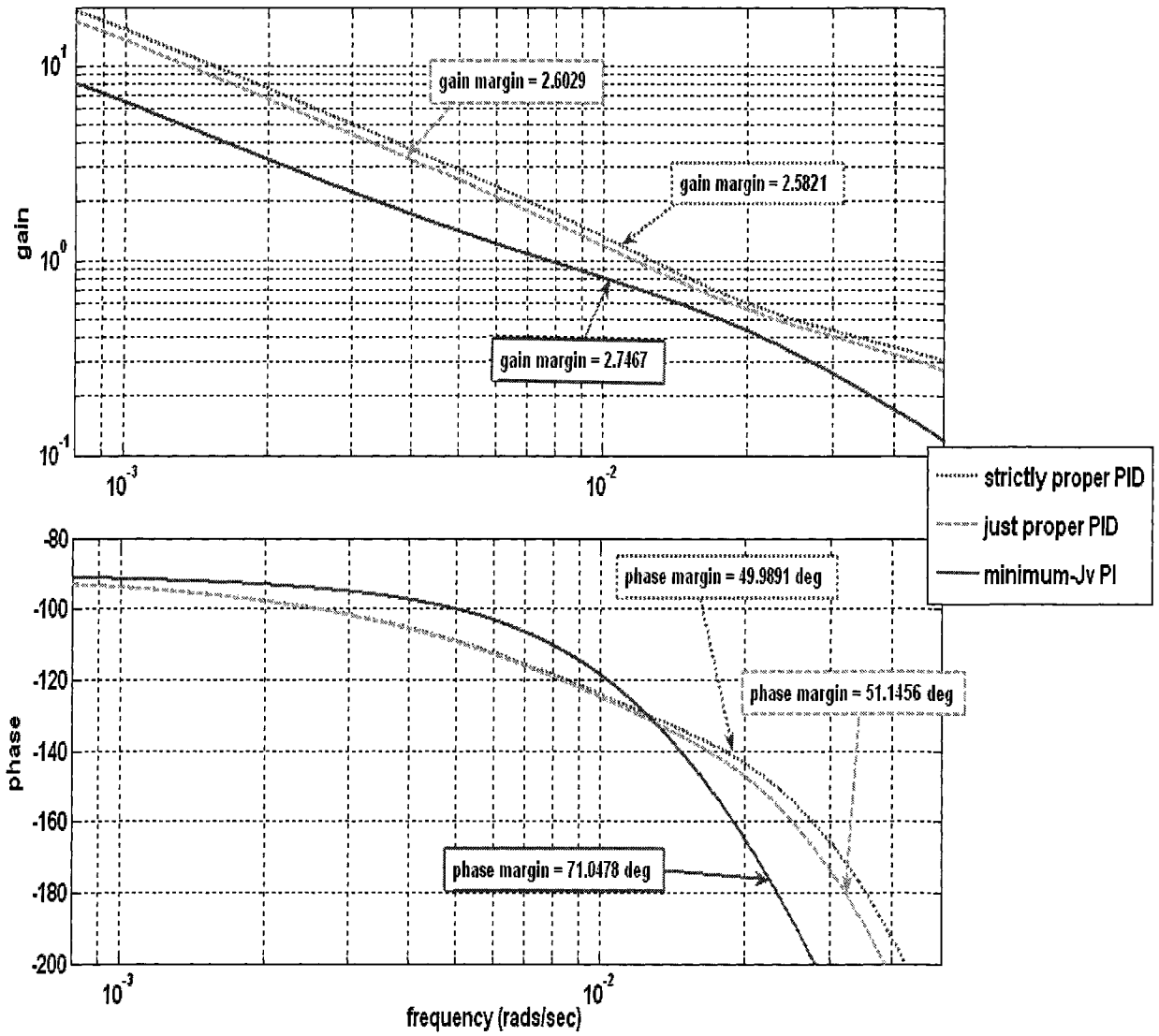

Figure 6.11: Bode diagram of Thermocouple 3's closed loops using minimum-J_v PI controller, selected just proper and strictly proper PID controllers.

All three controllers surpass the gain and phase margin minimum requirements of 2.4 and 45° respectively, as imposed by $GM_S \leq 1.7$. As expected, the minimum-J_v PI controller's loop is the most robust of the three, followed by the just proper PID controller's. The strictly proper PID controller's loop is slightly less robust than the just proper PID's loop, but also exceeds the imposed mid-frequency robustness requirement. Thus, the benefit of improved performance and tolerable control action provided by the strictly proper PID controller's closed loop, compared with the PI's closed loop, far outweighs its robustness cost.

The closed-loop performance comparisons of the PI and PID controllers have thus far been examined in simulation, using the transfer functions for the Heated Tank Process. However, some of the controllers were also experimentally implemented in the real process' closed loop. The performance-control action

profiles were computed for the responses of the selected controllers to input step and integrated white noise disturbances, as well as set point signal steps. Figure 6.12 shows the time domain performance-control action profiles for the closed loops controlled by optimal PI and PID controllers, in response to an integrated white noise disturbance. Figures 6.13(a) to 6.13(c) show the closed loop responses of selected controllers to the disturbance input. Figure 6.14 shows the time domain performance-control action profiles for the closed loops controlled by optimal PI and PID controllers, in response to a step in the process input load disturbance. Figures 6.15(a) to 6.15(c) show the closed-loop responses of some selected controllers to the disturbance input. Figure 6.16 shows the time domain performance-control action profiles for the closed loops controlled by optimal PI and PID controllers, in response to a step in the set point signal. Figures 6.17(a) to 6.17(c) show the closed loop responses of selected controllers to the step input.

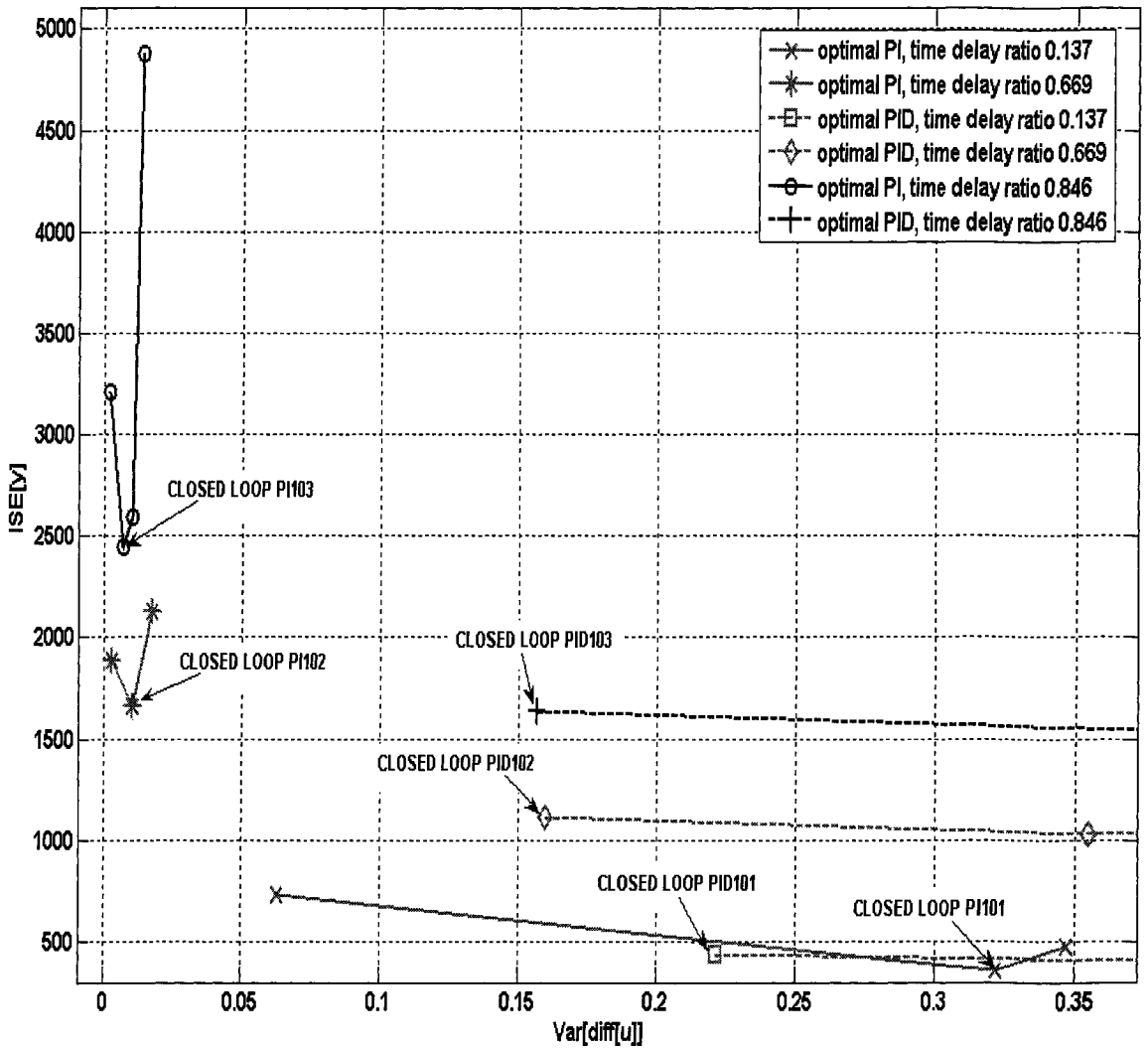

Figure 6.12: *ISE[y]-VAR[Δu]* profiles from experimental implementation of thermocouple closed loops perturbed by integrated white noise disturbances.

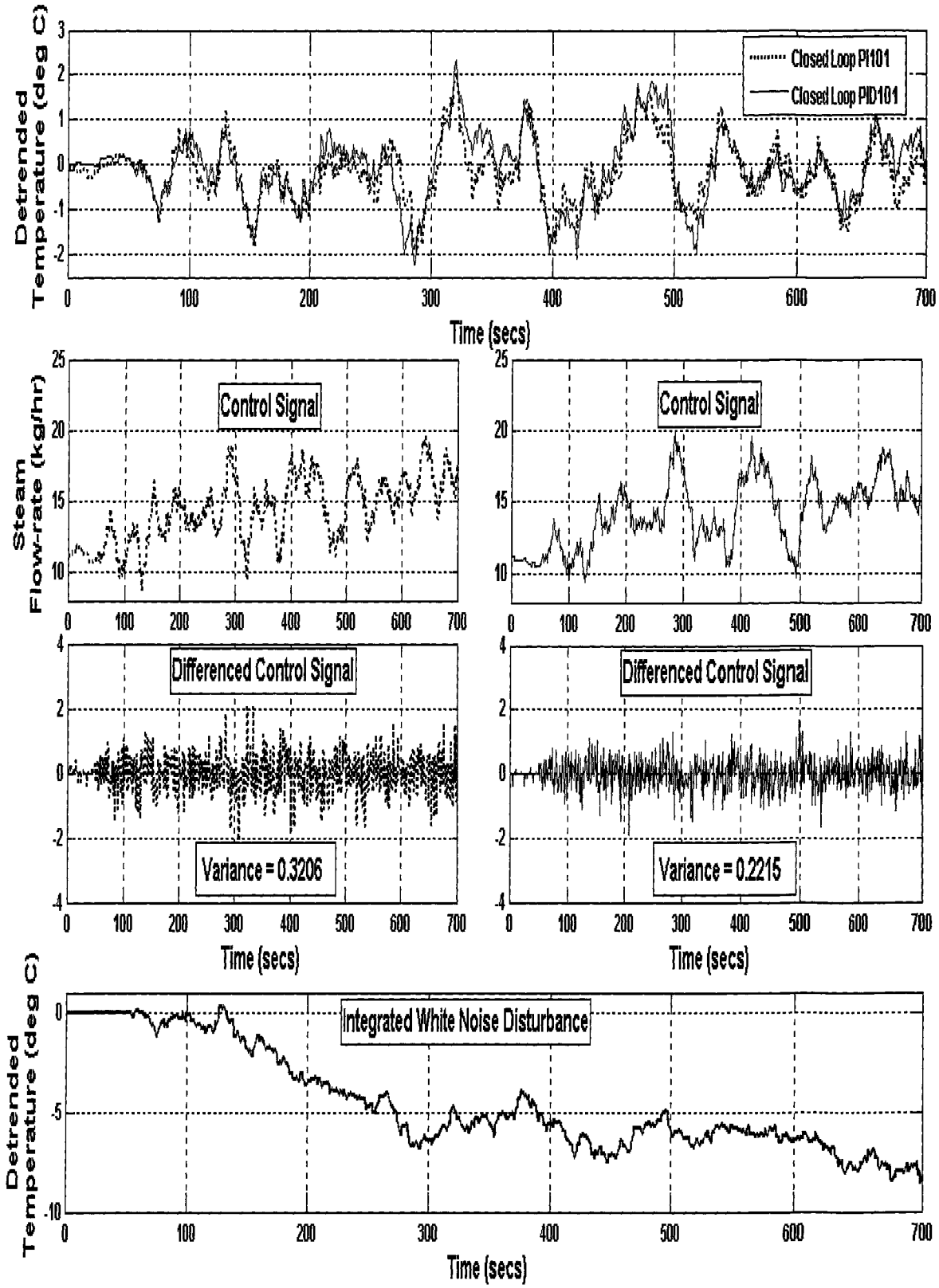

Figure 6.13(a): Temperature response of Thermocouple 1's experimentally implemented closed loops PI101 and PID101 to integrated white noise disturbance.

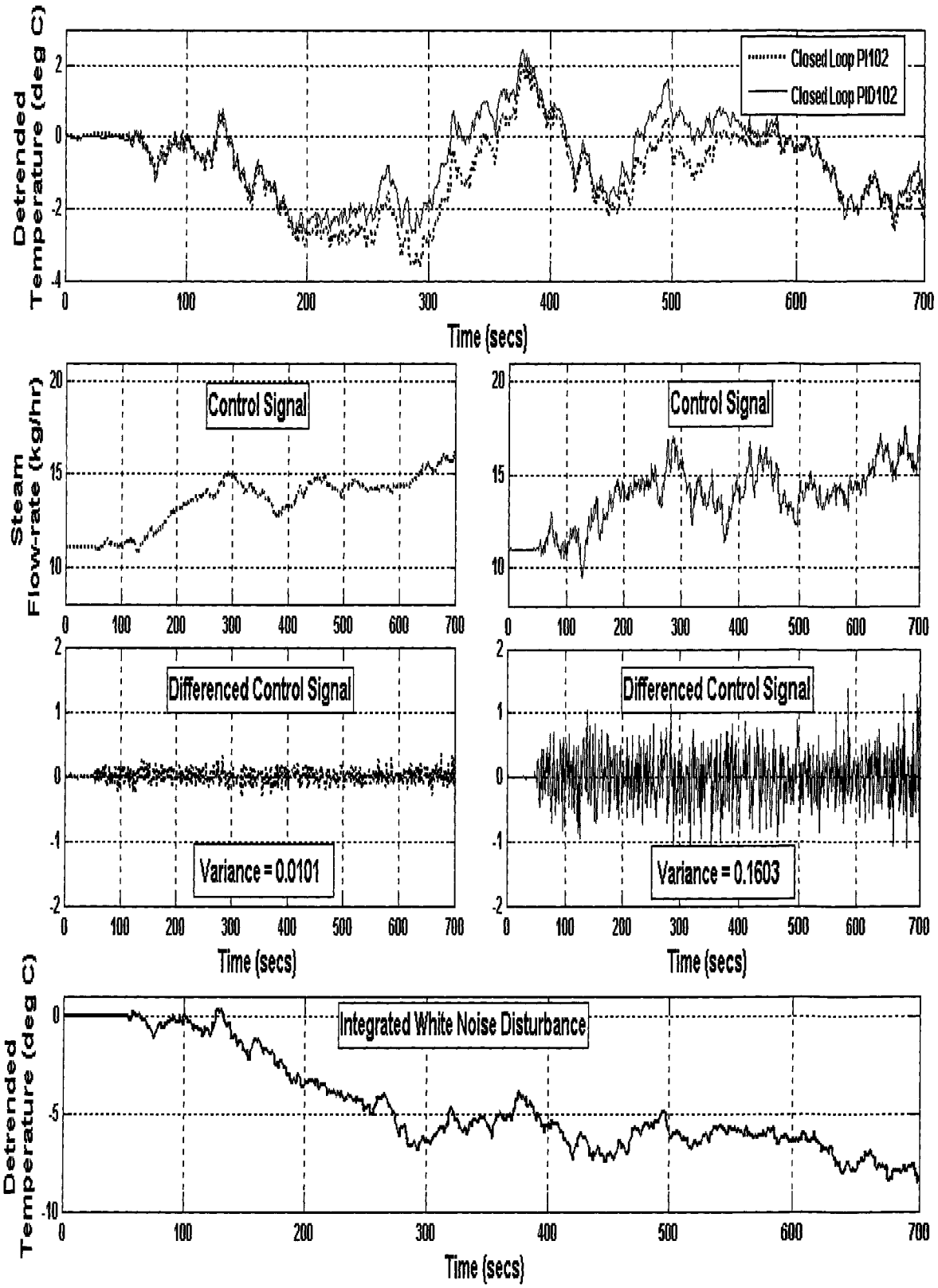

Figure 6.13(b): Temperature response of Thermocouple 2's experimentally implemented closed loops PI102 and PID102 to integrated white noise disturbance.

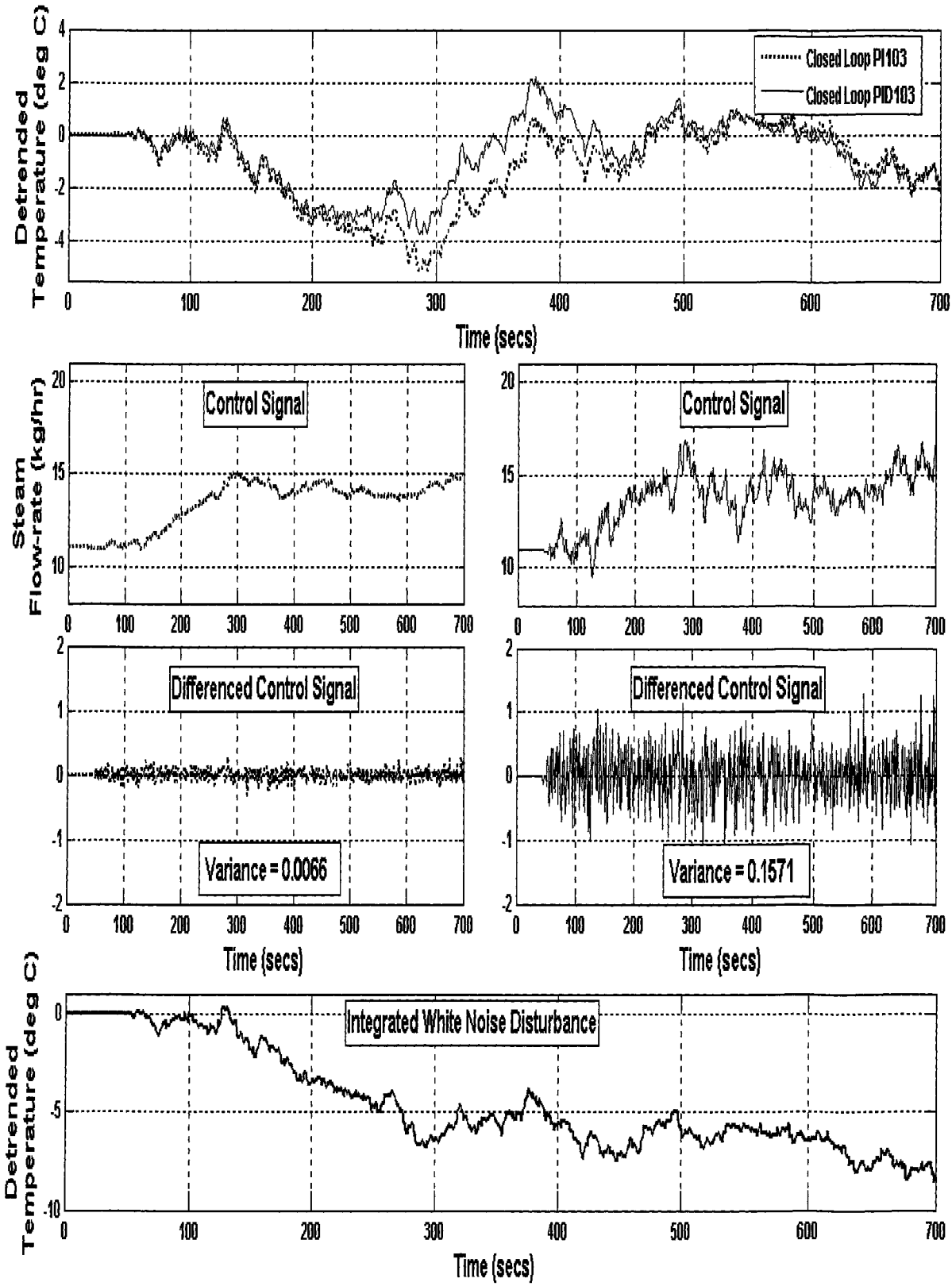

Figure 6.13(c): Temperature response of Thermocouple 3's experimentally implemented closed loops PI103 and PID103 to integrated white noise disturbance.

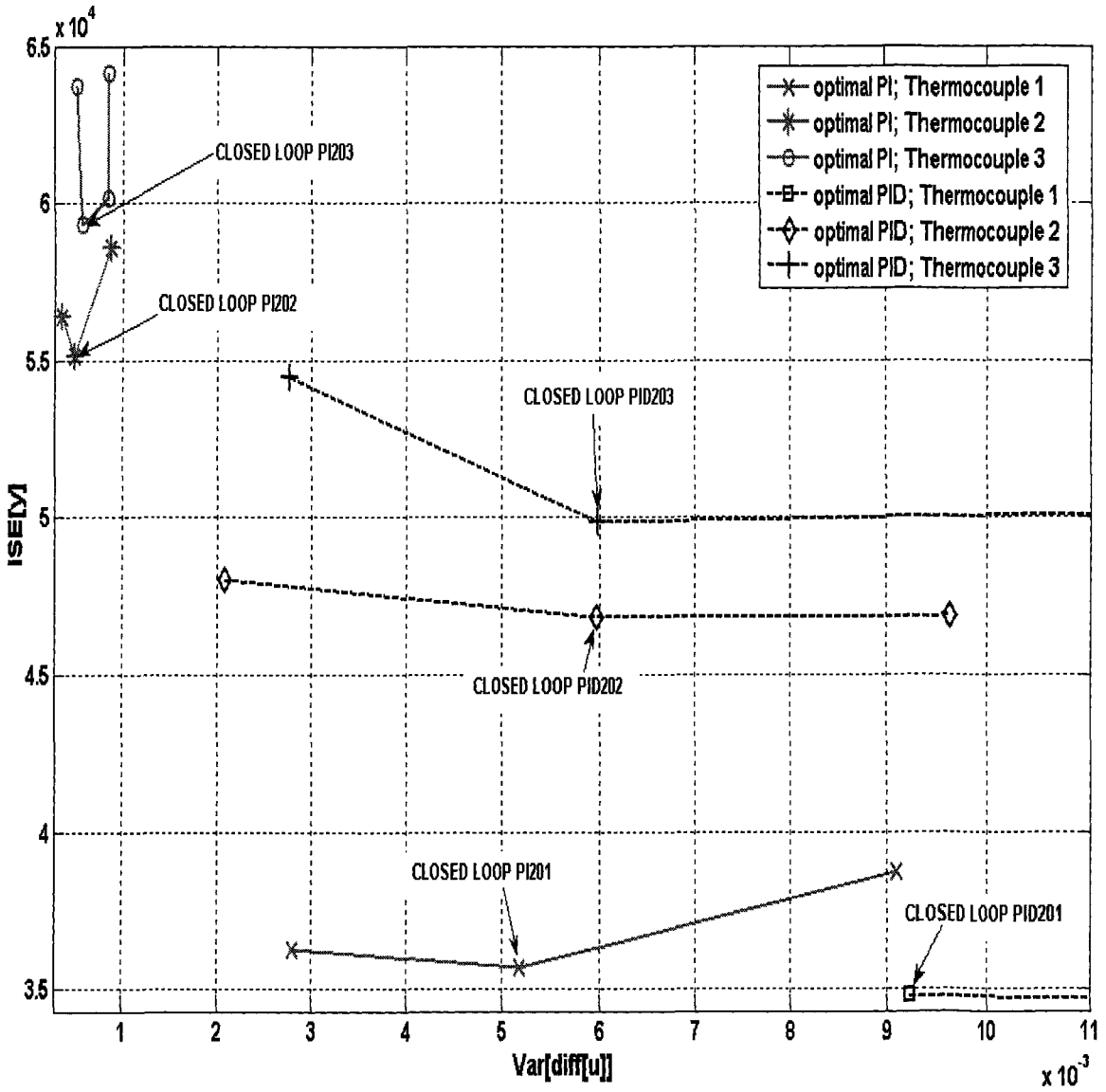

Figure 6.14: *ISE[y]-VAR[Δu]* profiles from experimental implementation of thermocouple closed loops perturbed by process input step disturbances.

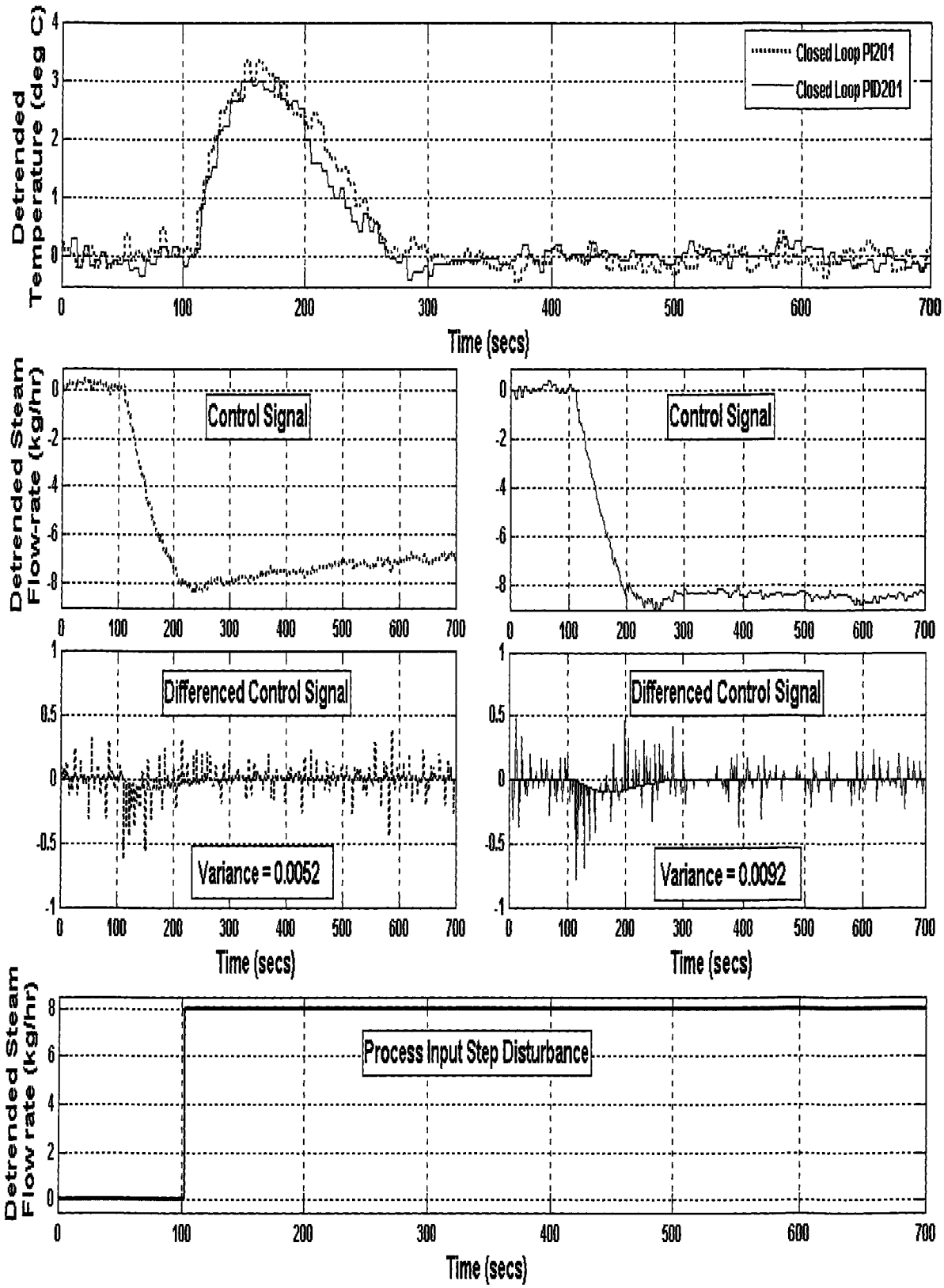

Figure 6.15(a): Temperature response of Thermocouple 1's experimentally implemented closed loops PI201 and PID201 to process input step disturbance.

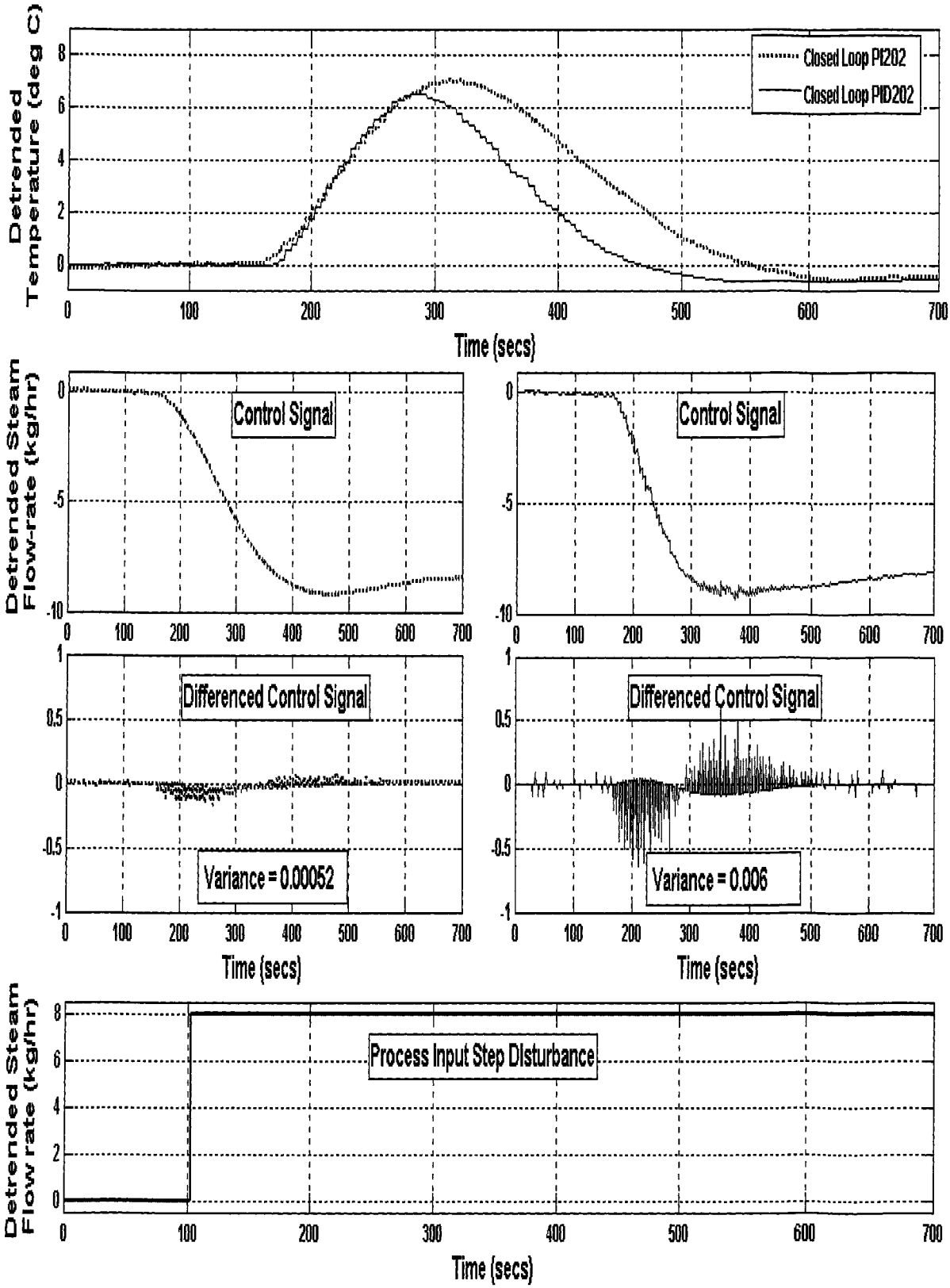

Figure 6.15(b): Temperature response of Thermocouple 2's experimentally implemented closed loops PI202 and PID202 to process input step disturbance.

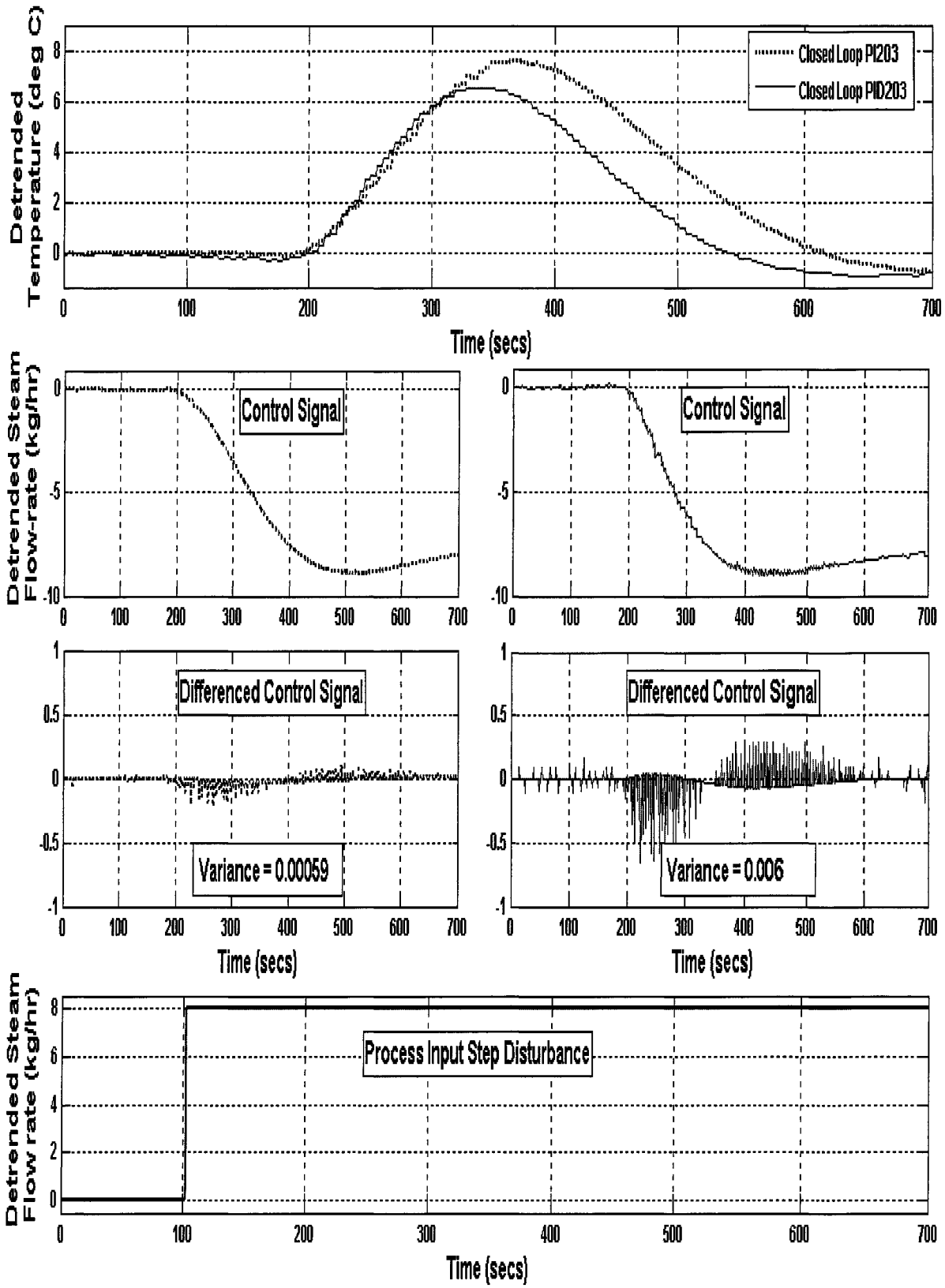

Figure 6.15(c): Temperature response of Thermocouple 3's experimentally implemented closed loops PI203 and PID203 to process input step disturbance.

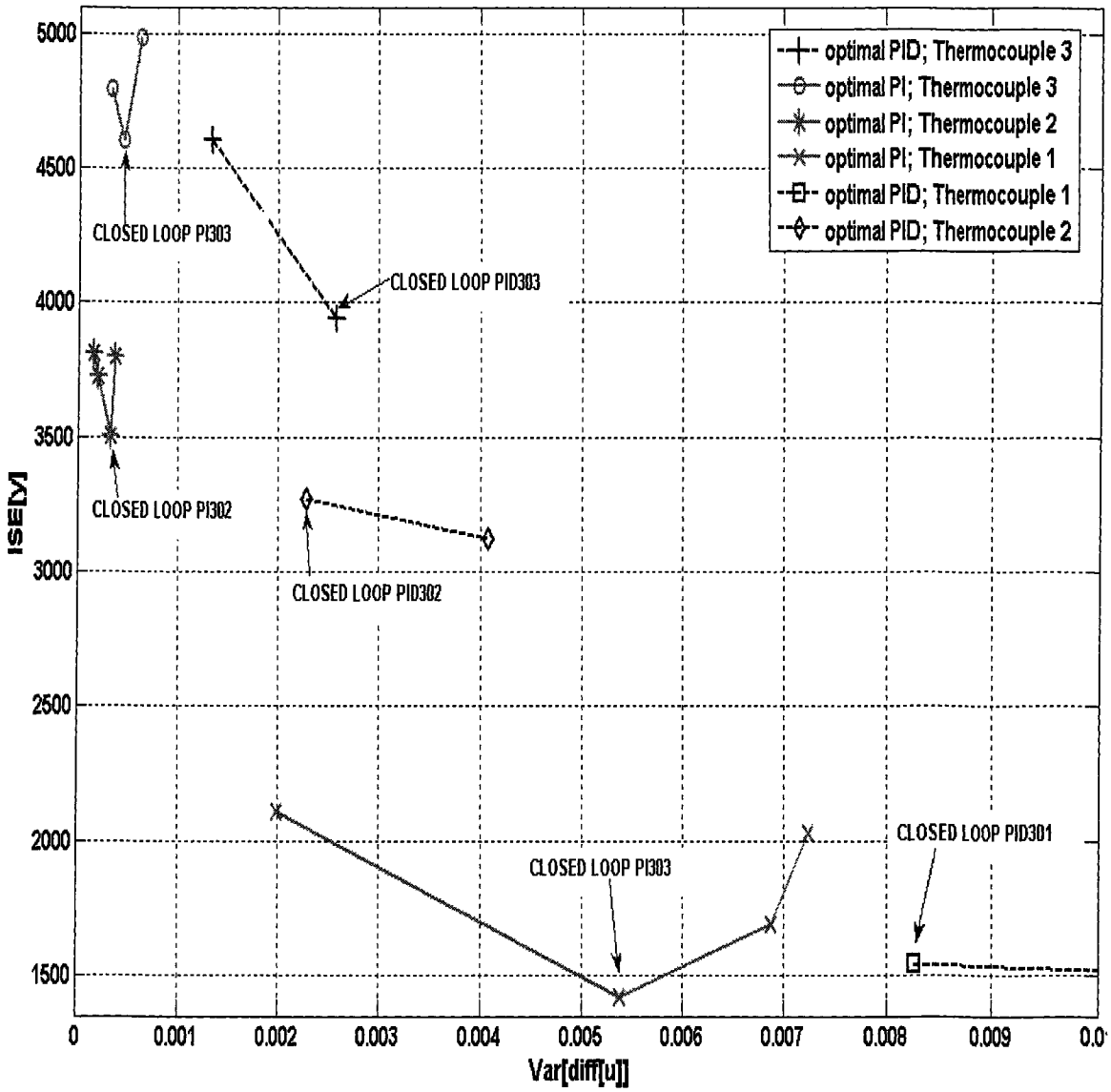

Figure 6.16: *ISE[y]-VAR[Δu]* profiles from experimental implementation of thermocouple closed loops perturbed by set point step.

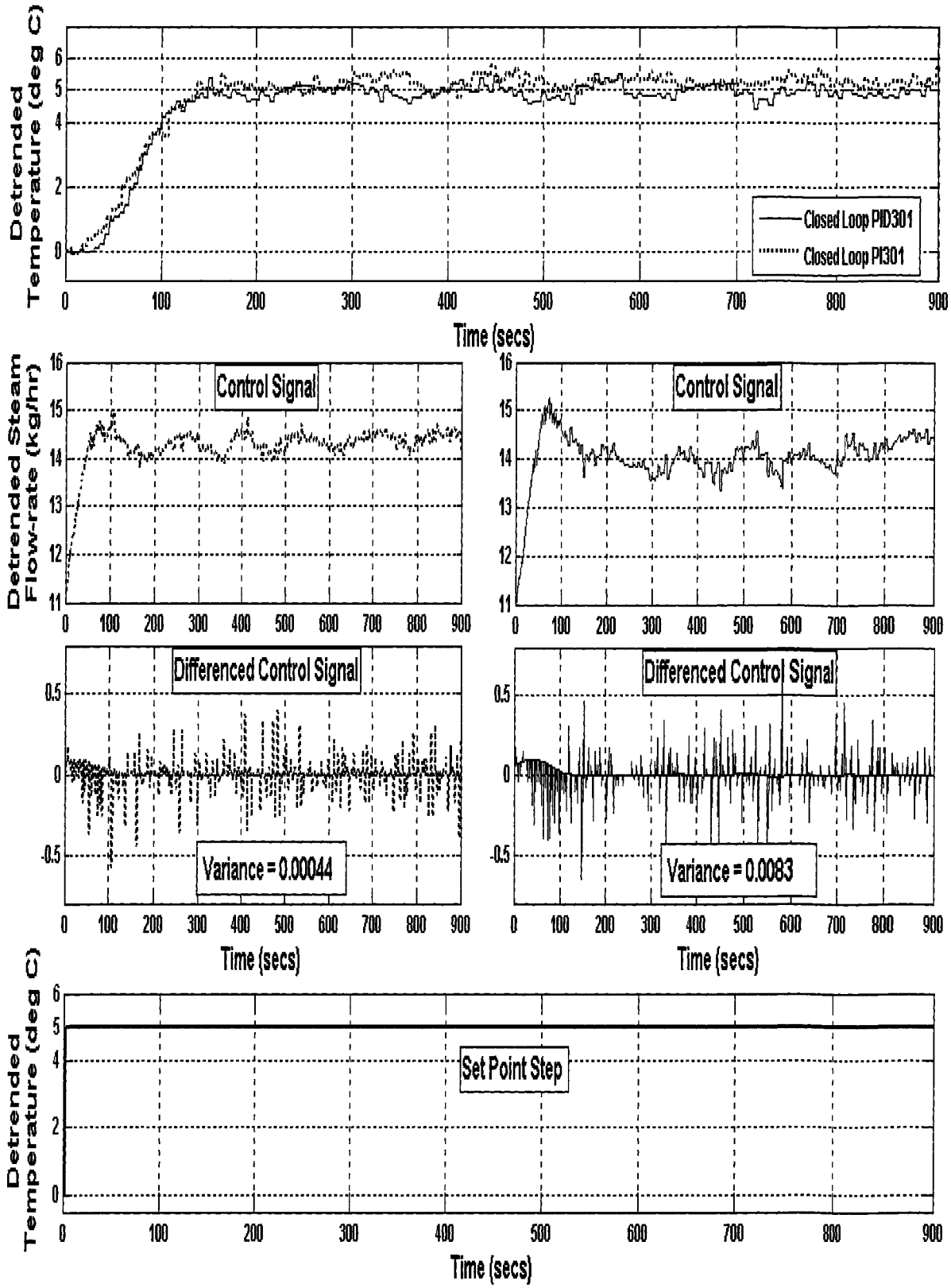

Figure 6.17(a): Temperature response of Thermocouple 1's experimentally implemented closed loops PI301 and PID301 to set point step.

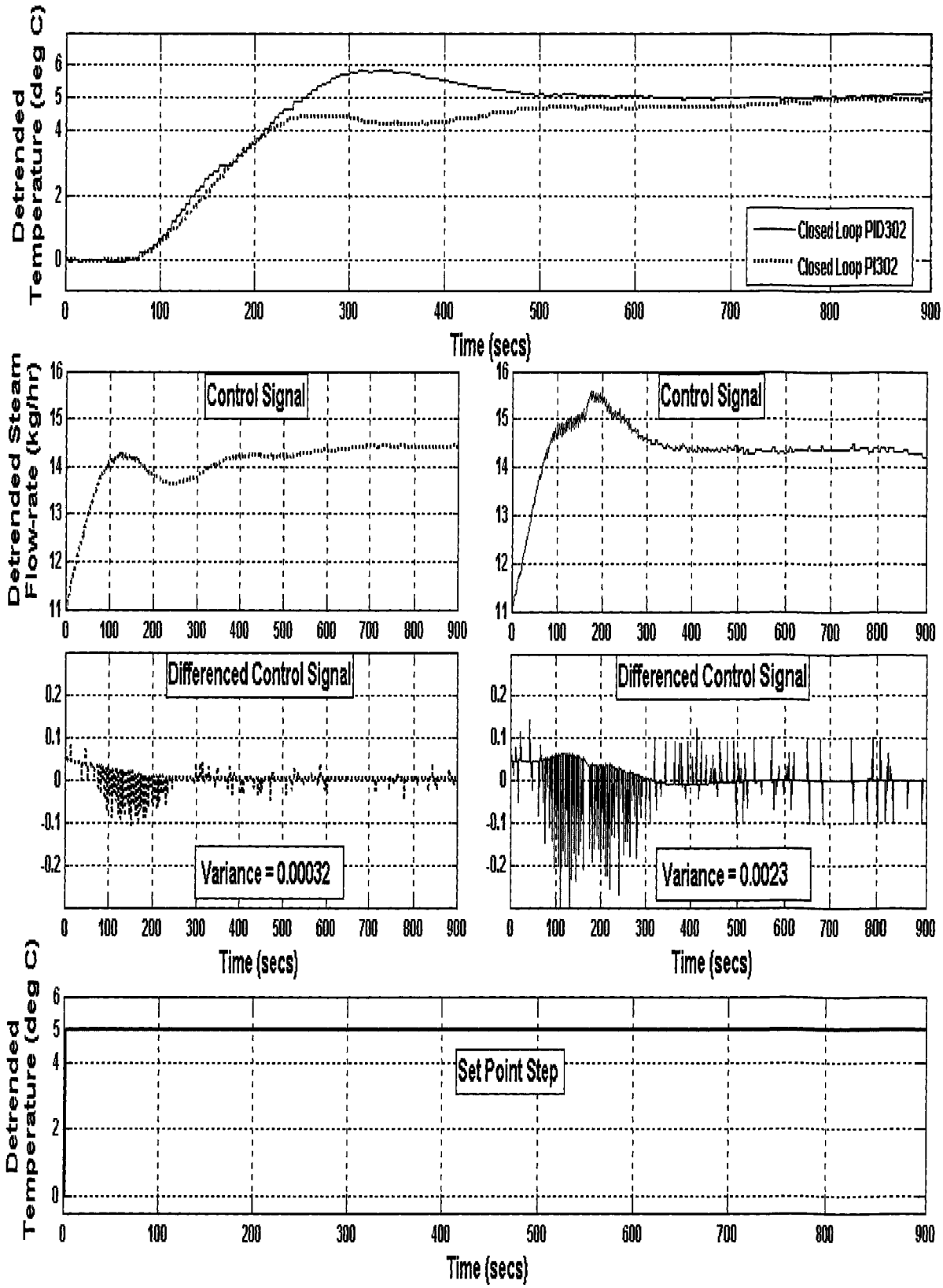

Figure 6.17(b): Temperature response of Thermocouple 2's experimentally implemented closed loops PI302 and PID302 to set point step.

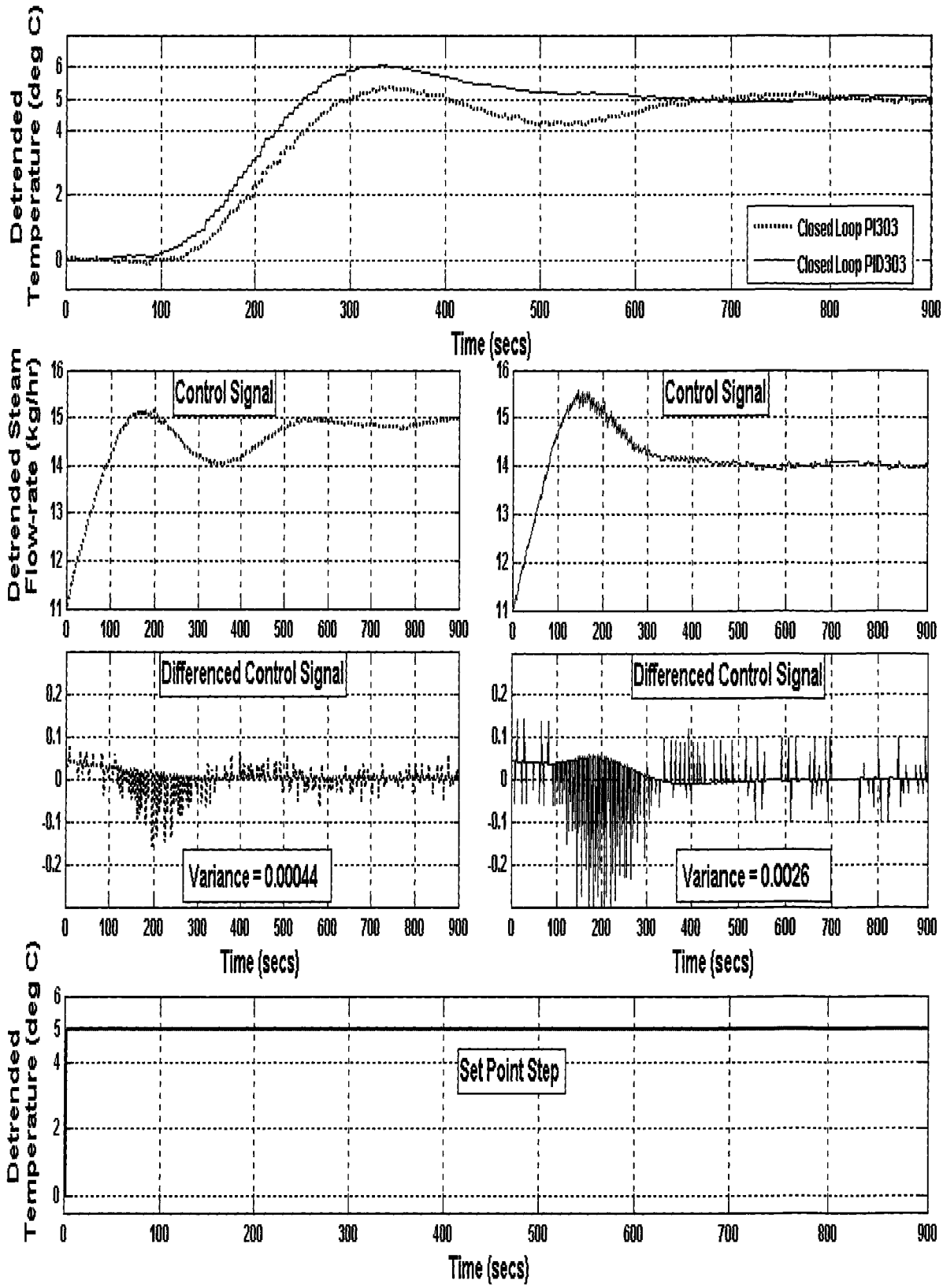

Figure 6.17(c): Temperature response of Thermocouple 3's experimentally implemented closed loops PI303 and PID303 to set point step.

The above figures show that for the three exogenous inputs considered, the PID controller's closed-loop performance is superior to the PI controller's for Thermocouples 2 and 3. However, for Thermocouple 1, which has a small time delay-time constant ratio, the PI controller performs almost equivalently with the PID controller. The figures demonstrate the increasing benefit the PID controller has over the PI controller with increasing time delay.

6.6 ECONOMIC BENEFITS OF OPTIMAL PID CONTROLLERS

Quite a number of controlled variables in industrial processes have control performance functions that directly or indirectly relate them to product yield, and thus income. Some of these control performance functions are inverse, non-linear relationships, so that the lower the mean value of the controlled variable, the higher the product yield (income). Craig and Koch [52] describe an industrial process having such a performance function – the Froth Flotation Process. The process is widely used in the concentration of mineral-bearing ores; it is usually the first step in the recovery of pyrite, the platinum group metals, copper, etc. The typical objective in this process is to maximize mineral recovery, since this determines the achievable income from the process. The controlled variable is the pulp level in the flotation cell, which determines the froth depth, and thus the recovered mineral concentrate's grade. Due to the dynamic nature of the process, the froth depth (grade) has an inverse, non-linear relationship with the mineral recovery. Therefore, product grade bears the cost for improved product recovery. Since the product grade is indirectly the controlled variable in this process, it would be expected that a minimum value constraint be imposed on it, so that product quality is not significantly sacrificed for product recovery. Thus, a secondary objective in the pulp level control of this process would be to ensure the product grade does not fall below a minimum value; that is, the pulp level in the flotation cell should not fall below a lower limit.

Craig and Koch [52] mathematically show how it is possible to improve product recovery in the flotation process by simply reducing the variability of the controlled variable, i.e., product grade, which is quantified by its standard deviation, σ, from the control set point, without violating the imposed grade constraint. This approach is generally applicable to processes with control performance functions that are linear with constraints, or non-linear with or without constraints. Reducing the variability of the controlled variable can be achieved by improving the loop performance of the controller utilized in the process. Because the utilized controller is likely to be of the PID structure, appropriate controller tuning or design can reduce variability. Variability reduction of the controlled variable around a set point makes it possible to move the set point, or the variable's mean value, to a more optimal position. In the Froth Flotation Process, for example, improved control of the concentrate grade allows its set point to be moved closer to the lower limit without violating it. Moving the set point closer to the limit leads to an increase in mineral recovery. Schubert et al. [53] point out that improved pulp level control could lead to an increase in recovery of about 1%. Another example of how improved control loop

performance can lead to economic benefits comes from [11], mentioned in Chapter 1, in which the Industrial Information Resources report reveals that major US process industries spend about thirty billion dollars annually on energy and over one hundred billion dollars on facility maintenance. According to the report, even a 1% improvement in either energy efficiency or improved controller maintenance direction represents hundreds of millions of dollars in savings to process industries.

The process description above provides an illustration of how controller closed-loop performance can be linked to a process' economic productivity, via the flexibility of moving the controlled variable's set point. To study this flexibility in detail, a hypothetical process, Process X, will be considered. The following assumptions are made about the process:

1) It has a controlled variable, y_X, which has the same non-linear control performance relationship, as the product grade in the Froth Flotation Process, with an income-related variable;

2) y_{XL} is the lower limit for y_X, hence $y_X \geq y_{XL}$;

3) Process X is controlled by either of two control systems – Control System 1 or Control System 2;

4) y_{X1} and y_{X2} are the responses of y_X, under the control of Control Systems 1 and 2 respectively; and

5) The set points for y_X under the control of Control System 1 and 2 are y_{XSP1} and y_{XSP2} respectively;

6) y_{X1} and y_{X2} are stochastic and are sampled for a sufficiently long duration, so that the variations around the respective set points y_{XSP1} and y_{XSP2} are approximately normally distributed with standard deviations σ_1 and σ_2 respectively and mean values approximately equal to y_{XSP1} and y_{XSP2} respectively.

According to [54], if the control systems are stable, or "in statistical control", then more than 99% of the data points in y_{X1} and y_{X2} are expected to respectively lie within the intervals:

$$y_{XSP1} - 3\sigma_1 \leq y_{X1} \leq y_{XSP1} + 3\sigma_1$$
$$y_{XSP2} - 3\sigma_2 \leq y_{X2} \leq y_{XSP2} + 3\sigma_2$$

Because $y_{X1}, y_{X2} \geq y_{XL}$, then in the worst case,

$$y_{XSP1} - 3\sigma_1 = y_{XL} \quad (6.2a)$$

$$y_{XSP2} - 3\sigma_2 = y_{XL} \quad (6.2b)$$

$$\Rightarrow y_{XSP1} - 3\sigma_1 = y_{XSP2} - 3\sigma_2 \quad (6.2c)$$

$$\Rightarrow y_{XSP1} - y_{XSP2} = 3\sigma_1 - 3\sigma_2 \quad (6.2d)$$

If Control System 1 leads to a greater variation in y_X than Control System 2, so that $\sigma_1 > \sigma_2$, (6.2) implies that $y_{XSP1} > y_{XSP2}$. Thus, in order for the two systems not to violate the linear constraint y_{XL}, y_{XSP1} must be raised higher than y_{XSP2}. Based on the non-linear control performance function, Control System 2 can be implemented at a target set point closer to the lower limit, and can therefore increase product yield relative to Control System 1. Figure 6.18 shows the distribution profiles of y_{X1} and y_{X2}, as well the relative positions of their mean points, y_{XSP1} and y_{XSP2}, with respect to the constraint y_{XL}.

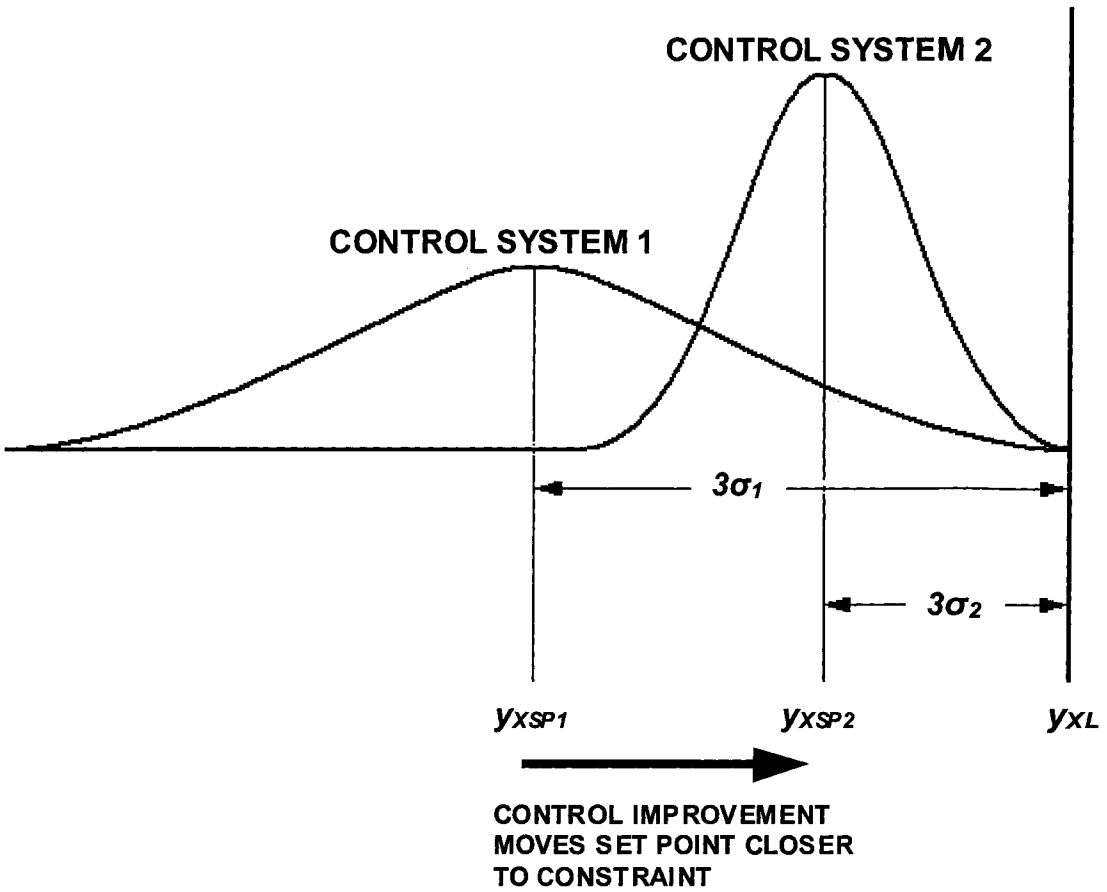

Figure 6.18: Movement of set point of controlled process variable towards constraint due to its reduced variation, brought about by controller performance improvement.

Now, for the Heated Tank Process, the controlled variable is the water temperature measured at each thermocouple. Figures 6.12, 6.13(b), and 6.13(c) have shown that the optimal PID controller can give smaller variations in the regulatory responses of temperatures than the optimal PI controller. As an illustration, let the Heated Tank Process be considered part of a hypothetical

integrated process, like Process X, in which the water temperature has an inverse, non-linear performance relationship with an economically beneficial variable. An example of such an integrated process could be a catalyzed chemical reaction, which is heated in a water bath. The nature of the reaction could be such that it ceases below a minimum temperature and consequently must be operated above that temperature. Therefore, the temperature of the water in the bath must in turn always be above a lower limit. On the other hand, the higher the temperature of the water bath above the lower limit, the greater the heat losses via convection and radiation since both processes are directly related to the source's temperature. Therefore, an economically beneficial variable for this process could be the heat savings from operating the chemical process at temperatures as close to the lower limit as possible, while the controlled variable is the temperature of the water bath, i.e. the Heated Tank Process. Figure 6.19 shows the hypothetical temperature control performance function for the integrated process.

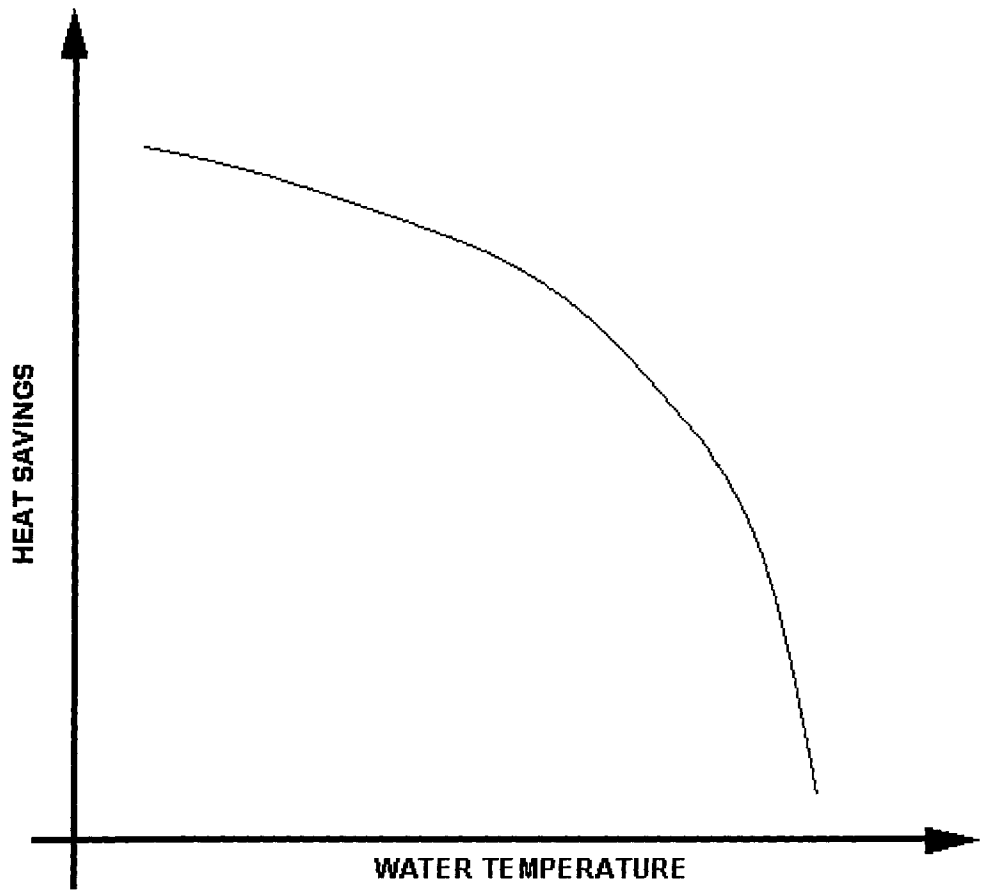

Figure 6.19: Temperature control performance function for integrated process.

Thus, the integrated process can be likened to Process X with Control System 1 being an optimal PI controller (Closed Loop PI402 in Figure 6.12). Control System 2 could be a just proper optimal PID controller (Closed Loop PID402) or

a strictly proper optimal PID controller. The control objective is to regulate the water temperature around a set point temperature such that at no instance does it fall below a lower limit. With the optimal PID controller's closed loop giving smaller variations than the optimal PI, it would be expected that the former control system's set point can be moved closer to a lower limit, without the actual temperature falling below this limit. Simulation and experimental examples are considered below to test this hypothesis. In each case, the assumptions made on Process X above, regarding the normality of the temperature responses, are assumed to be valid for this process.

Example 6.1: Closed loops of an optimal PI controller, an optimal just proper PID controller, and an optimal strictly proper PID controller are implemented in simulation, one after the other, for the Heated Tank Process. The control objective is to regulate the water temperature in response to an integrated white noise disturbance, so that it does not fall below 11°C, while keeping the set point temperature as close to this lower limit as possible.

Figure 6.20 shows the time trend of the integrated white noise disturbance sent added to each closed loop.

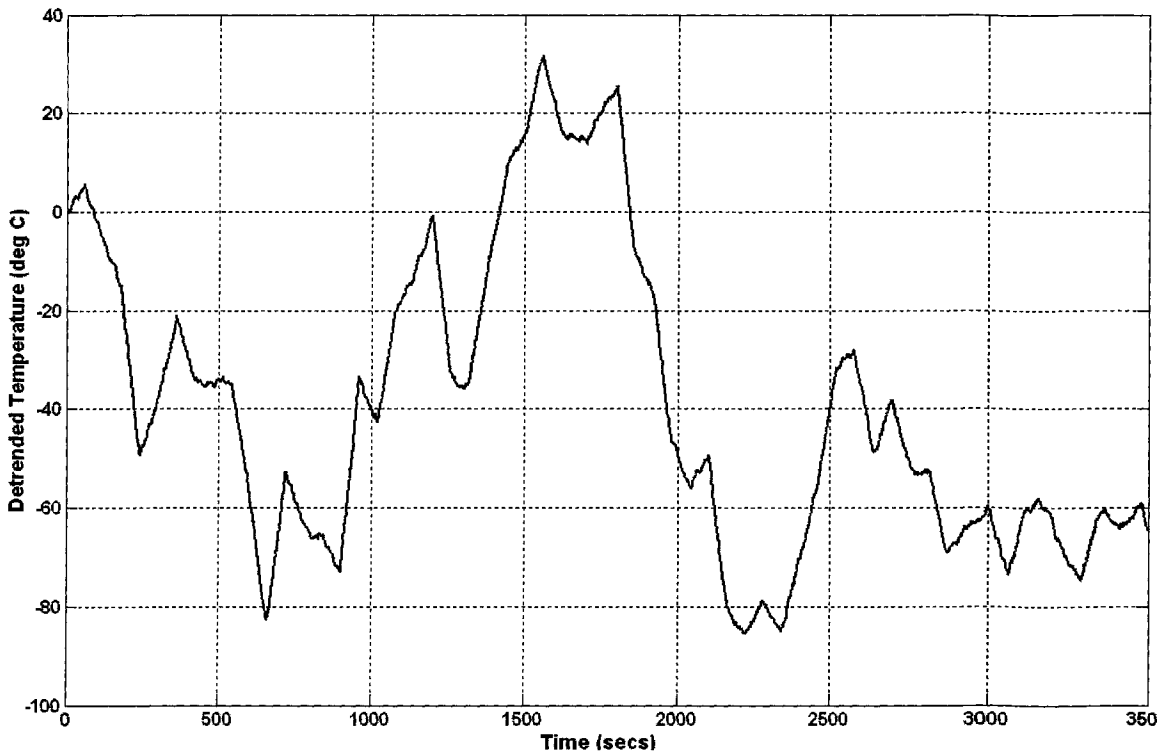

Figure 6.20: Integrated white noise disturbance sent to Heated Tank SIMULINK closed loop.

Table 6.3 shows the standard deviations, σ_{PI}, σ_{PID}, and σ_{PIDF} of the closed-loop temperature responses of the PI and the just and strictly proper PID controllers respectively, to the disturbance in Figure 6.20.

Table 6.3: Standard Deviations of Closed-Loop Temperature Responses of Optimal Controllers

CONTROLLER	STANDARD DEVIATION
Optimal PI	6.1533
Just proper optimal PID	5.0100
Strictly proper optimal PID	5.2500

From (6.2a) and (6.2b), the recommended temperature set points, y_{SP}^{PI}, y_{SP}^{PID}, and y_{SP}^{PIDF} respectively for the closed loops are:

$$\begin{aligned} y_{SP}^{PI} &= y_L + 3\sigma_{PI} \\ y_{SP}^{PID} &= y_L + 3\sigma_{PID} \\ y_{SP}^{PIDF} &= y_L + 3\sigma_{PIDF} \end{aligned} \tag{6.3}$$

where y_L is the lower limit temperature, 11°C.

Table 6.4 shows the recommended set point temperatures for the three closed loops, based on (6.3). Figure 6.21 shows the *ISE[y]-VAR[Δu]* profiles for the three closed loops. Figure 6.22 shows the temperature responses for the three loops using these set point temperatures, as well as the steam flow trend, its differenced trend (control activity), plus as their variances for each loop.

Table 6.4: Recommended Set Point Temperatures for Closed Loops of Optimal Controllers

CONTROLLER	RECOMMENDED TEMPERATURE SETPOINT (°C)
Optimal PI	29.46
Just proper optimal PID	26.03
Strictly proper optimal PID	26.75

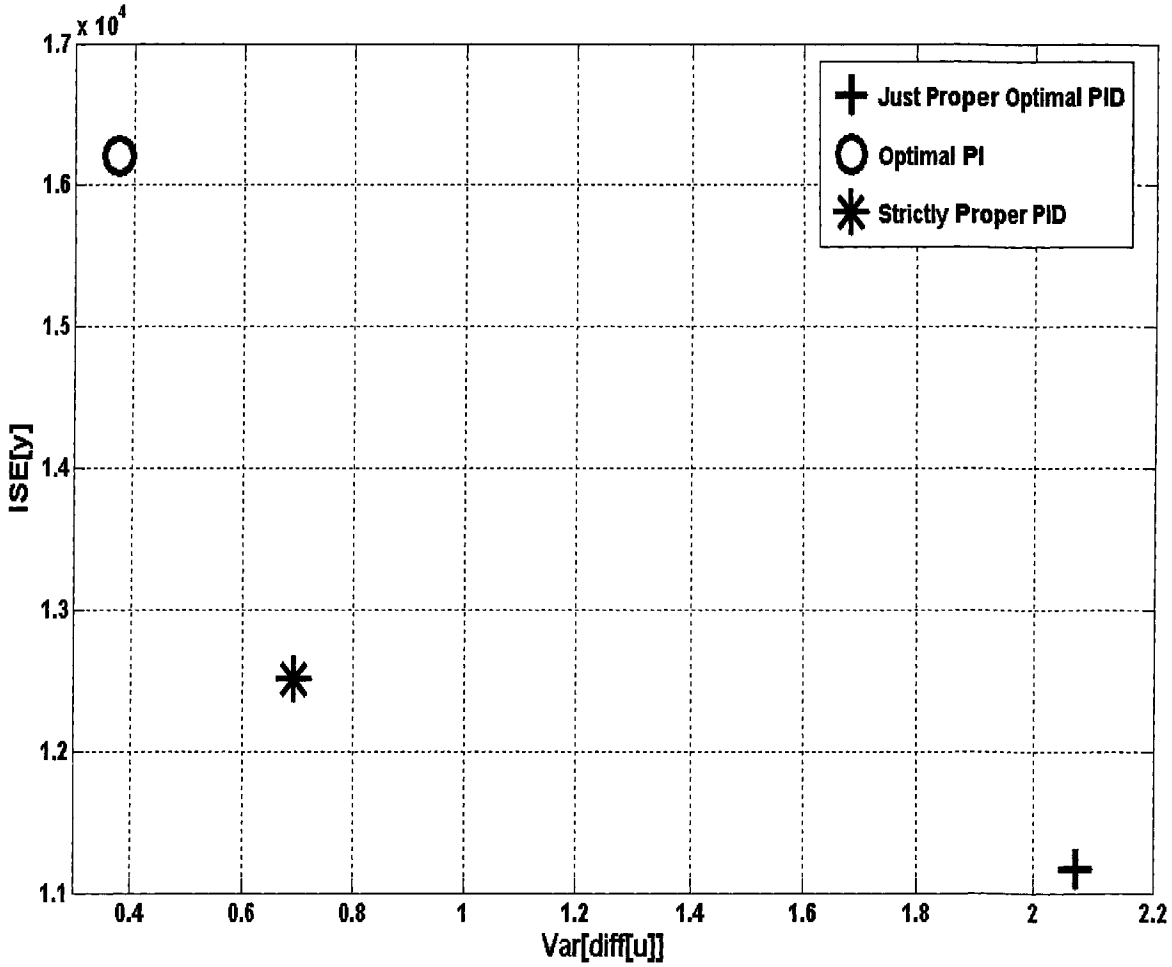

Figure 6.21: *ISE[y]-VAR[Δu]* profiles for simulated closed loops of optimal controllers.

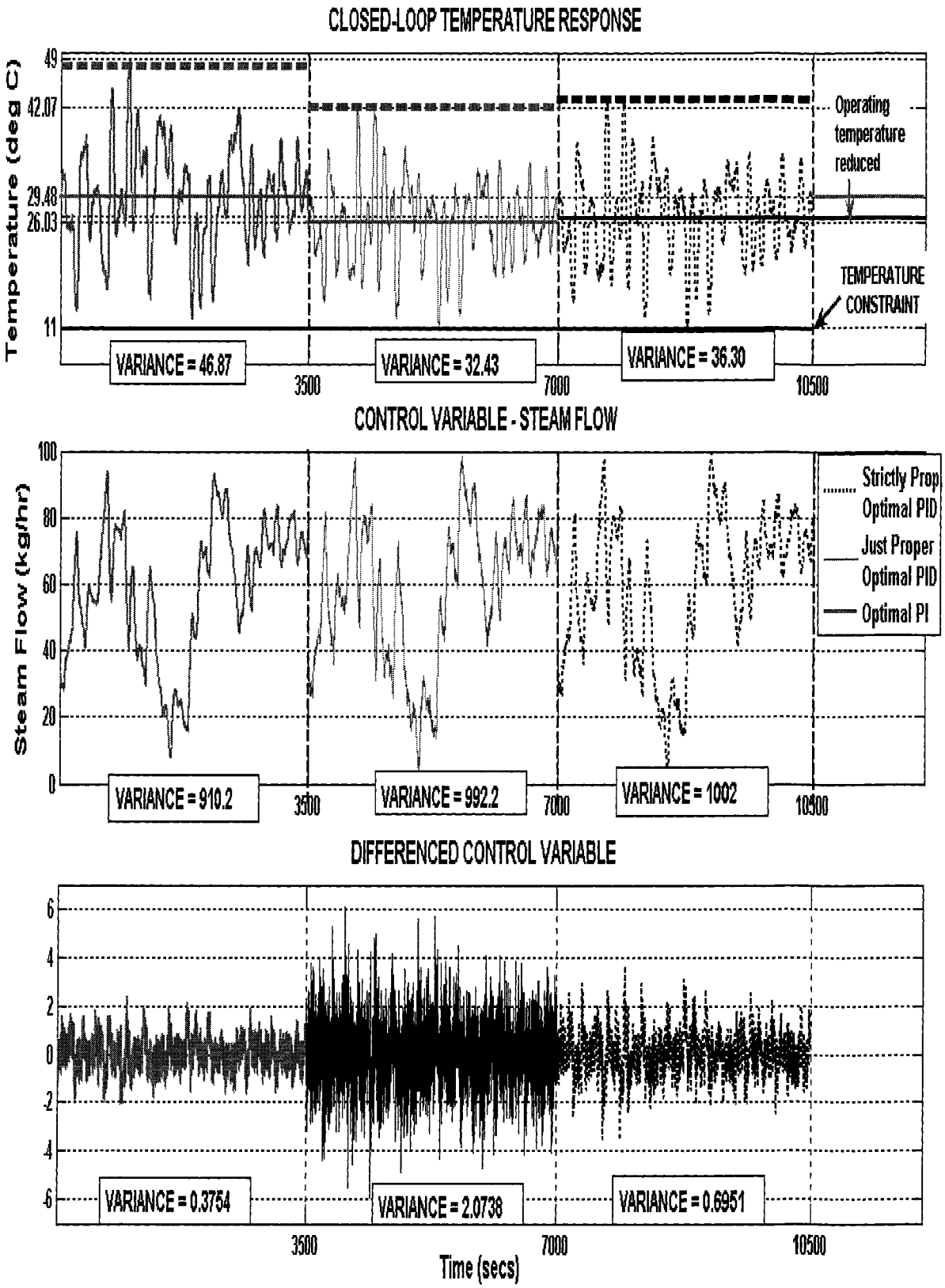

Figure 6.22: Simulated closed-loop temperature responses of optimal controllers to integrated white noise disturbance.

Figures 6.21 and 6.22 both show the reduced variation in the water temperature when controlled by the PID controllers, relative to the PI controller. All closed loops satisfy the control objective of regulating water temperature so that it does not fall below 11°C; the PID controllers are implemented at lower set points than the PI controller and can therefore give greater heat savings. The price to be paid by reduced variation in the controlled variable is increased variation in the PID control signal, as shown by the higher variance of the steam flow trend and its differenced trend. The strictly proper PID controller is able to strike a fair balance of giving lower temperature variation than the PI controller without an excessive increase in *VAR[Δu]* typical of the just proper PID controller.

Example 6.2: Closed loops of an optimal PI controller, an optimal just proper PID controller, and an optimal strictly proper PID controller are experimentally implemented, one after the other, on the Heated Tank Process. The control objective is to regulate the water temperature in response to an integrated white noise disturbance, so that it does not fall below 28°C, while keeping the set point temperature as close to this lower limit as possible.

Table 6.5 shows the standard deviations and recommended set point temperatures for the three closed loops, based on (6.3). Figure 6.23 shows the time trend of the integrated white noise disturbance sent to each closed loop. Figure 6.24 shows the *ISE[y]-VAR[Δu]* profiles for the three closed loops. Figure 6.25 shows the temperature responses for the three loops using these set point temperatures, as well as the steam flow trend, its differenced trend (control activity), plus their variances for each loop.

Table 6.5: Standard Deviations and Recommended Set Point Temperatures for Experimentally Implemented Closed Loops of Optimal Controllers

CONTROLLER	STANDARD DEVIATION	RECOMMENDED TEMPERATURE SETPOINT (°C)
Optimal PI	1.1667	31.5
Just proper optimal PID	1.000	31
Strictly proper optimal PID	1.0667	31.2

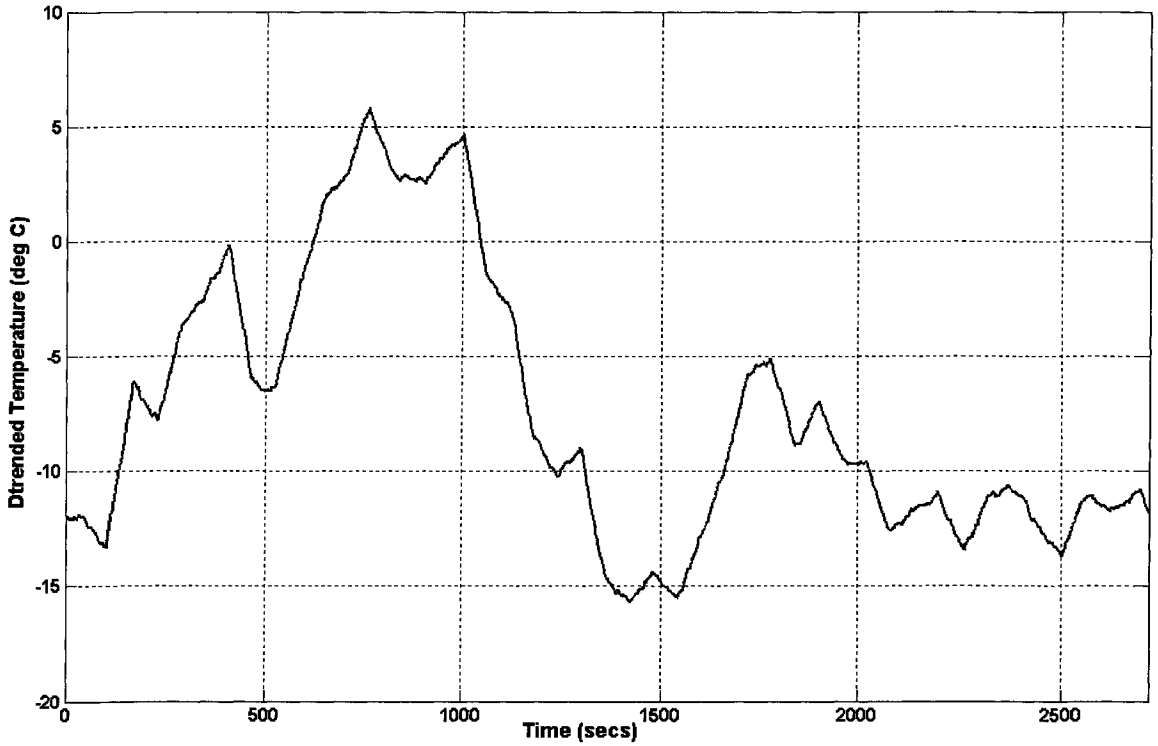

Figure 6.23: Integrated white noise disturbance sent to Heated Tank closed loop.

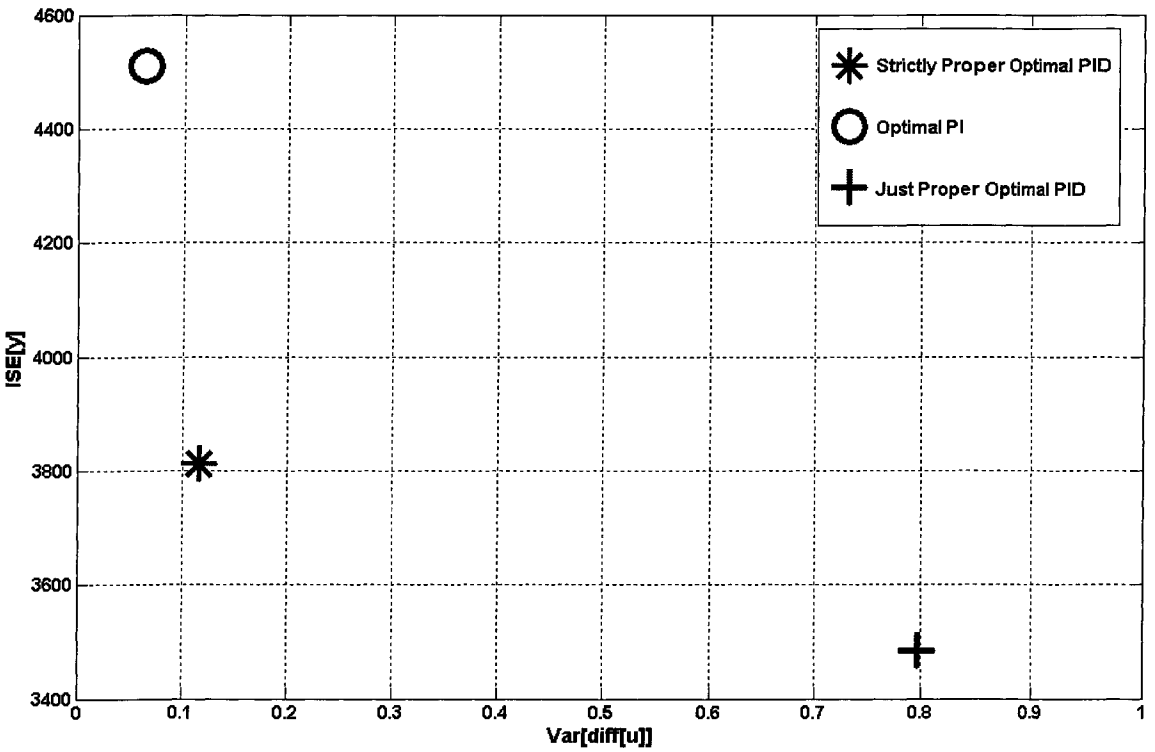

Figure 6.24: *ISE[y]-VAR[Δu]* profiles for experimentally implemented closed loops of optimal controllers.

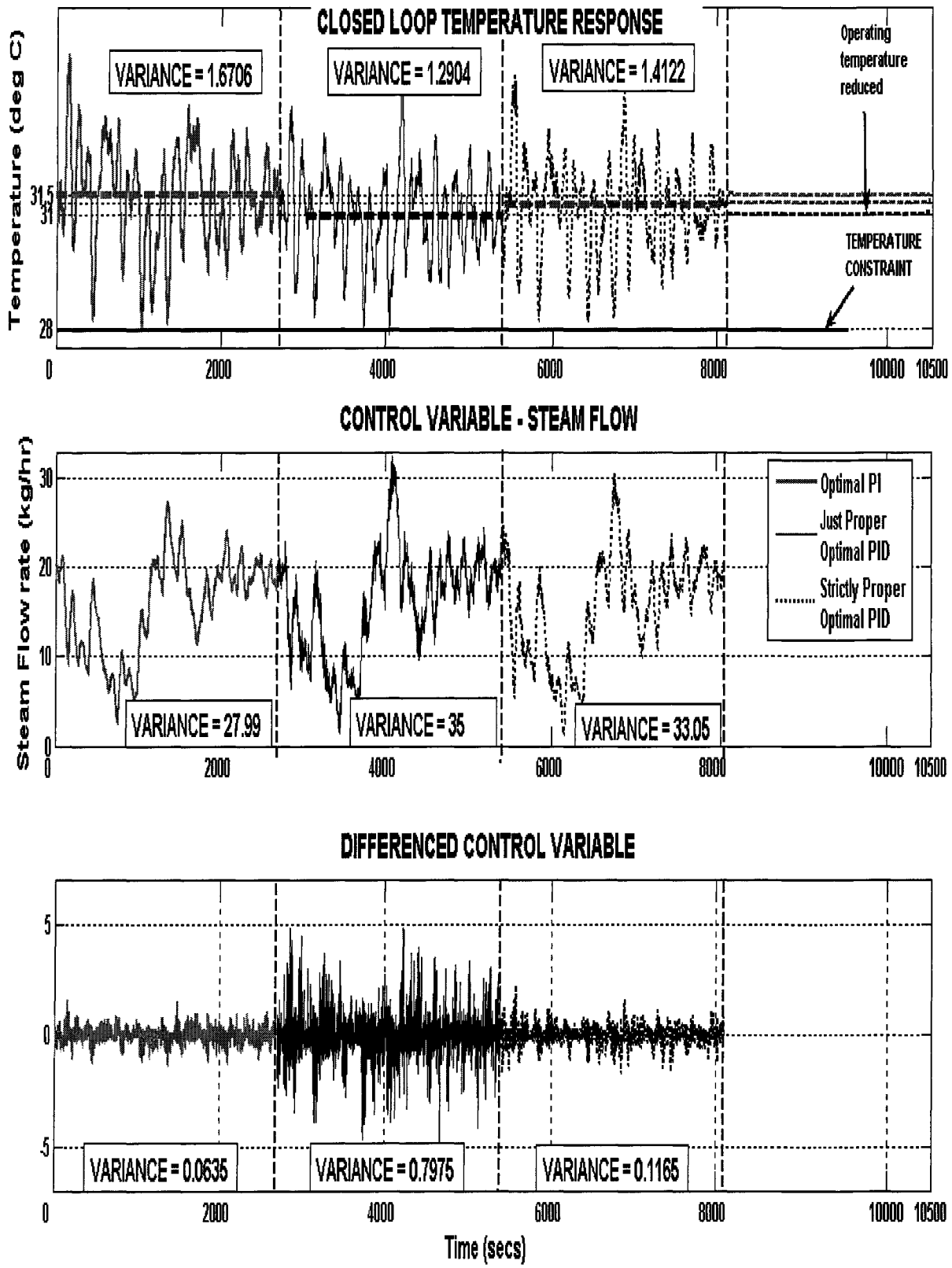

Figure 6.25: Experimentally implemented closed-loop temperature responses of optimal controllers to integrated white noise disturbance.

Figure 6.25 supports the simulation results shown in Figure 6.22. Hence, the optimal PID controller can deliver process variable response with smaller variation than the optimal PI controller, thus enabling the variable's set point to be placed closer to its constraint without violating it. This can lead to increases in economically significant process outputs. The price to be paid for this benefit is the increased variation in the control signal, which can be reduced significantly by utilizing a strictly proper PID controller.

In summary, this section has shown not only the potential technical benefits the PID controller has above the PI controller, but also how these benefits can be translated into economic benefits for the process industry.

CHAPTER 7

OPTIMAL PID CONTROLLERS AND SMITH PREDICTORS

7.1 INTRODUCTION

In Chapter 5, the presence of time delays in processes was shown to limit the performance of conventional feedback control systems. Systems with time delays can be controlled to some degree with PID control. However, the traditional tuning rules often give very poor results. Although derivative action is useful for lag-dominant processes, it is of limited value for systems that are delay-dominant [5, 20]. The reason for this is that prediction of the process output based on linear extrapolation is not effective. It is much better to make predictions based on inputs that have been fed into the system, but which have not yet shown up in the output.

To improve the performance of control systems containing significant time delays, the *Smith Predictor* technique [21, 22, 23, 24] is an effective control strategy for providing time delay compensation. Figure 7.1 shows the block diagram of a feedback loop augmented with a Smith predictor.

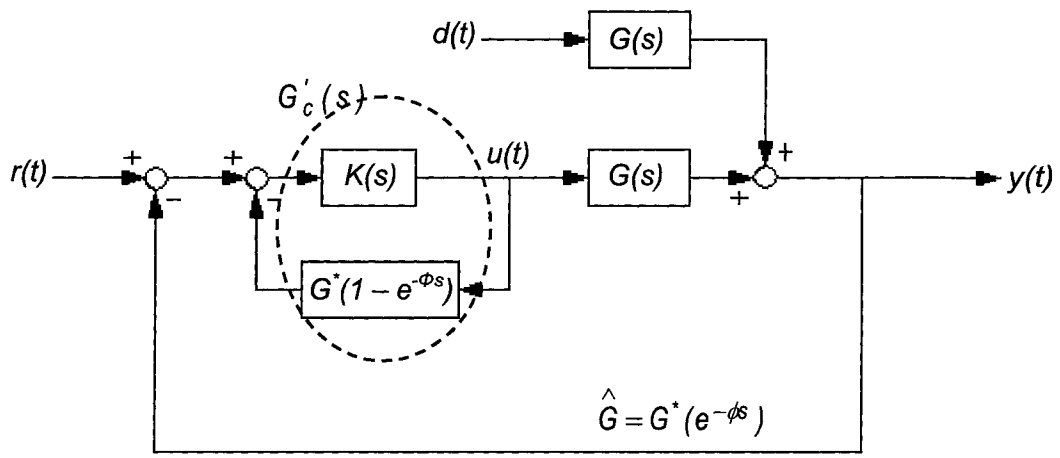

Figure 7.1: Block diagram of a SISO closed loop augmented with a Smith Predictor.

G^* is the delay-free form of the modeled transfer function $\hat{G}$ for the process G, so that $\hat{G} = G^*(e^{-\Phi s})$. G_c' is a composite controller consisting of controller K and the Smith predictor.

The objective of this chapter is to examine the performance comparisons of closed loops containing the Smith predictor, and those containing the plain PI or PID controllers, especially for processes with significant time delay dominance.

Traditionally, K is a controller, PI or PID, designed for G^*, i.e., the delay-free process, using typical tuning methods for SISO transfer functions [7]. Hence, optimal PI and PID controllers can be designed for G^* by solving (2.21) with the appropriate constraints. In [13], a proposed approach to designing K is to solve (2.21) for K', i.e., the composite controller, instead of K itself, and for $\hat{G}$ instead of G^*. The performance of a controller incorporating the Smith predictor for set-point changes has been found to be better than a conventional PI controller based on an integral-squared-error criterion [14]. However, the Smith predictor's performance may not be superior for all types of disturbances.

The sensitivity transfer functions for a closed loop having a Smith predictor are:

Sensitivity Function: $$S(s) = G_{er} = \frac{1 + K(G^* - \hat{G})}{1 + KG^*} \tag{7.1}$$

Complementary Sensitivity Function: $$T(s) = G_{yr} = \frac{K\hat{G}}{1 + KG^*} \tag{7.2}$$

Disturbance Sensitivity Function: $$\hat{G}(s)S(s) = G_{yd} = \frac{\hat{G} + \hat{G}KG^*(1 - e^{-\phi s})}{1 + KG^*} \tag{7.3}$$

Control Sensitivity Function: $$K(s)S(s) = \frac{K}{1 + KG^*} \tag{7.4}$$

(7.1) to (7.4) are based on the assumption that the modeled process time delay ϕ is equal to the actual time delay θ. If there is a significant mismatch in the two time delays, (7.2) and (7.3) respectively become:

Complementary Sensitivity Function:

$$T(s) = G_{yr} = \frac{K\hat{G}}{1 + KG^* + KG^* e^{-\theta s}(1 - e^{-(\phi - \theta)s})} \tag{7.5}$$

Disturbance Sensitivity Function:

$$\hat{G}(s)S(s) = G_{yd} = \frac{\hat{G} + \hat{G}KG^*(1 - e^{-\phi s})}{1 + KG^* + KG^* e^{-\theta s}(1 - e^{-(\phi - \theta)s})} \tag{7.6}$$

7.2 LIMITATIONS OF CLOSED LOOPS WITH SMITH PREDICTORS

Although the Smith predictor generally enhances the performance of the closed loop in which it is included, there are costs on others properties of the closed loop that limit the benefits of the Smith predictor augmentation. For traditional Smith predictor systems in which the PID controller is designed for the delay-free process transfer function G^*, it has been found [13] that their J_V values are typically lower than for Smith-augmented control systems designed by optimizing the disturbance sensitivity function for the entire structure, and for control systems using just PID controllers. However, the traditional Smith/PID system has a considerably smaller gain margin than other control systems. Above the phase crossover frequency, the loop gain attains very high values and in some frequency intervals, the phase angle shifts in the positive direction. Hence, its robustness is deteriorated. When the entire control structure is optimized, using the same constraints on GM_S as in (2.21), the resulting loop gain is still large at high frequencies, with J_V higher than the traditional Smith controller's, but lower than the optimal PID control system's. Its robustness is also unacceptable. For moderate delays, there are some benefits attainable by including a PID controller in a Smith predictor structure and optimizing (2.21) for the composite controller, compared to a PID controller without a Smith structure. It has also been observed [13] that an optimal PID controller (without a Smith predictor) can give better performance than the PI controller with or without the Smith predictor. To illustrate the observed features of the aforementioned Smith predictor-augmented closed loops, the following control systems are designed for the hypothetical modeled transfer function $\hat{G} = \frac{e^{-6s}}{10s+1}$, which has a time delay-time constant ratio of 0.6. The design of all the control systems is based on the assumption of insignificant mismatch of the modeled and actual time delays, i.e., $\phi \approx \theta$:

a) Traditional Smith/PID controller (Control System A) – designed by solving (2.21) for the s^{-1}-weighted form of (2.4), using delay-free G^* as the process transfer function;

b) Optimized Smith/PID controller (Control System B) – designed by solving (2.21) for the s^{-1}-weighted form of (7.3) with the definition of GM_S in (2.16) retained;

c) Optimized Smith/PI controller (Control System C) – designed by solving (2.21) for the s^{-1}-weighted form of (7.3) with the definition of GM_S in (2.16) retained;

d) Optimized PID controller (Control System D) – designed by solving (2.21) for the s^{-1}-weighted form of (2.4), using $\hat{G}$ as the process transfer function; and

e) Optimized PI controller (Control System E) – designed by solving (2.21) for the s^{-1}-weighted form of (2.4), using $\hat{G}$ as the process transfer function.

For Control Systems A, B, and D, the constraints $GM_S \leq 1.7$ and $J_u = 10.2$ are used, while the constraints on J_u and k_∞, which give optimal PI controllers with minimum J_v values, are used for Control Systems C and E, with the GM_S constraint retained. Figures 7.2 to 7.6 show the frequency responses of the five control systems, their performance-control action plots, and their closed-loop responses.

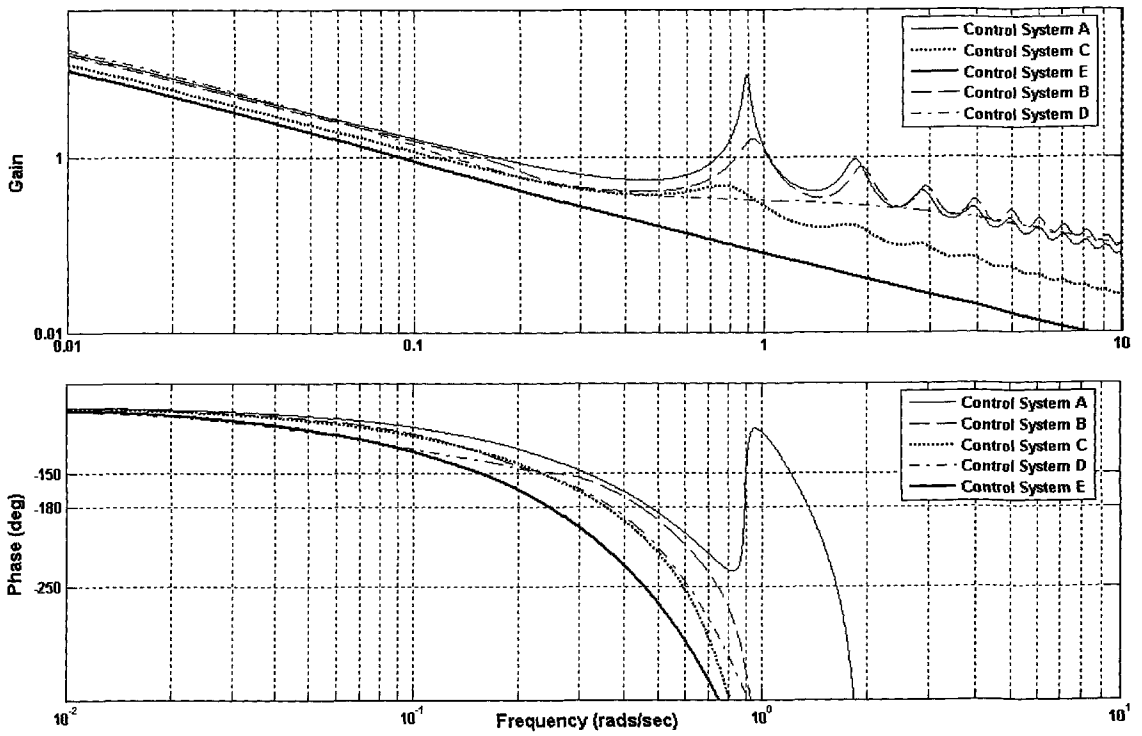

Figure 7.2: Bode plots for Control Systems A, B, C, D, and E.

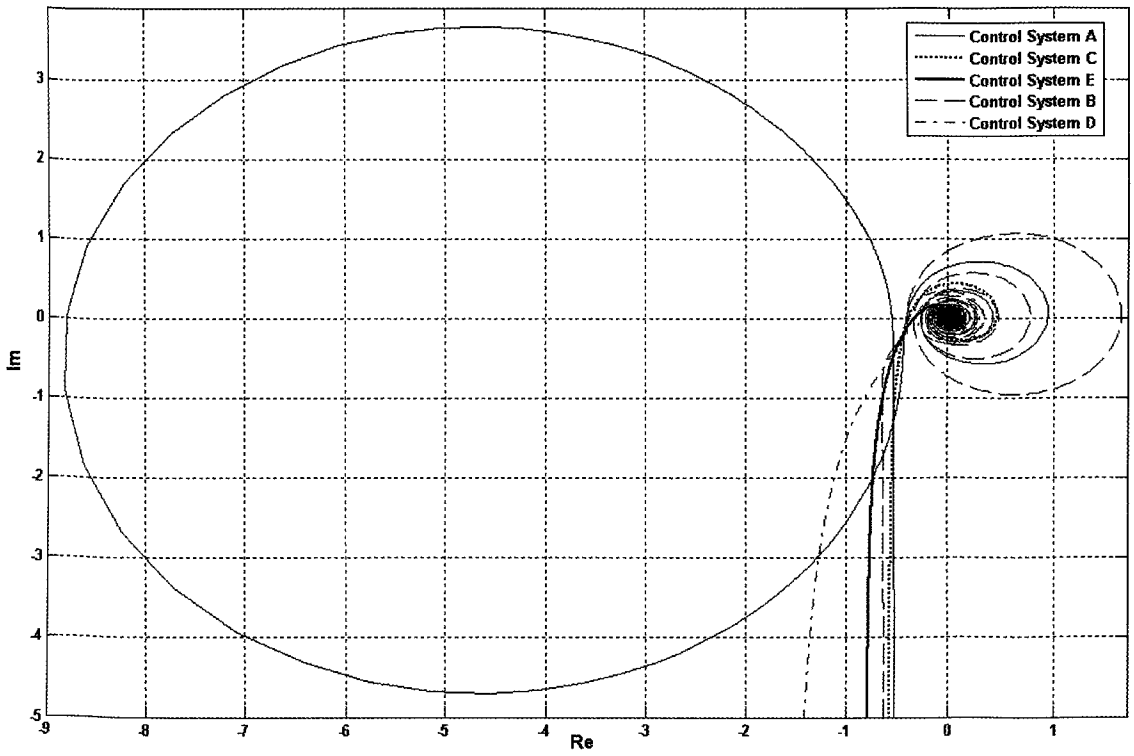

Figure 7.3: Nyquist plots for Control Systems A, B, C, D, and E.

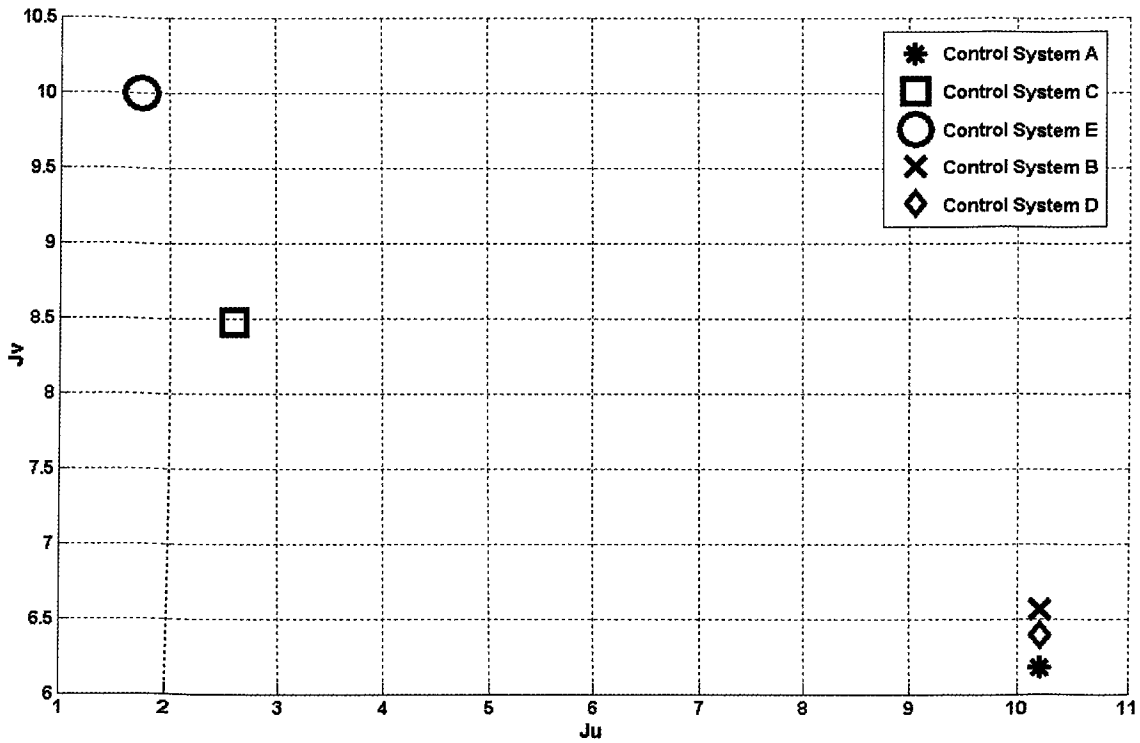

Figure 7.4: J_v-J_u plots for Control Systems A, B, C, D, and E.

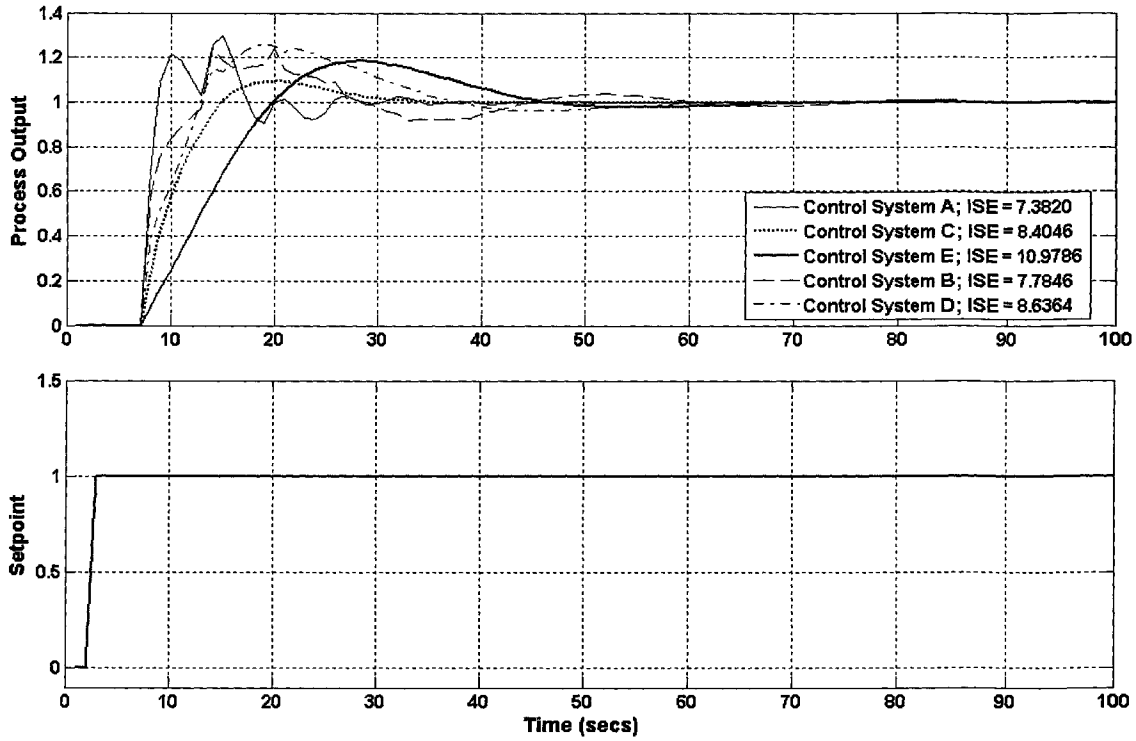

Figure 7.5: Closed-loop responses of Control Systems A, B, C, D, and E to set point step.

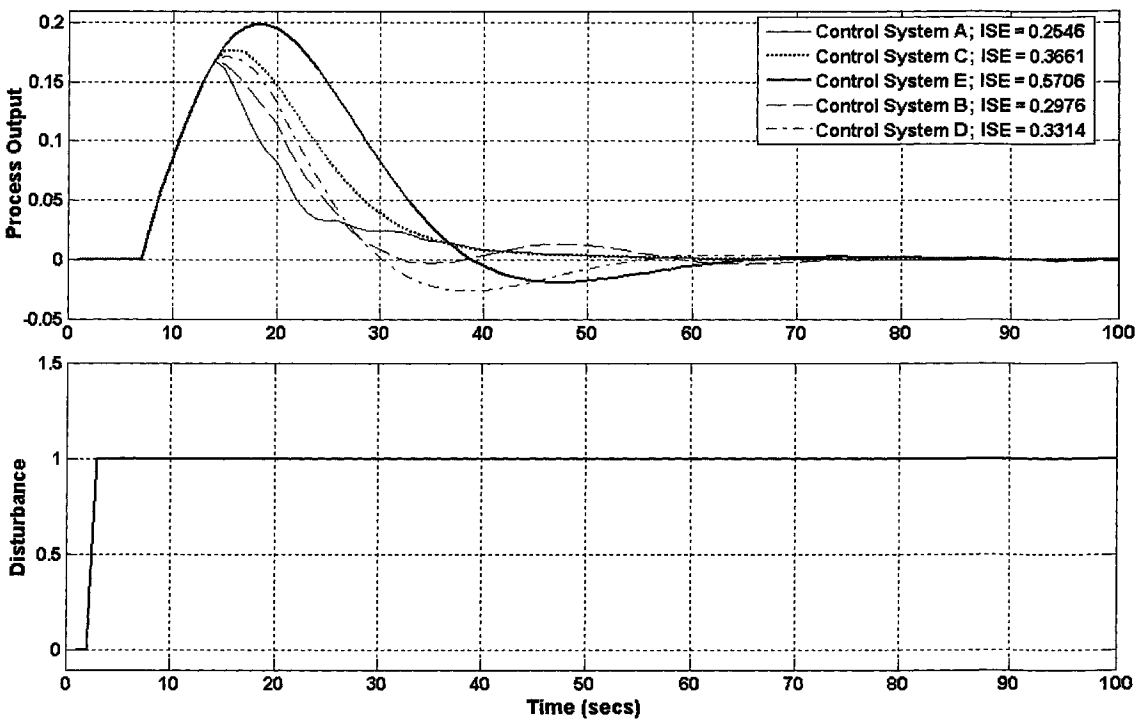

Figure 7.6: Closed-loop responses of Control Systems A, B, C, D, and E to disturbance step.

Figures 7.2 and 7.3 show the loop gain of Control System A (the traditional Smith/PID controller) developing resonance peaks above the phase crossover frequency, with one of the peaks causing an anti-clockwise encirclement of the point (-1, 0) on the Nyquist plot, thus making the system prone to instability. The unstable tendency of this system is shown in Figure 7.5, in which its set point response, though having the shortest rise time amongst all the control systems, has an oscillatory behaviour. Its disturbance rejection performance, as shown in Figure 7.6, is however the best amongst the systems, hence its position as the lowest on the J_v scale in Figure 7.4, as well as its low *ISE[y]* values as shown in Figures 7.5 and 7.6. Besides the high loop gain of Control System A above its phase crossover frequency, there is also an increase in its phase leading to a phase maximum and a second gain crossover frequency. The effect the growing loop gain has on the control system is high sensitivity to negative uncertainties in the process time delay θ [25] and thus low robustness to model parametric variations. According to [13], the combination of the post-crossover loop gain resonance peaks and the increase in phase angle is due to the factor $(1-e^{-\phi s})$ present in the denominator of the composite controller's transfer function. This factor is not taken into account in the design of Control System A because the procedure computes parameters for a closed loop consisting of a plain PID controller and a delay-free process.

Control System B's loop gain also has resonance peaks above its phase crossover frequency, which however are not severe enough to cause either an encirclement of point (-1, 0) on the Nyquist plot or a positive increase in its phase. Its high-frequency loop gain rises above 1, as shown in Figure 7.3, making its robustness to model uncertainties low. In Figure 7.5, it has the second shortest rise time, after Control System A, but the relatively low damping of its set point response briefly introduces oscillations, which eventually die down. Control System B's disturbance rejection performance is lower than Control System A's as shown in Figures 7.4 and 7.6. The price paid for the slight improvement in the high frequency robustness of Control System B is the deterioration in closed-loop performance.

It is useful to note that Control System D does not generate high loop gains beyond the phase crossover frequency and is therefore robust to model uncertainties, unlike Control Systems A and B.

It is also useful to note that Control System C (Optimized Smith/PI Controller), like Control System D, does not generate excessive loop gains at mid to high frequencies, unlike its PID counterpart. It offers better performance in set point tracking and disturbance rejection than the non-augmented optimal PI controller (Control System E). Thus it demonstrates that the Smith augmentation of a closed loop with a PI controller does enhance the performance of the controller for a process with significant time delay. The closed loops of the Optimized Smith/PI Controller (Control System C) and the plain Optimal PID Controller (Control System D) behave differently for set point tracking and disturbance rejection, as shown by their *ISE* values in Figures 7.5 and 7.6 respectively.

Control System C's set point tracking performance is slightly better than Control System D's, but slightly worse for disturbance rejection.

7.3 CONSTRAINT ON MID-TO-HIGH FREQUENCY LOOP GAINS OF SMITH PREDICTOR SYSTEMS

Although Control System B has better robustness properties above the phase crossover frequency relative to Control System A, it also exhibits unhealthy high loop gains in this frequency range, as shown by Figures 7.2 and 7.3. The reason is that the constraints imposed on $\|S\|_\infty$ and $\|T\|_\infty$ in (2.12) and (2.14) respectively place demands on the mid-frequency behaviour of *L(s)* and not its frequency response above the phase crossover region. For the typical closed-loop incorporating just the PID (or PI) controller, and not a Smith predictor, as well as the Optimized Smith/PI control system, (2.12) and (2.14) are adequate to constrain both the mid-frequency and high frequency properties of the system. However, for a PID control system incorporating a Smith predictor, such as Control System B, (2.12) and (2.14) are inadequate, and an additional constraint is required in (2.16). The additional constraint [13] is defined as:

$$\max_{\omega}\left|L(j\omega)-\frac{1}{m_{G_m}}\right|\le\frac{2}{m_{G_m}} \qquad \omega\ge\omega_{180_L} \tag{7.7}$$

where m_{Gm} is the minimum gain margin for the Smith-augmented control system, which has been chosen to be 3, and ω_{180L} is its phase crossover frequency. The geometrical interpretation of (7.7) is a circle on the Nyquist diagram, known as the M_L *circle*, with a radius of $2/m_{Gm}$ (i.e., $2/3$) and its centre at the point $(1/m_{Gm},0)$, as shown in Figure 7.7.

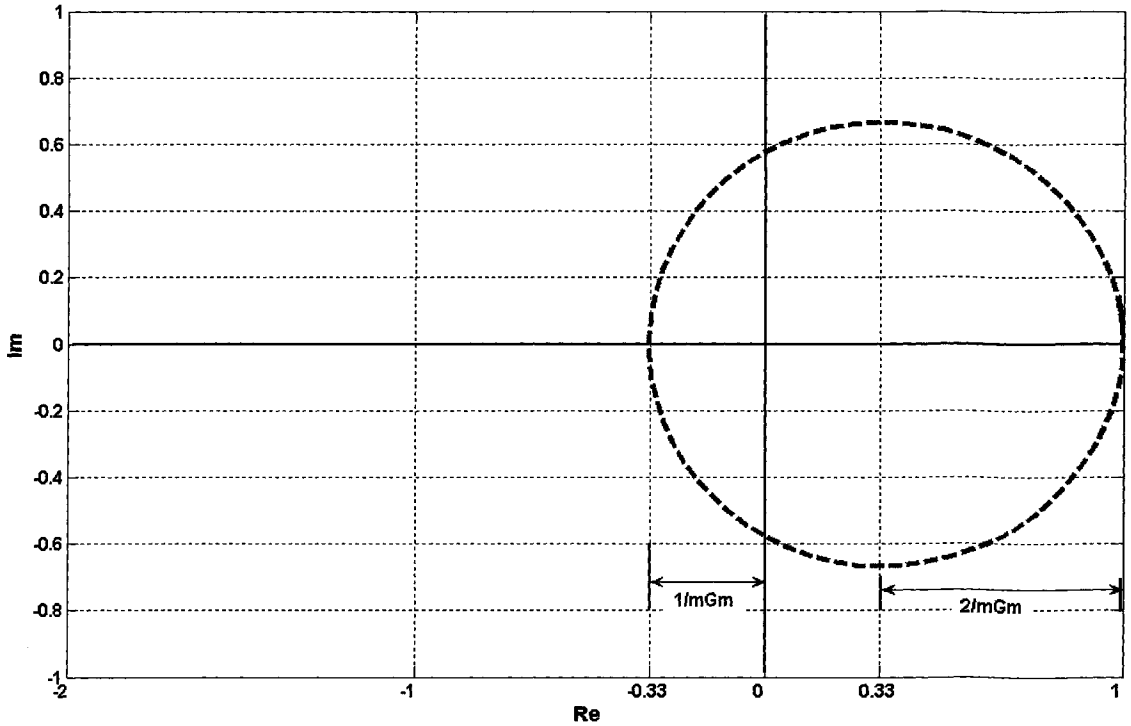

Figure 7.7: The M_L circle for restricting the loop gain of a Smith-Augmented control system above the crossover frequency.

The M_L circle ensures that loop gain $|L(j\omega)|$ does not exceed 1 for all frequencies above ω_{180L}. The additional constraint in (7.7) along with (2.12) and (2.14) lead to the formulation of a mid-frequency criterion, GM_{SL} [13], more comprehensive than GM_S in (2.16):

$$GM_{SL} = max\left(\|S\|_\infty, \alpha\|T\|_\infty, \gamma \max_{\omega} W_L(j\omega)\left|L(j\omega) - \frac{1}{m_{G_m}}\right| \right) \tag{7.8}$$

where $\gamma = 0.5 m_{G_m} M_S$ and $W_L(j\omega)$ is a weighting function defined as

$$W_L(j\omega) \rightarrow \begin{cases} 0 & \omega < \omega_{180L} \\ 1 & \omega \geq \omega_{180L} \end{cases}$$

With the mid-frequency constraint GM_{SL}, an optimal PID control system augmented with a Smith predictor, and having moderate loop gains at frequencies above ω_{180L}, can be designed:

f) Optimized Smith/PID controller (Control System F) – designed by solving (2.21) for the s^{-1}-weighted form of (7.3) with GM_{SL} taking the place of GM_S and setting $m_{Gm} = 3$ and retaining $M_S = 1.7, J_u = 10.2$.

Figures 7.8 to 7.11 show the frequency responses of Control System F, as well as Control Systems B and D, their performance-control action plots, and their closed-loop responses.

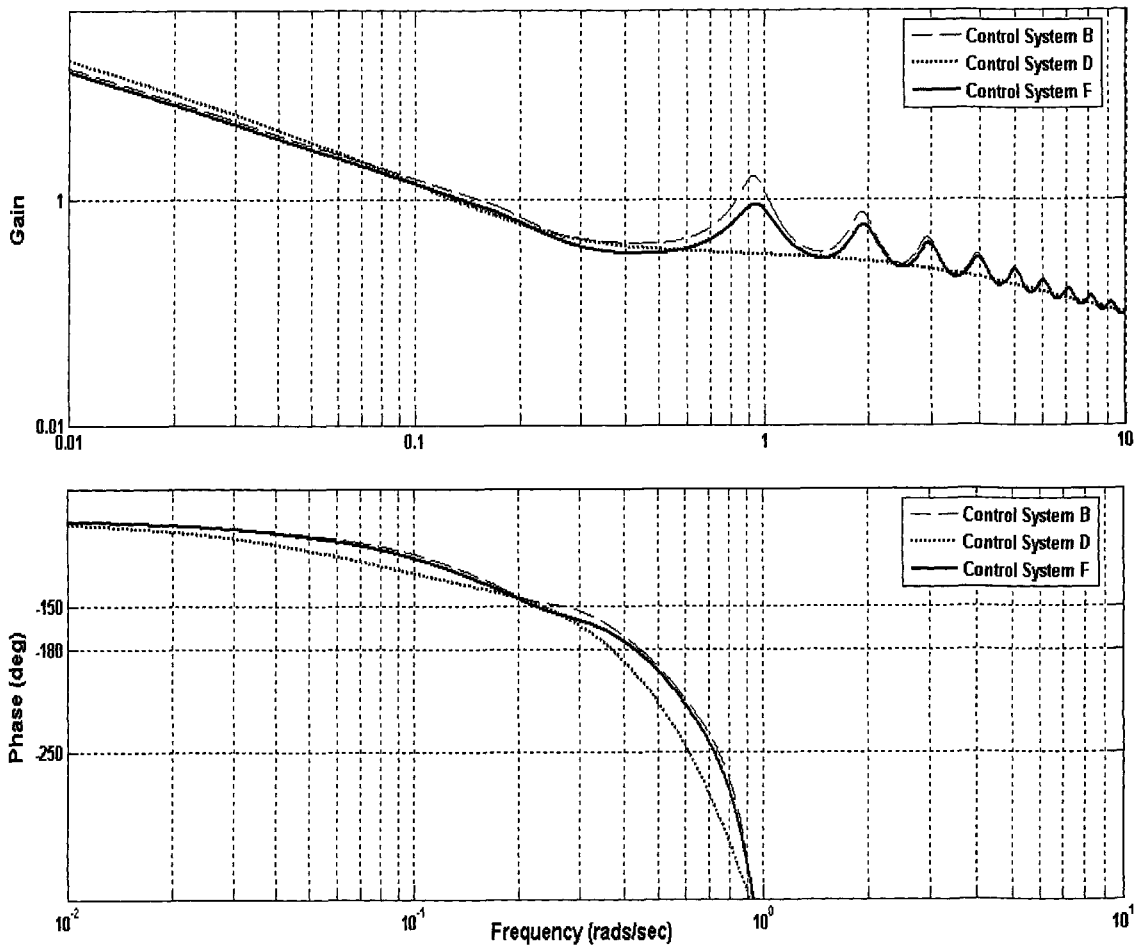

Figure 7.8: Bode plots for Control Systems B, D, and F.

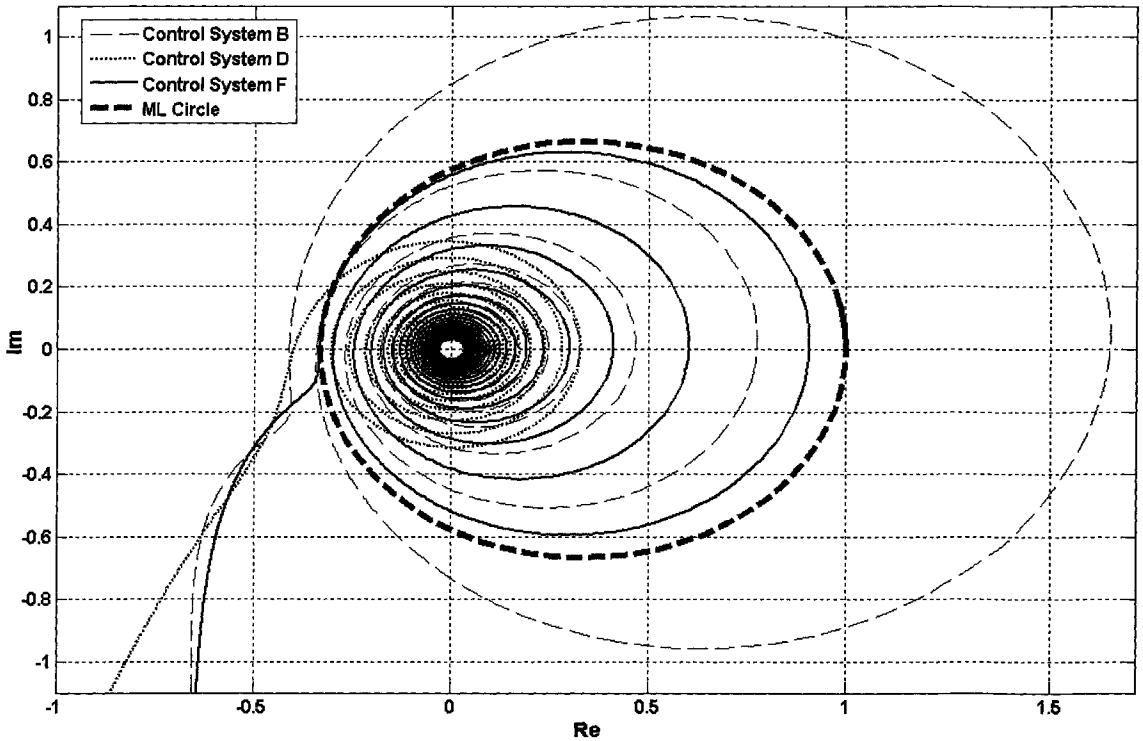

Figure 7.9(a): Nyquist plots for Control Systems B, D, and F.

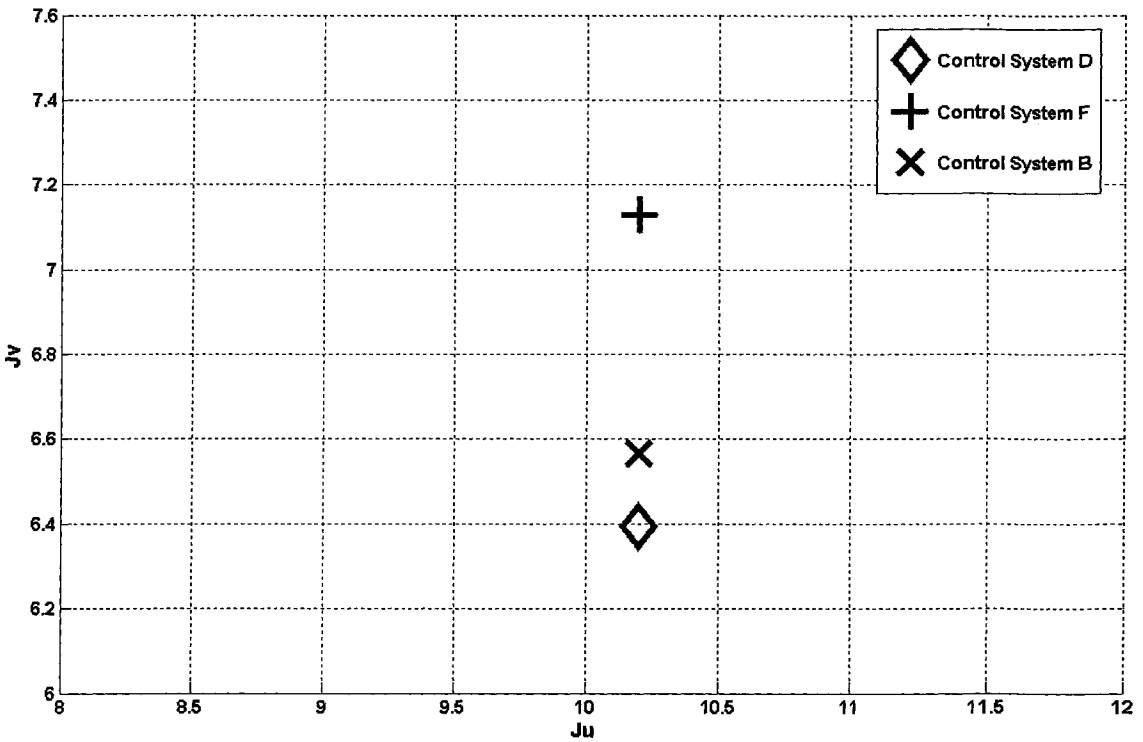

Figure 7.9(b): J_v-J_u plots for Control Systems B, D, and F.

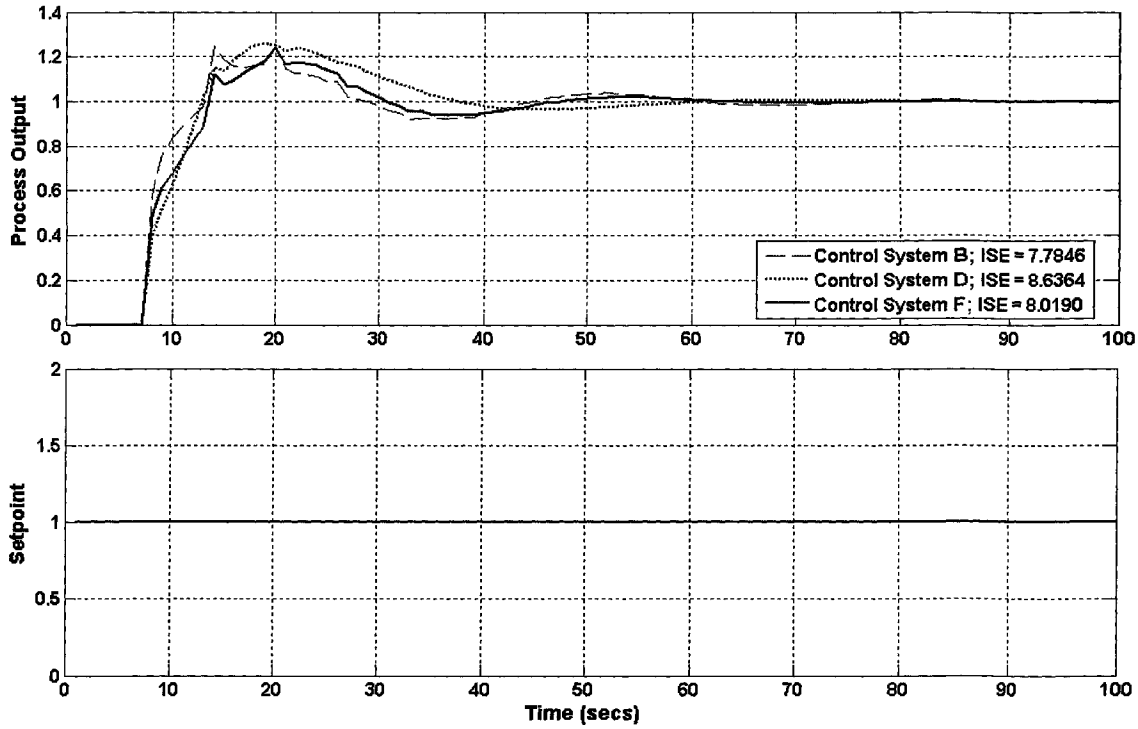

Figure 7.10: Closed-loop responses of Control Systems B, D, and F to set point step.

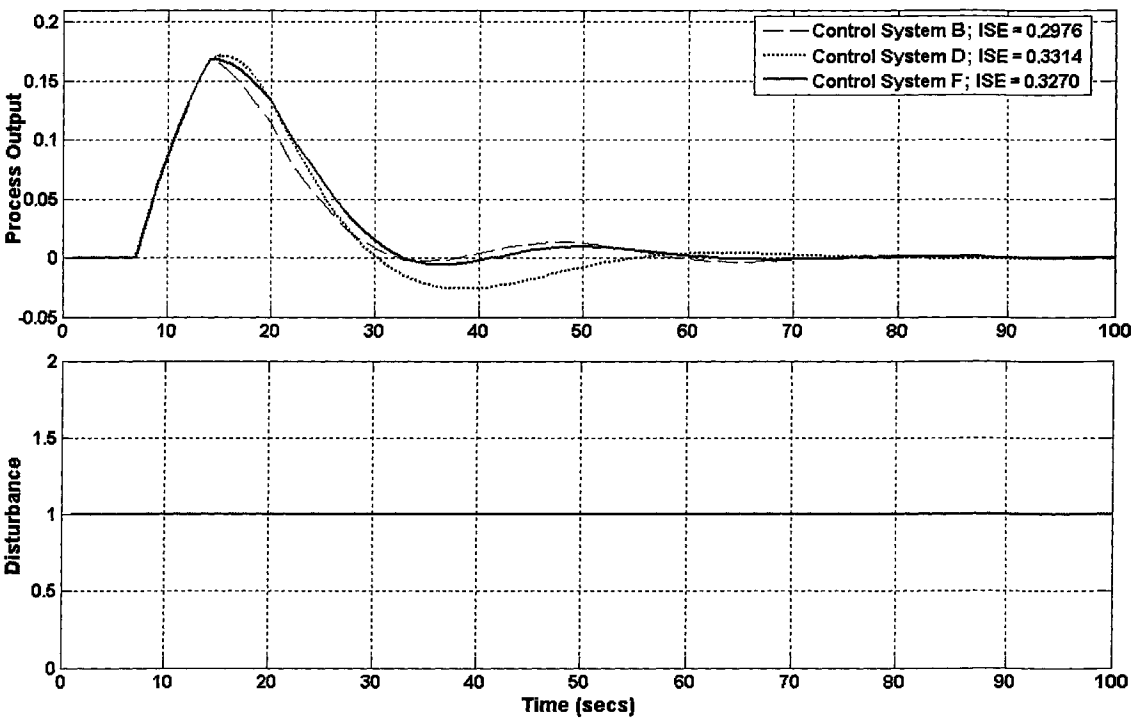

Figure 7.11: Closed-loop responses of Control Systems B, D, and F to disturbance step.

In Figure 7.8, the GM_{SL} constraint ensures the loop gain of Control System F does not exceed 1 beyond the phase crossover frequency. This is confirmed by the Nyquist plot in Figure 7.9(a), in which the Control System F's loop gain is restricted within the circumference of the M_L circle, thus ensuring sufficient robustness to model uncertainties. Control System B's loop gain, on the other hand, moves outside the circle. The *ISE[y]* values in Figures 7.10 and 7.11 show that Control System B's set point tracking and disturbance rejection performance exceeds those for Control System F. Thus, performance pays the price for the improved high frequency robustness of Control System F. However, it gives better closed-loop response than Control System D and therefore shows that Smith predictor augmentation does bring benefits to the PID-controlled closed loop for processes with significant time delays.

For disturbance rejection, it is useful to note from *ISE[y]* values in Figures 7.6 and 7.11 that the performance improvement going from Control System C to Control System D is more significant than going from Control System D to Control System F, all of which are better than Control System E. Hence, adding derivative control to the plain PI controller gives greater performance improvement than augmenting the PI controller with a Smith predictor. In contrast, the inclusion of the Smith predictor with the derivative control-augmented PI controller (i.e., PID controller) gives marginal improvement. The greatest performance gap amongst the aforementioned control systems exists between the Smith-augmented PI controller and the plain optimal PID controller.

7.4 PERFORMANCE COMPARISONS OF OPTIMAL PID AND SMITH PREDICTOR-AUGMENTED LOOPS

In the previous section, several control systems were designed for an arbitrary process with a significant time delay-time constant ratio. The simulation results showed that although the closed-loop response of a Smith-augmented PID control system, in which the PID controller was designed using the traditional approach, gave the best performance, it developed significant loop gains at frequencies above the phase crossover frequency and thus was insufficiently robust to model time delay uncertainties. It was found that designing the PID controller by optimizing the transfer function for the entire Smith-augmented closed loop, and imposing a constraint on the high frequency loop gain of the system, gave a closed loop whose response was not as superior as the traditional Smith/PID system, but was more robust to model uncertainties. The closed-loop performance of the optimal Smith/PID system was in turn found to be superior to the optimal Smith/PI's and the non-augmented optimal PID's.

For processes with large time delays, it is more common to use the PI than the PID controller [13], with or without Smith predictor-augmentation. However, the results from the previous section have shown that the three acceptable options for controlling such processes, while allowing for closed-loop robustness to model uncertainties, are the aforementioned control systems. It would be useful to study the performance of the three options for processes with various time

delay-time constant ratios. A concise summary [25] of the behaviour of the three systems for various time delay scenarios is that for both moderate and large time delays, augmenting a PI controller with a Smith predictor gives less improvement in performance than if it were augmented with derivative control. On the other hand, for a PID controller, the introduction of a Smith predictor implies some improvement for a process with moderate delay. However, when the delay is large, performance improvement is sacrificed to sustain the robustness demand on the control system placed by GM_{SL}, thus making the benefit of including the Smith predictor in the PID control system for a largely delay-dominant process questionable.

To experimentally investigate the advantages and disadvantages of the three control systems, each would be designed for the temperature response models for the thermocouples of the Heated Tank Process, discussed in Chapter 6 (Table 6.2). Because the temperature models have varying degrees of time delay dominance, they provide the physical basis to study the closed-loop performance of the controls systems for processes with varying time delay-time constant ratios, and would help in providing some insight into the issue of the benefits of the Smith predictor to PI and PID controllers. Controllers similar to Control Systems C, D, E and F (i.e., optimal PI and PID controllers with and without Smith predictors) were designed for Thermocouples 1, 2, and 3 of the Heated Tank Process, and implemented both experimentally and in simulation. Figures 7.12 to 7.16 show the performance-control activity profiles for the control systems using various pairs of evaluation criteria. GM_S (and GM_{SL}) ≤ 1.7.

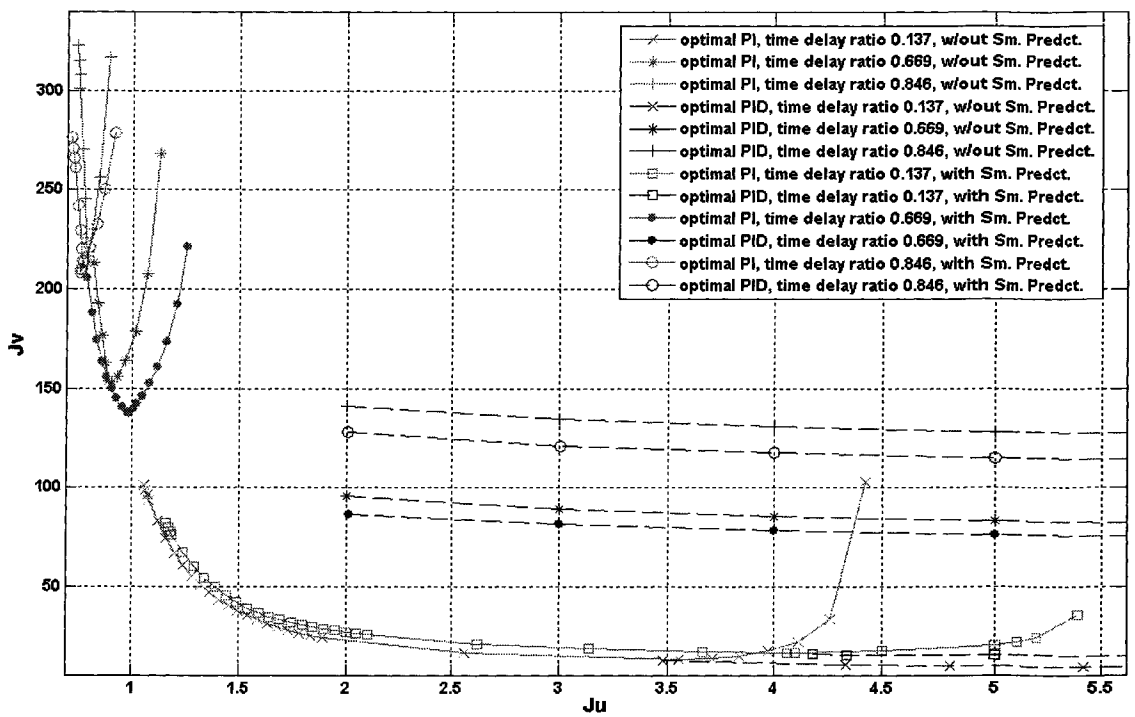

Figure 7.12: J_v-J_u profiles for optimal PI and PID control systems, with and without Smith Predictors, for Thermocouples 1 (0.137), 2 (0.669), and 3 (0.846).

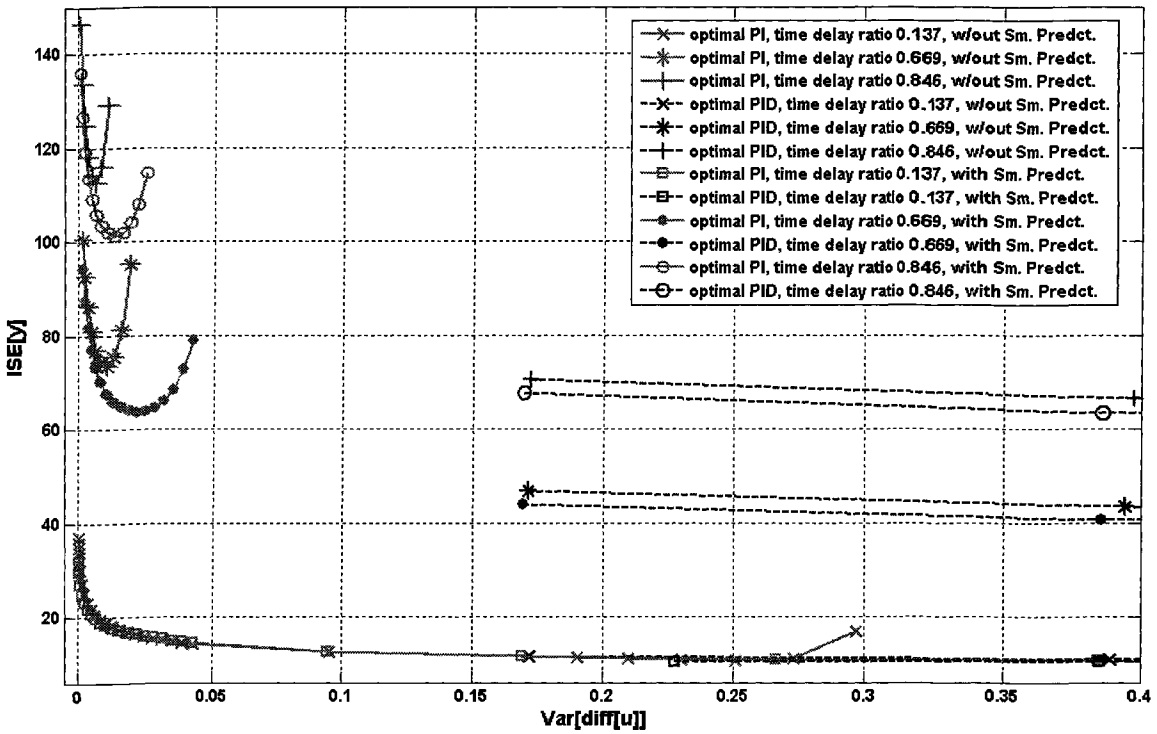

Figure 7.13: Simulated *ISE[y]-VAR[Δu]* profiles for optimal PI and PID control systems, with/ without Smith Predictors, for Thermocouples 1, 2, and 3 using integrated noise disturbance.

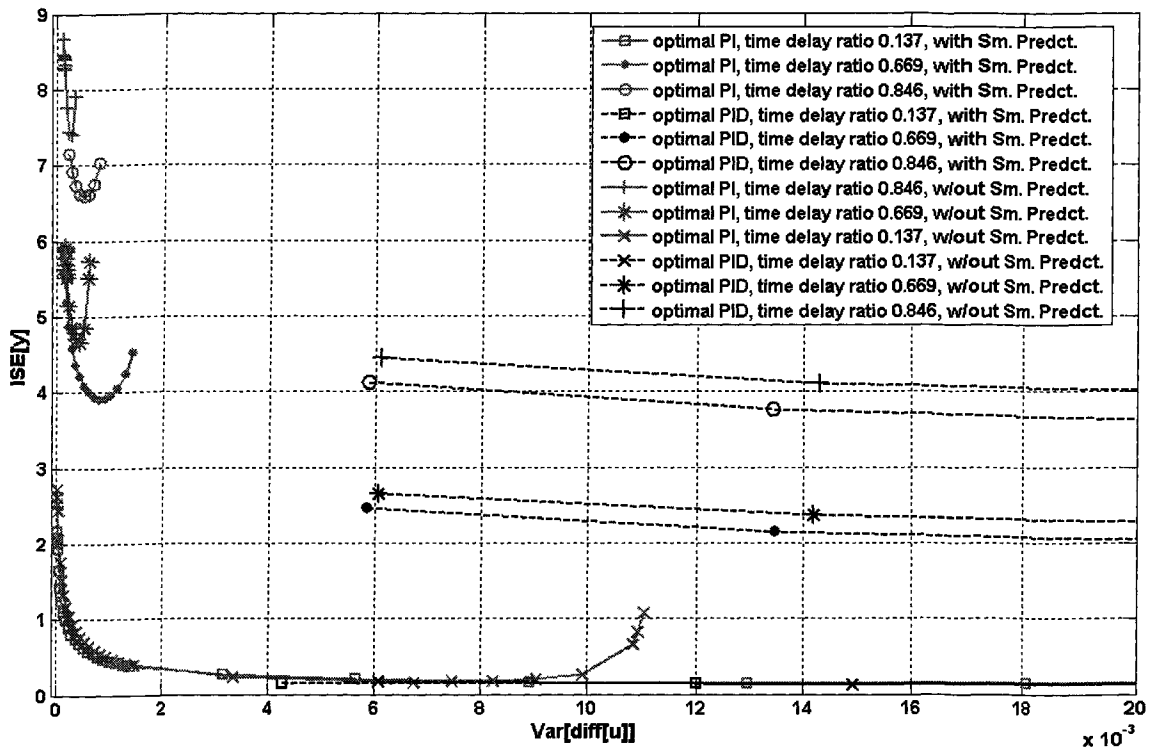

Figure 7.14: Simulated *ISE[y]-VAR[Δu]* profiles for optimal PI and PID control systems, with/ without Smith Predictors, for Thermocouples 1, 2, and 3 using step disturbance.

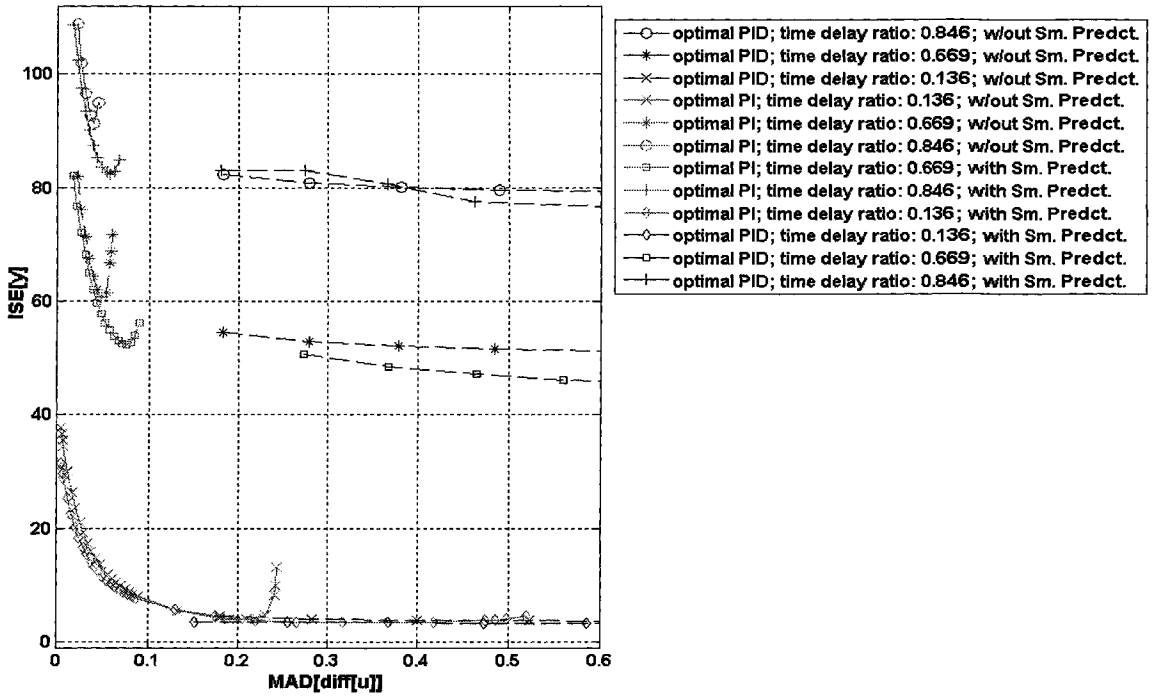

Figure 7.15: Simulated *ISE[y]-MAD[Δu]* profiles for optimal PI and PID control systems, with/ without Smith Predictors, for Thermocouples 1, 2, and 3 using step in set point signal.

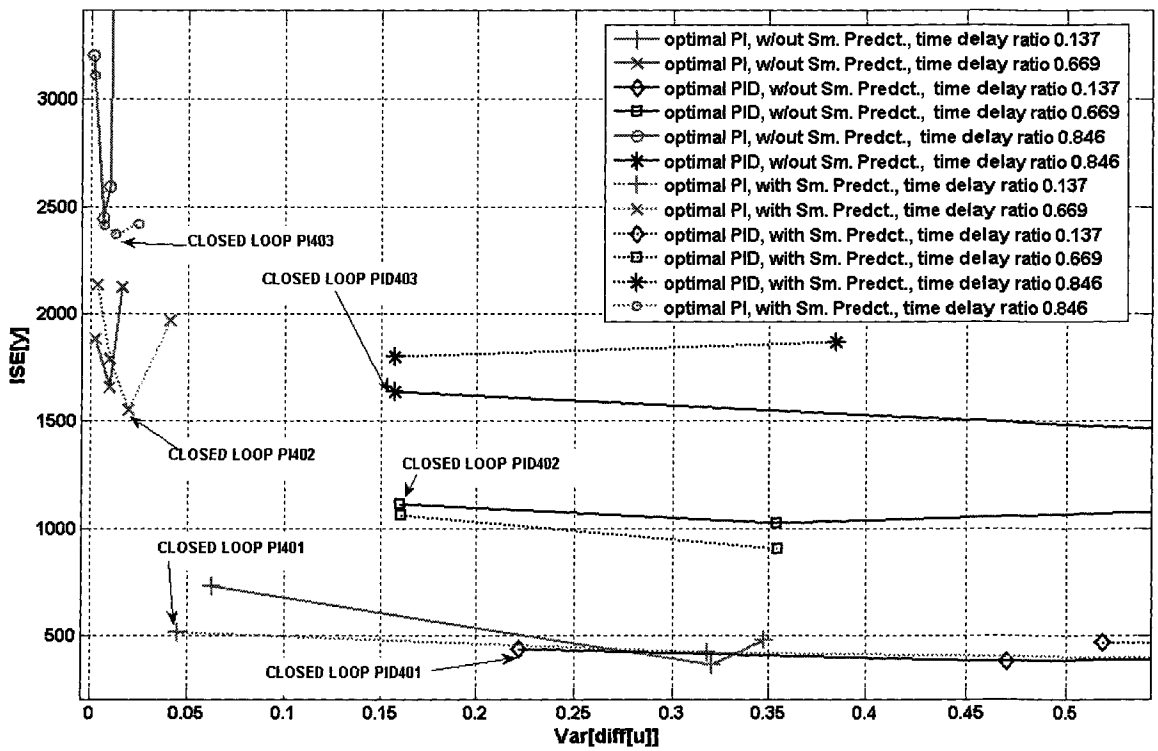

Figure 7.16: *ISE[y]-VAR[Δu]* profiles for optimal PI and PID control systems, with/without Smith Predictors, for experimentally implemented closed loops of Thermocouples 1, 2, and 3 with integrated white noise disturbance. Selected controllers are labelled.

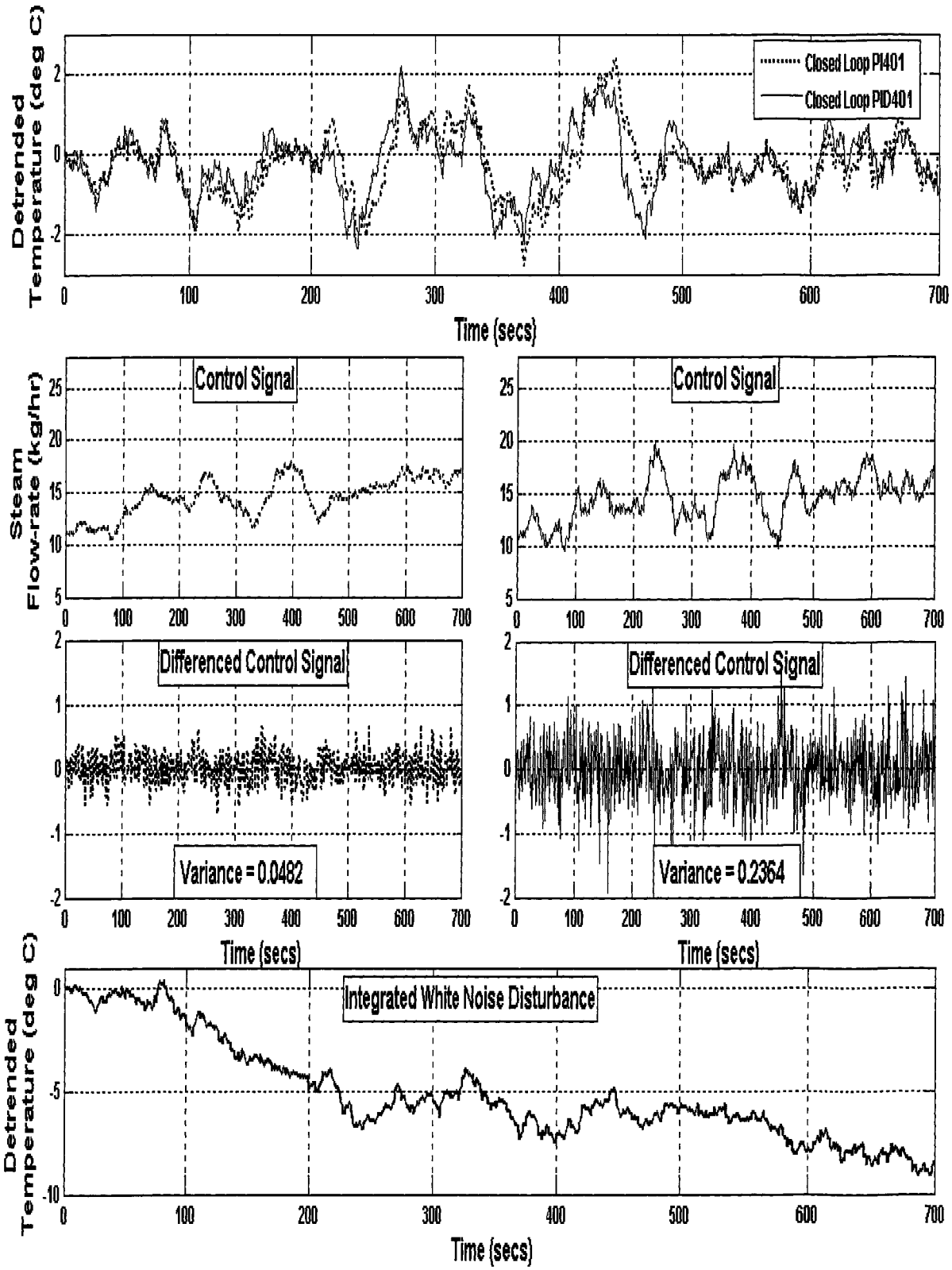

Figure 7.17(a): Temperature responses of Thermocouple 1's experimentally implemented closed loops PI401 and PID401 to integrated white noise disturbance.

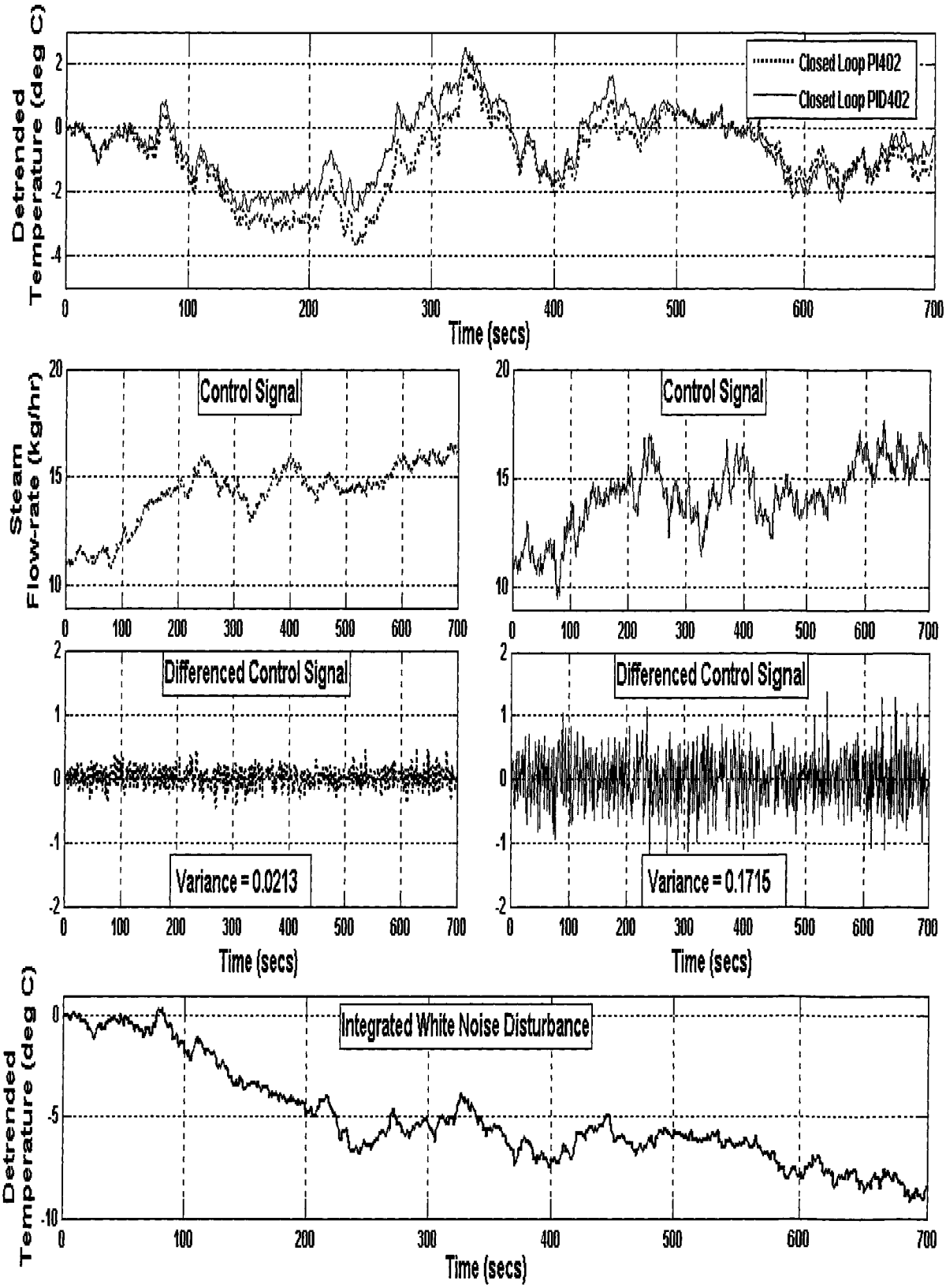

Figure 7.17(b): Temperature responses of Thermocouple 2's experimentally implemented closed loops PI402 and PID402 to integrated white noise disturbance.

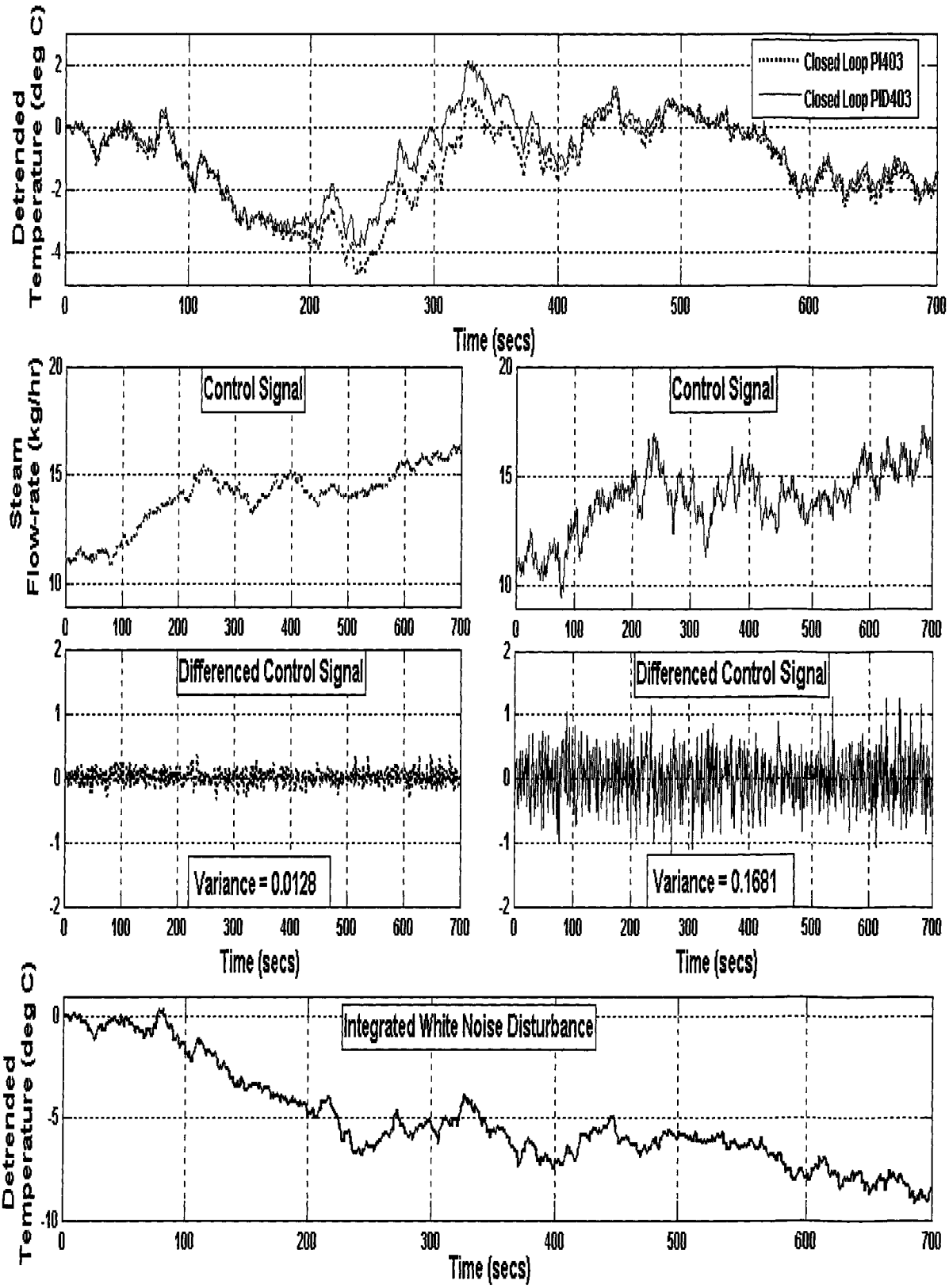

Figure 7.17(c): Temperature responses of Thermocouple 3's experimentally implemented closed loops PI403 and PID403 to integrated white noise disturbance.

Figures 7.12 to 7.15 show that for significant process time delays, the un-augmented PI controller's closed loop profile is highly restricted – both in terms of control activity and performance. Augmenting the PI controller with a Smith predictor widens its control activity range and leads to modest performance improvement. Figures 7.13, 7.14, and 7.16 clearly show that for step and integrated noise disturbance rejection, augmenting the PI controller with derivative control gives it better closed loop performance than augmenting it with a Smith predictor. Figures 7.17(b), and 7.17(c) compare the closed-loop time trends for the two types of augmentation to the PI controller, and demonstrate the regulatory superiority of the PID controller to the Smith-augmented PI controller where the process time delay is significant. Figure 7.17(a) shows that where the time delay isn't dominant, the Smith-augmented PI controllers have more or less the same closed-loop performance rating as the PID controller. Indeed, the performance-control activity profiles all show that for Thermocouple 1's temperature response, it might be pointless to augment the PI controller with either the Smith predictor or derivative control, since it can perform satisfactorily on its own in this case.

Figures 7.12, 7.13, 7.14, and 7.16 all show the performance improvement that the Smith predictor brings to the PI controller is marginal relative to derivative control's contribution where the process time delay is large. Hence, for disturbance rejection, augmenting the PI controller with derivative control, i.e., a PID controller, is more beneficial than augmenting the controller with a Smith predictor. On the other hand, Figure 7.15 shows that for the closed-loop set point tracking performance of a process with a large time delay, augmenting the PI controller with a Smith predictor brings significant improvement, while upgrading from a Smith predictor to a derivative controller gives only slight improvement. Hence, it can be argued that the Smith-augmentation covers most of the benefits offered by derivative control, and thus a case can be made for the utilization of the Smith predictor. However, since the PID controller closed loop has the comparatively lower *ISE[y]* limit and offers greater performance improvement for disturbance rejection, as well as a simpler structure for implementation, the overall conclusion is that derivative control is probably more beneficial to the PI controller than the Smith predictor.

All the performance-control activity profiles, i.e., Figures 7.12 to 7.16, show that even though the Smith-augmentation of the PID controller allows it to give the best closed-loop performance amongst the various control structures discussed, the improvement it brings to the un-augmented PID controller is marginal. Thus, implementing the PID controller, with or without the Smith predictor, gives better closed-loop performance than the PI controller, with or without the Smith predictor. The control engineer could choose between implementing a plain PID controller for a dead time dominant process, or a Smith-augmented PID controller. However, for closed-loop structural simplicity, and for processes in which the transfer function might either not be easily obtainable or whose parameters fall into a wide interval of uncertainty, it might be prudent to implement the un-augmented PID controller.

Another aspect of Smith-augmented controller implementation for which there is some interest is the robustness of the closed loops to model uncertainties. The reason for this interest is that because the Smith-augmented PI and PID controllers require process models for their implementation, unlike the plain PI and PID controllers, it is necessary to assess the closed-loop performance of these systems where there are variations in model parameters. The most common parametric variation to which Smith-augmented closed loops are sensitive is the process time delay uncertainty. Recall that the sensitivity transfer functions for Smith-augmented closed loops in (7.1) to (7.4) were derived based on the assumption that the modeled process time delay, ϕ, was equal to the actual time delay, θ. For traditional Smith-augmented closed loops, it has been shown that, due to the excessively high loop gains at high frequencies, variations in θ from the modeled value could lead to poor closed-loop performance or even unstable response. The mid-frequency robustness criterion, GM_{SL}, in (7.8) was introduced to restrict the Smith-augmented closed loop's high frequency loop gain, and enhance the system's robustness to time delay uncertainty. The Smith-augmented closed loops implemented in this section were designed with a constraint imposed on GM_{SL}, thereby making them robust.

A practical approach to assessing the time delay uncertainty robustness of the Smith-augmented PI and PID closed loops is to implement the controllers on the thermocouple temperatures for which they were designed, and other thermocouple temperatures. Consequently, the Smith-augmented PI and PID controllers designed for Thermocouple 2 would be implemented on Thermocouple 1's temperature, as well as Thermocouple 2's temperature and Thermocouple 3's. It should be noted that Thermocouple 1's temperature has the least time delay, while Thermocouple 3's temperature has the longest time delay.

$\theta > \phi$ (under-delayed) $\rightarrow$ closed-loop performance deteriorates

$\theta < \phi$ (over-delayed) $\rightarrow$ closed-loop performance improves

Thus, implementation of Thermocouple 2's Smith-augmented PI and PID controllers on Thermocouple 1's temperature is expected to enhance loop performance, while implementation of Thermocouple 2's controllers on Thermocouple 3's temperature is expected to reduce performance. Hence, these performance profile shifts, relative to the profile for the loop in which $\theta = \phi$, i.e., correctly delayed, for the Smith-augmented PI and PID closed loops would be compared with the performance profile shifts encountered in the un-augmented PID closed loop. The expectation for this experiment is that the farther the performance profiles for the under-delayed Smith-augmented closed loops are from the profiles for the correctly-delayed loops, relative to the performance profile distortions for the un-augmented PID closed loop, the less robust are the Smith-augmented closed loops to time-delay variations.

Figure 7.18 shows the performance-control activity profiles for the simulated Smith-augmented PI, PID, as well as un-augmented PID closed loops, in which

Thermocouple 2's controllers were implemented for its temperature, as well as the temperatures for Thermocouples 1 and 3.

Figure 7.19 shows the profiles for the laboratory implementation of the aforementioned simulated closed loops.

The exogenous signal sent to the loops was the integrated white noise disturbance.

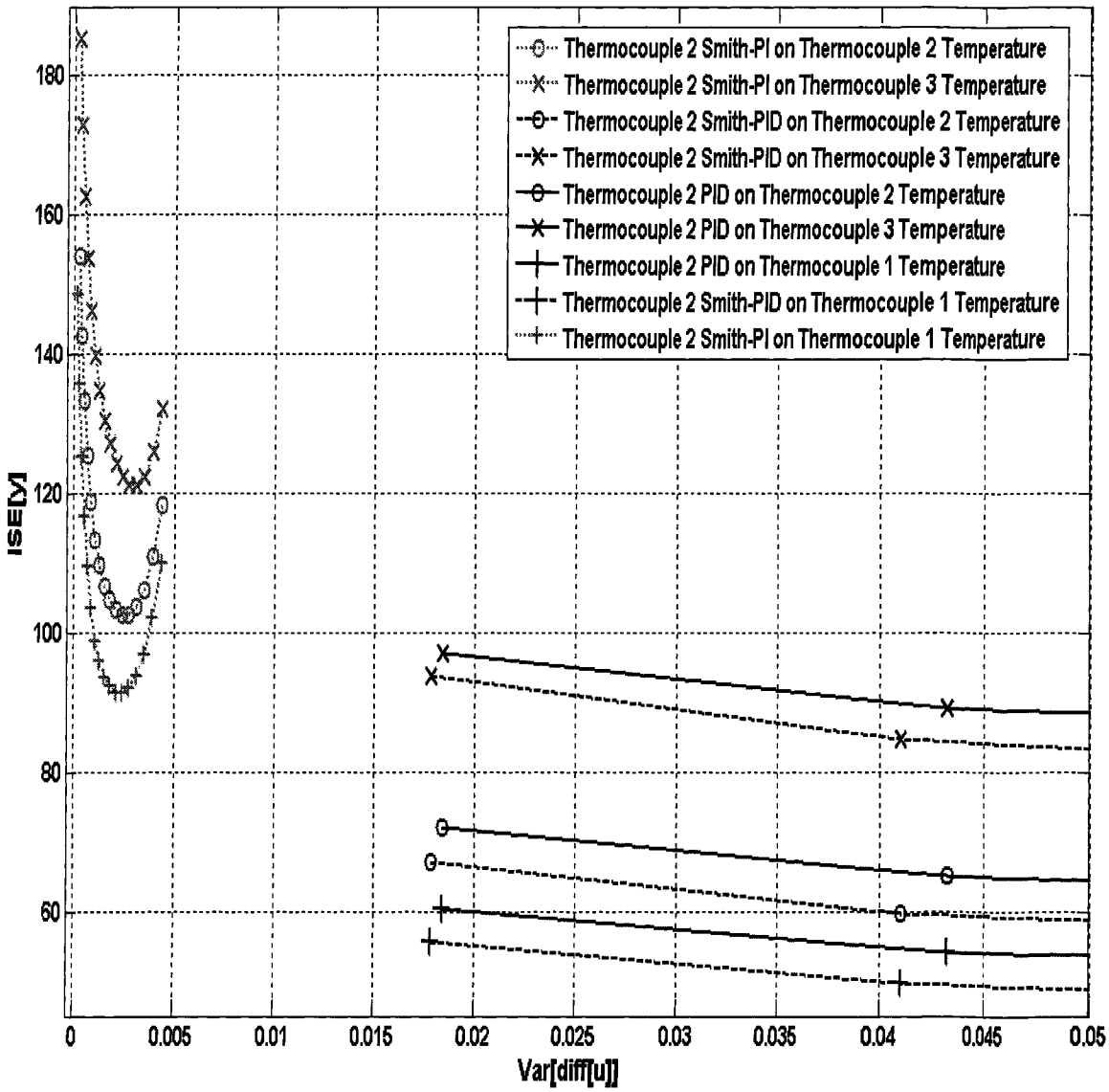

Figure 7.18: Simulation assessment of the time delay uncertainty robustness of the Smith-augmented PI and PID control loops, with respect to the un-augmented PID control loop.

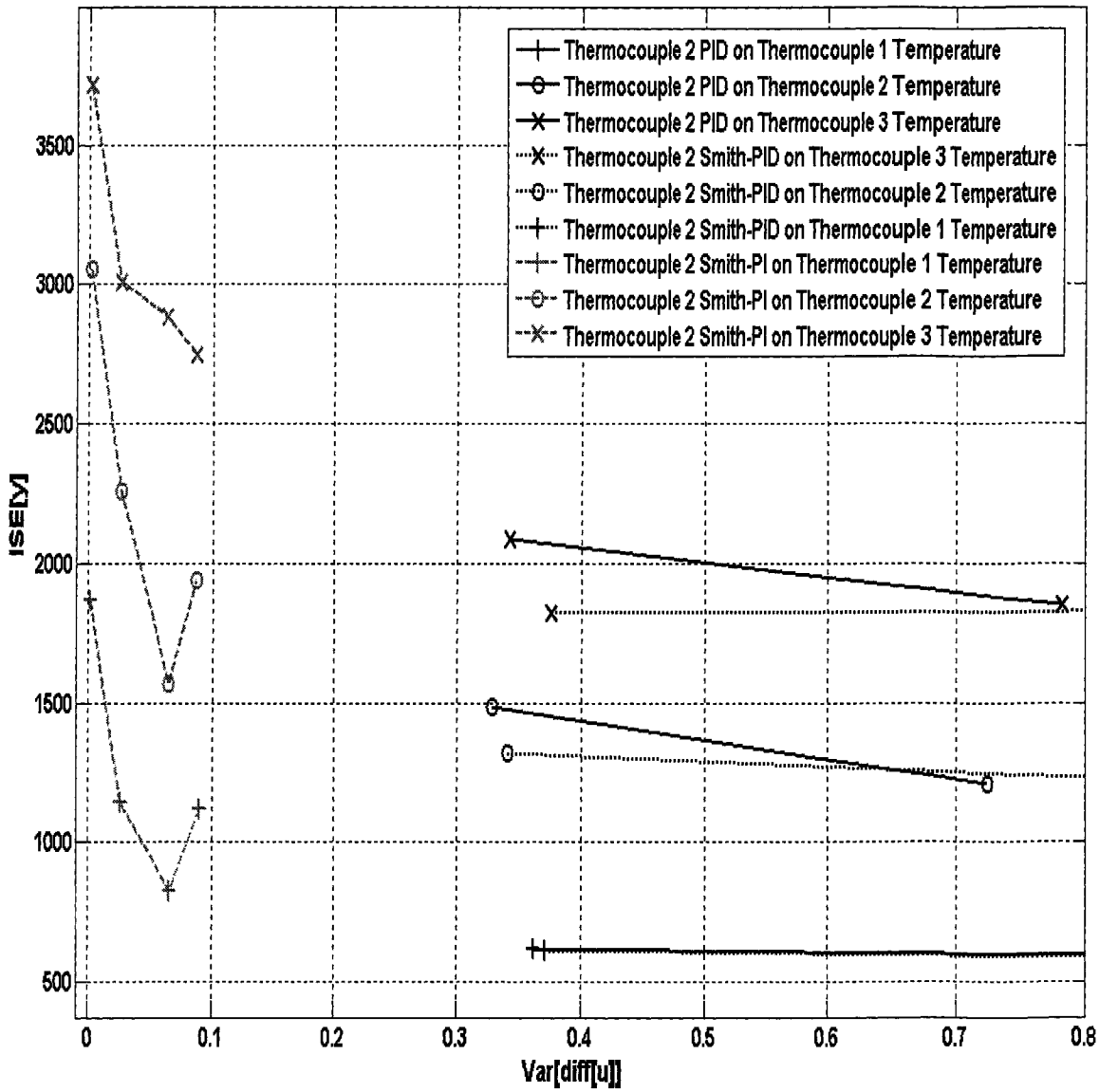

Figure 7.19: Experimental assessment of the time delay uncertainty robustness of the Smith-augmented PI and PID control loops, with respect to the un-augmented PID control loop.

Figures 7.18 and 7.19 show the profiles of all three groups of closed loops, for the under-delayed models, having approximately the same degree of performance displacement from the profiles of the correctly-delayed models. The same observation is made for the profiles of the over-delayed models. Thus, the closed loops of the Smith-augmented PI and PID controllers can be said to be as robust as the un-augmented PID closed loop to process time delay variations. This result illustrates the benefit of designing the Smith-augmented PI and PID controllers using GM_{SL} from (7.8) as the mid-frequency robustness criterion, and imposing an appropriate constraint on this criterion.

In summary, Kristiansson's [25] control system evaluation method has been applied to Smith-augmented control systems, demonstrating that the traditional

approach to designing the PI and PID controllers for such systems, as commonly described in literature, leads to a closed loop with significant loop gains at high frequency, thereby making the closed loop highly sensitive to variations in process time delays. To solve the problem of the high-frequency loop gain, an evaluation criterion, GM_{SL}, which restricts the loop gain in this frequency range, was introduced and incorporated into the optimal controller design formulation. Smith-augmented closed loops of optimal PI and PID controllers, designed by solving this modified design formulation, were implemented both in simulation and experimentally. The implementation results showed that for processes with small time delays, it was worthwhile to stay with the PI controller, as its closed loop performance compared well with other control structures. However, as time delay increased, both the Smith-augmented and un-augmented closed loops of the PID controller performed better than similar versions of the PI controller, with the Smith-augmented PID closed loop performing slightly better than the un-augmented PID closed loop. Various considerations of the advantages and disadvantages of utilizing either of the two control structures led to the conclusion that it might be more parsimonious to implement the un-augmented PID controller structure for processes with significant time delays, rather than the Smith-augmented PID controller. Practical time-delay uncertainty robustness analysis of the Smith-augmented PI and PID closed loops showed they were as robust as the un-augmented PID closed loop to the variations in the model parameter.

CHAPTER 8

INDUSTRIAL APPLICATION: PETRO-CANADA ISO-STRIPPER BOTTOMS TEMPERATURE LOOP

8.1 INTRODUCTION

The control system evaluation/design procedure, proposed in [25], has been applied to pilot-scale processes – the Quadruple-Tank Process and the Heated Tank Process - as discussed in previous chapters. In this chapter, the application of the procedure to an industrial control loop, the Petro-Canada Isostripper Bottoms Temperature Control Loop, will be presented.

The process/control objective of the loop will be briefly discussed, followed by the evaluation of the loop using Kristiansson's criteria in [25]. Using the GM_S value of the loop as a constraint, optimal PI, just proper, and strictly proper PID controllers will be designed for the temperature control loop. The closed loop evaluations of these three controllers will be compared with those of the current controller in the loop.

Finally, the closed loop time trends of the control systems, both from simulation and real-time implementation, and their comparisons will be presented.

8.2 PROCESS DESCRIPTION

The primary purpose of the Isostripper Tower at the Petro-Canada Edmonton Refinery is to control the Reid Vapour Pressure (RVP) of the alkylate (blending component of gasoline) at a target defined by the Refinery Planning Group. Lighter material in the C3 to C4 range is separated from the alkylate and sent in the overheads of the tower to eventually be recycled back into the process. The RVP controller cascades down to the temperature control loop, 12TC-3, to regulate the tower bottoms temperature and consequently the RVP of the alkylate. This temperature is controlled by manipulating the outlet steam flow from the bottom reboiler. Closing this valve, or reducing steam, will lower the tower temperature and raise the RVP. The process variable (PV) and the control variable (OP) are the bottoms temperature and steam flow rate, respectively. This tower is affected significantly by upstream swings in the process. Typical disturbances include variations in the tower feed rate, composition and temperature. Figure 8.1 is the process diagram of the isostripper tower.

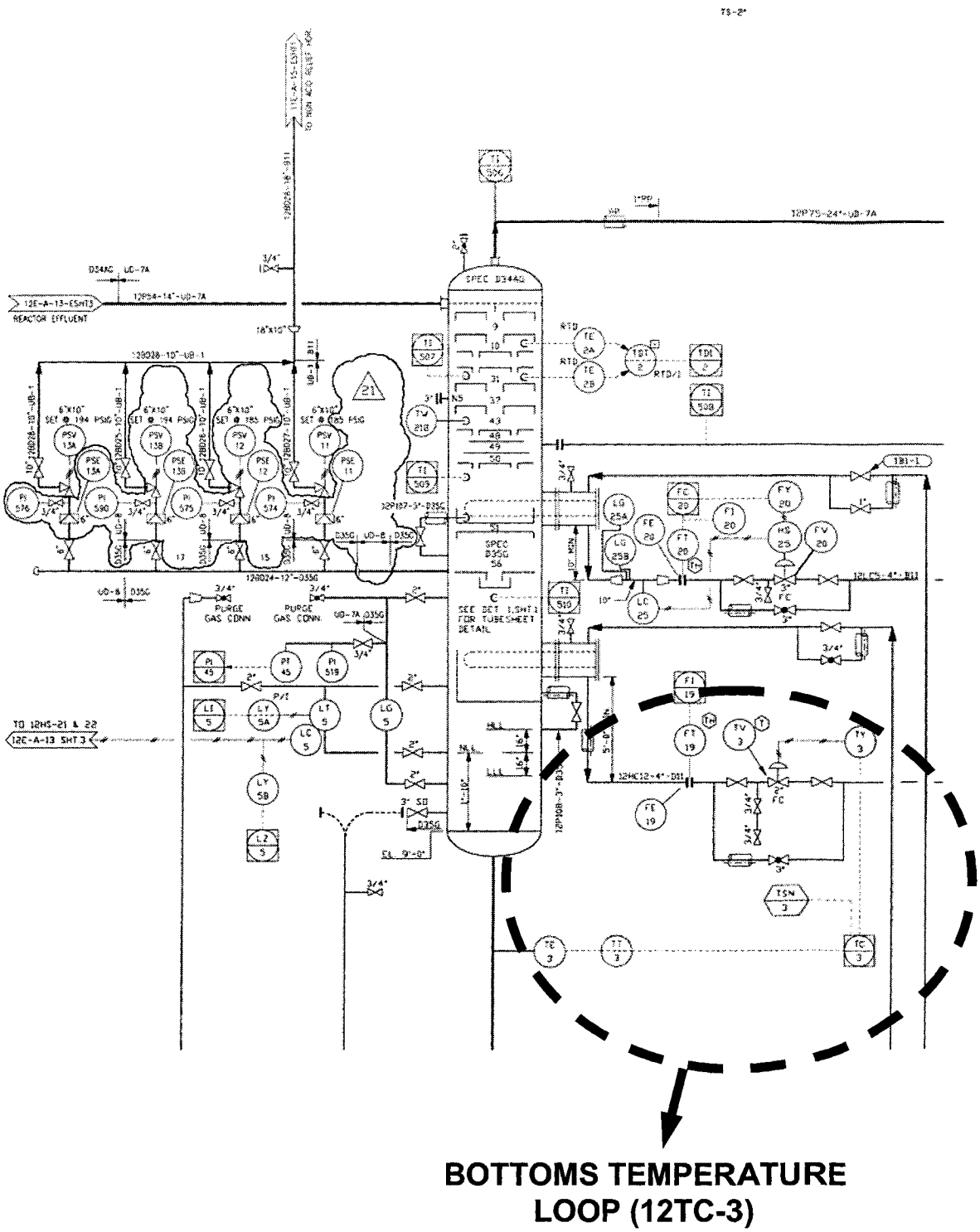

Figure 8.1: P & I diagram of the Petro-Canada Edmonton Refinery Isostripper Tower with the dashed circle showing the bottoms temperature control loop.

8.3 EVALUATION OF BOTTOMS TEMPERATURE CONTROL LOOP

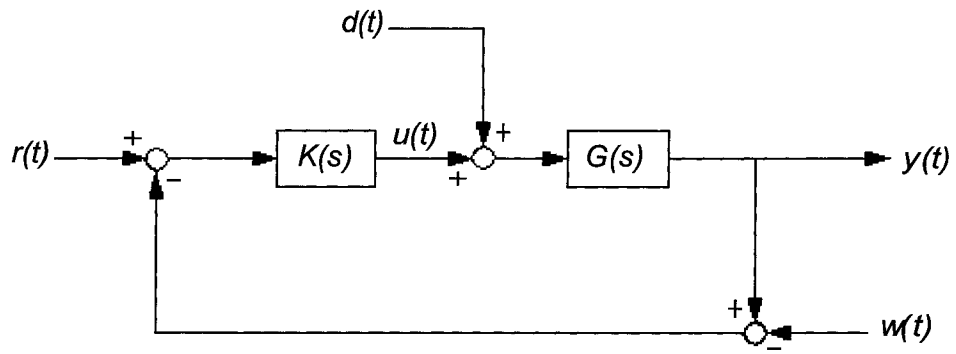

Figure 8.2: Simple block diagram of the bottoms temperature control loop.

The bottoms temperature control loop is assumed to have a block diagram similar to Figure 8.2, the variables are similar to those defined in Section 2.2.

From open-loop identification experiments, the transfer function for the temperature response to the steam flow perturbations has been calculated as:

$$G(s) = \frac{0.538e^{-240s}}{27720s^2 + 846s + 1} \qquad \textit{(time constants and delay in secs)} \qquad (8.1)$$

The transfer function of the PID controller (i.e. the Petro-Canada PID), currently being implemented in the loop, and its tuning parameters are:

$$K(s) = K_c\left(1 + \frac{1}{T_1 s}\right)\left[\frac{(T_2 s + 1)}{(\alpha T_2 s + 1)}\right] \qquad (8.2)$$

$$K_c = 1.4, T_1 = 1170\,\text{sec}\,s, T_2 = 78\,\text{sec}\,s, \alpha = 0.1$$

The Petro-Canada Refinery utilizes the Honeywell TDC Distributed Control System (DCS), which implements the PID loops. Because of the configuration of the DCS, the value of α has been set at 0.1. This restriction imposes a modified control activity constraint in the optimization formulation in (2.21) for the just proper optimal PID, i.e., $\alpha = 0.1$. The constraint substitutes those normally specified for J_u and J_{HF}.

Application of Kristiansson's criteria to evaluate the temperature loop computes the results in Table 8.1:

Table 8.1: Evaluation Results of Isostripper Bottoms Temperature Control Loop

CRITERION	CALCULATED VALUE
J_v	835.7143
GM_S	1.18 (M_S = 1.18, M_T = 1.0)
J_u	14.0
J_{HF}	14.0

According to Table 8.1, the values M_S = 1.18 and M_T = 1.0 imply gain and phase margins of 6.5 and 60° respectively. According to [2, 3], typical values of M_S range from 1.4 to 2.0, while recommended values of M_T range between 1.2 and 2.0. The designed optimal controllers that have been described in earlier chapters have M_S and M_T values of 1.7 and 1.3, respectively, based on the recommendation in [25]. Thus, the bottoms temperature control loop is significantly robust in the mid-frequency range. There exists the flexibility to slightly reduce the stability margins of the current temperature loop without jeopardizing loop stability, therefore obtaining some regulatory performance improvement.

8.4 DESIGN AND SIMULATION OF OPTIMAL PI AND PID CONTROLLERS

The constrained optimization formulation in (2.21) is solved for the bottoms temperature control loop to design an optimal PI controller and two optimal PID controllers – one PID with first order filtering (1°-PID) and the other with second order filtering (2°-PID). For the optimal PI and 1°-PID controllers, their transfer functions can easily be expressed in the form of (8.2) so that values for K_c, T_1, and T_2 are obtainable. For 2°-PID, the controller transfer function in (3.6) is used.

To ensure equal stability margins in the design of the optimal controllers, the Petro-Canada control loop's GM_S value is used as the respective constraint in (2.21). Thus, for the 1°-PID loop, (2.21) becomes

$$\min_{\rho}\{J_V(\rho): GM_S \le 1.18, \alpha = 0.1\} \tag{8.3}$$

For the 2°-PID controller, J_u and J_{HF} are set lower than the Petro-Canada control loop's values. (2.21) becomes

$$\min_{\rho}\{J_V(\rho): GM_S \le 1.18, J_u = 12.82, J_{HF} = 1.2\} \tag{8.4}$$

For the design of the optimal PI controller, no constraint is placed on J_u or J_{HF}. Solving the optimization formulation, unconstrained with respect to J_u and J_{HF}, calculates controller parameters whose closed loop attains the lower limit on J_V. Therefore, (2.21) becomes

$$\min_{\rho}\{J_V(\rho) : GM_S \leq 1.18\} \tag{8.5}$$

Table 8.2 presents the results for (8.3), (8.4) and (8.5):

Table 8.2: Parameters for Designed Optimal Controllers (PI, 1°-PID, 2°-PID)

	OPTIMAL PI	1°-PID	2°-PID
k_c	1.0938	1.2813	
T_1 (mins)	10.9227	8.5333	
T_2 (mins)	0	2.7231	
α	any	0.100	
k_i			0.0026
τ (secs)			250.25
ζ			1.3815
ζ_f			0.488
β			19.763
J_V	591.16	402.12	384.06
GM_S	1.18	1.18	1.18
J_u	1.9114	12.82	12.82
J_{HF}	1.9114	12.82	1.2

Table 8.2 shows the two optimal PID controllers having lower J_V values than the Petro-Canada PID controller in (8.2), while giving the same stability margins. Therefore, the optimal controllers can give better closed-loop performance. Figure 8.3 shows performance-control activity (J_V-J_u) profiles for the closed loops of the four controllers.

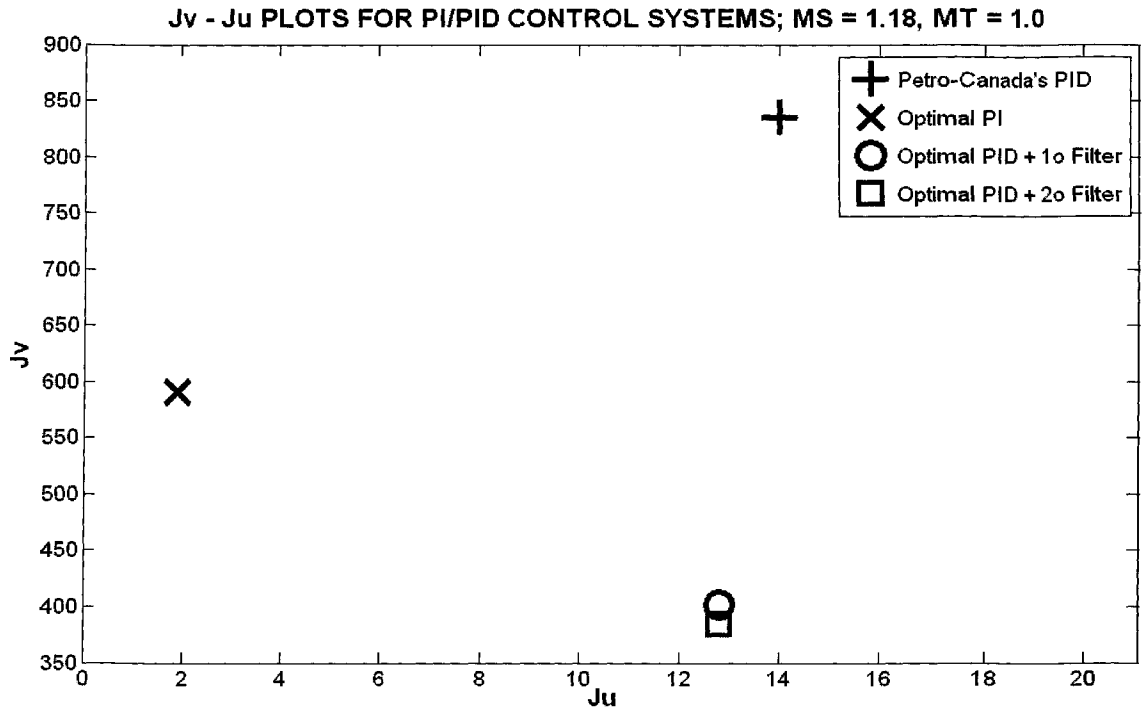

Figure 8.3: J_V-J_u profiles for the closed loops of the four controllers.

Figure 8.3 shows that the current Petro-Canada PID loop has high control activity, which implies higher sensitivity to high frequency sensor noise and lower robustness to model uncertainties. To obtain some insight into the performance variation amongst the four controllers' loops, their dynamic responses to steps in the set point and load disturbance (applied at process input) are simulated in SIMULINK. Gaussian noise signal is added to the process output as sensor noise in each closed loop. The performance-control activity profiles – using *ISE[y(t)]* and *VAR[Δu(t)* (or *MAD[Δu(t)]*) as alternative performance and control activity criteria respectively – are plotted in Figures 8.4 and 8.5. Figures 8.6 and 8.7 show the corresponding time trends of the closed loop responses to steps in the load disturbance (at process input) and set point.

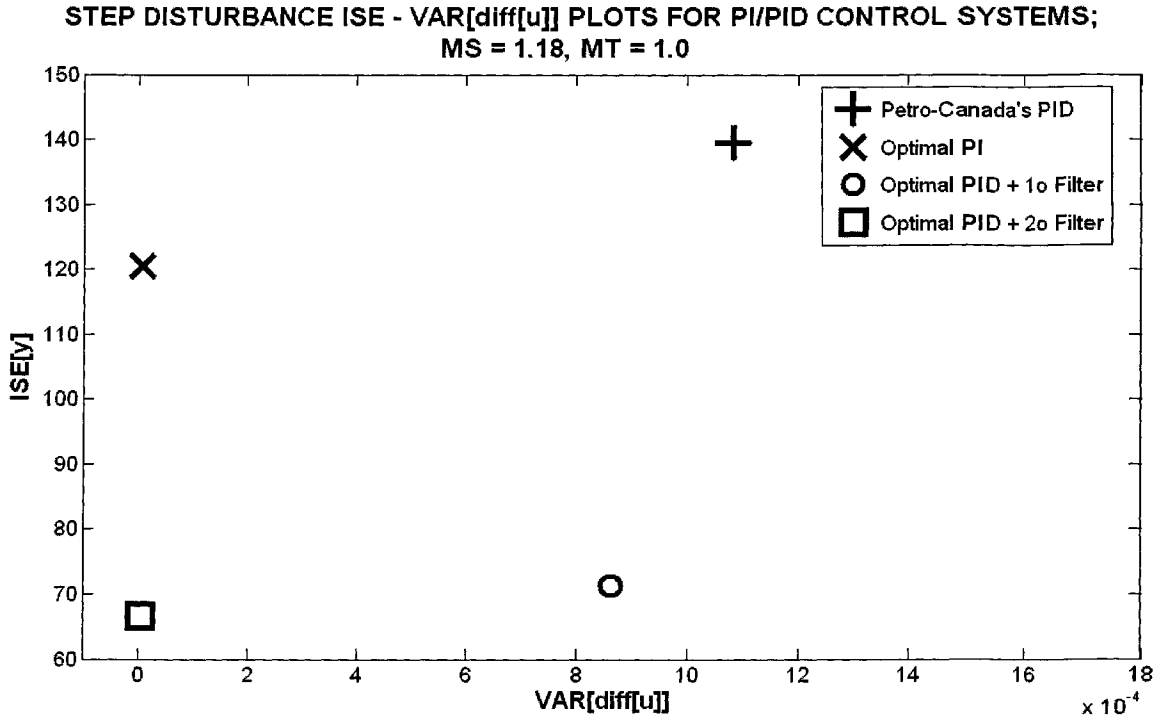

Figure 8.4: *ISE[y]-VAR[Δu]* profiles for step disturbance rejection of the four closed loops.

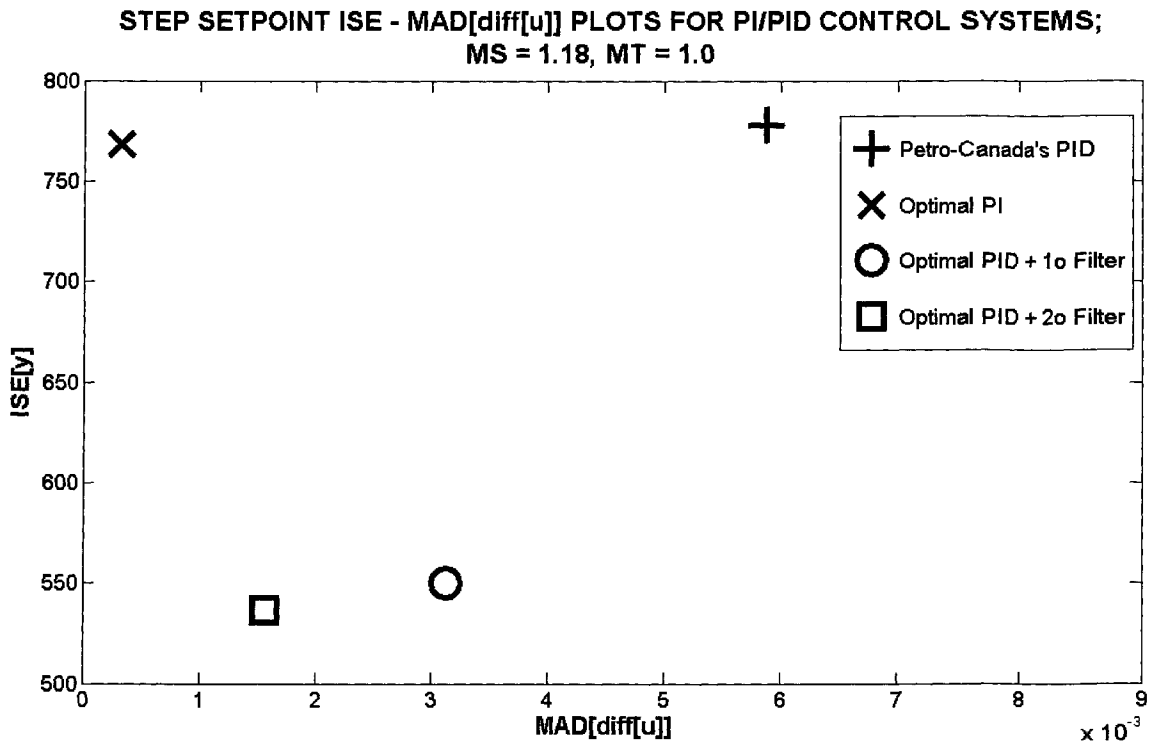

Figure 8.5: *ISE[y]-MAD[Δu]* profiles for step set point tracking responses of the four closed loops.

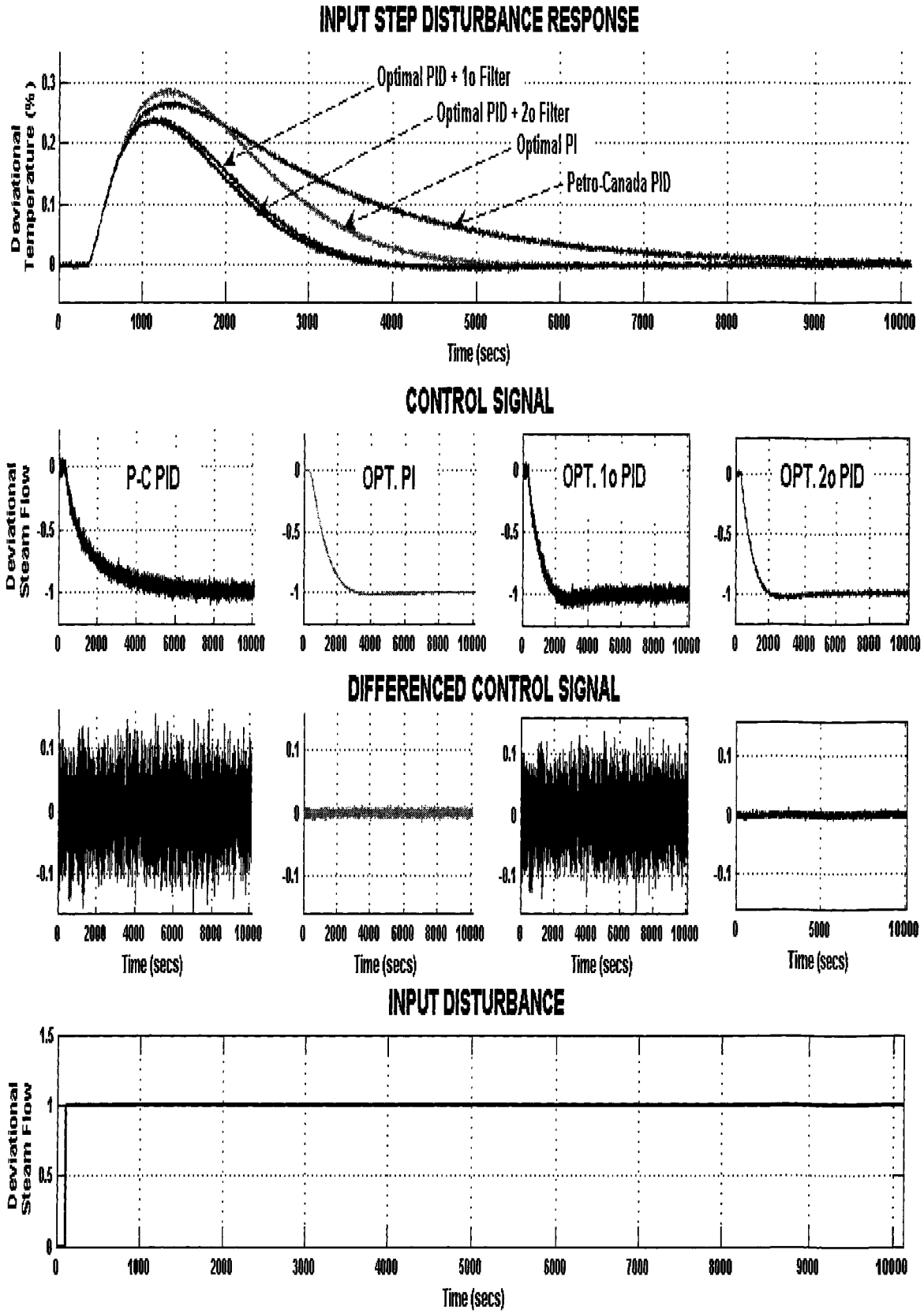

Figure 8.6: Step disturbance rejection responses of the four closed loops.

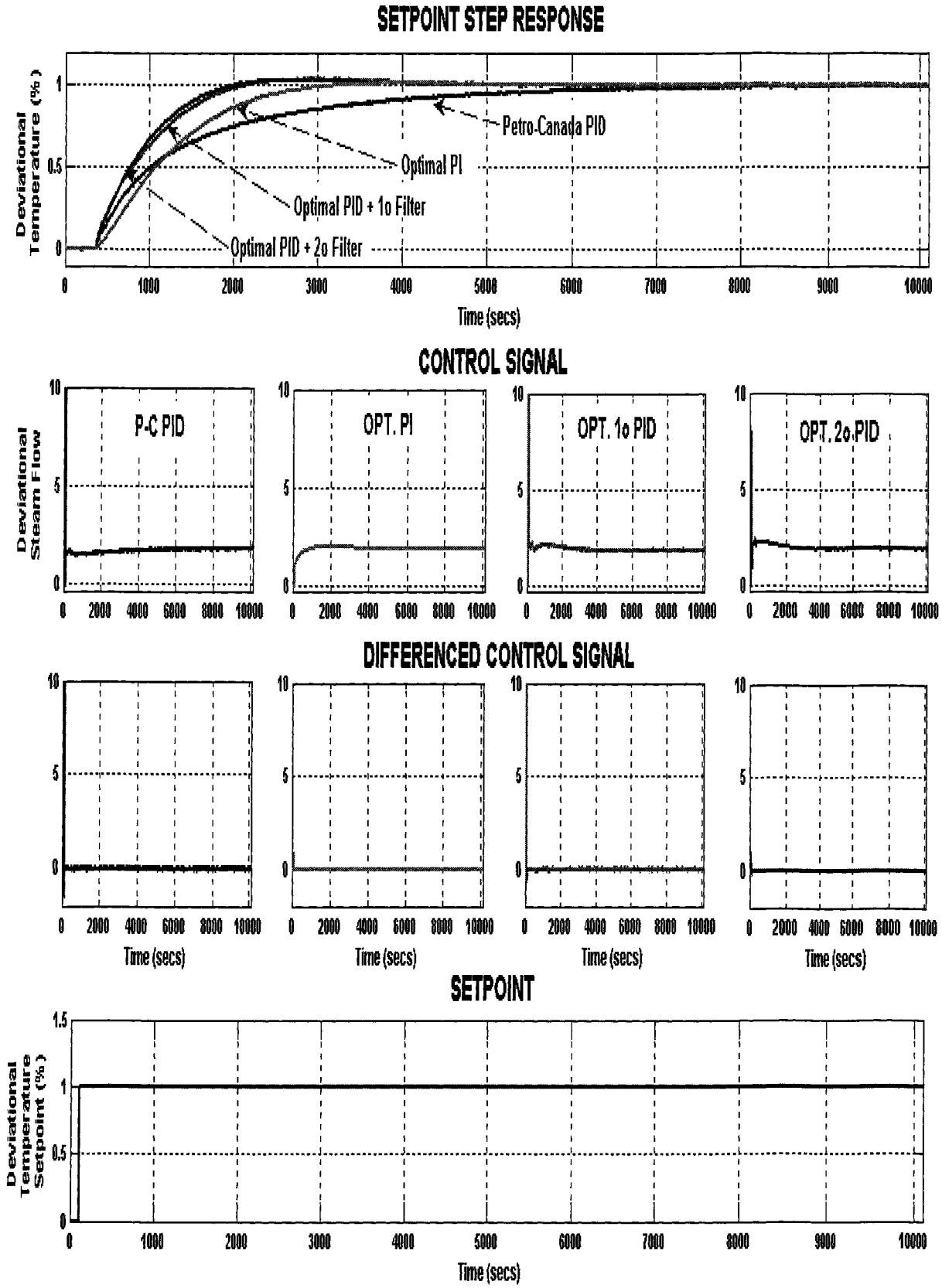

Figure 8.7: Step set point tracking responses of the four closed loops.

Figures 8.4 and 8.5 support the profiles in Figure 8.3 with respect to the optimal PI, optimal PID and Petro-Canada PID controllers. Thus, the optimal PID controllers can give better loop performance with lower control activity than the Petro-Canada PID. As explained, the restriction on α sets the value of J_u and does not provide the flexibility to reduce it to a desirable level, hence the proximity in the J_u values of the 1°-PID and Petro-Canada PID loop. The 1°-PID loop has a slightly lower J_u value than the Petro-Canada PID loop as confirmed by their *VAR[Δu(t)]* and *MAD[Δu(t)]* values. Therefore, improved loop performance is achieved with lower (though only slightly) control activity.

The profiles also show the performance superiority of the PID controller over the PI controller and demonstrate the benefit of including derivative control in the closed loop. According to the *VAR[Δu(t)]* values for the closed loops of the PI and 1°-PID controllers, the latter generates greater control activity, which is the price paid for superior performance. However, the 2°-PID's loop shows it can give performance comparable to the 1°-PID's and yet generate control activity comparable to the PI controller's.

The dynamic interpretation of the performance differences amongst the four controllers can be seen in Figures 8.6 and 8.7. From the step disturbance rejection responses in Figure 8.6, the optimal 1°- and 2°-PID controllers have the smallest overshoots and settling times. The Petro-Canada PID's overshoot is slightly higher than those of the optimal PID controllers. There is significant damping of its closed-loop response, thus leading to the loop's longer settling time. The PI controller has the highest overshoot but a shorter settling time than the Petro-Canada PID loop. Additionally, the differenced control signals of the four signals indicate that the Petro-Canada PID is the most aggressive controller, and the 2°-PID's control signal is as moderate as the PI controller's.

According to the set point tracking responses in Figure 8.7, the Petro-Canada PID loop's initial response is as fast as the optimal PID controllers', but the heavy damping of the loop's response makes it sluggish and significantly increases its settling time. The optimal PID controllers, on the other hand, have the shortest rise and settling times.

8.5 IMPLEMENTATION OF OPTIMAL PI AND PID CONTROLLERS

The optimal 1°-PID, optimal PI and Petro-Canada PID controllers were consecutively implemented in the bottoms temperature loop, each for at least an hour (3600 secs). The performance objective of the loop is to minimize the variability of the bottoms temperature (PV) about a set point temperature (SP) of 374.75°F. As described, the typical disturbances influencing this loop are variations in the tower feed rate, composition and temperature. It is difficult to implement each controller in the industrial loop for precisely the same duration. Thus, the length of the sampled closed-loop data for each controller varies, so that applying the *ISE[y(t)]* as the performance measure will lead to inconsistent loop comparisons.

To ensure the loop performance comparisons are reasonably consistent, the *Mean Square Error*, *MSE*, is the performance measure applied to the industrial implementation of the three controllers. The *MSE* of the closed loop error signal is defined as:

$$MSE = \frac{1}{N}\sum_{i=1}^{N}[SP(i) - PV(i)]^2 \qquad (8.6)$$

where:

N = sample size of PV (or SP)

Figure 8.8 shows the closed-loop responses of the three controllers, Figure 8.9 shows their *MSE-VAR[Δu(t)]* plots.

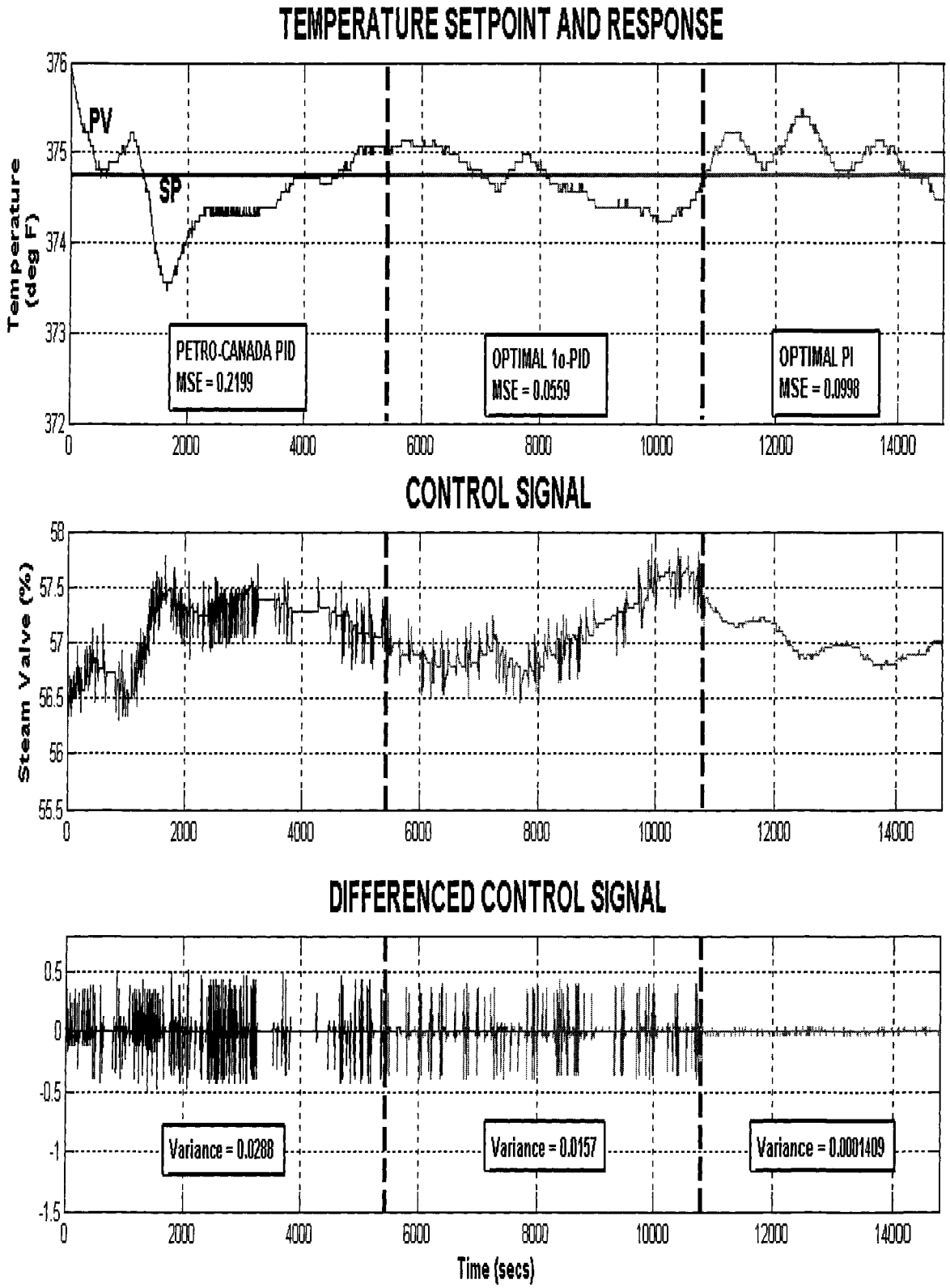

Figure 8.8: Implementation results of isostripper bottoms temperature closed loop, using the Petro-Canada PID, optimal PI and 1°-PID controllers.

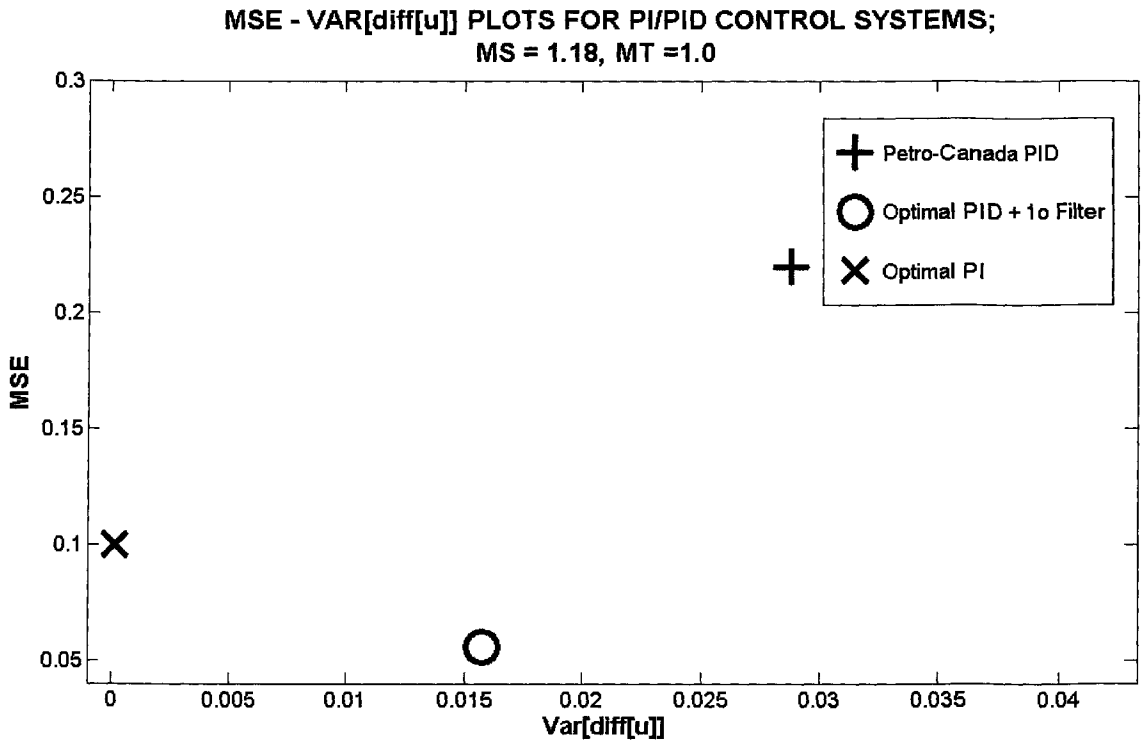

Figure 8.9: *MSE-VAR[Δu]* profiles for isostripper bottoms temperature closed-loop responses, using the Petro-Canada PID, optimal PI and 1°-PID controllers.

Figures 8.8 and 8.9 support the simulated comparisons in Figures 8.4 and 8.5, thus providing an industry-based corroboration that the inclusion of derivative control in a PI controller improves the controller's loop performance. The optimal 1°-PID controller reduces the variability of the isostripper bottoms temperature about its setpoint more effectively than the Petro-Canada's PID controller. Additionally, the optimal PID controller generates slightly less control activity than the Petro-Canada PI controller as shown by their *VAR[Δu(t)]* values in Figures 8.8.

In conclusion, Kristiansson's control system evaluation criteria have been applied to an industrial control loop. The criteria have shown how much insight the simultaneous evaluation of the various properties of a control loop provides, compared to the evaluation of just one property. The application of the criteria to the Petro-Canada isostripper bottoms temperature control loop has shown that the loop has very high stability margins, which could be reduced to improve loop performance. It has also shown that appropriate re-tuning of the PID controller, via the criteria, improves the controller's performance without necessarily increasing its aggressiveness.

CHAPTER 9

CONCLUSIONS

9.1 SUMMARY

In Chapter 1, a brief history of the development of the PID controller over a period of nearly eighty years was presented. Current issues encountered in its industrial application and the growing research interest shown by the academic community were discussed. Salient points made in the discussion were the relevance of the PID control algorithm to process industries despite the evolution of advanced control algorithms, and the importance of systematic procedures for evaluating the closed-loop properties of control systems.

In Chapter 2, the four criteria – J_v, J_u, GM_S, and J_{HF} – proposed by Kristiansson in [13], to evaluate the performance, stability and control activity of a Single-Input-Single-Output (SISO) closed loop, were presented. The criteria were graphically illustrated using numerical examples. The formulation of a constrained optimization function for the design of SISO optimal PI and PID controllers was briefly described.

In Chapter 3, the design of optimal PI and PID controllers, accomplished by the solution of the constrained optimization function introduced in Chapter 2, was presented in detail using numerical examples. The closed loops of the designed controllers were implemented in simulation. Although the design methodology was formulated for load disturbance rejection, it was shown that the closed loops could also perform servo tasks if they were augmented with set point pre-filters.

In Chapter 4, the design methodology discussed in Chapter 3 was applied to a pilot-scale process – the Quadruple Tank Process. The two dynamic phases of the process – the minimum and non-minimum phases – were discussed. Just proper and strictly proper PID controllers were designed for the two phases of the process using a modified version of Shen and Yu's sequential loop tuning method [17] that incorporated the optimal controller design technique. The optimal PID controllers were implemented in the multiloop framework for the minimum and non-minimum phases in simulation and experimentally.

In Chapter 5, the evaluation criteria were used to compute the loop performance-control activity (J_v-J_u) profiles of control loops utilizing optimal PI and PID controllers. The profiles showed that the loop performance of an optimal PI controller had a limit, which could be surpassed by the optimal PID controller. The cost of the optimal PID controller's improved performance was higher control activity. The profile comparisons of the two controllers' closed loops showed the performance benefit derivative action brought to a closed loop. Time domain-based evaluation criteria were also used to compute the performance-control activity profiles of control loops. The profiles exhibited the same characteristics

for the optimal controllers as shown by the J_V-J_u profiles, and thus corroborated the superiority of the PID controller over the PI controller. Closed-loop implementations of PID controllers with second order filters showed that the controller's performance improvement relative to the PI controller could be obtained without its control activity being excessive. The performance-control activity profiles also showed that as the time-delay dominance in a process increased, the closed-loop performance capability of the optimal PI controller became restricted. With the inclusion of derivative control, the restriction could be surpassed.

In Chapter 6, the design methodology discussed in Chapter 3 was applied to another pilot-scale process – the Heated Tank Process. The process' relevant feature was the adjustability in time delay of its temperature measurement. The variable delay in measurement provided an experimental basis for corroborating the closed-loop simulation results for time delay-dominant processes obtained in Chapter 5. The experimental and simulation results were similar. The economic benefit of the optimal PID's performance superiority over the PI controller's was discussed. It was shown that due to the improvement offered by the optimal PID controller, it could reduce a process output's variability more effectively than the optimal PI controller. Potential economic improvements in the process were linked to the reduction in the output's variability.

In Chapter 7, performance comparisons of closed loops augmented with the Smith predictor and those utilizing the plain optimal PI or PID controllers were examined. A constrained optimization procedure proposed by Kristiansson [13] for designing robust optimal controllers augmented with the Smith predictor was applied to the Heated Tank Process. The controller implementation results showed that for processes with small time delays, it was worthwhile to stay with the plain PI controller without augmenting it with a Smith predictor or derivative control. For processes with higher time delay dominance, both the Smith-augmented and un-augmented closed loops of the PID controller performed better than the Smith-augmented PI controller. The Smith-augmented PID closed loop gave marginally improved performance than the un-augmented PID closed loop. Based on preference for closed-loop structural simplicity, the un-augmented PID controller could be implemented for processes with significant time delays instead of the Smith-augmented PID controller.

In Chapter 8, the control system evaluation criteria were applied to an industrial control loop – an Isostripper bottoms temperature control loop at Petro-Canada's Edmonton refinery. Optimal PI and PID controllers were designed and implemented in this loop. The performance comparisons of the optimal controllers and Petro-Canada controller were presented.

9.2 CONTRIBUTIONS OF THESIS

The key contributions of this thesis are as follows:

- The application of Kristiansson's controller evaluation method [13] to the design of SISO and Multi-Input-Multi-Output (MIMO) PID-based control systems for pilot-scale and industrial processes, and the implementation of the designed control systems in simulation and real time; and
- The utilization of alternative evaluation criteria based on sampled data of closed loop variables to compute performance-control activity profiles. A few of the criteria were proposed in this thesis and others were obtained from literature. The characteristics of the profiles for optimal PI and PID control systems were similar to those of the J_v-J_u profiles presented in [13] and in this thesis.

9.3 RECOMMENDATIONS FOR FUTURE WORK

The results obtained during the course of this work suggest possible directions for future work. They are summarized below:

- Kristiansson's evaluation criteria have been applied to the design of optimal controllers for SISO closed loops and decentralized systems with strongly diagonal and non-diagonal process transfer matrices. **The application of the criteria should be extended to multivariable control systems because there are numerous MIMO industrial processes for which decentralized or SISO control may not perform satisfactorily.** These processes utilize multivariable control systems, e.g., Model Predictive Control (MPC).
- The criteria require process and controller transfer functions for their computation. However, transfer functions are not easily obtainable for some industrial processes. Although alternative criteria that use process data have been applied in this thesis, their application has been restricted to closed-loop evaluation and not controller design. Thus, the four criteria are still required for optimal controller design. **A useful direction for future work would be to develop techniques for computing Kristiansson's criteria using just process data, without requiring process transfer functions.** In [13] and [25], Kristiansson provides empirical tuning rules, which calculate optimal PI and PID controller parameters for processes, using minimal process information. However, the tuning rules have been formulated only for PI and PID closed loops having $GM_S \leq 1.7$.

BIBLIOGRAPHY

[1] K. H. Johansson (2000). "The quadruple tank process: A multivariable process with an adjustable zero." *IEEE Trans. Cont. Sys. Tech.* **8**(3), 456 – 465.

[2] Astrom, K.J., T. Hagglund, C.C. Hang, W.K. Ho (1993). "Automatic Tuning and Adaptation for PID Controllers – A Survey", *Control Engineering Practice* **1**(4), 699 – 714.

[3] Astrom, K.J., H. Panagopoulos, T. Hagglund (1998). "Design of PI Controllers based on Non-Convex Optimization", *Automatica* **34**(5), 585 – 601.

[4] Astrom, K.J., T. Hagglund (1995). "*PID Controllers: Theory, Design and Tuning*", Instrument Society of America.

[5] Astrom, K.J., T. Hagglund (2000). "The Future of PID Control". In: *Proceedings of PID'00. IFAC Workshop of Digital Control. Past, present and future of PID Control.* Terrassa, Spain.

[6] Bennett, S. (2000). "The Past of PID Control". In: *Proceedings of PID'00. IFAC Workshop of Digital Control. Past, present and future of PID Control.* Terrassa, Spain.

[7] Lelic, M., Z. Gajic (2000). "A Reference Guide to PID Controllers in the Nineties". In: *Proceedings of PID'00. IFAC Workshop of Digital Control. Past, present and future of PID Control.* Terrassa, Spain.

[8] Astrom, K.J., T. Hagglund (2000). "Benchmark Systems for PID Control". In: *Proceedings of PID'00. IFAC Workshop of Digital Control. Past, present and future of PID Control.* Terrassa, Spain.

[9] Yamamoto, S., I. Hashimoto (1991). "Present Status and Future Needs: The View from Japanese Industry". In: *Proceedings of the Fourth International Conference on Chemical Process Control.* Texas.

[10] Astrom, K.J., H. Panagopoulos, T. Hagglund (2002). "Design of PID Controllers based on Constrained Optimization", *IEE Proc.–D: Control Theory Appl* **149**(1), 32 – 40.

[11] Desborough, L., R. Miller (2001). "Increasing Customer Value of Industrial Control Performance Monitoring – Honeywell's Experience". In: *Preprints of CPC6.* Tucson, Arizona.

[12] Isaksson, A.J., S.F. Graebe (2002). "Derivative Filter as an Integral Part of PID Design", *IEE Proc.–D: Control Theory Appl* **149**(1), 41 – 45.

[13] Kristiansson, B. (2000). "*Evaluation and Tuning of PID Controllers*", Licentiate Thesis, Chalmers University of Technology, Sweden.

[14] Seborg, D.E., T.F. Edgar, D.A. Mellichamp (2003). "*Process Dynamics and Control*", John Wiley & Sons Inc, New Jersey.

[15] Kristiansson, B., B. Lennartson (2003). "Evaluation and Simple Tuning of PID Controllers with High Frequency Robustness", submitted to *J. Proc. Cont.*

[16] Kristiansson, B., B. Lennartson (2003). "Evaluation and Tuning of Robust PID Controllers", submitted to *Automatica*.

[17] Shen, S.H., C.C. Yu (1994). "Use of Relay-Feedback Test for Automatic Tuning of Multivariable Systems", *AIChE Journal* **40**(4), 627 – 646.

[18] Astrom, K.J. (2000). "Limitations on Control System Performance", In: *European Journal on Control*. Brussels, Belgium.

[19] Seron, M.M., J.H. Braslavsky, G.C. Goodwin (2003). "*Fundamental Limitations in Filtering and Control*", Springer, Berlin.

[20] Hagglund, T., Astrom, K.J. (1991). "Industrial adaptive controllers based on frequency response techniques", *Automatica* **27**(4), 599 – 609.

[21] Smith, O.J.M. (1957). "Closer Control of Loops with Dead Time", *Chem. Eng. Prog.* **53**, 217.

[22] Jiya, J., C. Shao, T.Y. Chai (1999). "Comparison of PID and PPI Design Techniques for a Process with Time Delay". In: *Preprints of 14th World Congress of IFAC*. Beijing, China.

[23] Kaya, I., D.P. Atherton (1999). "A New PI-PD Smith Predictor for Control of Processes with Long Time Delays". In: *Preprints of 14th World Congress of IFAC*. Beijing, China.

[24] Kristiansson, B., B. Lennartson. (1999). "Optimal PID Controller including Roll-Off and Smith Predictor Structure". In: *Preprints of 14th World Congress of IFAC*. Beijing, China.

[25] Kristiansson, B. (2003). "*PID Controllers: Design and Evaluation*", Chalmers University of Technology, Sweden.

[26] Clarridge, R.E. (1950). "A New Concept of Automatic Control", *Instruments* **23**, 1248 - 1292.

[27] Hazen, H.L. (1934). "Theory of Servomechanisms", *Journal of the Franklin Institute* **218**, 283 - 331.

[28] Grebe, J.J., Boundy, R.H., Cermak, R.W. (1933). "The Control of Chemical Processes", *Trans. AIChE* **29**, 211- 255.

[29] Ivanoff, A. (1934). "Theoretical Foundation of Automatic Regulation of Temperature", *Journal of the Institute of Fuel* **7**, 117 – 130.

[30] Ziegler, J.G., N.B. Nichols (1942). "Optimum Settings for Automatic Controllers", *Trans. ASME* **64**(11), 759 – 765.

[31] Skogestad, S. (2001). "Probably the best simple PID tuning rules in the world". In: *AIChE Annual Meeting.* Reno, USA.

[32] O'Dwyer, A. (2003). "*Handbook of PI and PID Controller Tuning Rules*", Imperial College Press, London.

[33] Shinskey, G. (1996). "*Process Control Systems: Application, Design, and Tuning*", McGraw-Hill, New York.

[34] Qin, S.J., T.A. Badgwell (1997). "An Overview of Industrial Model Predictive Control Technology". In: *Proceedings of Fifth International Conference on Chemical Process Control, CACHE, AIChE.*

[35] Katzer, J.R., M.P. Ramage, A.V. Sapre (2000). "Petroleum Refining: Poised for Profound Changes", *Chem. Eng. Prog.* **96**(7), 41- 51.

[36] Ender, D. (1993). "Process Control Performance: Not As Good As You Think", *Control Engineering*, 180 – 190.

[37] Bialkowski, W.L. (1993). "Dreams Vs. Reality: A View From Both Sides Of The Gap", *Pulp and Paper Canada* **94**(11), 19 – 27.

[38] Harris, T.J., C.T. Seppala, L.D. Desborough (1999). "A Review OF Performance Monitoring and Assessment Techniques For Univariate And Multivariate Control Systems", *J. Proc. Cont.* **9**, 1 – 17.

[39] Astrom, K., T. Hagglund (1984). "Automatic Tuning Of Simple Regulators With Specifications On Phase And Amplitude Margins", *Automatica* **20**(5), 645 – 651.

[40] Rivera, D., M. Morari (1990). "Low-Order SISO Controller Tuning Methods for the H_2, H_∞ and Objective Functions", *Automatica* **26**(3), 361 – 369.

[41] Rivera, D.E., M. Morari, S. Skogestad (1986). "Internal Model Control 4. PID Controller Design", *Ind. Eng. Chem. Proc. Des. And Dev.* **25**(1), 252 – 265.

[42] Cutler, C.R., B.L. Ramaker (1980). "Dynamic Matrix Control – A Computer Control Algorithm". In: *Proceedings of the American Control Conference.* San Francisco.

[43] Marlin, T.E. (1995). "*Process Control: Designing Processes and Control Systems for Dynamic Performance*", McGraw-Hill, New York.

[44] Schei, T.S. (1994). "Automatic Tuning of PID Controllers based on Transfer Function Estimation", *Automatica* **30**(12), 1983 – 1989.

[45] Bristol, E.H. (1966). "On a New Measure of Interactions for Multivariable Process Control", *IEEE Trans. Auto. Control* **11**, 133 – 134.

[46] Huang, H.P., J.C. Jeng, C.H. Chiang, W. Pan (2003). "A Direct Method for Multiloop PI/PID Controller Design", *Journal of Process Control* **13**(8), 769 – 786.

[47] Mayne, D.Q. (1973). "The Design of Linear Multivariable Systems", *Automatica* **9**(3), 201 – 207.

[48] O'Reilly, J., W.E. Leithead (1991). "Multivariable Control by Individual Channel Design", *Int. J. Control* **54**(1), 1 – 46.

[49] Chiu, M.S., Y. Arkun (1992). "A Methodology for Sequential Design of Robust Decentralized Control Systems", *Automatica* **28**(5), 997 – 1001.

[50] Loh, A.P., C.C. Hang, C.K. Quek, V.U. Vasnani (1993). "Autotuning of Multiloop Proportional – Integral Controllers Using Relay Feedback", *Ind. Eng. Chem. Res.* **32**(6), 1102 – 1107.

[51] Hovd, M., Skogestad, S. (1994). "Sequential Design of Decentralized Controllers", *Automatica* **30**(10), 1601 – 1607.

[52] Craig, I.K., Koch, I. (2003). "Experimental design for the economic performance evaluation of industrial controllers", *Control Engineering Practice* **11**(1), 57 – 66.

[53] Schubert, J. H., Henning, R. G. D., Hulbert, D. G., Craig, I. K. (1995). "Flotation control—a multivariable stabilizer", *XIX International Mineral Processing Congress*. San Francisco.

[54] Oakland, J.S. (2003). "*Statistical Process Control*", Butterworth-Heinemann.

[55] Davies, P.L., U. Gather (1993). "The identification of multiple outliers", *Journal of the American Statistical Association* **88**(423), 782 – 801.

APPENDIX A

CONTROLLER AND EVALUATION PARAMETERS FOR OPTIMAL CONTROL SYSTEMS

Tables A.1 to A.16 list the parameters of the optimal PI and just proper PID controllers designed for the simple process model considered in Chapter 5, the sequential loops [17] of the minimum and non-minimum phases of the Quadruple-Tank Process, and the closed loops of the Heated Tank Process' thermocouples. The tables also list the J_v and J_u values for plotting the performance-control activity profiles and the constraints on GM_S and k_∞. For the optimal PI and just proper PID controllers, $J_{HF} = J_u$.

Table A.1: Controller and Closed Loop Evaluation Parameters of Optimal PI Controllers for Process 1

J_u	J_v	k_i	τ	ζ	β	k_∞	GM_S	M_S	M_T
4	1.5681	0.64526	3.9874	1	1	2.5729	1.6369	1.3716	1.2517
4.5	1.3694	0.7404	3.8073	1	1	2.8189	1.6807	1.4181	1.2853
5	1.2208	0.82501	3.7646	1	1	3.1059	1.7	1.4582	1.3
5.5	1.1192	0.8937	3.8143	1	1	3.4089	1.7	1.4939	1.3
6	1.0483	0.95393	3.8616	1	1	3.6837	1.7	1.5297	1.3
6.5	0.99268	1.0074	3.9091	1	1	3.9379	1.7	1.5651	1.3
7	0.94781	1.0551	3.9588	1	1	4.1767	1.7	1.6	1.3
7.5	0.91114	1.0975	4.0121	1	1	4.4034	1.7	1.6346	1.3
8	0.88108	1.135	4.0708	1	1	4.6202	1.7	1.6688	1.3
8.5	0.86731	1.153	4.2006	1	1	4.8432	1.7	1.7	1.2912
9	1.0625	0.94114	5.5444	1	1	5.2181	1.7	1.7	1.171
9.1	1.1273	0.88709	5.9622	1	1	5.289	1.7	1.7	1.1465
9.2	1.2063	0.82896	6.4645	1	1	5.3588	1.7	1.7	1.1221
9.3	1.3043	0.76672	7.0789	1	1	5.4275	1.7	1.7	1.0982
9.4	1.4279	0.70032	7.8467	1	1	5.4952	1.7	1.7	1.0751
9.5	1.5883	0.62962	8.8337	1	1	5.5619	1.7	1.7	1.0532

Table A.2: Controller and Closed Loop Evaluation Parameters of Just Proper Optimal PID Controllers for Process 1

J_u	J_v	k_i	τ	ζ	β	k_∞	GM_S	M_S	M_T
8.4498	0.8004	1.2743	3.973	0.93181	0.96789	4.9	1.7	1.691	1.3
8.6255	0.78633	1.2979	3.7236	0.92375	1.0346	5	1.7	1.7	1.3
9.4939	0.72662	1.3844	2.2689	1.0053	1.9102	6	1.7	1.7	1.3
10.741	0.66413	1.5068	1.7477	1.1341	3.0378	8	1.7	1.7	1.3
11.598	0.62663	1.5959	1.5739	1.1962	3.9811	10	1.7	1.7	1.3
13.053	0.60117	1.6634	1.4833	1.2329	4.8635	12	1.7	1.7	1.3
15.123	0.5825	1.7167	1.4234	1.2617	5.7293	14	1.7	1.7	1.3
17.112	0.56816	1.7601	1.385	1.2787	6.5635	16	1.7	1.7	1.3
19.008	0.55676	1.7961	1.357	1.2913	7.3851	18	1.7	1.7	1.3
20.813	0.54746	1.8266	1.3363	1.2998	8.1935	20	1.7	1.7	1.3
22.523	0.53972	1.8528	1.32	1.3064	8.9951	22	1.7	1.7	1.3
24.141	0.53317	1.8756	1.3069	1.3116	9.7914	24	1.7	1.7	1.3
25.996	0.52755	1.8956	1.2967	1.3147	10.578	26	1.7	1.7	1.3
27.995	0.52267	1.9132	1.2877	1.3178	11.365	28	1.7	1.7	1.3
29.994	0.5184	1.929	1.2803	1.3201	12.147	30	1.7	1.7	1.3

Table A.3: Controller and Closed Loop Evaluation Parameters of Optimal PI Controllers for Loop 1 of the Minimum Phase Quadruple-Tank Process

J_u	J_v	k_i	τ	ζ	β	k_∞	GM_S	M_S	M_T
0.12027	677.91	0.001475	57.406	1	1	0.084682	1.458	1.1476	1.1149
0.16933	409.01	0.002445	48.08	1	1	0.11755	1.5763	1.1956	1.2054
0.2224	274.93	0.003638	42.628	1	1	0.15506	1.6485	1.2358	1.2606
0.28179	197.28	0.005069	38.628	1	1	0.1958	1.7	1.282	1.3
0.3508	151.76	0.006589	37.627	1	1	0.24794	1.7	1.3283	1.3
0.4321	123.06	0.008126	36.823	1	1	0.29923	1.7	1.3904	1.3
0.52495	103.76	0.009637	36.292	1	1	0.34976	1.7	1.46	1.3
0.62824	90.186	0.011088	36.08	1	1	0.40006	1.7	1.5358	1.3
0.74187	80.538	0.012416	36.267	1	1	0.4503	1.7	1.6171	1.3
0.75	79.998	0.0125	36.298	1	1	0.45373	1.7	1.6228	1.3
0.76	79.357	0.012601	36.339	1	1	0.45792	1.7	1.6299	1.3
0.77	78.738	0.0127	36.382	1	1	0.46207	1.7	1.6369	1.3
0.78	78.132	0.012799	36.424	1	1	0.46618	1.7	1.6439	1.3
0.79	77.549	0.012895	36.468	1	1	0.47026	1.7	1.651	1.3
0.8	76.986	0.012989	36.515	1	1	0.47431	1.7	1.658	1.3
0.82	75.923	0.013171	36.619	1	1	0.48233	1.7	1.6719	1.3
0.84	74.94	0.013344	36.738	1	1	0.49023	1.7	1.6858	1.3
0.86	74.037	0.013507	36.873	1	1	0.49804	1.7	1.6997	1.3
0.86287	74.8	0.013369	37.393	1	1	0.49991	1.7	1.7	1.294
0.87718	80.335	0.012448	40.963	1	1	0.5099	1.7	1.7	1.2572
0.878	80.7	0.012392	41.195	1	1	0.51047	1.7	1.7	1.2551
0.88	81.614	0.012253	41.774	1	1	0.51185	1.7	1.7	1.2499

Table A.4: Controller and Closed Loop Evaluation Parameters of Optimal PI Controllers for Loop 2 of the Minimum Phase Quadruple-Tank Process

J_u	J_v	k_i	τ	ζ	β	k_∞	GM_S	M_S	M_T
0.12027	698.47	0.001432	58.085	1	1	0.083161	1.4633	1.1647	1.119
0.16933	425.33	0.002351	49.268	1	1	0.11584	1.5811	1.2156	1.2091
0.2224	288.72	0.003465	43.972	1	1	0.15234	1.6556	1.2612	1.2661
0.28179	210.14	0.004759	40.674	1	1	0.19356	1.7	1.3097	1.3
0.3508	164.64	0.006074	39.993	1	1	0.24292	1.7	1.3636	1.3
0.4321	135.73	0.007368	39.514	1	1	0.29112	1.7	1.432	1.3
0.52495	116.09	0.008614	39.335	1	1	0.33884	1.7	1.5085	1.3
0.62824	102.37	0.009768	39.552	1	1	0.38635	1.7	1.5916	1.3
0.74187	93.02	0.01075	40.35	1	1	0.43378	1.7	1.6805	1.3
0.75	92.524	0.010808	40.435	1	1	0.43702	1.7	1.6867	1.3
0.76	91.943	0.010876	40.544	1	1	0.44097	1.7	1.6943	1.3
0.77	92.669	0.010791	41.305	1	1	0.44573	1.7	1.7	1.2928
0.78	97.688	0.010237	44.23	1	1	0.45277	1.7	1.7	1.2646
0.79	103.89	0.009626	47.757	1	1	0.45969	1.7	1.7	1.2361
0.8	111.64	0.008957	52.082	1	1	0.46651	1.7	1.7	1.2075
0.82	134.35	0.007443	64.468	1	1	0.47985	1.7	1.7	1.1508
0.84	175.87	0.005686	86.669	1	1	0.49281	1.7	1.7	1.097
0.86	271.97	0.003677	137.45	1	1	0.50539	1.7	1.7	1.0497
0.86287	296.98	0.003367	150.62	1	1	0.50716	1.7	1.7	1.0436
0.87718	574.39	0.001741	296.32	1	1	0.51589	1.7	1.7	1.0156
0.878	608.37	0.001644	314.15	1	1	0.51638	1.7	1.7	1.0142
0.88	712.01	0.001405	368.53	1	1	0.51758	1.7	1.7	1.0106

Table A.5: Controller and Closed Loop Evaluation Parameters of Optimal PI Controllers for Loop 3 of the Non-Minimum Phase Quadruple-Tank Process

J_u	J_v	k_i	τ	ζ	β	k_∞	GM_S	M_S	M_T
1.15	355.64	0.002812	227.59	1	1	0.63994	1.3387	1.3387	1
1.2	339.24	0.002948	219.71	1	1	0.64765	1.3581	1.3581	1
1.3	311.53	0.00321	207.48	1	1	0.666	1.397	1.397	1
1.4	288.92	0.003461	199.07	1	1	0.68902	1.4352	1.4352	1.0018
1.5	270.07	0.003703	192.22	1	1	0.71174	1.4732	1.4732	1.0256
1.6	254.09	0.003936	187.4	1	1	0.73754	1.51	1.51	1.0542
1.7	240.34	0.004161	183.4	1	1	0.76308	1.5463	1.5463	1.0851
1.8	228.38	0.004379	179.7	1	1	0.78687	1.5825	1.5825	1.1179
1.9	217.87	0.00459	177.84	1	1	0.81625	1.6164	1.6164	1.1487
2	208.66	0.004792	179.96	1	1	0.86246	1.6438	1.6438	1.1713
2.1	200.55	0.004986	181.81	1	1	0.90652	1.6706	1.6706	1.1942
2.2	193.34	0.005172	183.46	1	1	0.9489	1.697	1.697	1.2172
2.3	188.7	0.0053	197.73	1	1	1.0479	1.7	1.7	1.2077
2.4	186.18	0.005371	213.5	1	1	1.1467	1.7	1.7	1.1941
2.5	185.13	0.005402	229.36	1	1	1.2389	1.7	1.7	1.1816
2.6	185.22	0.005399	245.54	1	1	1.3257	1.7	1.7	1.1708
2.8	187.99	0.005319	279.68	1	1	1.4877	1.7	1.7	1.1548
3	193.61	0.005165	317.32	1	1	1.6389	1.7	1.7	1.1464
3.2	201.76	0.004956	359.71	1	1	1.7828	1.7	1.7	1.1443
3.4	212.47	0.004707	408.24	1	1	1.9214	1.7	1.7	1.1469
3.6	225.98	0.004425	464.59	1	1	2.0559	1.7	1.7	1.1531
3.8	242.76	0.004119	530.99	1	1	2.1873	1.7	1.7	1.1617
4	263.59	0.003794	610.51	1	1	2.3161	1.7	1.7	1.1719

Table A.6: Controller and Closed Loop Evaluation Parameters of Optimal PI Controllers for Loop 4 of the Non-Minimum Phase Quadruple-Tank Process

J_u	J_v	k_i	τ	ζ	β	k_∞	GM_S	M_S	M_T
1.15	363.7	0.00275	224.62	1	1	0.6176	1.374	1.374	1
1.2	347.47	0.002878	216.64	1	1	0.62347	1.3951	1.3951	1
1.3	320.05	0.003125	204.81	1	1	0.63993	1.4371	1.4371	1
1.4	297.68	0.003359	196.44	1	1	0.6599	1.4788	1.4788	1.0034
1.5	279.02	0.003584	190.11	1	1	0.68136	1.52	1.52	1.0296
1.6	263.18	0.0038	184.67	1	1	0.70169	1.5611	1.5611	1.0627
1.7	249.55	0.004007	181.16	1	1	0.72592	1.6006	1.6006	1.0966
1.8	237.69	0.004207	177.95	1	1	0.74866	1.6401	1.6401	1.1322
1.9	227.34	0.004399	179.2	1	1	0.78822	1.6734	1.6734	1.1601
2	218.56	0.004575	184.39	1	1	0.84364	1.7	1.7	1.179
2.1	214.28	0.004667	206.48	1	1	0.9636	1.7	1.7	1.1578
2.2	213.35	0.004687	228.15	1	1	1.0694	1.7	1.7	1.1381
2.3	214.75	0.004657	250.18	1	1	1.165	1.7	1.7	1.1213
2.4	217.97	0.004588	273.23	1	1	1.2535	1.7	1.7	1.1078
2.5	222.82	0.004488	297.9	1	1	1.337	1.7	1.7	1.0976
2.6	229.25	0.004362	324.73	1	1	1.4165	1.7	1.7	1.0903
2.8	247.22	0.004045	387.43	1	1	1.5672	1.7	1.7	1.0826
3	273.68	0.003654	467.88	1	1	1.7096	1.7	1.7	1.0812
3.2	312.68	0.003198	577.22	1	1	1.846	1.7	1.7	1.0835
3.4	372.85	0.002682	737.41	1	1	1.9777	1.7	1.7	1.0879
3.6	475.05	0.002105	1000.3	1	1	2.1056	1.7	1.7	1.0928
3.8	684.19	0.001462	1525.9	1	1	2.2302	1.7	1.7	1.0972
4	1351.4	0.00074	3178.3	1	1	2.3518	1.7	1.7	1.1001

Table A.7: Controller and Closed Loop Evaluation Parameters of Just Proper Optimal PID Controllers for Loop 1 of the Minimum Phase Quadruple-Tank Process

J_u	J_v	k_i	τ	ζ	β	k_∞	GM_S	M_S	M_T
0.79278	70.134	0.014612	33.314	0.90155	0.98609	0.48	1.7	1.642	1.3
0.8398	67.153	0.015299	32.313	0.89285	1.0114	0.5	1.7	1.6732	1.3
1.0475	59.246	0.016879	15.668	1.079	2.6469	0.7	1.7	1.7	1.3
1.0956	57.005	0.017542	13.329	1.2311	3.4128	0.798	1.7	1.7	1.3
1.0964	56.961	0.017556	13.299	1.2333	3.4266	0.8	1.7	1.7	1.3
1.1381	54.976	0.01819	12.194	1.3139	4.0577	0.9	1.7	1.7	1.3
1.1742	53.341	0.018747	11.531	1.3636	4.6258	1	1.7	1.7	1.3
1.5	48.276	0.020714	10.146	1.4635	7.137	1.5	1.7	1.7	1.3
2	45.62	0.02192	9.6433	1.4936	9.4615	2	1.7	1.7	1.3
2.5	43.962	0.022747	9.378	1.5063	11.719	2.5	1.7	1.7	1.3
3	42.822	0.023352	9.2156	1.5118	13.94	3	1.7	1.7	1.3
3.5	41.988	0.023816	9.1043	1.5147	16.142	3.5	1.7	1.7	1.3
4	41.349	0.024184	9.0213	1.5168	18.334	4	1.7	1.7	1.3
4.5	40.844	0.024483	8.9606	1.5173	20.512	4.5	1.7	1.7	1.3

Table A.8: Controller and Closed Loop Evaluation Parameters of Just Proper Optimal PID Controllers for Loop 2 of the Minimum Phase Quadruple-Tank Process

J_u	J_v	k_i	τ	ζ	β	k_∞	GM_S	M_S	M_T
0.80489	77.282	0.013127	27.188	0.90208	1.3449	0.48	1.7	1.7	1.3
0.82565	76.296	0.013198	24.146	0.92754	1.569	0.5	1.7	1.7	1.3
0.96896	70.217	0.014242	14.974	1.2098	3.2824	0.7	1.7	1.7	1.3
1.0105	67.525	0.014809	13.571	1.2991	3.9706	0.798	1.7	1.7	1.3
1.0111	67.476	0.01482	13.545	1.3011	3.9852	0.8	1.7	1.7	1.3
1.0475	65.282	0.015318	12.76	1.3522	4.6046	0.9	1.7	1.7	1.3
1.0784	63.498	0.015749	12.233	1.3875	5.1906	1	1.7	1.7	1.3
1.5	57.966	0.017252	11.048	1.4599	7.8698	1.5	1.7	1.7	1.3
2	55.049	0.018166	10.59	1.482	10.397	2	1.7	1.7	1.3
2.5	53.227	0.018787	10.338	1.4922	12.872	2.5	1.7	1.7	1.3
3	51.973	0.019241	10.184	1.4963	15.311	3	1.7	1.7	1.3
3.5	51.056	0.019586	10.079	1.498	17.729	3.5	1.7	1.7	1.3
4	50.354	0.01986	9.9997	1.4994	20.142	4	1.7	1.7	1.3
4.5	49.799	0.020081	9.9407	1.4998	22.543	4.5	1.7	1.7	1.3

Table A.9: Controller and Closed Loop Evaluation Parameters of Just Proper Optimal PID Controllers for Loop 3 of the Non-Minimum Phase Quadruple-Tank Process

J_u	J_v	k_i	τ	ζ	β	k_∞	GM_S	M_S	M_T
3.4875	111.88	0.008938	154.69	0.97175	1.4465	2	1.7	1.7	1.2994
4.1754	94.933	0.010676	138.99	0.94294	2.0218	3	1.7	1.7	1.2394
4.8361	84.465	0.012264	133.34	0.91411	2.446	4	1.7	1.7	1.2391
5.458	77.138	0.013936	128.59	0.8814	2.7901	5	1.7	1.7	1.259
6.0797	71.469	0.01617	123.64	0.82544	3.0012	6	1.7	1.7	1.3
8	63.485	0.018408	120.59	0.80647	3.6038	8	1.7	1.7	1.3
9	60.595	0.019375	119.6	0.79808	3.8838	9	1.7	1.7	1.3

Table A.10: Controller and Closed Loop Evaluation Parameters of Just Proper Optimal PID Controllers for Loop 4 of the Non-Minimum Phase Quadruple-Tank Process

J_u	J_v	k_i	τ	ζ	β	k_∞	GM_S	M_S	M_T
3.0699	145.68	0.007054	196.61	0.84084	1.4422	2	1.7	1.7	1.2601
3.4889	132.94	0.007957	177.31	0.77799	2.1266	3	1.7	1.7	1.2182
4.0004	127.39	0.008477	165.88	0.75261	2.8448	4	1.7	1.7	1.2061
5	124.53	0.008791	158.71	0.74163	3.5837	5	1.7	1.7	1.2122
6	122.66	0.009006	154.46	0.73579	4.3132	6	1.7	1.7	1.2209
8	122.94	0.009065	145.94	0.74134	6.0469	8	1.7	1.7	1.2351
9	123.26	0.009057	142.84	0.74662	6.9568	9	1.7	1.7	1.2419

Table A.11: Controller and Closed Loop Evaluation Parameters of Optimal PI Controllers for Closed Loop of Thermocouple 1 in Heated Tank Process

J_u	J_v	k_i	τ	ζ	β	k_∞	GM_S	M_S	M_T
1.058	101.54	0.012757	5.4873	1	1	0.07	1.7	1.6315	1.3
1.0657	98.87	0.013088	6.1126	1	1	0.08	1.7	1.6245	1.3
1.0734	96.323	0.013419	6.7069	1	1	0.09	1.7	1.6176	1.3
1.0811	93.887	0.013751	7.2722	1	1	0.1	1.7	1.611	1.3
1.1199	83.157	0.015418	9.7289	1	1	0.15	1.7	1.5807	1.3
1.1591	74.375	0.017096	11.699	1	1	0.2	1.7	1.5546	1.3
1.1988	67.072	0.018784	13.309	1	1	0.25	1.7	1.5321	1.3
1.2391	60.916	0.020481	14.647	1	1	0.3	1.7	1.5128	1.3
1.2799	55.666	0.022186	15.776	1	1	0.35	1.7	1.4962	1.3
1.3213	51.145	0.023897	16.738	1	1	0.4	1.7	1.482	1.3
1.3634	47.217	0.025614	17.568	1	1	0.45	1.7	1.47	1.3
1.4062	43.778	0.027335	18.292	1	1	0.5	1.7	1.4599	1.3
1.4498	40.748	0.029059	18.927	1	1	0.55	1.7	1.4516	1.3
1.4943	38.061	0.030785	19.49	1	1	0.6	1.7	1.445	1.3
1.5396	35.665	0.032511	19.993	1	1	0.65	1.7	1.4399	1.3
1.5859	33.519	0.034238	20.445	1	1	0.7	1.7	1.4362	1.3
1.6333	31.588	0.035962	20.855	1	1	0.75	1.7	1.4339	1.3
1.6819	29.844	0.037684	21.229	1	1	0.8	1.7	1.4329	1.3
1.7317	28.262	0.039402	21.572	1	1	0.85	1.7	1.4331	1.3
1.783	26.824	0.041115	21.89	1	1	0.9	1.7	1.4345	1.3
1.8358	25.512	0.042821	22.185	1	1	0.95	1.7	1.437	1.3
1.8902	24.313	0.04452	22.462	1	1	1	1.7	1.4407	1.3
2.5629	16.565	0.06076	24.687	1	1	1.5	1.7	1.5311	1.3
3.5531	13.476	0.074206	26.952	1	1	2	1.7	1.6872	1.3
3.7114	13.885	0.072021	29.158	1	1	2.1	1.7	1.7	1.2613
3.8365	15.243	0.065602	33.535	1	1	2.2	1.7	1.7	1.1945
3.9702	17.639	0.056693	40.569	1	1	2.3	1.7	1.7	1.1216
4.1119	22.302	0.044838	53.526	1	1	2.4	1.7	1.7	1.0477
4.2618	33.96	0.029447	84.899	1	1	2.5	1.7	1.7	1
4.4211	103.16	0.009694	268.21	1	1	2.6	1.7	1.7	1
4.4376	134.49	0.007436	351.01	1	1	2.61	1.7	1.7	1
4.4543	195.25	0.005122	511.55	1	1	2.62	1.7	1.7	1

Table A.12: Controller and Closed Loop Evaluation Parameters of Optimal PI Controllers for Closed Loop of Thermocouple 2 in Heated Tank Process

J_u	J_v	k_i	τ	ζ	β	k_∞	GM_S	M_S	M_T
0.60864	270.11	0.003702	74.444	1	1	0.27561	1.3481	1.3481	1
0.7	189.27	0.005284	60.439	1	1	0.31933	1.5276	1.5276	1
0.77996	171.72	0.005823	56.87	1	1	0.33118	1.6005	1.6005	1.028
0.78525	170.72	0.005858	56.619	1	1	0.33165	1.6053	1.6053	1.0318
0.79043	169.75	0.005891	56.517	1	1	0.33294	1.61	1.61	1.0349
0.79549	168.82	0.005923	56.297	1	1	0.33346	1.6146	1.6146	1.0387
0.81903	164.69	0.006072	55.538	1	1	0.33722	1.6361	1.6361	1.0557
0.8397	161.3	0.0062	54.942	1	1	0.34063	1.6549	1.6549	1.0712
0.85773	158.5	0.006309	54.444	1	1	0.3435	1.6713	1.6713	1.0852
0.87387	156.11	0.006406	54.115	1	1	0.34665	1.6857	1.6857	1.0975
0.88989	153.84	0.0065	53.848	1	1	0.35002	1.7	1.7	1.1096
0.90906	153.17	0.006529	61.267	1	1	0.4	1.7	1.7	1.0748
0.93524	156.09	0.006407	70.24	1	1	0.45	1.7	1.7	1.0317
0.97065	163.82	0.006104	81.909	1	1	0.5	1.7	1.7	1
1.0152	178.94	0.005589	98.408	1	1	0.54996	1.7	1.7	1
1.0681	207.69	0.004815	124.61	1	1	0.6	1.7	1.7	1
1.1286	268.1	0.00373	174.26	1	1	0.64997	1.7	1.7	1
1.1417	288.38	0.003468	190.34	1	1	0.66002	1.7	1.7	1
1.155	313.33	0.003192	209.92	1	1	0.66998	1.7	1.7	1
1.1687	345.21	0.002897	234.74	1	1	0.67998	1.7	1.7	1
1.1828	387.21	0.002583	267.18	1	1	0.69003	1.7	1.7	1
1.1971	443.87	0.002253	310.7	1	1	0.69997	1.7	1.7	1
1.2119	526.34	0.0019	373.7	1	1	0.71	1.7	1.7	1

Table A.13: Controller and Closed Loop Evaluation Parameters of Optimal PI Controllers for Closed Loop of Thermocouple 3 in Heated Tank Process

J_u	J_v	k_i	τ	ζ	β	k_∞	GM_S	M_S	M_T
0.6035	344.64	0.002902	60.645	1	1	0.17597	1.3876	1.3876	1
0.7	238.11	0.0042	69.889	1	1	0.29351	1.6124	1.6124	1
0.74025	227.09	0.004404	67.637	1	1	0.29784	1.654	1.654	1.0222
0.74403	226.13	0.004422	67.444	1	1	0.29825	1.6579	1.6579	1.0251
0.74765	225.23	0.00444	67.27	1	1	0.29868	1.6617	1.6617	1.0279
0.7511	224.37	0.004457	67.116	1	1	0.29913	1.6652	1.6652	1.0306
0.76571	220.87	0.004528	66.48	1	1	0.301	1.6804	1.6804	1.0425
0.77575	218.55	0.004576	66.128	1	1	0.30257	1.6908	1.6908	1.0507
0.78132	217.3	0.004602	65.841	1	1	0.303	1.6966	1.6966	1.0558
0.79105	218.87	0.004569	76.602	1	1	0.34999	1.7	1.7	1.0111
0.80973	230.02	0.004348	92.006	1	1	0.39999	1.7	1.7	1
0.84306	256.38	0.003901	115.37	1	1	0.44999	1.7	1.7	1
0.88924	316.81	0.003156	158.41	1	1	0.5	1.7	1.7	1
0.94733	499.9	0.002	274.94	1	1	0.55	1.7	1.7	1
0.97433	725	0.001379	413.25	1	1	0.57	1.7	1.7	1
0.98881	975.67	0.001025	565.89	1	1	0.58	1.7	1.7	1

Table A.14: Controller and Closed Loop Evaluation Parameters of Just Proper Optimal PID Controllers for Closed Loop of Thermocouple 1 in Heated Tank Process

J_u	J_v	k_i	τ	ζ	β	k_∞	GM_S	M_S	M_T
3.4784	13.056	0.077591	28.109	0.95961	0.917	2	1.7	1.67	1.3
4.3343	10.833	0.092809	13.424	1.0692	2.408	3	1.7	1.7	1.3
4.8099	9.981	0.10046	11.465	1.1488	3.4729	4	1.7	1.7	1.3
5.4254	9.472	0.10578	10.668	1.1868	4.4309	5	1.7	1.7	1.3
10.106	8.4045	0.11911	9.4947	1.2434	8.8427	10	1.7	1.7	1.3
14.469	8.0159	0.12487	9.1873	1.255	13.076	15	1.7	1.7	1.3
18.94	7.8112	0.12813	9.0441	1.2593	17.259	20	1.7	1.7	1.3
23.183	7.6844	0.13025	8.9655	1.2602	21.408	25	1.7	1.7	1.3
27.18	7.5978	0.13174	8.9105	1.2615	25.557	30	1.7	1.7	1.3
30.922	7.535	0.13284	8.8731	1.262	29.695	35	1.7	1.7	1.3
34.409	7.4872	0.13369	8.8461	1.2621	33.824	40	1.7	1.7	1.3
37.644	7.4498	0.13436	8.8255	1.262	37.949	45	1.7	1.7	1.3
40.634	7.4195	0.13491	8.8088	1.262	42.073	50	1.7	1.7	1.3
43.394	7.3946	0.13537	8.797	1.2616	46.185	55	1.7	1.7	1.3

Table A.15: Controller and Closed Loop Evaluation Parameters of Just Proper Optimal PID Controllers for Closed Loop of Thermocouple 2 in Heated Tank Process

J_u	J_v	k_i	τ	ζ	β	k_∞	GM_S	M_S	M_T
0.87314	161.12	0.006207	99.748	1.3009	0.48457	0.3	1.7	1.7	1.1285
0.90987	146.94	0.00686	56.238	0.95654	1.0368	0.4	1.7	1.7	1.1158
1.1222	112.43	0.009307	47.487	0.82089	2.2626	1	1.7	1.7	1.1448
2	95.95	0.011188	43.65	0.79058	4.0952	2	1.7	1.7	1.1817
2.9998	89.233	0.012182	42.311	0.78073	5.8203	3	1.7	1.7	1.2005
3.9995	85.498	0.012813	41.625	0.77533	7.5002	4	1.7	1.7	1.2118
4.999	83.097	0.013251	41.218	0.77164	9.1544	5	1.7	1.7	1.2191
9.9918	77.829	0.014337	40.402	0.76199	17.264	10	1.7	1.7	1.236
14.972	75.896	0.014781	40.117	0.75824	25.297	15	1.7	1.7	1.2425
19.935	74.888	0.015021	39.977	0.75618	33.305	20	1.7	1.7	1.2457
24.873	74.269	0.015186	39.886	0.75437	41.274	25	1.7	1.7	1.2484
29.781	73.849	0.015292	39.837	0.75327	49.246	30	1.7	1.7	1.2497
34.654	73.546	0.015358	39.797	0.75311	57.263	35	1.7	1.7	1.2502
39.486	73.317	0.01543	39.755	0.75216	65.207	40	1.7	1.7	1.2518

Table A.16: Controller and Closed Loop Evaluation Parameters of Just Proper Optimal PID Controllers for Closed Loop of Thermocouple 3 in Heated Tank Process

J_u	J_v	k_i	τ	ζ	β	k_∞	GM_S	M_S	M_T
1.9999	141.25	0.007632	52.62	0.76688	4.9801	2	1.7	1.7	1.1473
2.9998	134.36	0.008109	51.482	0.75819	7.1862	3	1.7	1.7	1.1603
3.9994	130.6	0.008394	50.923	0.75343	9.3578	4	1.7	1.7	1.1677
4.9989	128.23	0.008586	50.584	0.75034	11.512	5	1.7	1.7	1.1726
9.9909	123.14	0.009025	49.896	0.74392	22.206	10	1.7	1.7	1.1834
14.969	121.32	0.009197	49.682	0.74099	32.828	15	1.7	1.7	1.1875
19.927	120.39	0.009291	49.566	0.73932	43.429	20	1.7	1.7	1.19
24.857	119.82	0.009347	49.52	0.73812	54.01	25	1.7	1.7	1.191
29.754	119.43	0.009383	49.492	0.73751	64.605	30	1.7	1.7	1.1914
44.181	118.78	0.00945	49.388	0.73674	96.421	45	1.7	1.7	1.1935

APPENDIX B

MATLAB CODES FOR DESIGN OF OPTIMAL CONTROLLERS

The following MATLAB codes solve the constrained optimization formulation in (2.21) to design optimal PI and PID controllers for the Quadruple-Tank Process. Optimal PI and PID controllers were designed for other plant models by making appropriate modifications to the codes.

kiterator.m

```
% kiterator.m implements the iterative sequential loop-closing method
(Shen
% & Yu, 1994) and Kristiansson's loop evaluation criteria to compute
the
% parameters for the minimum-Jv PID controllers in the multiloop of the
% Quadruple-Tank Process

% code calls kanada_opt.m

global PARAMS1
global PARAMS2
global params

ki1=0.0123;tau1=143.0857;zeta1=0.8069;beta1=3.4078;
ki2=0.0092;tau2=143.5109;zeta2=0.7874;beta2=4.5247;
term=1;
params=[ki2 tau2 zeta2 beta2;ki1 tau1 zeta1 beta1];

while term==1;
plantnum=2001;                                  % 2001 refers to the
plant model in Loop 1
run kanada_opt                                  % solves the
constrained optimization formulation
                                                % to design a minimum-
Jv PID controller for plant 2001
plantnum=2002;                                  % 2002 refers to the
plant model in Loop 2
run kanada_opt                                  % solves the
constrained optimization formulation
                                                % to design a minimum-
Jv PID controller for plant 2001

clc
['ki0 = ' num2str(PARAMS2(1)) ' ' 'tau0 = ' num2str(PARAMS2(2)) ' '
'zeta0 = ' num2str(PARAMS2(3)) ' ' 'beta0 = ' num2str(PARAMS2(4))]
    ['ki2 = ' num2str(params(1,1)) ' ' 'tau2 = ' num2str(params(1,2)) '
' 'zeta2 = ' num2str(params(1,3)) ' ' 'beta2 = ' num2str(params(1,4))]
['ki0 = ' num2str(PARAMS1(1)) ' ' 'tau0 = ' num2str(PARAMS1(2)) ' '
'zeta0 = ' num2str(PARAMS1(3)) ' ' 'beta0 = ' num2str(PARAMS1(4))]
    ['ki1 = ' num2str(params(2,1)) ' ' 'tau1 = ' num2str(params(2,2)) '
' 'zeta1 = ' num2str(params(2,3)) ' ' 'beta1 = ' num2str(params(2,4))]

    term=input('Continue Iteration?  (1 / 0)    ');

end
```

kanada_opt.m

```
%Created in 2004 September 09 in Edmonton by Birgitta Kristiansson
%Tp and L are given values, T63 and Ld are measured values for
(ekvivalent) time constant and delay.
% This file minimizes Jv, while kinf (Ju) is given and  GMs is fixed
% for a proper PID controller (1:st ordn filter) with a possibly
complex zero.
% kinf = ki*tau*beta corresponds to Ju
% invariable: kinf
% parameters ki,zeta, tau are optimized. Starting values must be given
% outvariables: ki, zeta, tau and beta

% code calls the following functions: kanadaproc.m, kan_ixlf.m, and
% constrains.m

[ngp,dgp,kappa,wpip,nr,T63,Ld,kappa150,w150,Klf,Tp,L,ordn,w]=kanadaproc
(plantnum);  %takes in the plant model and the results of a simple
analyses of that model


format compact
w=logspace(-8,3,25000);
t=[0:0.02:2000];

maxs=1.7; maxt=1.3;  %maxt=maxs*1.3/1.7; minam=3.0;              %values
for GMS: max |S|, max |T| (and  min Gm)
                       % maxt is between 1.2 and 2.0; maxs is between
1.4 and 2.0

if ordn==1                                                        % 1st
order plant
  kinf=6;                                                         % kinf
is high-frequency PID controller gain
  ki=0.008;                                                       % sets
starting value for ki
  zeta=1.1;                                                       % sets
starting value for zeta
  tau=15;                                                         % sets
starting value for tau



elseif ordn==2                                                    % 2nd
order plant
  kinf=6;
  ki=0.0090;
  zeta=0.7878;
  tau=142;


elseif ordn==3                                                  % 3rd
order plant
  kinf=6;
```

```
  if kinf>25, kinf=25, end
  ki=0.0059;
  zeta=0.9153;
  tau=140.9720;
end

beta=kinf/(tau*ki)


global INDEXPAR
global WOMEGA
global NGPROCESS
global DGPROCESS


INDEXPAR(1)=kinf;
INDEXPAR(2)=wpip;


WOMEGA=w;
NGPROCESS=ngp;
DGPROCESS=dgp;


x0=[ki,zeta,tau];                                                    % sets
the initial values of ki, zeta, and tau

options = optimset('LargeScale','off','MaxFunEvals',350,'TolX',1e-
10,'TolCon',1e-10);
[x,Jv,EXITFLAG]=fmincon('kan_ixlf',x0,[],[],[],[],[0,0,0],[],'constrain
s', options)  %optimizes Jv

ki=x(1);
zeta=x(2);
tau=x(3);
```

kanadaproc.m

```
% kanadaproc.m computes the polynomial form of the plant's transfer
% function

% Created in 2004 September 03 in Edmonton by Birgitta Kristiansson
% called by kanada_opt.m

% code calls kanaproc.m to compute some frequency domain-based
parameters for the
% model

% nr refers to plant model number, e.g. 2001 for Loop 1 in the
% Quadruple-Tank's multiloop

function
[ngp,dgp,kappa,wpip,nr,T63,Ld,kappa150,w150,Klf,Tp,L,ordn,w]=kanadaproc
(plantnum);

nr=plantnum;
plantnum
w=logspace(-8,2,12000);

Tp=1;
Klf=1;
L=0;

global PARAMS1
global PARAMS2
global params

ki2=params(1,1);tau2=params(1,2);zeta2=params(1,3);beta2=params(1,4);
ki1=params(2,1);tau1=params(2,2);zeta1=params(2,3);beta1=params(2,4);

if nr==01,
    Tp=1;
    Klf=1;
    L=0.001;
      [npade,dpade]=pade(L, 4);
        ngp=Klf*npade;
        dgp=conv(dpade,[Tp 1]);
        ordn=1;

[wbp,wpip,kappa,T63,Ld,kappa150,w150,ymax]=kanaproc(ngp,dgp,w,nr);

elseif nr==03,
       Tp=10;
    Klf=1;
    L=0.3*Tp;
      [npade,dpade]=pade(L, 4);
        ngp=Klf*npade;
        dgp=conv(dpade,[(Tp) 1]);
        ordn=1;
```

```
[wbp,wpip,kappa,T63,Ld,kappa150,w150,ymax]=kanaproc(ngp,dgp,w,nr);

elseif nr==400,
       Tp1=41.875;Tp2=42.349;
       Klf=1.643;
       L=(0.4/0.669)*31.1;
      [npade,dpade]=pade(L, 4);
        ngp=Klf*npade;
        dgp=conv(dpade,[(Tp1*Tp2) (Tp1+Tp2) 1]);
        ordn=2;

[wbp,wpip,kappa,T63,Ld,kappa150,w150,ymax]=kanaproc(ngp,dgp,w,nr);

elseif nr==401,
       Tp=57.19;
    Klf=1.702;
    L=7.81;
      [npade,dpade]=pade(L, 4);
        ngp=Klf*npade;
        dgp=conv(dpade,[Tp 1]);
        ordn=1;

[wbp,wpip,kappa,T63,Ld,kappa150,w150,ymax]=kanaproc(ngp,dgp,w,nr);

elseif nr==402,
       Tp1=41.875;Tp2=42.349;
       Klf=1.643;
       L=31.1;
      [npade,dpade]=pade(L, 4);
        ngp=Klf*npade;
        dgp=conv(dpade,[(Tp1*Tp2) (Tp1+Tp2) 1]);
        ordn=2;

[wbp,wpip,kappa,T63,Ld,kappa150,w150,ymax]=kanaproc(ngp,dgp,w,nr);

elseif nr==403,
       Tp1=47.233;Tp2=45.707;
       Klf=1.657;
       L=48.4;
      [npade,dpade]=pade(L, 4);
        ngp=Klf*npade;
        dgp=conv(dpade,[(Tp1*Tp2) (Tp1+Tp2) 1]);
        ordn=2;

[wbp,wpip,kappa,T63,Ld,kappa150,w150,ymax]=kanaproc(ngp,dgp,w,nr);

elseif nr==02,
       Tp=input('Tp?   ');
       Klf=1;
       L=input('L?   ');
      [npade,dpade]=pade(L, 4);
        ngp=Klf*npade;
        dgp=conv(dpade,[Tp^2 2*Tp 1]);
        ordn=2;
```

```
[wbp,wpip,kappa,T63,Ld,kappa150,w150,ymax]=kanaproc(ngp,dgp,w,nr);

elseif nr==111,
       Tp=154.7;
       Klf=24.37;
       L=6.28;
      [npade,dpade]=pade(L, 4);
        ngp=Klf*npade;
        dgp=conv(dpade,[Tp 1]);
        ordn=1;

[wbp,wpip,kappa,T63,Ld,kappa150,w150,ymax]=kanaproc(ngp,dgp,w,nr);

elseif nr==112,
       Tp=120;
       Klf=11.15;
       L=8.7;
      [npade,dpade]=pade(L, 4);
        ngp=Klf*npade;
        dgp=conv(dpade,[Tp^2 2*Tp 1]);
        ordn=2;

[wbp,wpip,kappa,T63,Ld,kappa150,w150,ymax]=kanaproc(ngp,dgp,w,nr);

elseif nr==121,
       Tp=114;
       Klf=11.13;
       L=1;
      [npade,dpade]=pade(L, 4);
        ngp=Klf*npade;
        dgp=conv(dpade,[Tp^2 2*Tp 1]);
        ordn=2;

[wbp,wpip,kappa,T63,Ld,kappa150,w150,ymax]=kanaproc(ngp,dgp,w,nr);

elseif nr==122,
       Tp=157.8;
       Klf=24.57;
      L=7.12;
       [npade,dpade]=pade(L, 1);
        ngp=Klf*npade;
        dgp=conv(dpade,[Tp 1]);
        ordn=1;

[wbp,wpip,kappa,T63,Ld,kappa150,w150,ymax]=kanaproc(ngp,dgp,w,nr);

elseif nr==211,
       Tp=232.5;
       Klf=10.13;
       L=7.32;
      [npade,dpade]=pade(L, 4);
        ngp=Klf*npade;
        dgp=conv(dpade,[Tp 1]);
        ordn=1;
```

```
[wbp,wpip,kappa,T63,Ld,kappa150,w150,ymax]=kanaproc(ngp,dgp,w,nr);

elseif nr==212,
       Tp=155;
       Klf=1;
       L=49.3;
      [npade,dpade]=pade(L, 4);
        ngp=Klf*npade;
        dgp=conv(dpade,[24056 310.2 1]);
        ordn=2;
        [wbp,wpip,kappa,T63,Ld,kappa150,w150,ymax]=
kanaproc(ngp,dgp,w,nr);

elseif nr==221,
       Tp=162;
       Klf=1;
       L=33;
      [npade,dpade]=pade(L, 4);
        ngp=Klf*npade;
        dgp=conv(dpade,[Tp^2 2*Tp 1]);
        ordn=2;

[wbp,wpip,kappa,T63,Ld,kappa150,w150,ymax]=kanaproc(ngp,dgp,w,nr);

elseif nr==222,
       Tp=193.8;
       Klf=8.772;
       L=13.9;
      [npade,dpade]=pade(L, 4);
        ngp=Klf*npade;
        dgp=conv(dpade,[Tp 1]);
        ordn=1;

[wbp,wpip,kappa,T63,Ld,kappa150,w150,ymax]=kanaproc(ngp,dgp,w,nr);

elseif nr==1001,
        [np,dp]=pade(6.28,2); ngp11=24.37*np; dgp11=conv(dp,[154.7 1]);
G11=tf(ngp11,dgp11);
        [np,dp]=pade(8.70,2); ngp12=11.15*np; dgp12=conv(dp,[14340
250.8 1]); G12=tf(ngp12,dgp12);
        [np,dp]=pade(1.00,2); ngp21=11.13*np; dgp21=conv(dp,[13070
231.2 1]); G21=tf(ngp21,dgp21);
        [np,dp]=pade(7.12,2); ngp22=24.57*np; dgp22=conv(dp,[157.8 1]);
G22=tf(ngp22,dgp22);
       nf2=0.0205*[9.8262^2 2*1.4996*9.8262 1]; df2=[9.8262/29.7141 1
0]; F2=tf(nf2,df2);

d1221=conv(dgp12,dgp21);d1122=conv(dgp11,dgp22);n1221=conv(ngp12,ngp21)
        nf222=conv(nf2,ngp22);nf222=[0,nf222];df222=conv(df2,dgp22);
        nf21221=conv(nf2,n1221);t2=conv([0,nf21221],d1122);t2=[0,0,t2];
        sd=size(df222)
        sn=size(nf222)
        st2=size(t2)
        ngp1=conv(ngp11,d1221);size(ngp1)
        ngp2=conv(ngp1,(df222+nf222));np2=size(ngp2)
        ngp=conv(ngp1,(df222+nf222))-t2;
```

```
        d111221=conv(dgp11,d1221);
        dgp=conv(d111221,(df222+nf222));
        ordn=3;

[wbp,wpip,kappa,T63,Ld,kappa150,w150,ymax]=kanaproc(ngp,dgp,w,nr);

elseif nr==1002,
        [np,dp]=pade(6.28,2); ngp11=24.37*np; dgp11=conv(dp,[154.7 1]);
G11=tf(ngp11,dgp11);
        [np,dp]=pade(8.70,2); ngp12=11.15*np; dgp12=conv(dp,[14340
250.8 1]); G12=tf(ngp12,dgp12);
        [np,dp]=pade(1.00,2); ngp21=11.13*np; dgp21=conv(dp,[13070
231.2 1]); G21=tf(ngp21,dgp21);
        [np,dp]=pade(7.12,2); ngp22=24.57*np; dgp22=conv(dp,[157.8 1]);
G22=tf(ngp22,dgp22);
        nf1=0.0251*[8.8070^2  2*1.5251*8.8070 1]; df1=[8.8070/27.0910 1
0]; F1=tf(nf1,df1);

d1221=conv(dgp12,dgp21);d1122=conv(dgp11,dgp22);n1221=conv(ngp12,ngp21)
        nf111=conv(nf1,ngp11);nf111=[0,nf111];df111=conv(df1,dgp11);
        nf11221=conv(nf1,n1221);t2=conv([0,nf11221],d1122);t2=[0,0,t2];
        ngp1=conv(ngp22,d1221);
        ngp2=conv(ngp1,(df111+nf111));
        ngp=conv(ngp1,(df111+nf111))-t2;
        d221221=conv(dgp22,d1221);
        dgp=conv(d221221,(df111+nf111));
        ordn=3;

[wbp,wpip,kappa,T63,Ld,kappa150,w150,ymax]=kanaproc(ngp,dgp,w,nr);

elseif nr==2001,

PARAMS2(1)=ki2;PARAMS2(2)=tau2;PARAMS2(3)=zeta2;PARAMS2(4)=beta2;
        [np,dp]=pade(7.32,2); n11=0.3446*np; d11=conv(dp,[232.5 1]);
        [np,dp]=pade(49.3,2); n12=1*np; d12=conv(dp,[24056 310.2 1]);
        [np,dp]=pade(33.00,2); n21=1*np; d21=conv(dp,[26244 324 1]);
        [np,dp]=pade(13.9,2); n22=0.3046*np; d22=conv(dp,[193.8 1]);
        nf1=ki1*[(tau1^2) (2*zeta1*tau1) 1]; df1=[(tau1/beta1) 1 0];
        n12d21d22d11df1=conv(n12,d21)
        n12d21d22d11df1=conv(d22,n12d21d22d11df1);
        n12d21d22d11df1=conv(d11,n12d21d22d11df1);
        n12d21d22d11df1=conv(df1,n12d21d22d11df1);

        n12n21d22d11nf1=conv(n12,n21);
        n12n21d22d11nf1=conv(d22,n12n21d22d11nf1);
        n12n21d22d11nf1=conv(d11,n12n21d22d11nf1);
        n12n21d22d11nf1=conv(nf1,n12n21d22d11nf1);

        n22n11d12d21nf1=conv(n22,n11);
        n22n11d12d21nf1=conv(d12,n22n11d12d21nf1);
        n22n11d12d21nf1=conv(d21,n22n11d12d21nf1);
        n22n11d12d21nf1=conv(nf1,n22n11d12d21nf1);

        nf1n21d11d12d22=conv(nf1,n21);
        nf1n21d11d12d22=conv(d11,nf1n21d11d12d22);
        nf1n21d11d12d22=conv(d12,nf1n21d11d12d22);
```

```
        nf1n21d11d12d22=conv(d22,nf1n21d11d12d22);

        df1d21d11d12d22=conv(df1,d21);
        df1d21d11d12d22=conv(d11,df1d21d11d12d22);
        df1d21d11d12d22=conv(d12,df1d21d11d12d22);
        df1d21d11d12d22=conv(d22,df1d21d11d12d22);

        ngp=[zeros(1,2) n12n21d22d11nf1]+n12d21d22d11df1-
n22n11d12d21nf1;
        dgp=[zeros(1,2) nf1n21d11d12d22]+df1d21d11d12d22;

        ordn=3;


[wbp,wpip,kappa,T63,Ld,kappa150,w150,ymax]=kanaproc(ngp,dgp,w,nr);


elseif nr==2002,

PARAMS1(1)=ki1;PARAMS1(2)=tau1;PARAMS1(3)=zeta1;PARAMS1(4)=beta1;
        [np,dp]=pade(7.32,2); n11=0.3446*np; d11=conv(dp,[232.5 1]);
        [np,dp]=pade(49.3,2); n12=1*np; d12=conv(dp,[24056 310.2 1]);
        [np,dp]=pade(33.00,2); n21=1*np; d21=conv(dp,[26244 324 1]);
        [np,dp]=pade(13.9,2); n22=0.3046*np; d22=conv(dp,[193.8 1]);
        nf2=ki2*[(tau2^2) (2*zeta2*tau2) 1]; df2=[(tau2/zeta2) 1 0];
        n21d12d22d11df2=conv(n21,d12)
        n21d12d22d11df2=conv(d22,n21d12d22d11df2);
        n21d12d22d11df2=conv(d11,n21d12d22d11df2);
        n21d12d22d11df2=conv(df2,n21d12d22d11df2);
        n12n21d22d11nf2=conv(n12,n21);
        n12n21d22d11nf2=conv(d22,n12n21d22d11nf2);
        n12n21d22d11nf2=conv(d11,n12n21d22d11nf2);
        n12n21d22d11nf2=conv(nf2,n12n21d22d11nf2);
        n22n11d12d21nf2=conv(n22,n11);
        n22n11d12d21nf2=conv(d12,n22n11d12d21nf2);
        n22n11d12d21nf2=conv(d21,n22n11d12d21nf2);
        n22n11d12d21nf2=conv(nf2,n22n11d12d21nf2);
        nf2n12d11d21d22=conv(nf2,n12);
        nf2n12d11d21d22=conv(d11,nf2n12d11d21d22);
        nf2n12d11d21d22=conv(d21,nf2n12d11d21d22);
        nf2n12d11d21d22=conv(d22,nf2n12d11d21d22);
        df2d21d11d12d22=conv(df2,d21);
        df2d21d11d12d22=conv(d11,df2d21d11d12d22);
        df2d21d11d12d22=conv(d12,df2d21d11d12d22);
        df2d21d11d12d22=conv(d22,df2d21d11d12d22);
        ngp=[zeros(1,2) n12n21d22d11nf2]+n21d12d22d11df2-
n22n11d12d21nf2;
        dgp=[zeros(1,2) nf2n12d11d21d22]+df2d21d11d12d22;

        ordn=3;


[wbp,wpip,kappa,T63,Ld,kappa150,w150,ymax]=kanaproc(ngp,dgp,w,nr);

end
```

kanaproc.m

```
% kanaproc.m computes some characteristic parameters for the plant
model

% Created in 2004 September 03 in Edmonton by Birgitta Kristiansson
% function that analyses current plant.
% called by kanadaproc.m

function[wbp,wpip,kappa,T63,Ld,kappa150,w150,ymax]=kanaproc(ngp,dgp,w,n
r);


tsteg=0.02;
t=[0:tsteg:500];

[amp,fas]=bode(ngp,dgp,w);
amp1=amp(1)
K1f=amp(1)

ind=find(amp<(1/sqrt(2)));
wbp=w(ind(1));
if (max(fas)>-180) & (min(fas)<-180),
    ind=find(fas<=-180);
    wpip=w(ind(1));
    kappa=amp(ind(1))/amp(1);
else
    wpip=1000;
    kappa=100;
end

stegp=step(ngp,dgp,t);
i1=1;
        while stegp(i1)<0.63*stegp(length(t))
            i1=i1+1;
        end;
T63=t(i1);
i2=1;
        while stegp(i2)<0.05*stegp(length(t))
            i2=i2+1;
        end;
Ld=t(i2);
ymax =max(stegp);



if (max(fas)>-80) & (min(fas)<-150),
    ind=find(fas<=-150);
    w150=w(ind(1));
    kappa150=amp(ind(1))/amp(1);
else
    w150=1000;
    kappa150=100;
end
```

kan_ixlf.m

```
% kan_ixlf.m defines the objective function and uses the fmincon
function
% to solve the constrained optimization formulation

% Created in 2004 September 04 in Edmonton by Birgitta Kristiansson
% function to optimize Jv (Jr)
% called by kanada_opt

% code calls kreg.m, kkansl.m, kdistsen.m

function  Jv=kan_ixlf(x)


global INDEXPAR;
global WOMEGA;
global NGPROCESS;
global DGPROCESS;


kinf=INDEXPAR(1);
wpip=INDEXPAR(2);



w=WOMEGA;
ngp=NGPROCESS;
dgp=DGPROCESS;
[ampp,fip]=bode(ngp,dgp,w);

ki=x(1);
zeta=x(2);
tau=x(3);

beta=kinf/(tau*ki);

[ngr,dgr]=kreg(ki,tau,beta,zeta);                    % creates the
controller
[nl,dl]=kkrets(ngr,dgr,ngp,dgp,w);                   % creates the
loop
[ampl,fil]=bode(nl,dl,w);

[ns,ds,samp,ms,maxs_w,wmaxs_w]=kkansl(nl,dl,w);      % creates the
sensitivity function

[ngs,dgs]=kdistsen(ngp,dgp,ns,ds,w);                 % creates the
s-weighted disturbance sensitivity function
nix=ngs;
dix=conv([1 0],dgs);
[ixamp,ixfas]=bode(nix,dix,w);
[Jv,wind]=max(ixamp);                                % computes Jv
wmax=w(wind);
```

constrains.m

```
% constrains.m sets the constraints on the objective function. The
% constraints are typically on GMS and Ju (or kinf)

% Created in 2004 September 09 in Edmonton by Birgitta Kristiansson
% gives the constraints for the optimization
% called by kanada_opt

% code calls kkansl.m, kkompl.m and kreg.m


function[g,geq]=constrains(x)

geq=[];

maxs=1.7;  maxt=1.3;  %maxt=maxs*1.3/1.7;
lam=3;                                                    %lam= minimum
limit for gain margin
tsteg=0.02;
t=[0:tsteg:1500];

global INDEXPAR;
global WOMEGA;
global NGPROCESS;
global DGPROCESS;


kinf=INDEXPAR(1);
wpip=INDEXPAR(2);


w=WOMEGA;
ngp=NGPROCESS;
dgp=DGPROCESS;
[ampp,fip]=bode(ngp,dgp,w);

ki=x(1);
zeta=x(2);
tau=x(3);

beta=kinf/(tau*ki);

[ngr,dgr]=kreg(ki,tau,beta,zeta);

[nl,dl]=kkrets(ngr,dgr,ngp,dgp,w);
[ampl,fil]=bode(nl,dl,w);

[ns,ds,samp,ms,maxs_w,wmaxs_w]=kkansl(nl,dl,w);
[nt,dt,tamp,mt,wb]=kkompl(nl,dl,w);

g(1)=ms-maxs;                                  % imposes the constraint
max|S| <= MS
```

```
g(2)=mt-maxt;                                   % imposes the constraint
max|T| <= MT


g=[g(1) g(2)];
```

kreg.m

```
% Modified in  September 2004 in Edmonton by Birgitta Kristiansson

% kreg.m creates a PID controller with a 1st order filter, given the
% parameters ki, beta,zeta,tau
% code is called by kan_ixlf.m and constrains.m

function [ngr,dgr]=kreg(ki,tau,beta,zeta);

ngr=ki*[tau^2 2*zeta*tau 1];
dgr=conv([1 0], [tau/beta 1]);
```

kkrets.m

```
% Modified in  September 4004 in Edmonton by Birgitta Kristiansson

% kkrets.m creates the loop given the
% plant and the controller
% code is called by kan_ixlf.m and constrains.m

function [nl,dl]=kkrets(ngr,dgr,ngp,dgp,w);


nl=conv(ngr,ngp);
dl=conv(dgr,dgp);
    lnl=length(nl);ldl=length(dl);
    if lnl>ldl, dl=[zeros(1,lnl-ldl),dl];
    elseif ldl>lnl, nl=[zeros(1,ldl-lnl),nl];
    end
loopl=tf(nl,dl);
[ampl,fil]=bode(loopl,w);
index=find (fil<=-180);
```

kkansl.m

```
% Modified in  September 4004 in Edmonton by Birgitta Kristiansson

% kkansl.m creates the sensitivity function and the 1/s-weighted
sensitivity function given the loop
% It calculates Ms
% code is called by kan_ixlf.m and constrains.m

function [ns,ds,samp,ms,maxs_w,wmaxs_w]=kansl(nl,dl,w);


lnl=length(nl);
ldl=length(dl);
ns=dl;
    ds=nl+dl;
    [samp,sfas]=bode(ns,ds,w);
   [ms,sind]=max(samp);
   dsr=conv([1 0],ds);
   [s_w,s_wfas]=bode(ns,dsr,w);
   [maxs_w,swi]=max(s_w);
   wmaxs_w=w(swi(1));
```

kkompl.m

```
% Modified in  September 4004 in Edmonton by Birgitta Kristiansson

% kkompl.m creates the complementary sensitivity function T and the
bandwidth wb, given the
% loop
% code is called by kan_ixlf.m and constrains.m

function [nt,dt,tamp,mt,wb]=kkompl(nl,dl,w);

    nt=nl;
    dt=dl+nl;
        [tamp,tfas]=bode(nt,dt,w);
    [mt,tind]=max(tamp);

    indwb=find(tamp<(1/sqrt(2)));
    wb=w(indwb(1));                  %bandwith for the closed loop
```

kdisten.m

```
% Modified in  September 4004 in Edmonton by Birgitta Kristiansson

% kdisten.m creates the disturbance sensitivity function = Gvy

function[ngs,dgs,gsamp]=kdisten(ngp,dgp,ns,ds,w);

    ngs=conv(ngp,ns);
    dgs=conv(dgp,ds);
    [gsamp,gsfas]=bode(ngs,dgs,w);
```

kdisten.m

```
% Modified in  September 4004 in Edmonton by Birgitta Kristiansson

% kdisten.m creates the disturbance sensitivity function = Gvy

function[ngs,dgs,gsamp]=kdisten(ngp,dgp,ns,ds,w);

    ngs=conv(ngp,ns);
    dgs=conv(dgp,ds);
    [gsamp,gsfas]=bode(ngs,dgs,w);
```